



**unine**

UNIVERSITÉ DE  
NEUCHÂTEL

**University of Neuchâtel**

**Faculty of Science**

**Laboratory of Technologies for Heritage Materials  
and Laboratory of Microbiology**

**Fungal biogenic patina:  
optimization of an innovative conservation treatment  
for copper-based artefacts**

**Ph.D. dissertation of Monica Albini**

**March 23<sup>rd</sup>, 2017**



University of Neuchâtel  
Faculty of Science  
Laboratory of Technologies for Heritage Materials  
and Laboratory of Microbiology

**Fungal biogenic patina:  
optimization of an innovative conservation treatment  
for copper-based artefacts**

A dissertation submitted for the degree of  
*Docteur ès Sciences*

Presented by Monica Albini

Thesis co-directors:

Prof. Edith Joseph, University of Neuchâtel  
Prof. Pilar Junier, University of Neuchâtel

Jury members:

Prof. Edith Joseph, University of Neuchâtel, Switzerland  
Prof. Pilar Junier, University of Neuchâtel, Switzerland  
Prof. Katja Sterflinger-Gleixner, Universität für Bodenkultur Wien, Austria  
Dr. Elodie Guilminot, Laboratoire Arc'Antique, France

March 23<sup>rd</sup>, 2017



## IMPRIMATUR POUR THESE DE DOCTORAT

---

La Faculté des sciences de l'Université de Neuchâtel  
autorise l'impression de la présente thèse soutenue par

**Madame Monica ALBINI**

Titre:

**“Fungal biogenic patina: optimization  
of an innovative conservation treatment  
for copper-based artefacts”**

sur le rapport des membres du jury composé comme suit:

- Prof. ass. Edith Joseph, co-directrice de thèse, UniNE
- Prof. Pilar Junier, co-directrice de thèse, UniNE
- Dr Elodie Guilminot, Laboratoire Arc'Antique, Nantes, France
- Prof. Katja Sterflinger, University of Natural Resources and Applied Life Science, Vienne, Autriche

Neuchâtel, le 24 avril 2017

Le Doyen, Prof. R. Bshary





*“Life is not easy for any of us. But what of that?  
We must have perseverance and above all confidence in ourselves.  
We must believe that we are gifted for something and that this thing must be attained.”*

*Marie Curie*



## Abstract

Microorganisms are often considered harmful for cultural heritage. However, they can also be used for its safeguarding. Indeed, some fungal species are known for their ability to produce oxalic acid in order to immobilize toxic heavy metals and, therefore, detoxify their environment. Biotechnology already exploited this ability to immobilize heavy metals in the field of waste treatment forming metal oxalates. The “biopatina project” used this ability in order to modify active copper corrosion products into more stable and less soluble compounds such as copper oxalates. The presence of copper oxalates as green patinas was already discovered on outdoor bronze artefacts and it was not associated with active corrosion. Furthermore, copper oxalates are known to be extremely stable in polluted atmospheres with acidic conditions (pH 3), providing good protection to copper-based artefacts. The “biopatina project” aims to produce copper oxalates as passivating compound having the same composition as naturally occurring copper minerals (inorganic materials) enhancing the compatibility of this treatment with the corroded surface of artefacts. During previous projects (FP6-EU-ARTECH, 2004-2009 and FP7-BAHAMAS, 2010-2012), the most suitable fungal species to be used was identified and initial successful attempts to produce copper oxalates were performed. The aim of this thesis was to optimise this novel biological treatment for the conservation of copper-based artefacts in order to transfer it from the laboratory tests to real-praxis. This work focused on two main subjects: the study of the microorganism used for the production of biogenic copper oxalates and the treated material, namely copper and bronze. Regarding the treated material, the aim was to understand which protective mechanisms are involved in the biopatina treatment allowing to understand if such treatment acts as a corrosion inhibitor or as a coating. The biological treatment was compared to standard conservation treatment as microcrystalline wax (coating system) and benzotriazole (corrosion inhibitor) and its long-term behaviour was tested by natural and artificial ageing. Furthermore, the influence of alloying elements, particularly tin, on the behaviour of biopatina treatment was investigated. To do that, a complement of analytical techniques was used: high-performance liquid chromatography (HPLC), optical microscopy (OM), scanning electron microscopy (SEM) coupled with energy dispersive spectroscopy (EDS), infrared spectroscopy (FTIR), Raman spectroscopy, electrochemical impedance spectroscopy (EIS) and colorimetry. The outcomes of this work showed that the biopatina treatment is positioned in the range of corrosion inhibitors rather than protective coatings. Biopatina treatment can be used to replace benzotriazole (BTA) solutions as innocuous and more efficient treatment for archaeological objects. It can also be applied on outdoor objects, regardless the geometry of exposure conditions and its efficiency is not influenced by the bronze composition. Furthermore, the application protocol currently used on real artefacts was developed. Finally, based on the outcome of this study, a ready-to-use kit is currently under evaluation for commercialization and available for small trials to conservators-restorers.

## Keywords:

Biotechnology, conservation science, bronze, outdoor sculpture, archaeological artefact, benzotriazole, microcrystalline wax, FTIR, SEM, EIS

## Résumé

Les micro-organismes sont souvent considérés dangereux pour les biens culturels. Malgré cela, ils peuvent aussi être utilisés pour leur protection. En effet, certaines espèces fongiques sont connues pour leur capacité à produire de l'acide oxalique pour immobiliser des métaux lourds toxiques et, donc, détoxifier leur milieu. La biotechnologie a déjà exploité cette capacité d'immobiliser des métaux lourds sous forme d'oxalates métalliques dans le domaine du traitement des déchets. Le projet « biopatine » a tiré profit cette capacité pour modifier des produits de corrosion de cuivre actifs en des composés plus stables et moins solubles comme les oxalates de cuivre. La présence des oxalates de cuivre a été déjà observée sous forme de patines vertes sur des œuvres d'art en bronze à l'extérieur et ils n'ont pas été associés à de la corrosion cyclique. En outre, les oxalates de cuivre sont connus pour être extrêmement stables dans des atmosphères polluées en conditions acides (pH 3), fournissant une bonne protection aux sculptures à base de cuivre. Le projet « biopatine » a comme objectif la production de oxalates de cuivre comme composés passivant ayant la même composition que des minéraux de cuivre naturellement présents sur le patrimoine cuivreux (matériaux inorganiques) et l'amélioration de la compatibilité entre le traitement et la surface corrodée. Lors de projets précédents (FP6-EU-ARTECH, 2004-2009 et FP7-BAHAMAS, 2010-2012), l'espèce fongique la plus appropriée a été identifiée et des tentatives de production d'oxalates de cuivre ont été effectuées avec succès. L'objectif de cette thèse était d'optimiser le nouveau traitement biologique développé pour la conservation d'œuvres d'art en cuivre afin de transférer les tests de laboratoire à une mise en pratique sur le terrain. Ce travail de thèse s'est concentré sur deux sujets principaux : l'étude du micro-organisme utilisé pour la production des oxalates de cuivre biogéniques et les matériaux traités, notamment cuivre et bronze. En ce qui concerne les matériaux traités, le but était de comprendre quels mécanismes protecteurs sont impliqués dans le traitement biopatine permettant de déterminer si ce traitement agit comme un inhibiteur de corrosion ou comme un coating. Le traitement biologique a été comparé à des traitements de conservation standards, la cire microcristalline comme coating et le benzotriazole comme inhibiteur de corrosion, et son comportement à long terme a été évalué par des procédures de vieillissement naturel et artificiel. En outre, l'influence des éléments de l'alliage, l'étain en particulier, sur le comportement du traitement biopatine a été examinée. Pour ce faire, un complément de techniques analytiques a été utilisé: chromatographie liquide à haute performance (HPLC), microscopie optique (OM), microscopie électronique à balayage (SEM) couplé avec spectroscopie à rayons X à dispersion d'énergie (EDS), spectroscopie infrarouge (FTIR), spectroscopie Raman, Spectroscopie d'Impédance Electrochimique (EIS) et colorimétrie. Les résultats de ce travail ont montré que le traitement biopatine se place parmi les inhibiteurs de corrosion plutôt que les revêtements. Le traitement biopatine peut aussi être utilisé pour remplacer le benzotriazole (BTA) comme traitement sans risques pour la santé et l'environnement et plus efficace pour la stabilisation des objets archéologiques. Il peut aussi être appliqué sur des objets en extérieur et son efficacité n'est pas influencée par la composition de l'alliage. En outre, le protocole d'application actuellement utilisé sur des artefacts réels a été développé. Finalement, basé sur les résultats de cette étude, un kit prêt à l'emploi est actuellement en évaluation pour une commercialisation et est mis à disposition des conservateurs-restaurateurs.

## Mots clés:

Biotechnologie, science de la conservation, bronze, sculpture en extérieur, objets archéologiques, benzotriazole, cire microcristalline, FTIR, SEM-EDS, EIS

# TABLE OF CONTENT

## **CHAPTER 1**

<b>INTRODUCTION .....</b>	<b>15</b>
1.1 BASICS OF CORROSION .....	16
Corrosion as electrochemical reaction .....	16
Corrosion thermodynamic – Pourbaix diagrams .....	18
Corrosion rate .....	20
1.2 CORROSION OF COPPER AND BRONZE .....	21
Corrosion of outdoor monuments .....	22
Corrosion of archaeological artefacts .....	28
1.3 CURRENT TREATMENTS .....	33
Coatings .....	33
Acrylic coating .....	33
Waxes .....	34
Silanes .....	34
Corrosion inhibitors .....	35
Benzotriazole (BTA) .....	36
Carboxylates .....	36
“Green inhibitors” .....	37
1.4 BIOTECHNOLOGICAL INNOVATIVE APPROACH .....	37
1.5 RESEARCH OUTLINE .....	39
REFERENCES .....	41

## **CHAPTER 2**

<b>BEAUVERIA BASSIANA .....</b>	<b>47</b>
SUMMARY .....	48
ABSTRACT .....	49
INTRODUCTION .....	49
MATERIALS AND METHODS .....	51
Fungal strain .....	51
Liquid cultures .....	51
Sampling .....	52
Analytical methods .....	52
RESULTS AND DISCUSSION .....	53
CONCLUSIONS .....	55
SUPPLEMENTARY INFORMATION .....	56
Delivery system .....	59
REFERENCES .....	61

<b>CHAPTER 3</b>	
<b>BIOPATINA FOR ARCHAEOLOGICAL OBJECTS.....</b>	<b>63</b>
SUMMARY .....	64
3.1 FIRST STABILIZATION TESTS ON ARCHAEOLOGICAL OBJECTS.....	65
Abstract.....	65
Introduction .....	65
Materials and Methods .....	66
Artefacts .....	66
Treatments .....	66
Visual characterization.....	69
Fourier Transform Infrared Spectroscopy .....	69
Ageing procedures .....	69
Results .....	71
Test objects.....	71
Real objects.....	78
Conclusions.....	81
3.2 IN-DEPTH COMPARISON BETWEEN BENZOTRIAZOLE AND BIOPATINA.....	82
Abstract.....	82
Introduction .....	82
Materials and methods.....	83
Copper samples and artificial patina preparation .....	83
Treatments .....	83
Resin embedding and preparation of cross section .....	83
Optical Microscopy .....	84
Fourier Transform Infrared Spectroscopy (FTIR) .....	84
Scanning Electron Microscopy (SEM).....	85
Electrochemical impedance spectroscopy (EIS) .....	85
Results and discussion.....	85
Conclusions.....	91
REFERENCES.....	92

<b>CHAPTER 4</b>	
<b>BIOPATINA FOR OUTDOOR SCULPTURES.....</b>	<b>95</b>
SUMMARY .....	96
4.1 NATURAL PATINAS.....	97
Abstract.....	97
Introduction .....	97
Materials and Methods .....	98
Samples.....	98
Treatments .....	99
Natural ageing procedures.....	99
Fourier Transform Infrared Spectroscopy (FTIR) .....	99
Colorimetry.....	99
Scanning Electron Microscopy (SEM).....	99
Electrochemical impedance spectroscopy (EIS) .....	100
Results and discussion.....	100
Conclusions.....	105
Supplementary Information .....	106

Results and discussion.....	108
Conclusions.....	115
<b>4.2 ARTIFICIAL PATINAS .....</b>	<b>116</b>
Abstract.....	116
Introduction .....	116
Materials and Methods .....	116
Samples.....	116
Treatments .....	117
Natural ageing procedures.....	117
Fourier Transform Infrared Spectroscopy (FTIR).....	117
Colorimetry.....	118
Scanning Electron Microscopy (SEM).....	118
Results and discussion .....	118
Conclusions .....	126
<b>4.3 REAL OBJECTS.....</b>	<b>127</b>
Abstract.....	127
Fusion sculpture .....	127
Sculpture park Légende d’Automne.....	132
Conclusions .....	135
<b>REFERENCES .....</b>	<b>136</b>

## **CHAPTER 5**

<b>INFLUENCE OF TIN ENRICHMENT.....</b>	<b>139</b>
SUMMARY.....	140
ABSTRACT .....	141
INTRODUCTION .....	141
MATERIALS AND METHODS .....	143
Coupons .....	143
Pre-patination and ageing method .....	143
Biological treatment.....	144
Samples characterization.....	144
RESULTS AND DISCUSSION.....	145
Tin coupons.....	145
Tin-enriched bronze coupons.....	146
CONCLUSIONS.....	151
REFERENCES .....	152

## **CHAPTER 6**

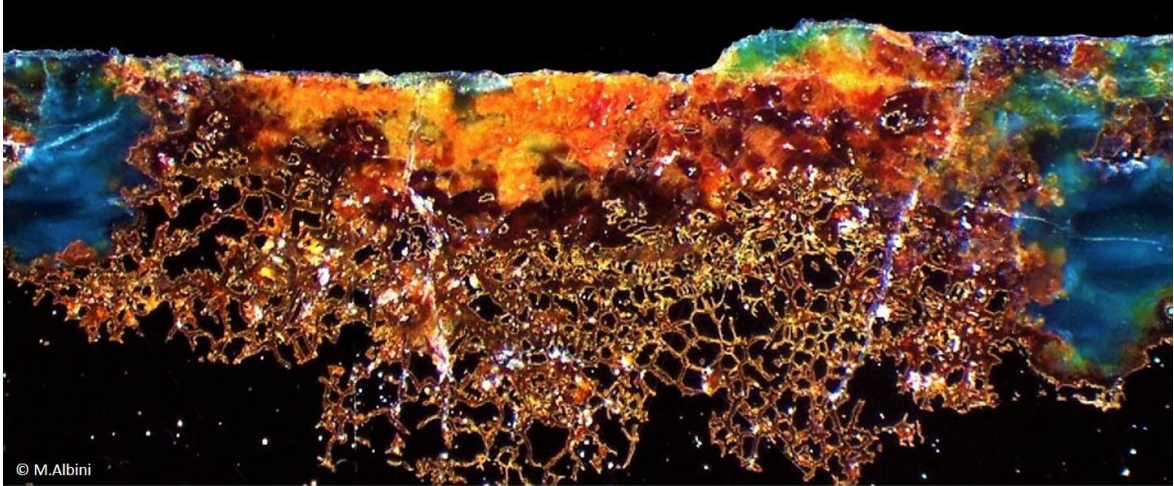
<b>INFLUENCE OF ALLOYING ELEMENTS.....</b>	<b>155</b>
<b>6.1 PRELIMINARY STUDY.....</b>	<b>157</b>
Abstract.....	157
Introduction .....	157
Materials and methods.....	158
Coupons .....	158
Fourier Transform Infrared Spectroscopy .....	160

Colorimetry.....	160
Scanning Electron Microscopy - Energy-Dispersive Spectroscopy (SEM-EDS).....	160
Results and discussion.....	161
Conclusions.....	164
6.2 STATISTICAL ANALYSIS .....	165
Abstract.....	165
Introduction.....	165
Materials and methods.....	165
Coupons.....	165
Treatments.....	166
Natural ageing procedures.....	166
Colorimetry.....	166
Electrochemical impedance spectroscopy (EIS) .....	167
ANOVA test .....	167
Results and discussion.....	172
Alloy's influence on colour .....	172
Alloy influence on electrochemical behaviour.....	172
Conclusions.....	173
REFERENCES.....	174
<b>CHAPTER 7</b>	
<b>FINAL DISCUSSION AND CONCLUSIONS .....</b>	<b>175</b>
REFERENCES.....	182
<b>ANNEX 1 – APPLICATION PROTOCOL OF BIOPATINA.....</b>	<b>183</b>
DESCRIPTION.....	183
PROPERTIES-CHARACTERISTICS:.....	183
ADVANTAGES .....	183
STABILITY .....	183
PROCEDURE .....	183
Phase 1- Preparation of the formulation .....	184
Phase 2- Application .....	184
Phase 3- Stop of the treatment.....	184
RISKS AND TOXICITY .....	184
PACKAGING .....	185
<b>ANNEX 2 – CV AND PUBLICATIONS .....</b>	<b>187</b>
<b>ACKNOWLEDGEMENTS .....</b>	<b>191</b>
<b>FIGURES INDEX.....</b>	<b>193</b>
<b>TABLES INDEX.....</b>	<b>199</b>

# Chapter 1

---

## INTRODUCTION



## 1.1 Basics of corrosion [1]

The definition of corrosion given by the International Organization for Standardization [2] is:

"Physicochemical interaction between a metal and its environment which results in changes in the properties of the metal and which may often lead to impairment of the function of the metal, the environment, or the technical system of which these form a part".

The International Union of Pure and Applied Chemistry (IUPAC) gives a wider definition of corrosion [3], also involving the degradation of non-metals as well as metallic materials:

"Corrosion is an irreversible interfacial reaction of a material (metal, ceramic, polymer) with its environment which results in consumption of the material or in dissolution into the material of a component of the environment. Often, but not necessarily, corrosion results in effects detrimental to the usage of the material considered. Exclusively physical or mechanical processes such as melting or evaporation, abrasion or mechanical fracture are not included in the term corrosion."

What is common to both definitions is that corrosion occurs due to the interaction of a material (e.g. metal) with the environment and that, in general, this interaction lead to its degradation and to a change in its characteristics. What is important for the field of cultural heritage conservation is that corrosion products are often aesthetically pleasant and the formation of such patinas is the reason why a specific metal was originally chosen for artistic production. Thus, not just the metal, but patina itself has an historical and artistic value that need to be considered, as long as the corrosion products do not cause damage to the artefact.

The cause of corrosion is the natural mechanism by which any metal reaches an equilibrium with the surrounding environment in a stable state. A stable state of a metal is, usually, one of its naturally occurring minerals rather than its metallic form and that is the reason for corrosion to occur.

In general, corrosion reactions can be divided in two groups: chemical and electrochemical, and both require the presence of a liquid electrolyte, either as moisture or as a thin water film. Chemical corrosion is due to the reaction of a metal and a corrosive agent involving the local transfer of charges among atoms. Electrochemical corrosion refers to the transfer of charges in different areas of the conductive metal due to an electrochemical potential. This latter mechanism is the most commonly involved in the corrosion of metallic heritage artefacts.

### Corrosion as electrochemical reaction

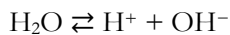
The corrosion process occurs as an oxidation-reduction (redox) reaction: the oxidation part of the reaction refers to the metal that loses electrons while the reduction part refers to the species that gain these electrons. Both reactions simultaneously occur on the metal surface. It is important to note that, despite its name, the term oxidation is not necessarily associated with oxygen.

A chemical reaction involving electron transfer is defined an electrochemical reaction. Since the corrosion process occurs as a redox reaction, it is important to define this reaction electrochemically. The anodic reaction is the one occurring as metal oxidation (anode) (Eq. 1). This reaction produces electrons that pass through the conducting metallic substrate to other sites (cathode) of the metal surface, where the cathodic reaction occurs and the oxidant is reduced (Eq. 2). These electrons can either combine with positive ions such as  $H^+$  or create negative ions.



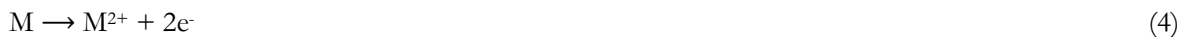
The chemical mechanism of corrosion is regulated by the pH of the water film surrounding the metal.

The acidity or alkalinity of a solution depends of the amount of  $H^+$  (hydrogen) or  $OH^-$  (hydroxyl) ions present. An excess of  $H^+$  will make the solution acidic while an excess of  $OH^-$  will make it alkaline or basic. The other ionic part of an acid or alkali added to water will not influence pH but just other properties of the liquid, such as its conductivity. Water itself dissociates to a small extent to produce equal quantities of  $H^+$  and  $OH^-$  ions displayed in the following equilibrium:



In acidic environments metals react with  $H^+$  ions of the solution producing hydrogen (Eq. 1-3). This means that, compared with neutral water solutions, low-pH acidic water accelerate corrosion by supplying hydrogen ions to the corrosion process.

In neutral solutions, these reactions can be written as:



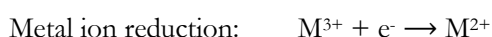
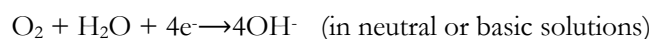
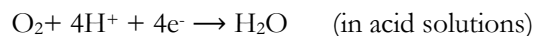
A factor that can increase the hydrogen ion concentration, even in pure water, is the dissolution of carbon dioxide ( $CO_2$ ). Indeed,  $CO_2$  can react with water to form carbonic acid ( $H_2CO_3$ ) and further dissociate in bicarbonate and carbonate ions (Eq. 7-9)



The corrosion of metals can also occur in fresh water, seawater, salt solutions and alkaline or basic media but, in order to become significant, it needs dissolved oxygen. The source of oxygen is generally supplied by the dissolution of the atmospheric oxygen in the water solution.

There are several possible cathodic reactions during the corrosion of metals:

Oxygen reduction:



Oxygen reduction and hydrogen ion reduction are very common cathodic reactions while metal ion reduction and metal deposition are less common but can cause severe corrosion issues.

Many anodic and cathodic reactions can occur during corrosion. Indeed, in corrosion processes of alloys, all metal components can be dissolved as ions in the solution and then be oxidized. In the same way, more than one cathodic reaction can occur at the metal surface which means that, for instance, acid solutions that contain dissolved oxygen or that are exposed to air are generally more corrosive than air-free acids.

It is possible to have an indication about the reactivity of metals in aqueous solution looking at the electrochemical series of standard reduction potentials (Table 1). These series are tables in which oxidants and reductants are ordered based on their oxidising or reducing strength. The more the electrode potential is positive the more the element oxidative power is high, the less it will be oxidized and it will resist to anodic process. Therefore, the more the electrode potential is negative the less will be its oxidative power the easier will be to undergo anodic/oxidation processes.

Half-Reaction	$E^{\circ}_{\text{red}}$
$\text{O}_3(\text{g}) + 2 \text{H}^+ + 2 \text{e}^- \rightleftharpoons \text{O}_2(\text{g}) + \text{H}_2\text{O}$	2.07
$\text{H}_2\text{O}_2 + 2 \text{H}^+ + 2 \text{e}^- \rightleftharpoons 2 \text{H}_2\text{O}$	1.776
$\text{Au}^+ + \text{e}^- \rightleftharpoons \text{Au}$	1.68
$\text{PbO}_2 + 4 \text{H}^+ + 2 \text{e}^- \rightleftharpoons \text{Pb}^{2+} + 2 \text{H}_2\text{O}$	1.467
$\text{Cl}_2(\text{g}) + 2 \text{e}^- \rightleftharpoons 2 \text{Cl}^-$	1.3583
$\text{O}_2 + 4 \text{H}^+ + 4 \text{e}^- \rightleftharpoons 2 \text{H}_2\text{O}$	1.229
$\text{Pt}^{2+} + 2 \text{e}^- \rightleftharpoons \text{Pt}$	1.2
$\text{H}_2\text{O}_2 + 2 \text{e}^- \rightleftharpoons 2 \text{OH}^-$	0.88
$\text{Hg}^{2+} + 2 \text{e}^- \rightleftharpoons \text{Hg}$	0.851
$\text{Ag}^+ + \text{e}^- \rightleftharpoons \text{Ag}$	0.7996
$\text{Hg}_2^{2+} + 2 \text{e}^- \rightleftharpoons \text{Hg}$	0.7961
$\text{Cu}^+ + \text{e}^- \rightleftharpoons \text{Cu}$	0.522
$\text{O}_2 + 2 \text{H}_2\text{O} + 4 \text{e}^- \rightleftharpoons 4 \text{OH}^-$	0.401
$\text{Cu}^{2+} + 2 \text{e}^- \rightleftharpoons \text{Cu}$	0.3402
$2 \text{H}^+ + 2 \text{e}^- \rightleftharpoons \text{H}_2$	0.0000...
$\text{Fe}^{3+} + 3 \text{e}^- \rightleftharpoons \text{Fe}$	-0.036
$\text{Pb}^{2+} + 2 \text{e}^- \rightleftharpoons \text{Pb}$	-0.1263
$\text{Sn}^{2+} + 2 \text{e}^- \rightleftharpoons \text{Sn}$	-0.1364
$\text{Ni}^{2+} + 2 \text{e}^- \rightleftharpoons \text{Ni}$	-0.23
$\text{Co}^{2+} + 2 \text{e}^- \rightleftharpoons \text{Co}$	-0.28
$\text{Fe}^{2+} + 2 \text{e}^- \rightleftharpoons \text{Fe}$	-0.409
$\text{Cr}^{3+} + 3 \text{e}^- \rightleftharpoons \text{Cr}$	-0.74
$\text{Zn}^{2+} + 2 \text{e}^- \rightleftharpoons \text{Zn}$	-0.7628
$\text{Mn}^{2+} + 2 \text{e}^- \rightleftharpoons \text{Mn}$	-1.04
$\text{Al}^{3+} + 3 \text{e}^- \rightleftharpoons \text{Al}$	-1.706
$\text{Mg}^{2+} + 2 \text{e}^- \rightleftharpoons \text{Mg}$	-2.375
$\text{Na}^+ + \text{e}^- \rightleftharpoons \text{Na}$	-2.7109
$\text{K}^+ + \text{e}^- \rightleftharpoons \text{K}$	-2.924

Table 1. Standard reduction potentials ( $E^{\circ}_{\text{red}}$ ) by decreasing order [1]

In the upper part of the table there are, thus, non-reactive metals and in the lower part the more reactive ones.

### Corrosion thermodynamic – Pourbaix diagrams

The corrosion of a metal in contact with an electrolyte deeply depends on the environment pH and on its oxidizing or reducing power. Generally, a metal can exhibit three different behaviours: inert, active or passive.

A metal is inert when it does not react with the environment ( $\Delta G = 0$ ). In this case corrosion mechanisms do not occur. When, instead, a metal has an active behaviour it reacts with the environment, corrosion

mechanisms occur, and the resulting corrosion products are soluble. On the contrary, when the metal is passivated corrosion mechanisms forms corrosion products that are insoluble.

A useful tool to predict in which condition a metal is inert, active or passive is given by potential-pH diagrams, commonly called Pourbaix diagrams [4]. The pH represents the acidity or alkalinity of the electrolyte while the potential represents its oxidative power. Thanks to these diagrams it is possible to foresee if corrosion can occur and to estimate the composition of the corrosion products (Figure 1).

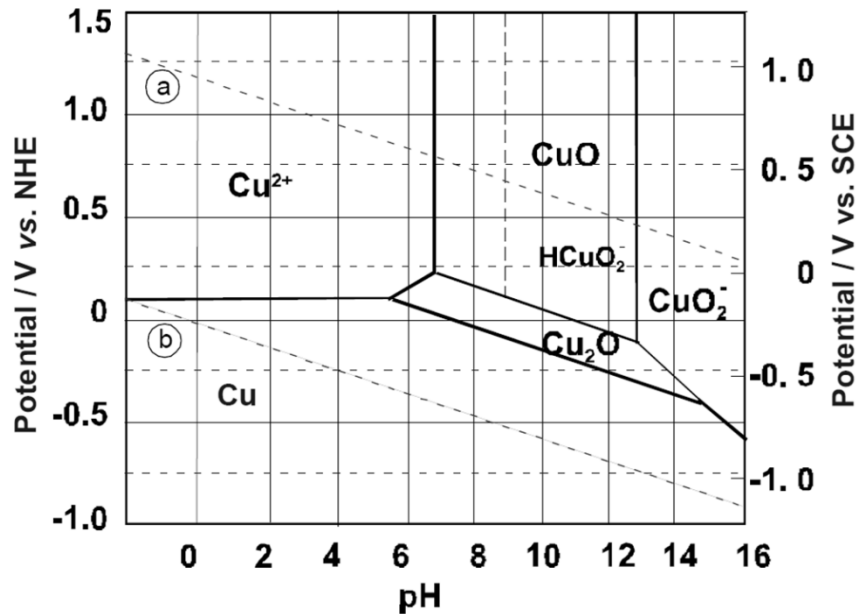
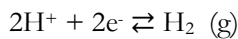


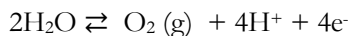
Figure 1. Potential – pH diagram of Cu in aqueous medium ( $10^{-6} \text{ mol} \cdot \text{dm}^{-3}$ ) [5]

Two diagonal lines are traced on Pourbaix diagrams. The first one (a), that start at a potential of zero, represent the following equilibrium:



Below this line there will be the production of hydrogen. In the case of copper (Cu) diagram, this line is located in the stability area of the metal which means that, in pure aqueous medium, there is no corrosion.

The second line (b) represents the following equilibrium:



Above this line there will be the oxidation of water and production of oxygen while below this line there will be the reduction of the dissolved oxygen in the electrolyte. Therefore, the dissolution of Cu will occur in aqueous medium with dissolved oxygen in the solution at acidic or at severely basic pH. The passivation zone is represented from the stability areas of  $\text{Cu}_2\text{O}$ ,  $\text{HCuO}_2$  and  $\text{CuO}$ .

### Corrosion rate

The limit of Pourbaix diagrams is to foresee only whether or not corrosion will occur without any information about the kinetics of the reaction. The rate of corrosion is defined as the mass loss per area unit over time:

$$CR = \frac{\Delta m}{A * t}$$

If the mass loss is constant over time it means that soluble corrosion products are formed due to the interaction with the environment and that these products are washed away from the surface. In the case of a decreasing mass loss, there is a passivation process occurring with the formation of insoluble and adherent corrosion products that protect the surface from further corrosion. If a damage of the passivation layer occurs the corrosion will start again causing an increase of the corrosion rate.

The corrosion rate is also generally used to define the corrosivity of a certain environment. Indeed, the higher is the corrosion rate the more the environment is corrosive. This evaluation is traditionally made by exposing standard coupons and measuring the mass loss over time. Indeed, the norm ISO 9226 defined the classification of outdoor atmospheric corrosivity based on mass loss of standard specimens of carbon steel, zinc, copper and aluminium exposed for one year.

Another definition of corrosion rate in terms of the corrosion current density ( $i_{corr}$ ) is calculated as:

$$CR = \frac{i_{corr} * a}{n * F}$$

where  $a$  is the atomic mass,  $n$  is the valence change and  $F$  is the Faraday's constant. The corrosion current density can be defined by electrochemical measurements such as polarization techniques or electrochemical impedance spectroscopy measurements. These measurements are particularly suitable to evaluate the protectiveness of a surface against corrosion defining the corrosion rate of metal in defined conditions.

In order to understand and evaluate corrosion processes occurring on metallic artefacts it is, thus, important to consider both the thermodynamic aspects, that are usually defined by the chemical species present in the environment, and the rate of corrosion, that define how and at what rate these species corrode the metal.

## 1.2 Corrosion of copper and bronze

Copper is an essential element of our lives. Human beings used this metal since millennia because of its numerous characteristics. Indeed, copper is a good conductor of heat and electricity. Therefore, it is possible to find this element in electrical conductors and superconductors, in cookware and heat exchangers. It also has good machinability that explains its use for the production of pipes and architectural features. But the most relevant characteristics for this study are its good resistance to corrosion and the pleasantness of its patina. These latter features made copper and its alloys the widest metals used for the production of sculptures, ornaments, monumental buildings and, in general, for artistic creations.

Since 6000 B.C. the use of copper spread among Middle-Eastern and European populations. At first, it was mainly employed in its native form for manufacturing small ornaments coexisting with the use of stone, this latter remaining the primary resource for tools and weapons production. Then, between 4000 and 3000 BC, the invention of melting was made. It was discovered that, throughout heating process of copper minerals (ores), metallic copper could be produced. Once developed, this extraction technique allowed the extensive use of copper without needing of its native form. The breakthrough happened around 3300 BC with the manufacturing of bronze that gave its name to a prehistoric period, the Bronze Age. It was discovered that the combination of two different metals made a resulting alloy with better features than the one of each single element. The discovery of bronze was probably accidental but very soon ancient metallurgists were able to intentionally extract copper and tin from ores and combine them together to produce bronze alloy. Bronze characteristics are extremely superior to those of copper and tin: it is significantly harder and has a superior tensile strength, which makes it perfect for the production of tools, weapons and armours; it also has a good cold machinability and a lower melting point than its constitutive elements and it has a good corrosion resistance. It was employed to produce measure weights, water pipes, roofs, vessels, polished mirrors, razors and for artistic decorations like jewellery and sculptures. The use of bronze was continuous and widespread until the Iron Age, between around 1200 and 600 BC, when iron became dominant for tools production. However, the use of copper alloys over the centuries continued for other applications, such as coinage and bell production, and bronze remained the preferred alloy for the use in statuary.

The term “bronze” is used to describe a multitude of copper alloys. The first known copper alloy was with arsenic (arsenical bronze) and its production was probably fortuitous. In fact, copper minerals at their natural form contain a certain amount of arsenic impurities and possibly during melt operations this element was incorporated in the cast. The “pure” bronze is defined as an alloy of copper (90%) and tin (10%) but it is possible to have the addition of other metals such as lead, zinc, aluminium, manganese and nickel in different amount depending on the final use of the cast and on the production period. For instance, the alloy for statuary production changed over the century, passing from a binary alloy of copper and tin during the Bronze Age to arrive to a ternary (copper, tin and lead) alloy during the classical age and quaternary (copper, tin, lead and zinc) alloy in contemporary sculptures. The proportion between the elements contributes to different properties of the cast.

The production of bronze artefacts has deep roots in history and that is why it is possible to find them in several sites. Particularly, sculptures and architectural elements embellish many outdoor locations while archaeological findings bring to light ancient artworks after long-term burial. The surrounding atmosphere in all these environments interact with the metal resulting in corrosion of the bulk and possible loss of shape and can lead, in severe conditions, to the complete loss of the artefact. The corrosion of copper and bronze is closely related to the surrounding atmosphere and a brief description of the corrosion mechanisms occurring to outdoor sculptures and archaeological objects is given below.

## Corrosion of outdoor monuments

Outdoor artefacts undergo atmospheric corrosion, which is caused by the interaction of the metallic substrate with the surrounding environment. Traditionally, outdoor environments have been classified into four basic types:

*Urban and Industrial:* both are characterized by the presence of two main classes of pollutants, sulphur compounds such as sulphur dioxide ( $\text{SO}_2$ ) and nitrogen oxides ( $\text{NO}_x$ ). In presence of moisture and oxygen they generate sulfuric and nitric acid that are the major cause of acid rain. The additional presence of dew and fog results in the formation of an acid film on exposed surfaces that enhance corrosion. Furthermore, the presence of other corrosive pollutants, such as chlorides, may lead to more active corrosion.

*Marine:* this atmosphere is characterized by the presence of salt crystals deposited on the exposed surfaces. The amount of the crystals can vary depending on the weather conditions and can result in extreme corrosion. Indeed, the high presence of chlorides made this environment highly corrosive, in particular if there is the co-presence of urban or industrial pollutants. The harshest condition is represented from the areas where sea splashing and heavy sea spray are present. This condition increases the presence of salts and adds the detrimental corrosive effect of wet and dry cycles on the exposed surfaces.

*Rural:* rural environments do not contain strong chemical contaminants and are the mildest atmospheres resulting in slow corrosion rate.

As just mentioned, the most important atmospheric compounds that can affect the corrosion of copper-based alloys are:

- Moisture;
- gaseous molecules: oxygen ( $\text{O}_2$ ), sulphur dioxide ( $\text{SO}_2$ ); nitrogen dioxide ( $\text{NO}_2$ ), hydrogen chloride ( $\text{HCl}$ ), hydrogen sulphide ( $\text{H}_2\text{S}$ ), carbon dioxide ( $\text{CO}_2$ ), ammonia ( $\text{NH}_3$ ), nitric acid ( $\text{HNO}_3$ ), ozone ( $\text{O}_3$ ), hydrogen peroxide ( $\text{H}_2\text{O}_2$ ) and formaldehyde ( $\text{HCHO}$ );
- particulate matter: sodium chloride ( $\text{NaCl}$ ), ammonium sulphates ( $(\text{NH}_4)_2\text{SO}_4$ ,  $\text{NH}_4\text{HSO}_4$ ), ammonium chloride ( $\text{NH}_4\text{Cl}$ ) and sodium sulphate ( $\text{Na}_2\text{SO}_4$ ).

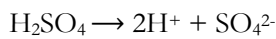
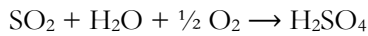
All these compounds can affect the corrosion mechanisms but their synergy appeared to be much more relevant for the corrosion rate. In particular, the combined effect of  $\text{SO}_2$ ,  $\text{NO}_2$ ,  $\text{O}_3$ , moisture and particulate matter, such as  $\text{NaCl}$ , may be highly aggressive[6].

Moisture is the most important element for atmospheric corrosion and its presence or absence can be significant to understand outdoor corrosion. Indeed, the highest the moisture content in the atmosphere, the highest the corrosion effects on metallic surfaces. On the contrary, in absence of moisture little or no corrosion effects will be observed, even in highly polluted atmospheres. The presence of moisture can occur in form of rain, dew or high relative humidity (RH). The RH present in the atmosphere, as well as dew, can form a thin water layer on copper-based surfaces. It is worth mentioning that all the potentially-corrosive gases are water soluble as well as a part of atmospheric particulates. Therefore, the water layer present on the metal acts as a solvent enhancing the corrosion processes. Frequent rain washing can, instead, contribute to dilute and wash away surface contamination. It is particularly important to know the time during which a corrosion-stimulating liquid film exists on the surface, the so-called Time of Wetness (TOW). Indeed, the chemical reactions endangering the metal substrate occur inside the liquid layer while the surface is wet. Hence, the longer the TOW, the harsher corrosion will occur [7]. TOW is an estimated parameter based on the length of time when the relative humidity is greater than 80% at a temperature greater than  $0^\circ\text{C}$  and can be expressed as the hours or days per year

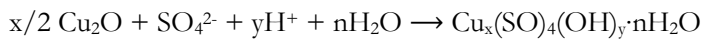
or the annual percentage of time. Also, the wetting and drying cycles occur at the metal surface changing the pH of the water layer from neutral or slightly acidic in high liquid layer thickness to highly acidic in low liquid layer thickness [8].

Gaseous molecules have great importance in the corrosion of copper and bronze outdoor artefacts. Indeed, the first corrosion product that is formed is a passivating dark-red to orange red layer of cuprous oxide (*cuprite*,  $\text{Cu}_2\text{O}$ ) due to the interaction between copper and oxygen [9]. This layer is formed within seconds after the exposure to the environment which means that copper alloys start corroding from the moment of their production. Cuprite continues to grow during the entire artefact lifetime and it was found that, on an average, it represents half of the total patina mass of copper corrosion products, regardless the composition of the exposure environment [10]. A less abundant copper oxide is the dull black *tenorite* ( $\text{CuO}$ ).

In polluted atmospheres, harmful compounds are those containing sulphur, particularly sulphur dioxide. In presence of moisture and oxygen, sulphur dioxide is oxidized into sulphuric acid that dissociate in water forming sulphate ions:



Thereafter, cuprous oxide reacts with sulphate ions forming basic copper hydroxysulphates:



Basic copper hydroxysulphates are the main copper corrosion products identified in urban and industrial environments. Based on their composition they are classified as [10, 11]:

*Posniakite* ( $\text{Cu}_4(\text{SO})_4(\text{OH})_6 \cdot \text{H}_2\text{O}$ ): Blue to dark blue. It is the hydrated form of brochantite and its precursor. Mainly found in unsheltered conditions.

*Brochantite* ( $\text{Cu}_4(\text{SO})_4(\text{OH})_6$ ): Green-bleu. It is nearly always the most common component of the green patina formed on copper after long atmospheric exposure. It can be found in both sheltered and unsheltered conditions

*Antlerite* ( $\text{Cu}_3(\text{SO})_4(\text{OH})_4$ ): Deep green. It is stable in more acidic conditions than brochantite. Some evidence showed that antlerite may form at earlier stages of the patination process than brochantite. It is suggested that acid rain is converting brochantite to less protective antlerite, which is more susceptible to erosion. Mainly found in sheltered conditions.

The stability conditions for each compound are indicated in the Pourbaix diagram specific for the system  $\text{Cu} - \text{SO}_4 - \text{H}_2\text{O}$  (Figure 2).

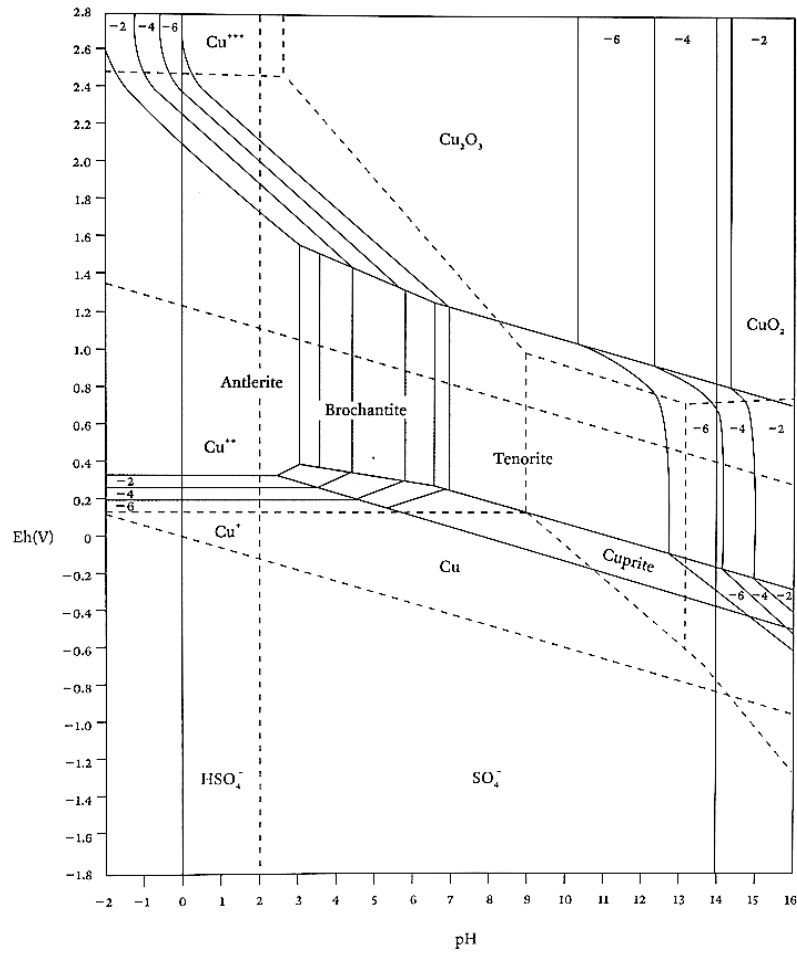
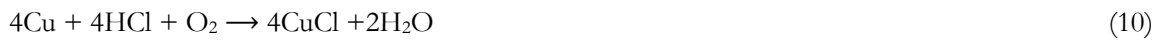
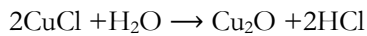


Figure 2. Pourbaix diagram for the system Cu – SO<sub>4</sub> – H<sub>2</sub>O at 20°C with 46 ppm of SO<sub>4</sub> [12]

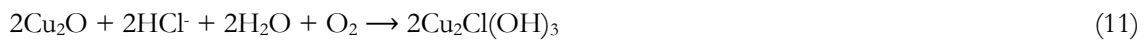
Another group of pollutants that is, as a matter of fact, the most harmful for copper-based artefacts is the one of chlorine-containing species. Chloride ions are predominant in marine environments and in presence of moisture and oxygen can form hydrochloric acid that react with copper ions to form nantokite (CuCl) [13, 14].



Thereafter, the hydrolysis of nantokite can occur and form again hydrochloric acid and also cuprite.



At this point the chemical pathway can follow two directions: hydrochloric acid can react either with copper and form again nantokite (Eq. 10) or with cuprous oxide forming copper hydroxychlorides (Eq 11), generating a cycling reaction.



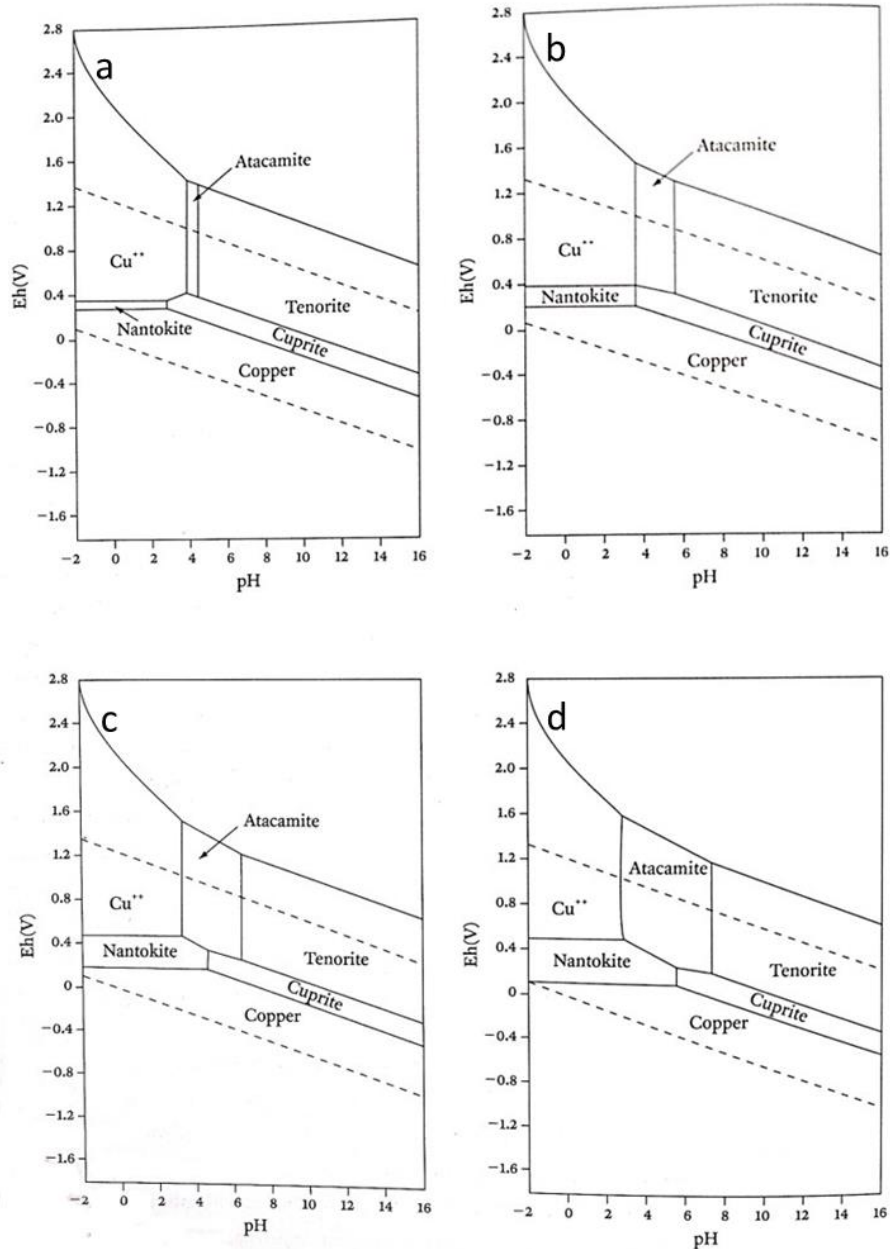


Figure 3. Pourbaix diagram for the system Cu – Cl – H<sub>2</sub>O at 20°C at chlorine concentration of 35 ppm (a), 350 ppm (b), 3550 ppm and 35500 ppm (d) [12]

The most common copper chlorides corrosion products are [10, 11, 14]:

*Nantokite* (CuCl): From grey to pale green. It is the precursor of atacamite, paratacamite and botallackite. It is usually found at the interface between the metallic bulk and the cuprite.

*Atacamite* (Cu<sub>2</sub>Cl(OH)<sub>3</sub>): Powdery, green to yellow-green. It is soluble in weak acid. Usually is present in same amount or more abundant than brochantite in marine atmosphere. It is not found on specimens exposed for short periods. Mostly detected in sheltered areas.

*Paratacamite* or *clinoatacamite* (Cu<sub>2</sub>Cl(OH)<sub>3</sub>): Powdery, dark green to greenish black. It is an isomeric compound of atacamite. The uncertainty in the name is due to the identification of its crystalline form



- the consumption of copper ions or copper species by the external environment (rainfall). In this case the deposit is not stable, porous, not adherent and formed by both copper and tin corrosion products. The deposit is not protective and after the removal of this layer by rainfall new copper species will be dissolved from the alloy and washed away. This is a cyclic mechanism of corrosion promoted by the rainfall that bring to the complete dissolution of the alloy.

These two mechanisms describe the corrosion of bronze alloys and reported tin corrosion products as component of the patina but they were still not complete. Alloy elements, such as tin, lead and zinc, have an important role in bronze corrosion processes. In particular, copper and tin corrosion products can both activate and passivate bronze corrosion processes [18-20]. Furthermore, the surface exposure to rainfall is of great importance to understand corrosion thermodynamic and kinetic. Indeed, two main surface categories can be distinguished: exposed to rainfall (unsheltered areas) and protected from direct rainfall (sheltered areas). The first ones generally are made of pale green corrosion products (mainly brochantite and rarely antlerite) that surround small black islands [21]. Elemental analyses revealed that these compounds have a high elemental tin concentration. Sheltered areas are made of green deposits (brochantite and rarely antlerite) and/or opaque black crusts that contains atmospheric particles. These areas have very low elemental tin content. According with the kind of surface, two different corrosion pathways can be envisaged [21]. The first two steps are shared and consist in:

1. the selective dissolution of copper with the contemporary formation of tin oxide. Tin oxide is usually stable over a large pH range and remain in the inner part of the corrosion layer while copper corrosion products, as copper oxides, can be found on top of it
2. the increase of the copper patina thickness according with the local atmosphere composition. This step is controlled by the diffusion of copper ions from the bulk to the outer patina layer.

The third step is the one mainly influenced by the surface exposure conditions. In unsheltered areas, the deposit of corrosion products is washed away and the surface is susceptible to further corrosion. The corrosion process is cyclic and related to precipitation frequency.

From the rain-exposed surfaces soluble copper compounds are leached. The deposit described in the second step is progressively destroyed. Therefore, the artefact surface undergo again the first step of the corrosion process (i.e. selective dissolution of copper and internal oxidation of tin of the first step). The corrosion proceeds from a cyclic mechanism that is strongly correlated with the precipitation frequency. Some studies investigated the nature of pale green patinas from unsheltered areas of outdoor quaternary bronze monuments [22-24]. They revealed that the dissolution process in unsheltered areas depended to repetitive pH drop due to the rainfall that destabilises the patina. Furthermore, the corrosion processes are related to the selective dissolution of copper, zinc and lead and to the surface enrichment in stable, poorly crystallised tin species in the form of  $\text{SnOx}(\text{OH})_y$ . The amount of dissolved copper and zinc is proportional to their concentration in the alloy, independently of the tin content. Nevertheless, with respect to Cu, a preferential corrosion of Zn and Pb occur. Also, it appeared that the instability of the patinas that underwent to acid rain precipitation is more probably related to the loss of properties of tin species and their dissolution rather than to the transformation of copper compounds. Indeed, in such acidic conditions they are unable to act as a stabilising structural agent.

In sheltered areas, the corrosion follows a different mechanism. In stagnant rain condition, the surface is periodically subjected to wetting, stagnation and evaporation of wet deposition, with a consequent change in pH. The outcome of a research on atmospheric corrosion of quaternary bronze in stagnant rain water [25] revealed that the oxidation of bronze is governed by diffusion through a porous layer that is formed at the beginning of exposure and grows during time. The patina consists in two layers: an external layer mainly formed by copper and lead corrosion products and an inner layer enriched in tin and difficult to detect by surface analyses. In this kind of surface exposure tin compounds are not

dissolved and remain as passivation layer at the interface with the alloy. It seems that Pb corroded preferentially probably because of its solid immiscibility in the copper matrix that create globules which act as sacrificial anodes. In this condition, the amount of Cu and Pb remaining in the patina are higher than in unsheltered areas while Zn dissolved in the environment regardless the exposure conditions.

To summarise, the atmospheric corrosion of bronze and copper alloys is related to several factors. Indeed, it is closely related to the type of exposure environments (urban, industrial, marine or rural), which are influenced from content of moisture and pollutants. Also, it depends from the bronze composition in terms of alloying elements and from its surface exposure to rain precipitation. It is thus important to consider all these variables when approaching an outdoor artefact for a conservation-restoration intervention

### **Corrosion of archaeological artefacts**

Archaeological artefacts undergo important corrosion processes during their period of burial. Therefore, the properties of the soil have an important role in the understanding of corrosion mechanisms.

Soil is an aggregate of minerals, organic matter, water, and gases (mostly air). Different types of soils have different proportions of these components. In particular, the texture of a soil depends on the distribution and size of mineral particles. For example, soils with a high proportion of sand have very limited storage capacity for water, whereas clays are excellent in retaining water. The properties of the soil also vary as function of depth.

The corrosion rates in buried environment are usually influenced by soil properties such as water content, degree of aeration, pH, resistivity, soluble ionic species (salts) and microbiological activity [1].

As for outdoor environment, corrosion can evolve in buried environment only if there is the presence of an electrolyte, in this case water. Water movement in soil can occur by gravity, capillarity, osmotic pressure (from dissolved species), and/or electrostatic interaction with soil particles. The water-holding capacity of a soil is strongly dependent on its texture. Coarse sands retain very little water, while fine clay soils store water to a high degree.

Also, oxygen, as previously mentioned, is important for corrosion mechanisms. In coarse and dry soils the transport of oxygen is more rapid than in fine, waterlogged textures. Excavation can increase the degree of aeration in soil and usually the corrosion rate in undisturbed soil is lower than in disturbed, highly oxygenated soil. Oxygen concentration decreases with depth making the conditions anoxic and corrosion difficult to occur. However, the presence of anaerobic microbes such as sulphate-reducing bacteria (SRB) can lead to high corrosion rate. The degree of aeration in soil is indicated with the redox potential. A high redox potential indicates a high oxygen level.

In soil pH usually varies between 5 and 8. In this range its effect is not dominant on corrosion mechanisms but some factors as mineral leaching, decomposition of acidic plants, industrial wastes and acid rain can have a great effect on the corrosion rate. On the contrary, alkaline soils with high contents of sodium, potassium, magnesium and calcium, form protective deposits on buried artefacts.

The corrosivity of a soil can be indicated by its resistivity. High soil resistivity usually slows down corrosion reactions since ionic current flow is associated with corrosion. The increases of water content and of the concentration of ionic species usually reduce the resistivity of the soil. Nevertheless, a high soil resistivity alone does not guarantee the occurring of corrosion processes.

The burial condition of bronze artefacts is usually of the order of hundreds of years, much longer than when artefacts are exposed outdoor. Therefore, even if the main parameters that influence the corrosion processes are the same, the extent of the corrosion processes and the products formed differ. Several studies were made in order to model the corrosion rate of buried copper-alloys but resulted to be

inadequate for such long burial periods. Nevertheless, in 1998, Robbiola proposed a convincing phenomenological model of bronze (Cu-Sn alloy) corrosion based on several observations reported for archaeological objects [26]. The model was divided in three main corrosion steps:

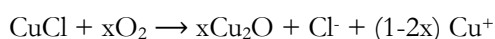
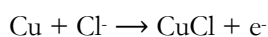
- Phase 1: an initial fast step of alloy dissolution which leads to the formation of a surface corrosion layer
- Phase 2: a propagation step controlled by migration of ionic species through the deposits from the alloy to the soil and vice versa. During this phase the corrosion rate decreases with time down to values close to zero reaching a steady phase.
- Phase 3: possible corrosion resumptions during ageing of the previously formed structures

The first two phases are much shorter than the third one since the reaching of the steady face is rapid compared to the total burial time.

The structures of the corrosion layers were also analysed and divided into two main types (Type I and Type II). Depending on the structure type the resulting corrosion products of each phase differed.

In Type I structures, also defined as “even surfaces” or “passive layers”, the first phase consists in the alloy oxidation with the formation of an inner amorphous tin oxides layer associated to copper oxidation ( $\text{Cu}_2\text{O}$ ) and also to copper dissolution. The copper portion dissolved in the environment can reprecipitate onto the surface as cupric compounds, hydroxycarbonates, hydroxychlorides, or others copper minerals depending on the ion species present in soil. This precipitation usually forms a porous outer layer. Therefore, during the first phase of the Type I structure there is the formation of a passive layer enriched with tin compounds and the tin-soil interface corresponds to the original object surface. Phase 2 corresponds to the growth of the corrosion layer through the previously formed passive deposit until steady state is reached. Deviations of the Type I basic model have been observed probably due to the ageing of the corrosion layers occurring in phase 3. Indeed, during phase 3 chemical modifications can occur inside the corrosion layers due to the evolution of the archaeological soil over time. Cracks can also occur inside the corrosion layers with the increase of the localized corrosion rate due to the rupture of the passivating layer. The colour of the patina in Type I structures is not related to the tin content in the alloy but mostly to the nature and amount of soil elements. Furthermore, since no soil elements such as Si, P or Cl are contained in the inner tin-enriched layer, the formation of the outer layer is probably a secondary step. An important feature of this corrosion structure is that it well preserves the original surface of the artefact as well as the inner metallurgical structure, presenting “ghost” sulphides or grain boundaries originally present in the alloy.

In Type II structures, also defined as “coarse surfaces”, the formation of stabilizing tin oxides is not observed because of the severe initial alloy dissolution that leads to a strong local enrichment in copper cations. This is due to the aggressiveness of the environment or to the presence of heterogeneities in the alloy, in the environment or in the geometry of the artefact. The external patina is rich in copper corrosion products, such as  $\text{Cu}_2\text{O}$  and green cupric compounds and the formation of these compounds results in a porous barrier layer which limits alloy dissolution in a second step. During this phase, also tin compounds are formed in the internal layer mixed with cuprous oxide. Nevertheless, in the inner layer there is usually also the presence of some chlorides. Their accumulation in this layer is an autocatalytic process, similar to bronze disease and that follows the reported reactions:



In phase two the kinetic of the corrosion process is thus controlled by the migration of negative species from the soil, mainly oxygen and chloride ions, which lead to the formation of the orange to brown inner layer enriched in tin and chlorine underneath the red cuprous oxide layer. As for Type I, the phase 3 of Type II structures corresponds to the ageing of the corrosion layer, such as the transformation of cuprite into malachite, or the rupture of the corrosion layers.

These models allowed to explain a great number of observations reported in the literature for bronzes dating from many periods and excavated from very different environments.

As just mentioned, the corrosion products common to all artefacts are cuprite and tin oxides. These corrosion products are usually covered by other copper minerals according with the ion species present in soil, such as  $\text{HCO}_3^-$ ,  $\text{SO}_4^{2-}$ ,  $\text{Cl}^-$  and  $\text{H}_2\text{PO}_4^-$ . Nevertheless, basic copper carbonates and copper chlorides are the most abundant.

Copper chloride minerals founded on archaeological objects are the same ones found on outdoor monuments (nantokite, atacamite, paratacamite and botallackite) and their description and formation mechanism had been previously discussed.

Two important basic copper carbonates are commonly found as corrosion products [12]:

*Malachite* ( $\text{CuCO}_3 \cdot \text{Cu}(\text{OH})_2$ ): it forms a compact, stable, green patina on top of the cuprite layer. It is one of the most common patina formed in almost every burial environment. As mineral it is an important copper ore and was used in ancient world to extract pure copper.

*Azurite* ( $2\text{CuCO}_3 \cdot \text{Cu}(\text{OH})_2$ ): deep blue copper mineral usually associated with malachite and cuprite. Less common as corrosion product compared with malachite due to the specific thermodynamic conditions needed for its formation.

Both minerals can be formed by the action of water charged with carbon dioxide. Azurite, as less stable than malachite, can be converted to it in presence of moisture due to loss of carbon dioxide. This transformation is promoted by an increase of temperature at alkaline pH. The Pourbaix diagrams for the system copper-water- carbon dioxide illustrate the formation of both species (Figure 5). The presence of azurite is reported only above  $\text{CO}_2$  concentration of 4400 ppm while malachite is formed already at 44 ppm. The increase of carbon dioxide content results in the stabilization of malachite over tenorite and cuprite at high pH values. As the amount of carbon dioxide increases, azurite becomes the stable product instead of malachite.

To summarise, in Figure 6 the main corrosion products formed on outdoor monuments and on archaeological objects are showed.

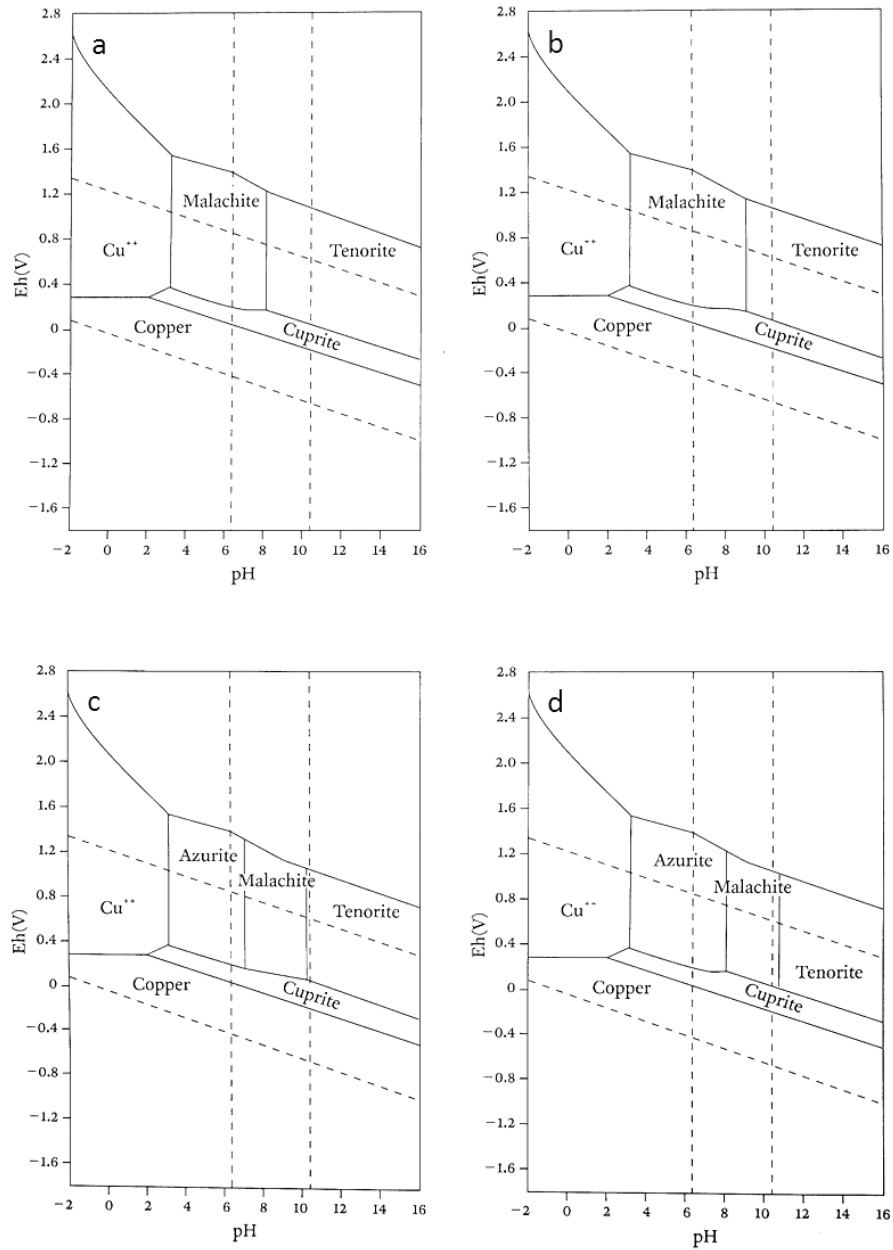


Figure 5. Pourbaix diagram for the system  $\text{Cu} - \text{CO}_2 - \text{H}_2\text{O}$  at  $20^\circ\text{C}$  at carbon dioxide concentrations of 44 ppm (a), 440 ppm (b), 4400 ppm and 44000 ppm (d) [12]














<b>Cu Chlorides</b>	$\text{CuCl}$	$\text{Cu}_2\text{Cl}(\text{OH})_3$	$\text{Cu}_2\text{Cl}(\text{OH})_3$	$\text{Cu}_2\text{Cl}(\text{OH})_3$
				
	<i>Nantokite</i>	<i>Atacamite</i>	<i>Paratacamite</i>	<i>Botallackite</i>
<b>Cu Sulphates</b>	$\text{Cu}_4(\text{SO})_4(\text{OH})_6 \cdot \text{H}_2\text{O}$	$\text{Cu}_4(\text{SO})_4(\text{OH})_6$	$\text{Cu}_3(\text{SO})_4(\text{OH})_4$	
				
	<i>Posniakite</i>	<i>Brochantite</i>	<i>Antlerite</i>	
<b>Cu Carbonates</b>	$\text{CuCO}_3 \cdot \text{Cu}(\text{OH})_2$	$2\text{CuCO}_3 \cdot \text{Cu}(\text{OH})_2$		
				
<i>Malachite</i>	<i>Azurite</i>			
<b>Cu Oxides</b>	$\text{Cu}_2\text{O}$	$\text{CuO}$		
				
<i>Cuprite</i>	<i>Tenorite</i>			
<b>Cu Nitrates</b>	$\text{Cu}_2(\text{NO})_3(\text{OH})_3$			
				
<i>Gerhardtite</i>				
<b>Sn Oxide</b>	$\text{SnO}_2$			
				
<i>Cassiterite</i>				

Figure 6. Main copper and tin minerals found on corroded bronze artefacts

### 1.3 Current treatments [27]

Corrosion can lead to serious damages of metallic artefacts. Therefore, conservation treatments are required in order to preserve the artistic and historic values of the objects. Indeed, the research for appropriate protective systems began in the ancient world, when natural waxes, oils and resins were used to protect copper alloys from corrosion. Nowadays, different strategies are applied in order to avoid or, at least, to decrease corrosion mechanisms. It is possible either to isolate the metal from the aggressive environment using coating systems or to try to decrease the corrosion rate modifying the metal reactivity to the environment using corrosion inhibitors. Nevertheless, these materials are usually developed for industrial purposes and often cannot be used on heritage metals without careful evaluation. Indeed, in order to be applied on cultural heritage, conservation products need to fulfil several requirements [28, 29]:

- none or minimal aesthetical impact
- reversibility, or at least retreatability
- long-term and predictive performance
- easy application
- non-toxicity

Moreover, most of the time conservation treatments are required to have high performance on porous, uneven, fragile and chemically unstable metal surfaces while industrial coatings are usually applied on bare polished metals. The removal of “historical” patinas is ethically not well perceived by the conservation community unless their nature is detrimental for the object or the “original” object surface and its details need to be revealed. Therefore, conservation products need to be developed also considering the patinas features.

The most used coating systems and inhibitors for copper and its alloys conservation are here presented with the addition of new approaches recently developed.

#### Coatings

Conservation coatings act as physical barriers in order to avoid the direct contact of gas, moisture and particulates with the artefacts’ surface, offering a conservation strategy when pollution cannot be avoided. They are extensively use in conservation practice but, due to the nature of the treated surfaces, their application often results in a large number of imperfections. Furthermore, due to lack of standardized application protocols, it is difficult to identify the best coating for each environmental context. In order to better perform, coatings need surface preparation such as the removal of soluble corrosion products and pollutants by cleaning. They can be used alone or in combination with other products. Brostoff and de la Rie [30] proposed a multi-layer system made of primer, main coat and top coat. The primer enhances the adhesion of the main coat to the surface, the main coat provides the protection from the environment and the top coat is used as a sacrificial layer.

According with their chemical nature, coatings can be divided in acrylic coatings, waxes and silanes.

#### *Acrylic coating*

One of the most used acrylic coating for general purposes in conservation practice is Paraloid B72™ [31], made of a methyl methacrylate and ethyl acrylate copolymer. It is considered reversible even after

long time and it can be applied not just as coating but also as consolidant and adhesive, explaining it extensively used in conservation practice, particularly for archaeological objects. Nevertheless, after long-term exposure it results to fail at object edges resulting in filiform corrosion that makes its application problematic on objects with multiple and thin edges.

Another extensively used acrylic coating is Incralac™ which is made of Paraloid B44™ (ethyl methacrylate and butyl acrylate copolymer), benzotriazole (BTA) as UV absorber and epoxidized soybean oil as levelling agent [12]. Incralac™ is used both for archaeological and outdoor artefacts but its use change the aesthetical appearance of the objects, darkening the surface. The protective efficiency of this treatment resulted to be satisfying for fresh applications but after natural ageing it resulted in poor protectiveness, giving the same electrochemical results as untreated surfaces [32]. Poor long-term performance was also point out in a 10-years aged treatment [12]. In fact, it was highly insoluble and completely cracked. Usually, before Incralac™ treatment, the surface is prepared applying corrosion inhibitors as benzotriazole. Nevertheless, for outdoor usage, Incralac™ results in poor performance in terms of protection, low maintenance and reversibility. Despite that it is still used for outdoor applications while for archaeological objects its use decreased in favour of Paraloid B72™ [31].

### *Waxes*

On outdoor monuments, microcrystalline waxes are currently used in order to coat and smooth the corroded surfaces. Nevertheless, waxes are also used on ethnographic metals [33]. The most common commercial waxes are Cosmoloid 80H™ and Renaissance™. Compared to acrylic coatings, waxes are considered a better option for the protection of outdoor bronzes but they are also often used as topcoat for underlying acrylic layer. Indeed, a multilayer system can have an enhanced protection because of the synergy between a corrosion inhibitor used as primer, usually BTA, a central acrylic layer, mainly Incralac™, and a microcrystalline wax as top coat. Due to their hydrophobic nature, low vapor permeability and transparency waxes could be considered ideal candidate for the treatment of heritage metals. However, several studies have demonstrated that their use should be more carefully evaluated. Reversibility issues can be experienced and the application of wax coatings for archaeological objects has been discouraged [33]. Furthermore, waxes used on outdoor monuments have a short lifetime, poor barrier properties, and susceptibility to photodegradation, as well as a high volatile organic compound (VOC) content and removal difficulties [34-36]. A study from 2015 gave recommendations to conservator-restorers as the reapplication of waxes at an interval of less than 9 months and application of thick films, 100-200 μm ideally or as thick as possible [37]. Also, aged wax films contained oxidation products that could enhance the corrosion of the underlying metal since they are polar and more acidic than fresh waxes.

### *Silanes*

The use of silane in conservation practice is recent compared with waxes and acrylics and many studies have been conducted in order to find an appropriate formulation to use on heritage artefacts. Organosilicon compounds are good hydrophobic and transparent coatings often used for industrial purposes capable to create strong bonding with corrosion products. Alkoxysilanes can be used as coupling agents in order to apply silaned materials by sol-gel processes. This process can be summarised as the creation of an oxides network by polymerization of a monomeric precursor in a liquid medium. The advantages of sol-gel coatings are the possibility to produce thin films on complex shapes, the absence of toxic waste and of washing step after treatment and the use of environmentally friendly compounds [38]. They can be applied by brush, spray or immersion. Also, the addition of inorganic particles such as SiO<sub>2</sub> or TiO<sub>2</sub> enhances barrier properties of silanes reducing water permeability and

also increasing their reversibility. The need of decreased water permeability is due to the fact that the bond Si-O-M is reversible by hydrolysis and thus, when water reaches the interface metal-silane, the protective features of silane coatings are eventually lost. The use of a thicker film is not an option for silane coatings since the layer becomes then brittle and difficult to apply.

One of the first applications of organic-inorganic copolymer system on bronze was the product Ormocer™. In laboratory tests, it performed better than waxes but the metal surface was darkened. Furthermore, it needs the use of methylene chloride to be removed, which is a highly toxic solvent. Hence, the use of this product should be evaluated under ethical perspective. The EU-ARTECH project (EU-6FP, 2005-2009) evaluated, among others, silane coatings in comparison with Incralac™ coating and waxes. This study showed that the tested silanes have a comparable protectiveness to Incralac™ which, as previously discussed, has poor long-term protective features. However, these silane formulations performed less than waxes [39]. The project PROMET (EU-6FP, 2004-2008) also tested silanes but all materials failed over the tested period [40]. Works from 2013 and 2015, showed good preliminary results obtained from PropS-SH (3-mercaptopropyl-trimethoxy-silane) on quaternary bronzes exposed to a 3.5 wt.% NaCl solution or a concentrated artificial rain [41, 42]. Nevertheless, in order to have an almost complete polymerisation a curing time of 30 days at room temperature was needed. However, even with a curing time of 10 days at room temperature the treatment achieved good protective capabilities after ageing tests. The protective efficiency of the silane PropS-SH was further tested on artificially aged substrates to reproduce corroded patina conditions in stagnant and runoff artificial rain conditions [41, 42]. It appeared that the silane coating was less efficient when exposed to runoff conditions than to stagnant rain conditions. However, it limited the formation of corrosion products and the colour alteration of the exposed surfaces and reduced as well the metal release in the artificial rain. The coating appeared to be a selective barrier towards the metal release acting more efficiently to avoid Cu release than Zn release. Also, the exposure conditions had an influence on the Pb release that was higher under runoff exposure. The same organo-silane was also evaluated for its response to UV radiation and temperature cycles in humid conditions [43]. Results showed microscale cracking and flaking during natural exposure but this phenomenon was reduced in TiO<sub>2</sub>-amended formulation. After thermal/UV cycles in climatic chamber the treated samples showed a visible yellowish colour variation. Better results were achieved in terms of photostability in presence of TiO<sub>2</sub> nanoparticles that probably absorb UV radiation.

It seems that, in order to fulfil the ethical requirement for application on heritage materials, further investigation on silane coatings need to be performed. However, they could be a good alternative to traditional protective systems used on copper-based artefacts.

### Corrosion inhibitors

According with ISO standard 8044, corrosion inhibitors are defined as “a chemical substance that decreases the corrosion rate when present in the corrosion system at suitable concentration, without significantly changing the concentration of any other corrosion agent” [2]. As previously mentioned, corrosion inhibitors can be used alone or as part of a protective multilayer system combined with different coatings. As well as for coatings, the use of corrosion inhibitors for heritage metals has to deal with the ethical requirements of minimal aesthetical alteration, reversibility or at least re-treatability, non-toxicity, application ease and predictive performance. The toxicity issue is currently a central part in the development of new corrosion inhibitors since the products used so far are toxic for the operators and the environment. Indeed, many efforts were made in order to find less toxic alternatives, possibly using natural products. Corrosion inhibitors are able to form stable chemical bonds with the patina limiting the eventual reaction with external corrosive agents. Most of the time, the film that they form on the treated surfaces is so thin to appear visible. However, there are cases where visual changes are clearly

perceived. However, the low film thickness applied renders such films ineffective against mechanical stress and therefore they are often covered by further coating layers in outdoor environment. The main use of copper corrosion inhibitors in the field of conservation-restoration is in presence of copper chlorides (bronze disease) in order to decrease the corrosion rate. Indeed, most of the time corrosion inhibitors are tested in presence of chlorine. The inhibition mechanisms can involve either the anodic, cathodic or both reactions.

#### *Benzotriazole (BTA)*

As mentioned above, the most used corrosion inhibitor for copper-based alloys is 1,2,3-benzotriazole (BTA). No tested protocol has been produced despite it is employed since more than 50 years. The most common recipes are solutions of 3% of BTA in ethanol or 1% of BTA in water. Regarding the application method, BTA is applied either by brush, by immersion of objects under vacuum conditions for few hours or by soaking objects for several days [27]. Factors such as the condition state of the object (in particular the oxidation state of its reactive surface), the potential, temperature, pH, content of chlorine and oxygen can affect the reaction between BTA and copper. In fact, the nature of the complexes formed when BTA is chemically absorbed on the metal depends on the copper oxidation state (i.e. Cu(I) or Cu(II)) [44]. The study of BTA inhibition mechanism, described for the first time in 1963, and its application in conservation-restoration vault a vast scientific literature even if conflicting evidence and opinions about its effectiveness have been raised [31, 45-51]. It seems that BTA efficiency is lower on copper alloys than on pure copper. Indeed, there are some concerns about its effectiveness on bronze disease since the cupric chloride-BTA complex layer formed upon treatment would only be superficial and therefore subject to eventual disruption and reactivation of the corrosion processes underneath [52]. The low pH condition necessary during application has been proposed to explain the several failures against bronze disease corrosion processes. At low pH BTA molecules would be absorbed by the surface but no complexes would be formed [53]. Furthermore, on tin-enriched parts when reacting with CuCl, BTA produces a black-green thin coating that cause darkening of the surface and has low efficiency [27, 54]. On outdoor sculptures, the use of BTA requires frequent maintenance due to the water solubility and low vapour pressure of BTA that may be washed away by rainfall. However, the most controversial argument about the extended use of BTA is its toxicity. As reported by Cano and Lafuente [55], some authors referred to benzotriazole as an environmental and health hazardous product recommending to handle it with care [12], while others are incline to describe it as slightly toxic. Numerous studies have been conducted in order to produce less toxic alternative to its molecule [5, 56-61]. Nevertheless, most of these molecules did not perform as well as BTA during performance tests.

#### *Carboxylates*

Sodium salts of carboxylic acids have been studied in the last decades as low-toxic corrosion inhibitors. Indeed, sodium carboxylates ( $\text{CH}_3(\text{CH}_2)_n\text{COONa}$ ,  $n =$  usually C10 or C12) have been used on copper in order to form copper carboxylates. The first tested carboxylate molecule was sodium heptanoate showing good corrosion inhibition as well as sodium decanoate. Recent research also focused on the combination of carboxylate functional groups with azole and thiol groups derivative but their effectiveness needs to be further investigated [62]. Also, carboxylates were tested on bare and artificially corroded bronze coupons but they resulted to be soluble and with poor protective features against moisture and gaseous pollutants [63, 64]. However, the use of carboxylates is mostly focused on the inhibition of iron, lead and zinc corrosion.

*“Green inhibitors”*

In the last decades, the interest about alternative sustainable and safe corrosion inhibitors increased. Products from plant extracts [65-68] and amino acids [69-73] have been studied even if no tests on real objects have been conducted so far. These products benefit of their easy availability and non-toxic nature as well as their natural biodegradability. However, they present the drawback of their complex nature and high variability. Recent works also focused on the use of expired medical drugs to inhibit corrosion mechanism. Among others, domperidone [74] and several antibiotics [75] were tested even if serious concerns about the possibility of an increased antibiotic concentration in the environment and their harmful effect on bacterial resistance could be raised.

## 1.4 Biotechnological innovative approach

In the field of metal cultural heritage, the corrosion layers on an artefact, naturally or artificially generated, is defined as patina. This term has another signification in the field of geosciences as biofilm (or biopatina), referring to an aggregate of microorganisms in which cells, that are frequently embedded within a self-produced matrix of extracellular polymeric substance (EPS), adhere to each other and/or to a surface. Finally, when microorganisms and their metabolites interact with a surface, forming new inorganic compounds, those compounds are referred as biogenic patina, indicating their biological formation mechanisms rather than due to purely chemical (abiotic) reactions.

These three definitions are important for the understanding of this thesis. Indeed, throughout this work, the term “biopatina” will be used to refer to a novel conservation treatment that allows the formation of a protective biogenic patina. In fact, the aim of the “biopatina project” is to develop an alternative biological conservation treatment on copper-based artefacts using selected microorganisms.

Some fungal species are known for their ability to produce oxalic acid in order to immobilize of toxic heavy metals and, therefore, detoxify their environment [76-78]. Indeed, free ions of toxic metals can be complexed by oxalic acid forming biogenic high insoluble crystals of metal oxalates reducing the toxicity of the medium [79, 80]. Biotechnology already exploited this ability to immobilize heavy metals in the field of waste treatment [81-83]. This ability can be used to modify existing corrosion products into more stable and less soluble compounds while preserving the artefacts physical appearance. Indeed, instead of use a sacrificial layer as organic coatings mentioned above, this research aims to produce passivating compounds having the same composition as naturally occurring copper minerals (inorganic materials) enhancing the compatibility of this treatment with the corroded surface of artefacts. The presence of copper oxalates as green patinas was already discovered on outdoor bronze artefacts but not associated with active corrosion [15]. Furthermore, copper oxalates are known to be extremely stable in polluted atmospheres with acidic conditions (pH 3), providing good protection to copper-based artefacts [84, 85]. Therefore, the biosynthesis of these minerals is proposed in the “biopatina” project as new biotechnological innovative approach to the preservation of outdoor corroded bronze.

The “biopatina project” started in 2005 in the framework of the EU-ARTECH project (EU-6FP, 2005-2009) which was followed by a second project, BAHAMAS (Biological patinA for archAeological and Artistic Metal ArtefactS, EU-7FP-IEF, 2010-2012).

During the first project (EU-ARTECH), a new approach was proposed, considering the compatibility with the inorganic corrosion products present on monuments and the toxicity of the treatments commonly applied. In fact, organic coatings such as waxes, acrylic resins and corrosion inhibitors, traditionally used in industry, are used without adaptation to the conservation field and may not be compatible with the corroded inorganic metal substrates [86]. These products simply create an artificial barrier against aggressive environments, a sacrificial layer that needs frequent maintenance in order to

fulfil its protective role. Furthermore, the use of organic treatment implies some disadvantages: as previously mentioned they need frequent maintenance; also, they induce surface darkening (wax), shiny aspect of the treated surface and brittleness of the film (acrylic resin) and the most used corrosion inhibitor, benzotriazole, is toxic and a well-known human carcinogen [86]. Therefore, the possibility to produce biogenic copper oxalates to protect metallic artefacts was proposed. During this study, five wild fungal strains were selected for their ability to produce oxalic acid: *Aspergillus niger*, *Penicillium* sp., *Aspergillus alliaceus* and two fungal strains isolated from vineyards in Switzerland, *Beauveria bassiana* and *Fusarium* sp.. These five strains were incubated in malt-agar culture medium, pure or amended with copper sulphates, copper hydroxychlorides or copper oxide powder and their conversion into copper oxalates was evaluated. *B. bassiana* showed the best efficiency in terms of formation speed and amount of copper oxalates and was used to attempt a first application on corroded copper sheets. Results showed that almost 100% of brochantite (copper sulphate) were transformed in moolooite (copper oxalate  $\text{CuC}_2\text{O}_4 \cdot n\text{H}_2\text{O}$ ,  $n < 1$ ) while for atacamite (copper chloride) the transformation was only partial [39, 87].

The efficiency of this novel biological treatment has been further investigated within the BAHAMAS project. In particular, the newly formed biogenic copper oxalates were characterized in order to define the formation mechanisms, the adhesion to the treated surface and the final aesthetical appearance [86, 88-90]. Furthermore, first tests on fungal inoculation and application procedures on metal sheets were conducted. The best application method resulted to be the application of colonised malt-agar turned on top of metal coupons, with the fungal mycelium in direct contact with the treated surface.

The timeline of biopatina project and the main outcomes of the two previous studies are summarized in Figure 7.

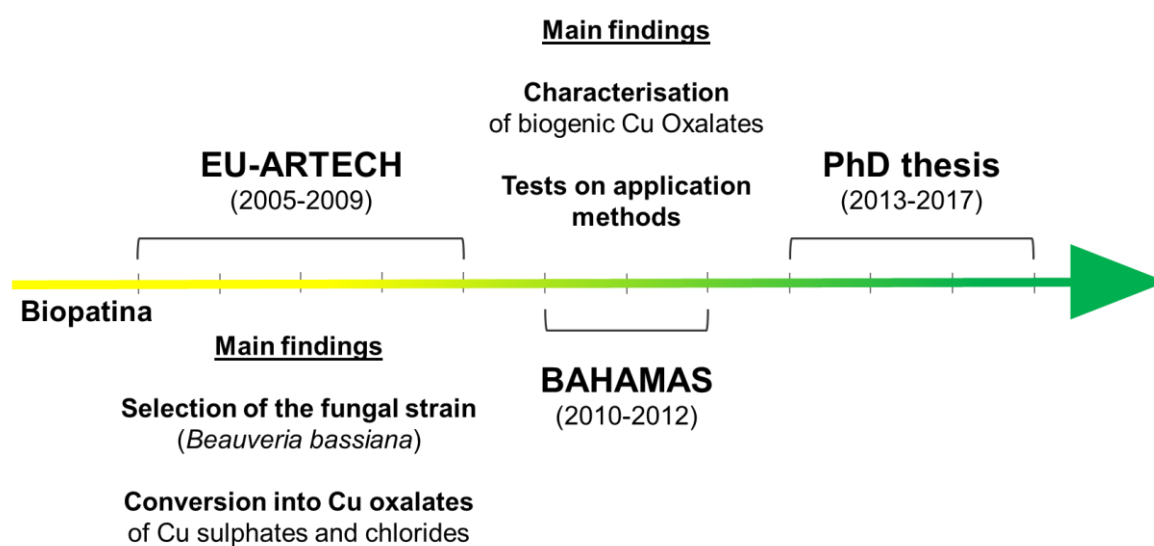


Figure 7. Chronological timeline of biopatina projects and main outcomes of previous studies

## 1.5 Research outline

The results obtained within EU-ARTECH and BAHAMAS projects are the basis of this PhD thesis. The aim of this work is to further investigate and optimise biopatina treatment, in order to transfer this treatment from the laboratory tests to real-praxis. To do that, this work focused on two main subjects: the study of the microorganism used for the production of biogenic copper oxalates and the treated material, namely copper and bronze. Regarding the treated material, the aim was to understand which protective mechanisms are involved in the biopatina treatment allowing to understand if such treatment acts as a corrosion inhibitor or as a coating. Furthermore, the influence of alloying elements, particularly tin, on the behaviour of biopatina treatment was investigated. A summary of the main focuses of this thesis is given in **Figure 8**.

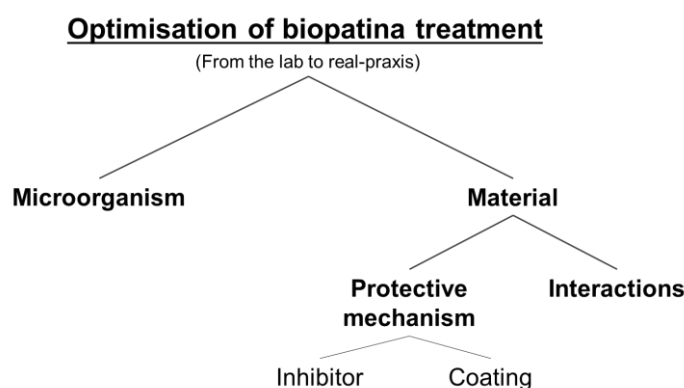


Figure 8. Summary of the main focuses of this PhD project

Each part of this work focused its attention on one specific issue. The ability of a specific strain of *B. bassiana* to produce oxalic acid is investigated in chapter 2, using liquid fungal cultures in presence and absence of a copper source. The analyses performed allowed to better understand the metabolism of this specific strain, particularly in terms of oxalic acid production.

The use of the biological treatment for archaeological and outdoor artefacts is further addressed in chapters 3 and 4. In the case of outdoor sculpture, the biopatina protective mechanism was compared with a microcrystalline wax, since wax coatings are the reference products used outdoor. Whereas, in the case of archaeological objects, it was compared to a corrosion inhibitor (BTA) commonly used for such artefacts, usually stored indoor. For both applications, the treatment was tested on standardized specimens and on real objects and underwent either artificial or natural ageing. Furthermore, different delivery systems were tested in order to propose a user-friendly product, suitable to real praxis by conservators-restorers.

In chapter 5, the issue of surfaces exposed to rainfall and surface tin enrichment is considered. Indeed, biopatina treatment was tested on tin-enriched specimens aged through simulated unsheltered conditions.

The influence of alloying elements on the behaviour of biopatina treatment is further investigated in chapter 6. Through a complement of several analytical techniques, the impact of tin, lead and zinc alloying elements on the corrosion patina formed and on the protective treatment when applied is assessed.

Finally, in chapter 7, the main results of the thesis are discussed and the conclusions of this PhD project are presented.

**Due to the potential industrial application of this work, the fungal culture conditions and the specific preparation of the delivery system as well as the preparation method will not be disclosed in the present manuscript.**

## References

1. Roberge, P.R., Corrosion Engineering. 2008: McGraw-Hill New York, NY, USA:.
2. ISO, 8044:1999 Corrosion of metals and alloys - Basic terms and definitions.
3. IUPAC, Compendium of Chemical Terminology - Gold Book. International Union of Pure and Applied Chemistry. 2014.
4. Pourbaix, M., Atlas of electrochemical equilibrium in aqueous solution. 1966, New York: Pergamon Press
5. Marušić, K., Protection of patinated bronze by non-toxic inhibitors. 2010, Fakultet kemijskog inženjerstva i tehnologije, Sveučilište u Zagrebu.
6. Tidblad, J., V. Kucera, and S. Sherwood, Corrosion, in *The Effects of Air Pollution on Cultural Heritage*, R. Hamilton, et al., Editors. 2009, Springer US: Boston, MA. p. 53-103.
7. Schindelholz, E. and R.G. Kelly, Wetting phenomena and time of wetness in atmospheric corrosion: a review. 2012.
8. Leygraf, C., et al., Atmospheric corrosion. 2016: John Wiley & Sons.
9. Graedel, T., Copper patinas formed in the atmosphere—II. A qualitative assessment of mechanisms. *Corrosion Science*, 1987. 27(7): p. 721-740.
10. Krätschmer, A., I. Odnevall Wallinder, and C. Leygraf, The evolution of outdoor copper patina. *Corrosion Science*, 2002. 44(3): p. 425-450.
11. de la Fuente, D., J. Simancas, and M. Morcillo, Morphological study of 16-year patinas formed on copper in a wide range of atmospheric exposures. *Corrosion Science*, 2008. 50(1): p. 268-285.
12. Scott, D.A., *Copper and Bronze in Art: Corrosion, Colorants, Conservation*. 2002: Getty Publications.
13. Grayburn, R., et al., Tracking the progression of bronze disease—A synchrotron X-ray diffraction study of nantokite hydrolysis. *Corrosion Science*, 2015. 91: p. 220-223.
14. Scott, D.A., Bronze Disease: A Review of Some Chemical Problems and the Role of Relative Humidity. *Journal of the American Institute for Conservation*, 1990. 29(2): p. 193-206.
15. Nassau, K., et al., The characterization of patina components by X-ray diffraction and evolved gas analysis. *Corrosion Science*, 1987. 27(7): p. 669-684.
16. Lins, A. and T. Power, The Corrosion of Bronze Monuments in Polluted Urban Sites: A Report on the Stability of Copper Mineral Species at Different pH Levels, in *Ancient & Historic Metals: Conservation and Scientific Research*. 1994, Getty Conservation Institute. p. 119-151.
17. Cicileo, G.P., M.A. Crespo, and B.M. Rosales, Comparative study of patinas formed on statuary alloys by means of electrochemical and surface analysis techniques. *Corrosion Science*, 2004. 46(4): p. 929-953.
18. Robbiola, L. and L. Hurltel, Nouvelle contribution à l'étude des mécanismes de corrosion des bronzes de plein air: caractérisation de l'altération de bronzes de Rodin. *Mémoires et Études Scientifiques Revue de Métallurgie*, 1991. 12: p. 809.
19. Wadsak, M., et al., Multianalytical in situ investigation of the initial atmospheric corrosion of bronze. *Corrosion Science*, 2002. 44(4): p. 791-802.

20. Sidot, E., et al., Study of the corrosion behaviour of Cu–10Sn bronze in aerated Na<sub>2</sub>SO<sub>4</sub> aqueous solution. *Corrosion science*, 2006. 48(8): p. 2241-2257.
21. Robbiola, L., C. Fiaud, and S. Pennec. New model of outdoor bronze corrosion and its implications for conservation. in *ICOM Committee for Conservation tenth triennial meeting*. 1993.
22. Chiavari, C., et al., Composition and electrochemical properties of natural patinas of outdoor bronze monuments. *Electrochimica acta*, 2007. 52(27): p. 7760-7769.
23. Robbiola, L., et al., New insight into the nature and properties of pale green surfaces of outdoor bronze monuments. *Applied Physics A*, 2008. 92(1): p. 161-169.
24. Bernardi, E., et al., The atmospheric corrosion of quaternary bronzes: The leaching action of acid rain. *Corrosion Science*, 2009. 51(1): p. 159-170.
25. Chiavari, C., et al., The atmospheric corrosion of quaternary bronzes: The action of stagnant rain water. *Corrosion Science*, 2010. 52(9): p. 3002-3010.
26. Robbiola, L., J.-M. Blengino, and C. Fiaud, Morphology and mechanisms of formation of natural patinas on archaeological Cu–Sn alloys. *Corrosion Science*, 1998. 40(12): p. 2083-2111.
27. Watkinson, D., Preservation of Metallic Cultural Heritage, in *Shreir's Corrosion*, J.A.R. Tony, Editor. 2010, Elsevier: Oxford. p. 3307-3340.
28. Brandi, C., *Teoria del restauro*. Vol. 318. 1981: Ed. di storia e letteratura.
29. Appelbaum, B., *Conservation treatment methodology*. 2007, Oxford: Elsevier.
30. Brostoff, L. and E. De la Rie. Research into protective coating systems for outdoor bronze sculpture and ornamentation. in *Conférence internationale sur la conservation des métaux*. 1997.
31. Argyropoulos, V., et al. A survey of the types of corrosion inhibitors and protective coatings used for the conservation of metal objects from museum collections in the Mediterranean basin. in *Strategies for Saving our Cultural Heritage. Proceedings of the International Conference on Conservation Strategies for Saving Indoor Metallic Collections 2007*. Cairo (Egypt): TEI of Athens.
32. Townsend, J., K. Eremin, and M. Adriaens, *Conservation science 2002: papers from the conference held in Edinburgh, Scotland, 22-24 May 2002*. 2003: Archetype.
33. Moffett, D.L., Wax coatings on ethnographic metal objects: justifications for allowing a tradition to wane. *Journal of the American Institute for Conservation*, 1996. 35(1): p. 1-7.
34. Grissom, C.A., et al., Evaluation of coating performance on silver exposed to hydrogen sulfide. *Journal of the American Institute for Conservation*, 2013. 52(2): p. 82-96.
35. Considine, B.B., *Conserving outdoor sculpture: the Stark collection at the Getty Center*. 2010: Getty Publications.
36. Jaeger, T., Short Communication Removal of Paraffin Wax in the Re-treatment of Archaeological Iron. *Journal of the American Institute for Conservation*, 2008. 47(3): p. 217-223.
37. Swartz, N. and T.L. Clare, On the protective nature of wax coatings for culturally significant outdoor metalworks: microstructural flaws, oxidative changes, and barrier properties. *Journal of the American Institute for Conservation*, 2015. 54(3): p. 181-201.
38. Zucchi, F., *Sol-gel coatings for the preservation of metallic heritage artefacts*. 2013, Elsevier Inc. Chapters.
39. Joseph, E., et al. Innovative treatments for the protection of outdoor bronze monuments. in *Proceedings of the Interim Meeting of the ICOM-CC Metal WG, Amsterdam, Netherlands*. 2007.

40. Argyropoulos, V., *Metals and museums in the Mediterranean: protecting, preserving and interpreting*. 2008: Technological educational institute of Athens.
41. Chiavari, C., et al., Protective silane treatment for patinated bronze exposed to simulated natural environments. *Materials Chemistry and Physics*, 2013. 141(1): p. 502-511.
42. Chiavari, C., et al., Atmospheric corrosion of fire-gilded bronze: corrosion and corrosion protection during accelerated ageing tests. *Corrosion Science*, 2015. 100: p. 435-447.
43. Chiavari, C., et al., Organosilane coatings applied on bronze: Influence of UV radiation and thermal cycles on the protectiveness. *Progress in Organic Coatings*, 2015. 82: p. 91-100.
44. Brostoff, L.B., *Coating strategies for the protection of outdoor bronze art and ornamentation*. 2003, University of Amsterdam. p. 180.
45. Hassairi, H., et al., Evaluation of the inhibitive effect of benzotriazole on archeological bronze in acidic medium. *Applied Physics A*, 2013. 113(4): p. 923-931.
46. Hassairi, H., et al., Characterization of archaeological bronze and evaluation of the benzotriazole efficiency in alkali medium. *Materials and Corrosion*, 2008. 59(1): p. 32-40.
47. Abu-Baker, A.N., et al., A comparative study of salicylaldoxime, cysteine and benzotriazole as inhibitors for the activechloride-based corrosion of copper and bronze artifacts. *European Scientific Journal*, 2013. 9(33).
48. Mezzi, A., et al., Investigation of the benzotriazole inhibition mechanism of bronze disease. *Surface and Interface Analysis*, 2012. 44(8): p. 968-971.
49. Balbo, A., et al., Effectiveness of corrosion inhibitor films for the conservation of bronzes and gilded bronzes. *Corrosion Science*, 2012. 59: p. 204-212.
50. Faltermeier, R., *Testing Corrosion Inhibitors for the Conservation of Archaeological Copper and Copper Alloys*. *Journal of Conservation and Museum Studies*, 1997. 3.
51. MacLeod, I.D., Conservation of corroded copper alloys: a comparison of new and traditional methods for removing chloride ions. *Studies in Conservation*, 1987. 32(1): p. 25-40.
52. Sease, C., Benzotriazole: a review for conservators. *Studies in Conservation*, 1978. 23(2): p. 76-85.
53. Finšgar, M. and I. Milošev, Inhibition of copper corrosion by 1, 2, 3-benzotriazole: a review. *Corrosion science*, 2010. 52(9): p. 2737-2749.
54. Faltermeier, R., Colour changes induced when treating copper and copper alloy archaeological artefacts with the corrosion inhibitors benzotriazole and amino-mercapto-thiadiazole. *SSCR Journal*, 1998. 9(1): p. 5.
55. Cano, E. and D. Lafuente, Corrosion inhibitors for the preservation of metallic heritage artefacts, in *Corrosion and conservation of cultural heritage artefacts*, P. Dillmann, et al., Editors. 2013, Woodhead Publishing. p. 570-594.
56. Cotton, J. and I. Scholes, Benzotriazole and related compounds as corrosion inhibitors for copper. *British Corrosion Journal*, 1967. 2(1): p. 1-5.
57. Trachli, B., et al., Protective effect of electropolymerized 3-amino 1, 2, 4-triazole towards corrosion of copper in 0.5 M NaCl. *Corrosion Science*, 2002. 44(5): p. 997-1008.
58. Muresan, L., et al., Protection of bronze covered with patina by innocuous organic substances. *Electrochimica Acta*, 2007. 52(27): p. 7770-7779.

59. Marušić, K., et al., Comparative studies of chemical and electrochemical preparation of artificial bronze patinas and their protection by corrosion inhibitor. *Electrochimica Acta*, 2009. 54(27): p. 7106-7113.
60. Rahmouni, K., et al., Protection of ancient and historic bronzes by triazole derivatives. *Electrochimica Acta*, 2009. 54(22): p. 5206-5215.
61. Dermaj, A., et al., Inhibition of bronze corrosion in 3% NaCl media by novel non-toxic 3-phenyl-1, 2, 4-triazole thione formulation. *Corrosion Engineering, Science and Technology*, 2015. 50(2): p. 128-136.
62. Tansuğ, G., et al., A new corrosion inhibitor for copper protection. *Corrosion Science*, 2014. 84: p. 21-29.
63. Elia, A., Application of electrochemical methods for the study and protection of heritage copper alloys. 2013, Ghent University.
64. Rapp, G., et al., The application of non-toxic corrosion inhibitors for the temporary protection of iron and copper alloy in uncontrolled environments. *Metal*, 2010: p. 185-190.
65. Abiola, O.K. and A. James, The effects of Aloe vera extract on corrosion and kinetics of corrosion process of zinc in HCl solution. *Corrosion Science*, 2010. 52(2): p. 661-664.
66. Banerjee, S., V. Srivastava, and M. Singh, Chemically modified natural polysaccharide as green corrosion inhibitor for mild steel in acidic medium. *Corrosion Science*, 2012. 59: p. 35-41.
67. Deng, S. and X. Li, Inhibition by Ginkgo leaves extract of the corrosion of steel in HCl and H<sub>2</sub>SO<sub>4</sub> solutions. *Corrosion Science*, 2012. 55: p. 407-415.
68. El-Haddad, M.N., Chitosan as a green inhibitor for copper corrosion in acidic medium. *International journal of biological macromolecules*, 2013. 55: p. 142-149.
69. Wang, T., J. Wang, and Y. Wu, The inhibition effect and mechanism of l-cysteine on the corrosion of bronze covered with a CuCl patina. *Corrosion Science*, 2015. 97: p. 89-99.
70. Badawy, W.A., K.M. Ismail, and A.M. Fathi, Corrosion control of Cu–Ni alloys in neutral chloride solutions by amino acids. *Electrochimica Acta*, 2006. 51(20): p. 4182-4189.
71. Ismail, K.M., Evaluation of cysteine as environmentally friendly corrosion inhibitor for copper in neutral and acidic chloride solutions. *Electrochimica Acta*, 2007. 52(28): p. 7811-7819.
72. Khaled, K., Corrosion control of copper in nitric acid solutions using some amino acids—A combined experimental and theoretical study. *Corrosion Science*, 2010. 52(10): p. 3225-3234.
73. Zhang, D.-Q., H. Wu, and L.-X. Gao, Synergistic inhibition effect of l-phenylalanine and rare earth Ce (IV) ion on the corrosion of copper in hydrochloric acid solution. *Materials Chemistry and Physics*, 2012. 133(2): p. 981-986.
74. Wang, D., et al., Corrosion control of copper in 3.5 wt.% NaCl solution by domperidone: experimental and theoretical study. *Corrosion Science*, 2014. 85: p. 77-86.
75. Rotaru, I., et al., Antibacterial drugs as corrosion inhibitors for bronze surfaces in acidic solutions. *Applied Surface Science*, 2014. 321: p. 188-196.
76. Burford, E.P., M. Fomina, and G.M. Gadd, Fungal involvement in bioweathering and biotransformation of rocks and minerals. *Mineralogical Magazine*, 2003. 67(6): p. 1127-1155.
77. Gadd, G.M., Interactions of fungi with toxic metals. *New Phytologist*, 1993. 124(1): p. 25-60.

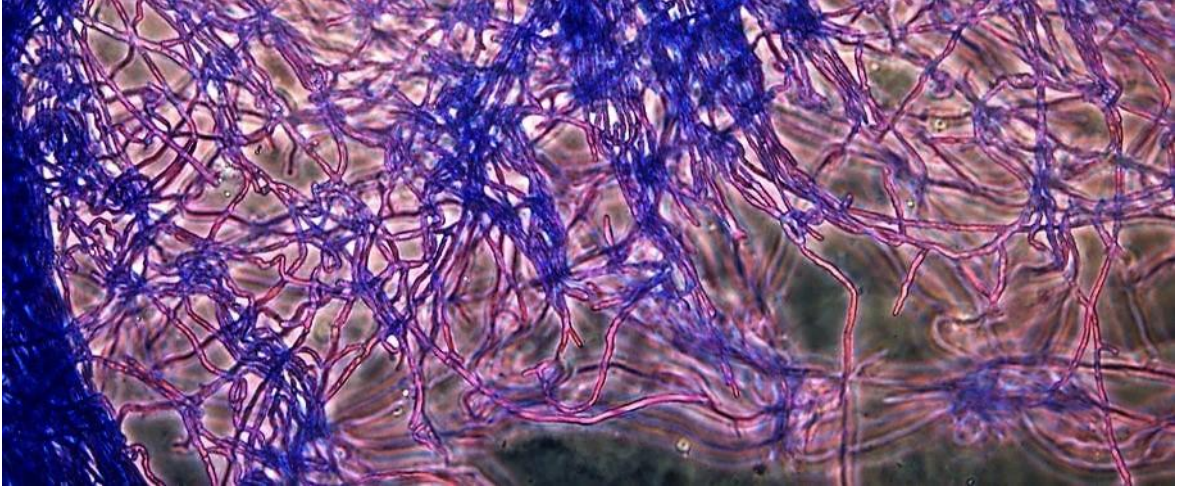
78. Jarosz-Wilkolazka, A. and G.M. Gadd, Oxalate production by wood-rotting fungi growing in toxic metal-amended medium. *Chemosphere*, 2003. 52(3): p. 541-547.
79. Gadd, G.M., Geomycology: biogeochemical transformations of rocks, minerals, metals and radionuclides by fungi, bioweathering and bioremediation. *Mycological Research*, 2007. 111(1): p. 3-49.
80. Gadd, G.M., Metals, minerals and microbes: geomicrobiology and bioremediation. *Microbiology*, 2010. 156(3): p. 609-643.
81. Tabak, H.H., et al., Developments in bioremediation of soils and sediments polluted with metals and radionuclides–1. Microbial processes and mechanisms affecting bioremediation of metal contamination and influencing metal toxicity and transport. *Reviews in Environmental Science and Bio/Technology*, 2005. 4(3): p. 115-156.
82. Godlewska-Żylkiewicz, B., Microorganisms in inorganic chemical analysis. *Analytical and bioanalytical chemistry*, 2006. 384(1): p. 114-123.
83. Saylor, G.S., R. Fox, and J. Blackburn, *Environmental biotechnology for waste treatment*. Vol. 41. 2013: Springer Science & Business Media.
84. Marabelli, M. and R. Mazzeo, La corrosione dei bronzi esposti all'aperto: problemi di caratterizzazione. *METALLURGIA ITALIANA*, 1993. 85: p. 247-247.
85. Mazzeo, R., G. Chiavari, and G. Morigi, Identificazione ed origine di patine ad ossalato sui monumenti bronzei: il caso del portale centrale del duomo di Loreto (AN), in *Le pellicole ad ossalati: origine e significato nella conservazione delle opere d'arte*. 1989, Centro. p. 271-280.
86. Joseph, E., et al., Development of an analytical procedure for evaluation of the protective behaviour of innovative fungal patinas on archaeological and artistic metal artefacts. *Analytical and Bioanalytical Chemistry*, 2011. 399: p. 2899-2907.
87. Simon, A., Etude et optimisation de la formation fongique d'oxalate de cuivre sur du vert-de-gris en vue de la protection de monuments, in *Laboratory of microbiology*. 2007, University of Neuchâtel: Neuchâtel.
88. Joseph, E., et al., Protection of metal artefacts with the formation of metal-oxalates complexes by *Beauveria bassiana*. *Frontiers in Microbiology*, 2012. 2.
89. Joseph, E., et al., Spectroscopic characterization of an innovative biological treatment for corroded metal artefacts. *Journal of Raman Spectroscopy*, 2012. 43(11): p. 1612-1616.
90. Joseph, E., et al. Assessment of a biological approach for the protection of copper alloys artefacts. in *Metal 2013: interim meeting of the ICOM-CC metal working group Edinburgh*. 2013.



## Chapter 2

---

### BEAVERIA BASSIANA



## Summary

In this chapter the production of oxalic acid by the strain S6 of *Beauveria bassiana* and its use for copper oxalates biosynthesis will be discussed. An introduction about *B. bassiana* and its characteristics is given. Furthermore, an assessment of the production of organic acids by strain S6 with and without the use of a copper source was attempted. This allowed a better understanding of the biological mechanisms occurring during the treatment of copper-based artefacts and the interaction between the fungus and copper corrosion products. The characterization and quantification of organic acids was made by high-performance liquid chromatography (HPLC).

## Abstract

*Beauveria bassiana* is known to be a cosmopolitan entomopathogenic fungus. One of the determinant pathogenic metabolites that this fungus produces is oxalic acid. Indeed, this organic acid is able to solubilise specific cuticular proteins of the host. This ability allows it to be a perfect candidate for the treatment of copper based artefacts, as oxalic acid is able to chelate copper ions forming copper oxalates. Furthermore, it has been demonstrated that this species does not cause harm to human health and to the environment. Nevertheless, toxic metals, as copper, are usually detrimental for microorganisms. Indeed, fungal growth and, consequently, relative metabolic activity can be inhibited by a high concentration of copper. In order to overcome this problem, many fungal species have developed resistance mechanisms. One of this is the overexcretion of oxalic acid that immobilize metals (and metallic ions) in insoluble forms detoxifying the medium. It has also been suggested that in environments highly contaminated with toxic metals a selection for resistant ecotypes may occur. An evaluation of the organic acids produced and the possible over-production of oxalic acid in copper amended media was here assessed with this strain.

## Introduction [1-3]

*Beauveria bassiana* is a cosmopolitan anamorphic ascomycete fungus. Its colonies are white, later yellowish or occasionally reddish while the reverse is uncoloured or yellowish to pinkish (Figure 9 and Figure 10). It is an entomopathogenic fungus that attaches as spore to insect's cuticle and germinates colonizing the host with its hyphae. It is able to colonize more than 700 hosts species [4] and it was isolated both in uncultivated and in cultivated habitats [5, 6]. Due to these characteristics, *B. bassiana* was always considered an optimal biological control agent for pests in organic agriculture and it was employed in the development of several commercial products [4].

Despite its primary pathogenic behaviour this fungus can also live in soils as a saprophyte, but extensive proliferation and dispersal are limited [7, 8]. In this environment, the population survival depends on the production of infective conidia that are released from the host cadaver over time after sporulation [9]. Furthermore, some evidence showed that *B. bassiana* could be included in the range of endophytic fungi. Its presence in plant tissues of corn [10], cacao [11] and poppy [12] could protect the plants against herbivorous insects [13, 14]. *B. bassiana* was also isolated in air samples [15, 16] and air transport and deposition could be an explanation of its occurrence on plants phylloplanes [17].

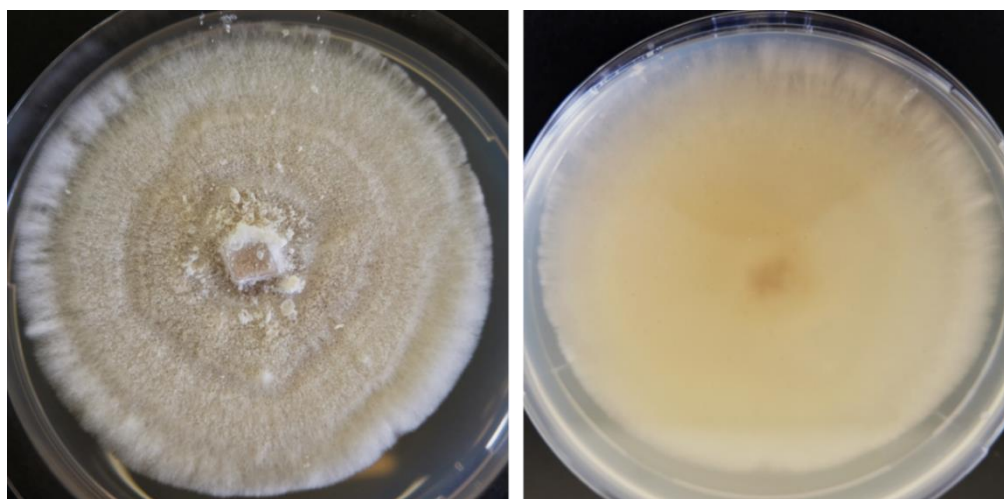


Figure 9. Front and reverse of *Beauveria bassiana* colony in Malt Agar

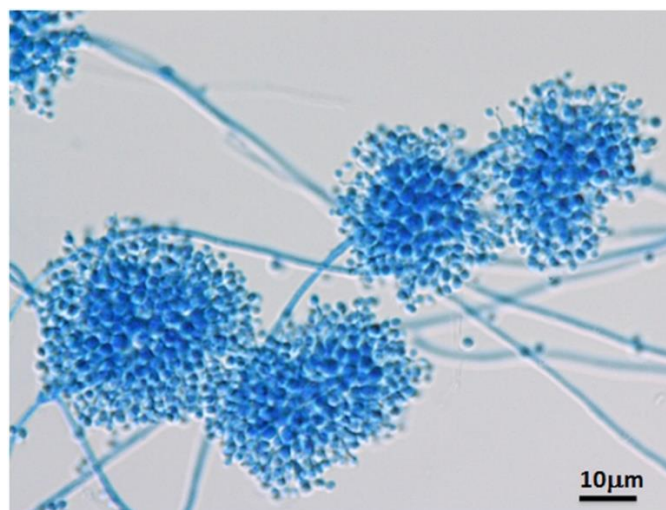


Figure 10. Microscopic aspect of *B. bassiana* conidia [18]

Some abiotic factors can affect the development and survival of *B. bassiana*, namely temperature, humidity or moisture and solar radiation. In fact, non-optimal temperature can inactivate or activate spores' germination and reduce or accelerates mycelial growth. In *B. bassiana*, the optimum temperature is between 23 and 28°C, the minimum between 5 and 10°C and the maximum at about 30-38°C, depending on the strain [2]. The synergic effect of high-temperature and high or low humidity has an effect on spores' viability. The optimal range of relative humidity is between 100 and 92% [19]. The UV component of solar radiation, in particular UV-A and B is the most dangerous factor for fungal survival and in simulated sunlight irradiation experiments just half of *B. bassiana* conidia were still viable.

The use of this fungus as biological control agent led to the production of extensive literature about its toxicity and risks related to human health and to untargeted organisms. The risks related to human exposure has been demonstrated to be extremely rare. Based on the wide natural occurrence of *B. bassiana* and the low toxicity profile demonstrated by ecotoxicology studies conducted on relative commercial products, the ecological risk due to exposure to this microorganism is expected to be minimal. This fungus is, thus, a perfect candidate to be used in conservation-restoration practice because of the limited risks for operators and environment. For an extensive review on *B. bassiana* effects on human health and on other microorganisms, vertebrates, plants and mammals, useful articles by Langle (2006), Zimmerman (2007), and Shahid (2012) are advised [2, 20, 21].

In terms of biodiversity, *B. bassiana* presents some cryptic species [22, 23]. This is because the diversity of fungal species is usually assessed by morphological characteristics and only few characters are used for species separation. Furthermore, its anamorphic life cycle makes the comparison of the specific characters and the distinction based of the morphological diversity more difficult to perform. However, molecular biology techniques revealed a high genetic diversity of the morphological species of *B. bassiana* [24]. Indeed, the morphological species of *B. bassiana* are paraphyletic, consisting in two separates clades, one more related to *Beauveria brongniartii* and a second one, also called 'pseudobassiana' [22, 23]. The identification of the strain S6 was done by the Mycothèque de l'Université Catholique de Louvain (Belgian Coordinated Collections of Micro-organisms BCCM/MUCL) using a morphological assessment and, thus, for the purpose of this study, the name *B. bassiana* is here used referring to the morphological species since no genetic information is so far available.

Entomopathogenic fungi, and microorganisms in general, are able to produce different metabolites in order to perform specific activities and functions. Secondary metabolites of the genus *Beauveria* are bassianin, bassiacridin, beauvericin, bassianolide, beauverolides, tenellin and oosporein [25, 26].

*B. bassiana* also secret an important extracellular organic acid: oxalic acid [27], which is able to solubilise specific cuticular proteins and is a determinant pathogenic metabolite [28]. Oxalic acid is one of the strongest organic acids and it is produced by many fungi, including brown-rots, white-rots, mycorrhizae and plant pathogens. Its production, aside its role related to pathogenic infection processes, is often associated to metal solubilisation, increasing their bioavailability. Indeed, fungal growth needs the availability of essential elements, such as sodium, potassium, copper, zinc, cobalt, calcium, magnesium, manganese and iron. Among these elements, all metals, particularly heavy metals, can become toxic if present in high concentration. The production of oxalic acid is also related to this issue providing metal immobilization and, therefore, environmental detoxification [29-31]. Indeed, free ions of toxic metals can be complexed by oxalic acid forming highly insoluble biogenic crystals of metal oxalates and thus reducing the toxicity of the medium [3, 32]. During fungal growth, the production of organic acids is influenced by the pH and the buffering capacity of the environment, the carbon sources and the presence of certain metals. In the presence of toxic metals, though, the production of oxalic acid may increase [33]. For instance, brown-rot basidiomycetes produce higher amount of organic acids in presence of copper [34]. Fomina (2004) also correlated an over-excretion of oxalic acid to the metal tolerance exhibited by *Beauveria caledonica* [33]. Thus, in response to high concentration of toxic metals, fungi may adopt as resistance mechanism the formation of metal oxalates [3]. It has also been suggested that in environments highly contaminated with toxic metals a selection for resistant ecotypes may occur [35, 36].

The strain S6 of *B. bassiana* used in this study was already known for its ability to biosynthesise copper oxalates (Figure 11), as already described in chapter one. Nevertheless, a study about the correlation between the presence of copper ions in the medium and an overproduction of oxalic acid was never made. It is worth mentioning that this strain was isolated in a vineyard site highly contaminated with copper-based anti-cryptogamic solutions. Therefore, this strain may have developed a resistance mechanism that would induce an over-excretion of oxalic acid. This ability could be then exploited on copper corrosion products in order to convert them into copper oxalates with an high efficiency of the process compared with non-resistant strains. In order to evaluate the production of oxalic acid by strain S6 of *B. bassiana*, liquid cultures amended or not with a copper source were prepared. The culture media were collected over one month and up to six months and the production of organic acids was evaluated through high-performance liquid chromatography (HPLC).

## Materials and methods

### *Fungal strain*

The strain S6 of *B. bassiana* belongs to the fungal culture collection of the Laboratory of Microbiology, Department of Biology, Faculty of Science of the University of Neuchatel. The culture was maintained on malt-agar (12 g.L<sup>-1</sup> and 15 g.L<sup>-1</sup> respectively) plates and slants.

### *Liquid cultures*

The fungus was cultivated in Pyrex 100mL-bottles with 57.6 mL of malt medium (12 g.L<sup>-1</sup>). The control medium MA contained exclusively malt. The medium MB was amended with 0.4 g.L<sup>-1</sup> of copper (II) sulphate pentahydrate (CuSO<sub>4</sub>·5H<sub>2</sub>O) from Sigma-Aldrich. The medium MC was amended with 3 g.L<sup>-1</sup> of copper (I) oxide (Cu<sub>2</sub>O) from Sigma-Aldrich. The difference in concentration between the two copper minerals depended on the fungal growth. Indeed, for concentration above 0.4 g.L<sup>-1</sup> of copper (II) sulphate no fungal growth was observed. Each medium was prepared in triplicates. The bottles were inoculated with a spores suspension and incubated under orbital shaking (150 rpm) at room temperature.

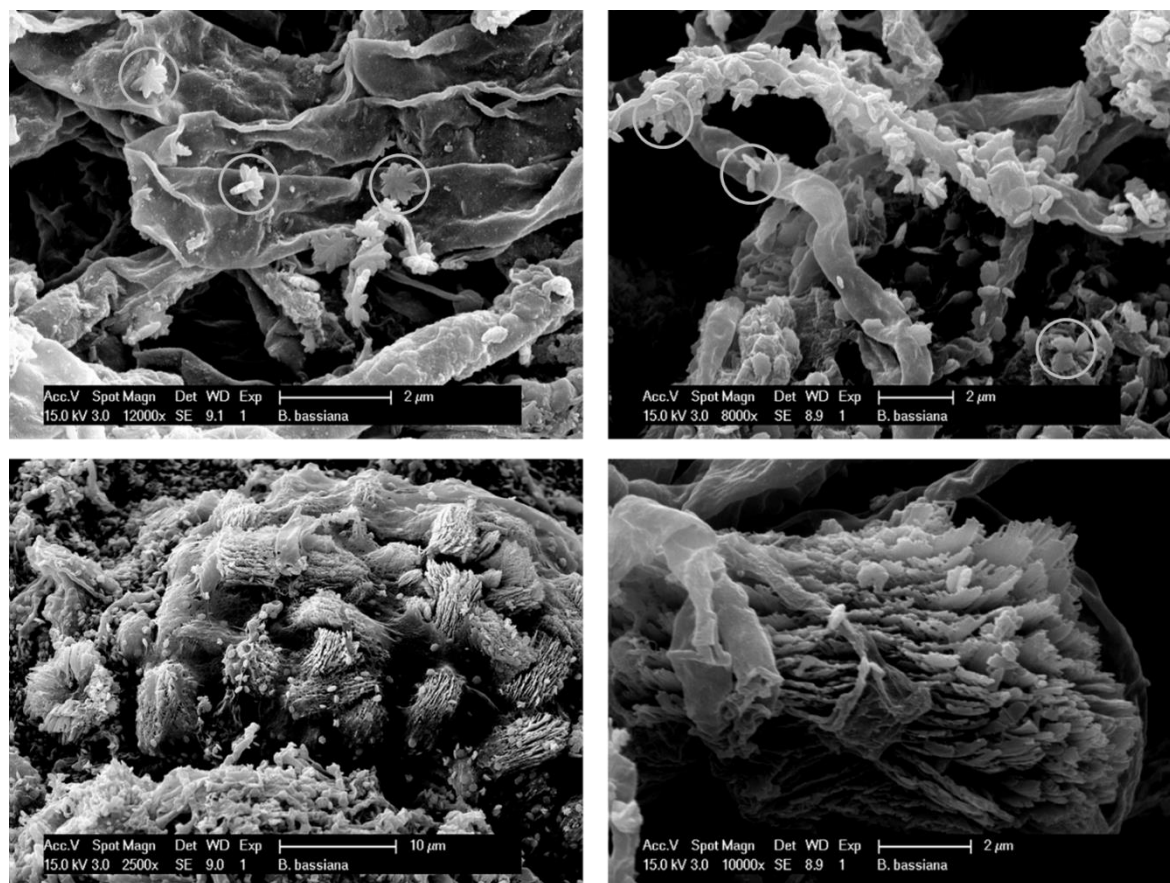


Figure 11. Secondary electron micrographs of *B. bassiana* hyphae and biosynthesised crystals of copper oxalates. On the top images some copper oxalates crystals are indicated by circles

### *Sampling*

Samples of 1 mL were collected daily during the first week, then every three days during the first month and finally once per month until a total of six months of incubation. Samples were taken in sterile conditions from growing cultures under agitation. Hydrochloric acid (HCl) and ammonium hydroxide ( $\text{NH}_4\text{OH}$ ) were added to dissociate any precipitates of copper oxalates or calcium oxalates formed during incubation. Mycelium was removed by filtration using 13mm PTFE syringe filters with  $0.22\ \mu\text{m}$  pores from BGB (USA) and the filtrates were stored at a temperature of  $-20^\circ\text{C}$  until chromatographic analyses were performed.

### *Analytical methods*

The frozen filtrates were left at room temperature for one hour and diluted then with deionized water in order to arrive at an overall dilution factor of 5 and to avoid the clog of the column due to the density of the solvents (HCl and  $\text{NH}_4\text{OH}$ ). The solutions were analysed by high-performance liquid chromatography HPLC (Agilent 1100 series HPLC, Santa Clara, CA, USA) using an BP-100+ carbohydrate analysis column ( $300\ \text{mm} \times 7.8\ \text{mm}$ ) with guard column (same phase,  $50\ \text{mm} \times 4.6\ \text{mm}$ ) by Benson Polmeric™ (USA). The column was equilibrated in 20 mM  $\text{H}_2\text{SO}_4$  at  $40^\circ\text{C}$  and samples were eluted at a  $0.4\ \text{mL}\cdot\text{min}^{-1}$  flow rate. Organic acids were detected with a UV detector at 210 nm (G1315A, Agilent HPLC 1100 series). Data were acquired with ChemStation software (Agilent, Hewlett Packard, Waldbronn, Germany). Oxalic, citric, itaconic, oxalacetic, tartaric, malonic, succinic, propionic, acetic and fumaric acids were used as external standards.

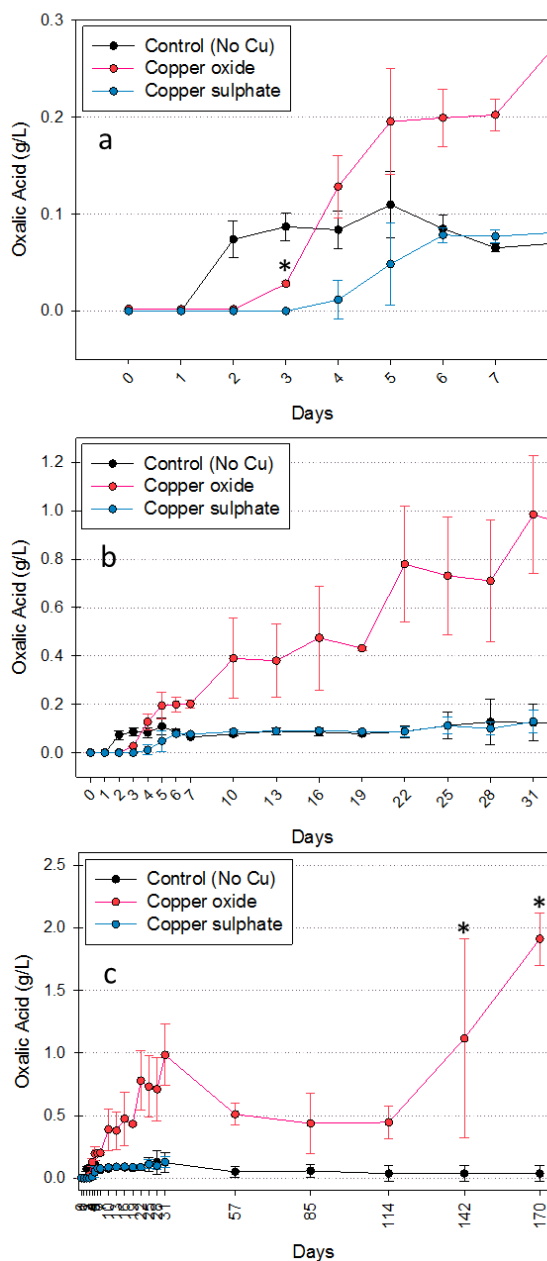
## Results and discussion

Oxalic acid was observed in all media at a retention time between 14, and 15.1 minutes.... A second peak was detected at a retention time of 26 minutes in the control at day 0 and day 1 and in MC (copper oxide amended) cultures from day 0 to day 7. The nature of this peak was not identified among the external standards used and further investigation will be conducted for its identification. Regarding oxalic acid, its production in the control medium started at day 2 and slightly increased during the following three days (Figure 12a). From day 5 a threshold was reached until the end of the first month (Figure 12b). After two months of incubation one of the control triplicates did not show the presence of oxalic acid while in the other two controls the amount of oxalic acid produced it halved. After four months of incubation, the presence of oxalic acid was not detected neither in the remaining control triplicates (Figure 12c). The highest concentrations of oxalic acid in MA were recorded at day 5 ( $0.11 \pm 0.03 \text{ g}\cdot\text{L}^{-1}$ ) and at day 28 ( $0.13 \pm 0.09 \text{ g}\cdot\text{L}^{-1}$ ). These results are assumed as the average production of oxalic acid by the strain S6. In the MB medium (amended with copper sulphate) the production of oxalic acid was slower. Indeed, the first record of oxalic acid was at day 4 (Figure 12a). This behaviour is probably due to the high toxicity of copper sulphate. In fact, this compound is completely soluble in water allowing the copper ions to rapidly get in direct contact with the fungus and inhibit its growth. Thereafter, at day 8 an oxalic acid concentration of  $0.8 \pm 0.01 \text{ g}\cdot\text{L}^{-1}$  was reached and remained stable until day 25, when a slight increase of oxalic acid production was observed (Figure 12b). For MB medium, samples were collected only during the first month and long term consideration cannot be extrapolated. However, during the first 31 days, the curve of oxalic acid production in MB medium follows the same trend as the control. Therefore, aside the slower initial production, the introduction of  $0.4 \text{ g}\cdot\text{L}^{-1}$  of copper sulphate in the medium did not affect the output of oxalic acid. It is worth noticing here that above this concentration no fungal growth was observed. Hence, either the copper content is still too toxic and does not allow fungal development or it may have reached a too low concentration being not enough toxic to trigger a resistance mechanism influencing the oxalic acid production. In order to verify which is the correct hypothesis, the analysis should be repeated at lower concentrations of copper sulphate to compare the oxalic acid production.

Regarding the MC medium, the fungal behaviour appeared to be considerably different. The fungus needed three days to produce oxalic acid, one day more than in the control medium, but already from the day 4 its amount was higher than in control (Figure 12a). At day 5 the oxalic acid content was double compared with the control, reaching a first threshold ( $0.20 \pm 0.05 \text{ g}\cdot\text{L}^{-1}$ ). Between day 10 ( $0.39 \pm 0.17 \text{ g}\cdot\text{L}^{-1}$ ) and 19 ( $0.43 \pm 0.17 \text{ g}\cdot\text{L}^{-1}$ ) a second threshold occurred, four times higher than in the control (Figure 12b). A third threshold was reached at day twenty-two ( $0.78 \pm 0.24 \text{ g}\cdot\text{L}^{-1}$ ), almost nine times higher than the control. After 31 days of incubation it seemed that the content of oxalic acid in the MC cultures was still growing arriving at  $0.98 \pm 0.25 \text{ g}\cdot\text{L}^{-1}$  (Table 2). During the following three months, the production of oxalic acid decreased except after five month of incubation when a new increment was observed, arriving at  $1.19 \pm 0.21 \text{ g}\cdot\text{L}^{-1}$  (Figure 12c).

From these data, it appeared that in the case of poorly soluble copper source the fungus reacted differently compared with the previous media. Indeed, in the case of copper oxide amended medium the production of oxalic acid was almost ten times higher than the amount found both in the control and in the copper sulphate amended media. Hence, the response to toxicity may vary according to the solubility of copper source. Results also showed that the production of oxalic acid in  $\text{Cu}_2\text{O}$  medium cultures did not followed a linear trend. This behaviour could be due to a discontinuous detoxification of the medium. Indeed, oxalic acid chelates copper ions in the solution forming insoluble copper oxalates and decreasing the content of copper ions. Once the Cu ions concentration is below the toxicity threshold, the fungus seems to stop the over-production of oxalic acid. However, as opposite reaction, the presence of oxalic acid decreased the pH of the solution solubilizing more copper oxide in the medium. Hence,

new copper ions are released and the fungus then continues producing more oxalic acid as response. This hypothesis could also explain the relatively low production of oxalic acid in the MB medium. In fact, this copper source was completely soluble and all copper ions were in solution reacting directly with oxalic acid produced at that time, forming copper oxalates and allowing the detoxification of the fungal environment. Therefore, an over-production of oxalic acid was not needed.



Day of measure	Control	Cu oxide	Cu sulphate
0	0.00 ± 0.00	0.00 ± 0.00	0.00 ± 0.00
1	0.00 ± 0.00	0.00 ± 0.00	0.00 ± 0.00
2	0.07 ± 0.02	0.00 ± 0.00	0.00 ± 0.00
3	0.09 ± 0.01	0.03* ± 0.00	0.00 ± 0.00
4	0.08 ± 0.02	0.13 ± 0.03	0.01 ± 0.02
5	0.11 ± 0.03	0.20 ± 0.05	0.05 ± 0.04
6	0.08 ± 0.01	0.20 ± 0.03	0.08 ± 0.01
7	0.07 ± 0.00	0.20 ± 0.02	0.08 ± 0.01
10	0.08 ± 0.01	0.39 ± 0.17	0.09 ± 0.01
13	0.09 ± 0.01	0.38 ± 0.15	0.09 ± 0.00
16	0.09 ± 0.02	0.47 ± 0.21	0.09 ± 0.01
19	0.08 ± 0.01	0.43 ± 0.01	0.09 ± 0.00
22	0.09 ± 0.02	0.78 ± 0.24	0.09 ± 0.02
25	0.11 ± 0.05	0.73 ± 0.24	0.11 ± 0.03
28	0.13 ± 0.09	0.71 ± 0.25	0.10 ± 0.03
31	0.12 ± 0.08	0.98 ± 0.25	0.13 ± 0.05
57	0.05 ± 0.05	0.51 ± 0.09	n.a.
85	0.06 ± 0.05	0.44 ± 0.24	n.a.
114	0.04 ± 0.06	0.45 ± 0.13	n.a.
142	0.04 ± 0.07	1.12* ± 0.80	n.a.
170	0.04 ± 0.06	1.19* ± 0.21	n.a.

Figure 12. Plots of the oxalic acid concentration in control (black), copper oxide (red) and copper sulphate (blue) amended culture media during the first seven (a), thirty-one (b) and hundred-seventy (c) days. The asterisks indicate the sets where one outlier was excluded from the calculation of the mean.

Table 2. Mean and standard deviation of the oxalic acid concentration measured in control, copper oxide and copper sulphate amended culture media. The asterisks indicate the sets where one outlier was excluded from the calculation of the mean.

Results also showed that, from the second up to the fourth month of incubation, in MC cultures the production of oxalic acid dramatically decreased and started again during the last two months. This could be due to the use of copper oxalates previously formed as carbon source or for other metabolic activities. Indeed, a previous study demonstrated that, in absence of other carbon sources, some fungi are able to degrade calcium oxalates and use it as carbon source [37]. Therefore, it may be possible that the strain of *B. bassiana* used here adopted this survival mechanism. It could also be suggested, as a daring theory, that the over-production of oxalic acid under prolonged stress conditions may be a storage mechanism of carbon source envisaging a lack of nutrients or the entrance in a dormant state. Nevertheless, no evidence from this study can support this hypothesis.

Regarding the use of the strain S6 for the treatment of copper-based alloys artefacts, some consideration can be done. It would be important to consider that the response in terms of oxalic acid production may vary depending on the copper source. Therefore, different corrosion products could induce a differential production of oxalic acid and, thus, a different formation of copper oxalates. Indeed, the presence of soluble corrosion products could inhibit the over-secretion of oxalic acid avoiding the formation of a homogenous layer of copper oxalates. However, copper oxide is formed as first corrosion product on copper-based objects and its presence should allow the fungus to behave as in the  $\text{Cu}_2\text{O}$  amended medium.

## Conclusions

In this study the production of oxalic acid by a specific strain of *B. bassiana* was assessed. Furthermore, the use of amended media allowed to evaluate the production of oxalic acid as a defensive mechanism against toxic copper. It appeared that the copper content initially inhibited fungal growth depending on the solubility of the product used. The higher the solubility of the copper source the more the degree of growth inhibition. The amount of oxalic acid produced by the fungus was counterintuitive with respect to the toxicity of the copper source. Furthermore, the production of oxalic acid was not linear over time but proceeded by a sequence of incremental steps. This is probably due to a cyclic reaction between the formation of copper oxalates and the dissolution of further solid copper phases due to medium acidification. Also, it seemed that the strain used for this study may be able to degrade copper oxalates previously formed in order to use them as carbon source. In order to confirm this hypothesis, further investigation in this direction needs to be performed. Finally, the use of *B. bassiana* for the transformation of copper corrosion products into copper oxalates seemed appropriate due to the high production of oxalic acid when in contact with the most common copper corrosion product, namely copper oxide.

## Supplementary Information

### *HPLC chromatograms*

A comparison between the control, MB (copper sulphate) and MC (copper oxide) media is here reported as supplementary information. Chromatograms of samples after 3, 5, 10 and 31 days of incubation are shown (Figures 13, 14, 15 and 16).

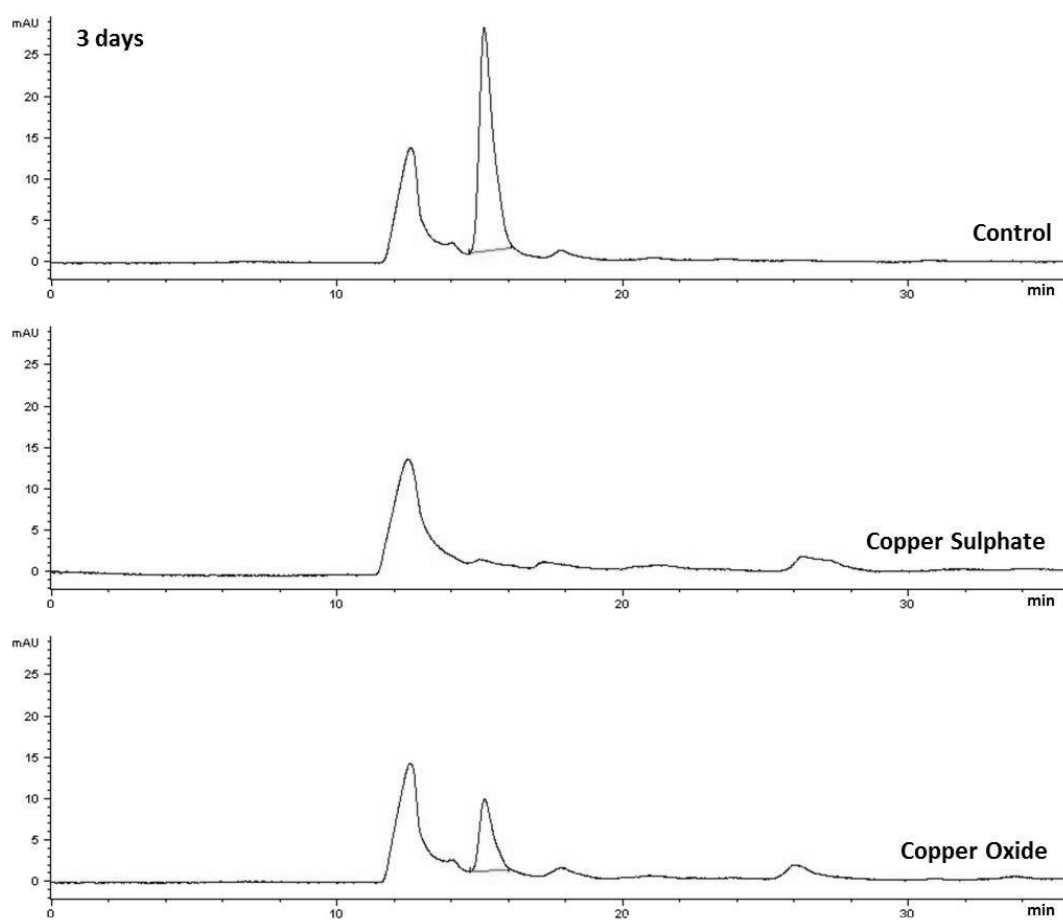


Figure 13. HPLC chromatograms of control, copper sulphate and copper oxide amended culture media after 3 days of incubation

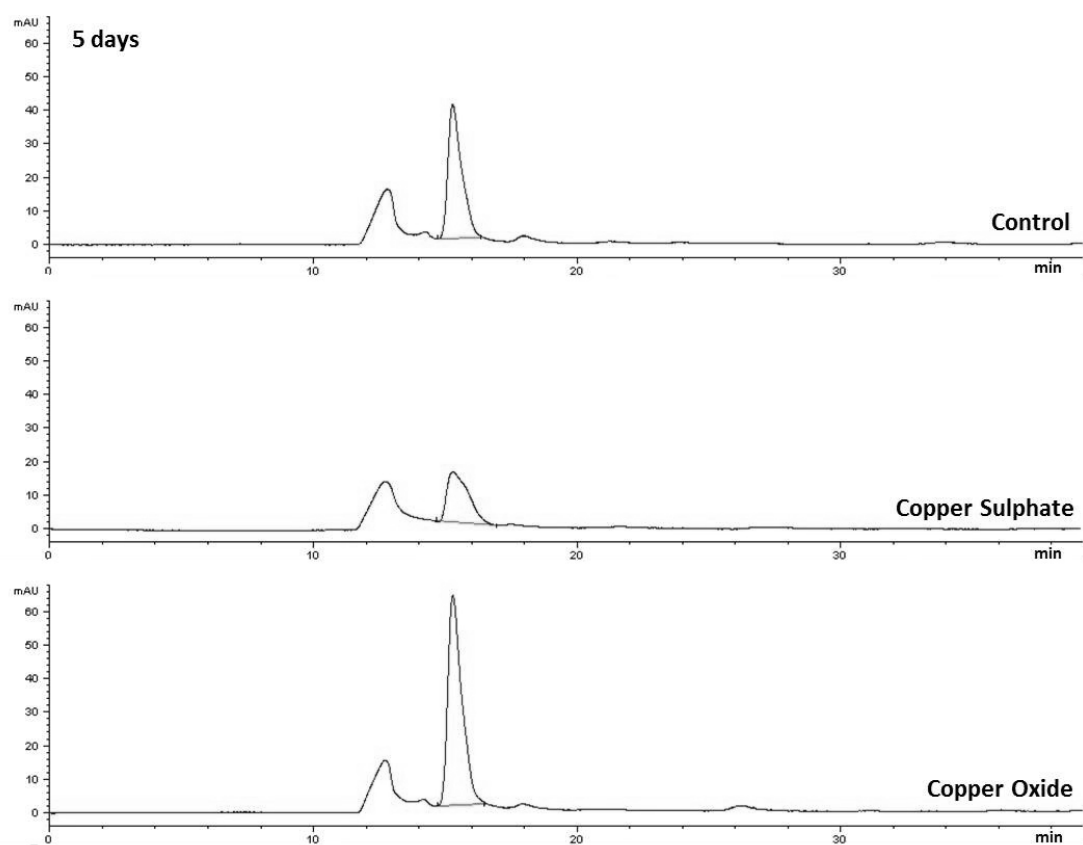


Figure 14. HPLC chromatograms of control, copper sulphate and copper oxide amended culture media after 5 days of incubation

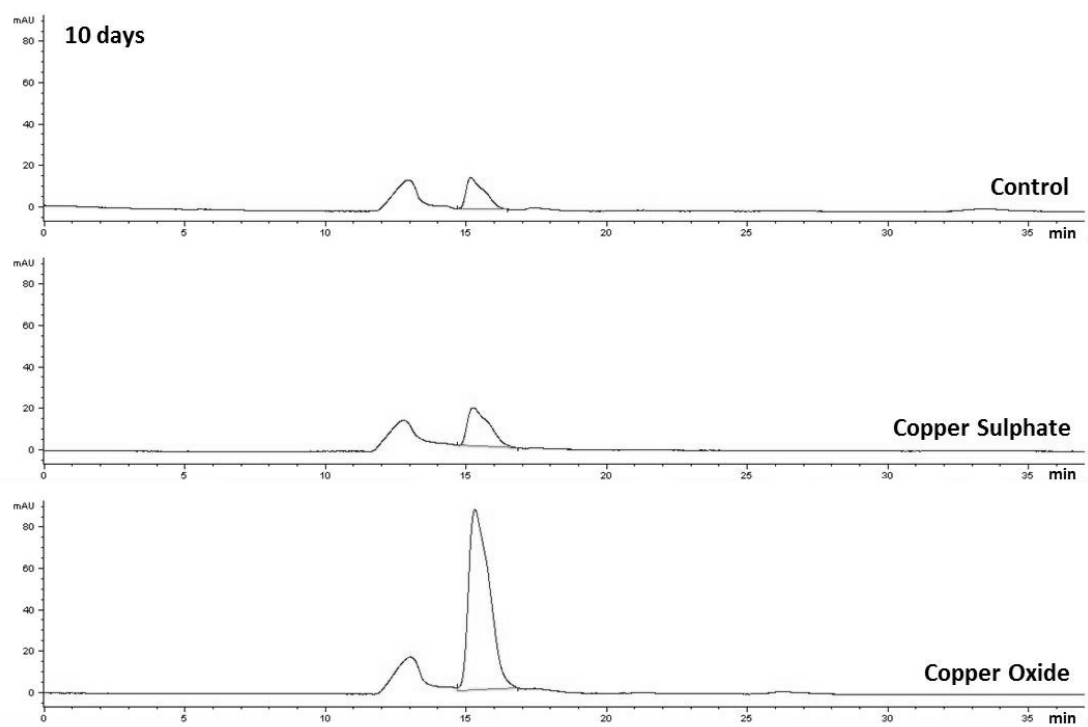


Figure 15. HPLC chromatograms of control, copper sulphate and copper oxide amended culture media after 10 days of incubation

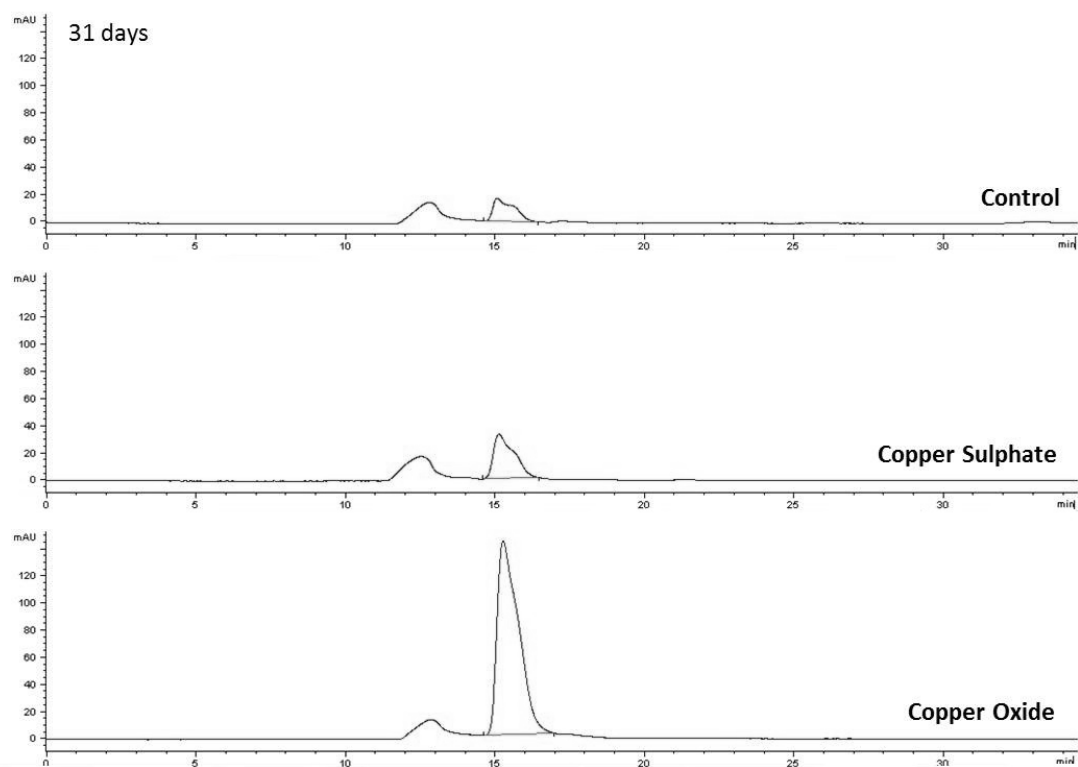


Figure 16. HPLC chromatograms of control, copper sulphate and copper oxide amended culture media after 31 days of incubation

*Delivery system*

In order to define the optimal delivery system for the biological treatment several substrates were tested. For this purpose, different known conservation-restoration products were used. The aim was to identify a delivery system that could be easily applied on metal artefacts, taking into account the three-dimension aspect of real objects, and that remained adherent on vertical surfaces for the duration of the treatment. Furthermore, the delivery system needs to be inert with the metallic treated substrate and with the microorganism. For this reason, transparency would be an undoubtable value allowing to verify the fungal growth and the appearance of the characteristic green colour of copper oxalates. Also, it needs to be easily removed from the treated surface, leaving no marks or residues. All products were prepared at different concentrations in order to obtain an optimal density. Thereafter, they were applied on vertical surfaces of copper-based objects, let in place for several days in order to simulate a real treatment and then removed. Due to the application of trade secret, the name of one of the tested delivery system is not disclosed and is here named as GelX. In Table 3 the main characteristics of the different tested substrates are summarised.

Substrate	Tested concentration	Transparency	Application ease	Vertical adhesion	No reactivity	Removal ease	Comments
Methylan®	30 to 50 gL <sup>-1</sup>	X	X	±	X	±	Cold preparation
Lutum® (ready-to-use)		-	X	X	X	±	Cold preparation
Lutum® (home recipe)		-	X	X	X	±	Cold preparation; Needs appropriate ratio between sand and clay components
GelX	10 to 40 gL <sup>-1</sup>	X	X	X	X	X	Cold preparation
Carbogel®	2.5 to 10 gL <sup>-1</sup>	X	-	±	±	X	Cold preparation
Carbopol®	6 to 10 gL <sup>-1</sup> + NaOH (%M)	X	X	X	±	X	Cold preparation; Needs pH neutralization
Cellulose pulp	200 gL <sup>-1</sup>	-	X	X	X	X	Cold preparation
Klucel®	2 to 50 gL <sup>-1</sup>	X	n.a.	n.a.	X	n.a.	Not gelling
Carboxymethyl-cellulose	100 gL <sup>-1</sup>	X	±	x	X	±	Similar to Methylan® but higher amount of product required
Tylose®	40 to 60 gL <sup>-1</sup>	x	±	X	X	-	Cold preparation
Arabic gum	50 gL <sup>-1</sup>	x	±	-	x	-	Cold preparation

Table 3. Main characteristics of the different substrates tested (x: yes; -: no; ±: partially)

Based on their characteristics and the results of the tests, three substrates based on Lutum®, Methylan® and GelX® were selected for further assays. Their behaviour will be presented in Chapters 3 and 4. Carbopol® was a promising candidate due to its transparency and gel consistence but it required a neutralization step that can impair fungal growth and it was discarded. The final protocol currently used and available for small trials to conservators-restorers is described in Annex 1.

## References

1. Meyling, N.V. and J. Eilenberg, Ecology of the entomopathogenic fungi *Beauveria bassiana* and *Metarhizium anisopliae* in temperate agroecosystems: potential for conservation biological control. *Biological control*, 2007. 43(2): p. 145-155.
2. Zimmermann, G., Review on safety of the entomopathogenic fungi *Beauveria bassiana* and *Beauveria brongniartii*. *Biocontrol Science and Technology*, 2007. 17(6): p. 553-596.
3. Gadd, G.M., Geomycology: biogeochemical transformations of rocks, minerals, metals and radionuclides by fungi, bioweathering and bioremediation. *Mycological Research*, 2007. 111(1): p. 3-49.
4. Inglis, G.D., et al., Use of hyphomycetous fungi for managing insect pests. *Fungi as biocontrol agents*, 2001: p. 23-69.
5. Bidochka, M.J., J.E. Kasperski, and G.A. Wild, Occurrence of the entomopathogenic fungi *Metarhizium anisopliae* and *Beauveria bassiana* in soils from temperate and near-northern habitats. *Canadian Journal of Botany*, 1998. 76(7): p. 1198-1204.
6. Meyling, N.V. and J. Eilenberg, Occurrence and distribution of soil borne entomopathogenic fungi within a single organic agroecosystem. *Agriculture, ecosystems & environment*, 2006. 113(1): p. 336-341.
7. Keller, S. and G. Zimmermann, Mycopathogens of soil insects. *Insect-fungus interactions*, 1989: p. 239-270.
8. Hajek, A.E., Ecology of terrestrial fungal entomopathogens, in *Advances in microbial ecology*. 1997, Springer. p. 193-249.
9. Gottwald, T. and W. Tedders, Studies on conidia release by the entomogenous fungi *Beauveria bassiana* and *Metarhizium anisopliae* (Deuteromycotina: Hyphomycetes) from adult pecan weevil (Coleoptera: Curculionidae) cadavers. *Environmental Entomology*, 1982. 11(6): p. 1274-1279.
10. Bing, L.A. and L.C. Lewis, Occurrence of the entomopathogen *Beauveria bassiana* (Balsamo) Vuillemin in different tillage regimes and in *Zea mays* L. and virulence towards *Ostrinia nubilalis* (Hübner). *Agriculture, ecosystems & environment*, 1993. 45(1-2): p. 147-156.
11. Posada, F. and F.E. Vega, Establishment of the fungal entomopathogen *Beauveria bassiana* (Ascomycota: Hypocreales) as an endophyte in cocoa seedlings (*Theobroma cacao*). *Mycologia*, 2005. 97(6): p. 1195-1200.
12. Quesada-Moraga, E., et al., Endophytic colonisation of opium poppy, *Papaver somniferum*, by an entomopathogenic *Beauveria bassiana* strain. *Mycopathologia*, 2006. 161(5): p. 323-329.
13. White, J.F., et al., Clavicipitalean fungal epibionts and endophytes—development of symbiotic interactions with plants. *Symbiosis*, 2002. 33(3): p. 201-213.
14. Elliot, S., et al., Can plants use entomopathogens as bodyguards? *Ecology Letters*, 2000. 3: p. 228-235.
15. Shimazu, M., H. Sato, and N. Maehara, Density of the entomopathogenic fungus, *Beauveria bassiana* Vuillemin (Deuteromycotina: Hyphomycetes) in forest air and soil. *Applied entomology and zoology*, 2002. 37(1): p. 19-26.
16. Ulevičius, V., et al., Field study on changes in viability of airborne fungal propagules exposed to UV radiation. *Environmental toxicology*, 2004. 19(4): p. 437-441.
17. Meyling, N.V. and J. Eilenberg, Isolation and characterisation of *Beauveria bassiana* isolates from phylloplanes of hedgerow vegetation. *Mycological research*, 2006. 110(2): p. 188-195.

18. Mitani, A., et al., Fungal keratitis caused by *Beauveria bassiana*: drug and temperature sensitivity profiles: a case report. *BMC research notes*, 2014. 7(1): p. 677.
19. Hallsworth, J.E. and N. Magan, Water and temperature relations of growth of the entomogenous fungi *Beauveria bassiana*, *Metarhizium anisopliae*, and *Paecilomyces farinosus*. *Journal of invertebrate pathology*, 1999. 74(3): p. 261-266.
20. Längle, T. *Beauveria bassiana* (Bals.-Criv.) Vuill.—A biocontrol agent with more than 100 years of history of safe use. in *Workshop on Current Risk Assessment and Regulation Practice* Salzau, Germany. 2006.
21. Shahid, A.A., et al., Entomopathogenic fungi as biological controllers: new insights into their virulence and pathogenicity. *Archives of Biological Sciences*, 2012. 64(1): p. 21-42.
22. Rehner, S.A. and E. Buckley, A *Beauveria* phylogeny inferred from nuclear ITS and EF1- $\alpha$  sequences: evidence for cryptic diversification and links to *Cordyceps* teleomorphs. *Mycologia*, 2005. 97(1): p. 84-98.
23. Rehner, S.A., et al., Phylogenetic origins of African and Neotropical *Beauveria bassiana* sl pathogens of the coffee berry borer, *Hypothenemus hampei*. *Journal of invertebrate pathology*, 2006. 93(1): p. 11-21.
24. Glare, T., Molecular characterization in the entomopathogenic fungal genus *Beauveria*. *Laimburg Journal*, 2004. 1: p. 286-298.
25. Strasser, H., A. Vey, and T.M. Butt, Are there any risks in using entomopathogenic fungi for pest control, with particular reference to the bioactive metabolites of *Metarhizium*, *Tolyocladium* and *Beauveria* species? *Biocontrol Science and Technology*, 2000. 10(6): p. 717-735.
26. Quesada-Moraga, E. and A. Vey, Bassiacridin, a protein toxic for locusts secreted by the entomopathogenic fungus *Beauveria bassiana*. *Mycological research*, 2004. 108(4): p. 441-452.
27. Roberts, D., *Toxins of entomopathogenic fungi. Microbial control of pests and plant diseases, 1970-1980*, 1981.
28. Vey, A., R.E. Hoagland, and T.M. Butt, 12 Toxic Metabolites of Fungal Biocontrol Agents. *Fungi as biocontrol agents*, 2001: p. 311.
29. Burford, E.P., M. Fomina, and G.M. Gadd, Fungal involvement in bioweathering and biotransformation of rocks and minerals. *Mineralogical Magazine*, 2003. 67(6): p. 1127-1155.
30. Gadd, G.M., Interactions of fungus with toxic metals. *New Phytologist*, 1993. 124(1): p. 25-60.
31. Jarosz-Wilkolazka, A. and G.M. Gadd, Oxalate production by wood-rotting fungi growing in toxic metal-amended medium. *Chemosphere*, 2003. 52(3): p. 541-547.
32. Gadd, G.M., Metals, minerals and microbes: geomicrobiology and bioremediation. *Microbiology*, 2010. 156(3): p. 609-643.
33. Fomina, M., et al., Role of oxalic acid overexcretion in transformations of toxic metal minerals by *Beauveria caledonica*. *Applied and Environmental Microbiology*, 2005. 71(1): p. 371-381.
34. Clausen, C.A. and F. Green, Oxalic acid overproduction by copper-tolerant brown-rot basidiomycetes on southern yellow pine treated with copper-based preservatives. *International Biodeterioration & Biodegradation*, 2003. 51(2): p. 139-144.
35. Colpaert, J.V., et al., Genetic variation and heavy metal tolerance in the ectomycorrhizal basidiomycete *Suillus luteus*. *New Phytologist*, 2000. 147(2): p. 367-379.
36. Sharples, J., et al., Genetic diversity of root-associated fungal endophytes from *Calluna vulgaris* at contrasting field sites. *New Phytologist*, 2000. 148(1): p. 153-162.
37. Guggiari, M., et al., Experimental calcium-oxalate crystal production and dissolution by selected wood-rot fungi. *International Biodeterioration & Biodegradation*, 2011. 65(6): p. 803-809.

## Chapter 3

---

### BIOPATINA FOR ARCHAEOLOGICAL OBJECTS



This chapter is based on the results of the following published article:

E. Domon Beuret, L. Mathys, L. Comensoli, L. Brambilla, M. Albini, C. Cevey, R. Bertholon, P. Junier, E. Joseph. *Biopatines: des champignons au service des alliages cuivreux*. In “Journées des restaurateurs en archéologie 2014: restaurer l'ordinaire, exposer l'extraordinaire : du site au musée“. Atelier de Conservation-Restauration du Musée Départemental Arles Antique (MDAA) et A-CORROS, Arles, 16th-17th October 2014. Cahier technique de l'ARAAFU 2015, 22, 45-48.

This part of the research was implemented in collaboration with Laténium Archaeological Park and Museum (Hauterive, Switzerland) and the Institute of Marine Sciences CNR-ISMAR (Genoa, Italy).

## Summary

In this chapter the use of the biological treatment (biopatina) for the stabilization of archaeological objects is discussed. In the first part of the chapter, the results of the comparison of three different delivery systems for the application of biopatina are presented. This allowed to select the most suitable delivery system in terms of effective copper oxalates production adherence to the surface, application and removal ease. Then, a first attempt of comparison between the biological treatment and benzotriazole (BTA), a corrosion inhibitor commonly used on archaeological artefacts, was performed. Accelerated ageing was performed on the treated coupons in order to evaluate the inhibition effect of both treatments on the active corrosion products present. This first part relies mostly on visual observations and Fourier Transform Infrared Spectroscopy.

The second part of the chapter is devoted to an in-depth comparison between benzotriazole and biopatina. The purpose of this section is to compare the two treatments in terms of conversion and corrosion stabilization of an artificial patina composed of copper hydroxychlorides, i.e. atacamite. The biological treatment and benzotriazole were applied on triplicates of copper coupons covered with synthesized copper hydroxychlorides. The surface and cross-section of the samples were fully characterized by Fourier Transform Infrared Spectroscopy, Scanning Electron Microscopy and Electrochemical Impedance Spectroscopy. Results demonstrated that the biological treatment converted almost all atacamite present and enhanced the surface inhibition against corrosion giving better results than benzotriazole. This research gives a significant contribution to the current development of non-toxic and efficient inhibitors that could replace benzotriazole, highly suspected carcinogen.

### 3.1 First stabilization tests on archaeological objects

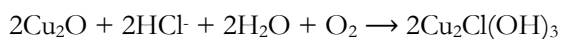
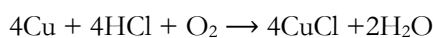
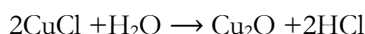
#### Abstract

Archaeological artefacts undergo to changes of state after excavation. Indeed, they need to reach equilibrium with the new environment and, in some cases, dormant corrosion processes can be activated. A dangerous cyclical mechanism can occur due to the presence of copper chlorides and is commonly defined as “bronze disease”. In this study, the biopatina treatment was used in order to stabilise active corrosion processes on archaeological objects. Different delivery systems were tested in order to identify the most appropriate one to be used on such delicate artefacts. A clay mixture based on Lutum®, Metylan® gel and GelX® were tested. Furthermore, the inhibition properties of the biological treatment were compared to a reference inhibitor, benzotriazole (BTA), through accelerated ageing procedures. Promising results about the inhibition effect of biopatina were achieved. Indeed, it seems that the biological treatment is as efficient as the BTA in terms of corrosion inhibition on chlorine-contaminated objects.

#### Introduction

After excavation, archaeological artefacts tend to suffer from changes of their state in order to find equilibrium with the new environment. These modifications can lead to the activation of corrosion mechanisms that were dormant while burial. Moreover, the storage and display conditions inside museums are unfortunately often uncontrolled, with frequent fluctuation of temperature and relative humidity that enhances corrosion processes. Furthermore, the presence of pollutants in indoor environment can cause the development of further corrosion [1].

The most common corrosion products that can be found on bronze archaeological objects are cupric oxide (cuprite), basic copper carbonates (malachite and azurite), copper phosphates (libethenite) and copper hydroxychlorides (nantokite, atacamite and paratacamite) [2]. The latter are considered the most dangerous corrosion products for copper-based alloys and form the so called “bronze disease”. Indeed, the presence of nantokite, oxygen and moisture in contact with copper triggers a series of cyclical reactions that form cupric oxide and atacamite bringing to severe damages and finally loss of the artefact [3, 4], as described by the following reactions:



In order to prevent or stop ongoing corrosion processes conservation treatments are then needed. At first, mechanical or chemical cleaning of powdery and uncoherent corrosion products is performed followed by the consolidation of the objects. Finally, protective treatments are applied. Nowadays, protective coating such as Incralac®, Paraloid B72 or microcrystalline waxes, inhibitors as benzotriazole or a combination of the two are commonly used by conservator-restorers on archaeological objects [5]. Nevertheless, these treatments interact with the artefact changing its aspect, particularly its colour and brightness [6]. Moreover, they are not completely efficient in the protection of the object and most of them are toxic for the operators and the environment [7]. For this reason, conservator-restorers are looking for novel efficient and harmless alternatives to such treatments.

In this study the use of biopatina was evaluated as corrosion inhibitor in comparison with BTA as reference treatment. Furthermore, different delivery systems were tested in order to optimize the application protocol for archaeological objects. Also, the validation on real artefacts allowed to demonstrate the efficiency of biopatina on different copper corrosion products. All treated objects underwent to accelerated ageing procedures in order to estimate the long-term behaviour of both biopatina and reference treatment.

## Materials and Methods

### *Artefacts*

#### Test objects

In order to compare different treatment application protocols and minimize the possible risks occurring when testing new products several “test objects” were selected (Laténium collection). A total amount of twenty-two bronze artefacts were chosen for the possible presence of active corrosion induced by copper chlorides (Table 4). The patina layers were formed after a long burial period and post-excavation storage under uncontrolled environmental conditions. At the time of the study there was no information about the exact nature of the copper alloys, the objects provenance or eventual past conservation-restoration interventions.

#### Real objects

As well as for the “test objects” the “real artefacts” chosen came from the Laténium collections and were selected due to the possible presence of active corrosion induced by copper chlorides (Table 5). At the time of the study, there was no information about the exact nature of the copper alloys, the objects provenance or eventual past conservation-restoration interventions.

### *Treatments*

The treatment commonly used by the Laténium conservation-restoration department for archaeological copper-based objects, when corroded by chlorides, is the following. A first mechanical cleaning of the corrosion layers is performed aiming to access the original surface where details are well conserved. The localization of this surface, also known as *limitos*, should indeed be determined before any intervention on the object by establishing a stratigraphy of the corrosion products and a visual documentation as complete as possible. Then, 1% w/w benzotriazole (BTA) solution in ethanol is applied as corrosion inhibitor by immersion for 1 hour followed by a layer of acrylic resin (usually 20% w/w Paraloid B72 solution in acetone), doubled with microcrystalline wax protective coating. On archaeological samples, the biopatina was compared with BTA in terms of performance, efficiency and durability. The objects selected were divided into 3 groups (Untreated, Biopatina treatment and BTA treatment) according to their composition and dimensions (Table 4 and Table 5).

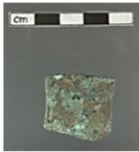
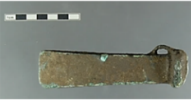
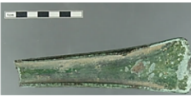
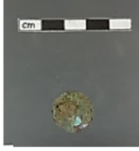

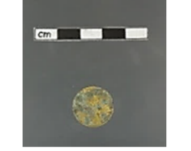


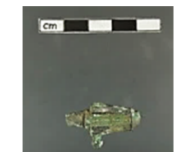

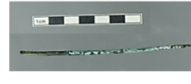
Untreated	Biopatina	BTA
 <p><b>A-6 Coin fragment</b></p> <p><i>Main patina components</i></p> <p>Cu chlorides Cu sulphates</p>	 <p><b>F-23 Axe blade</b></p> <p><i>Main patina components</i></p> <p>Cu chlorides Cu carbonates Cu sulphates Organic substance</p>	 <p><b>F-Agen-15 Axe blade</b></p> <p><i>Main patina components</i></p> <p>Cu chlorides Cu carbonates Silicates</p>
 <p><b>A-2 Coin</b></p> <p><i>Main patina components</i></p> <p>Cu chlorides</p>	 <p><b>A-5 Coin</b></p> <p><i>Main patina components</i></p> <p>Cu chlorides Organic substance</p>	 <p><b>A-3 Coin</b></p> <p><i>Main patina components</i></p> <p>Cu chlorides Cu carbonates Cu sulphates Organic substance</p>
 <p><b>A-12 Indetermined fragment</b></p> <p><i>Main patina components</i></p> <p>Cu chlorides Silicates Organic substance</p>	 <p><b>A-11 Belt strap</b></p> <p><i>Main patina components</i></p> <p>Cu chlorides Cu carbonates Organic substance</p>	 <p><b>A-10 Fibula</b></p> <p><i>Main patina components</i></p> <p>Cu chlorides Cu carbonates Silicates Organic substance</p>
	 <p><b>CH-518 Pin</b></p> <p><i>Main patina components</i></p> <p>Cu carbonates Cu sulphates Organic substance</p>	
	 <p><b>CH-947 Pin</b></p> <p><i>Main patina components</i></p> <p>Cu carbonates Cu sulphates Organic substance</p>	

Table 4. Test objects: patina composition determined by FTIR analysis and respective treatment assignment



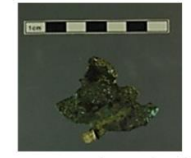



Untreated	Biopatina	BTA
 <p><b>Unnumbered Spearhead</b></p> <p><i>Main patina components</i></p> <p>Cu chlorides Silicates Organic substance</p>	 <p><b>Eg-530 Osiris statuette</b></p> <p><i>Main patina components</i></p> <p>Cu chlorides Organic substance</p>	 <p><b>CH-287 Indetermined fragment</b></p> <p><i>Main patina components</i></p> <p>Cu chlorides Organic substance</p>
 <p><b>EU-52 Necklace</b></p> <p><i>Main patina components</i></p> <p>Cu chlorides Organic substance</p>	 <p><b>Unnumbered Bracelet</b></p> <p><i>Main patina components</i></p> <p>Cu chlorides Organic substance</p>	 <p><b>Unnumbered Fibula</b></p> <p><i>Main patina components</i></p> <p>Cu chlorides Cu carbonates Cu sulphates Silicates Organic substance</p>

Table 5. Real objects: patina composition determined by FTIR analysis and respective treatment assignment

### Benzotriazole (BTA)

Since the most concerning problem of archaeological objects is the reactivation of corrosion mechanisms, it was decided to compare the biopatina treatment with BTA, a commonly used corrosion inhibitor. BTA does not remove copper chlorides from the corrosion layers but forms a layer of Cu-BTA polymeric complexes. Hence, a preliminary mechanical cleaning was necessary, in particular on chlorides pustules and craters. After this step, the samples were impregnated under vacuum with a 1% w/w benzotriazole solution in deionized water (pH 6) for 3 hours [8] using a vacuum chamber Salvis® (50 mbar pressure) and then immersed for 28 days under agitation in the same solution. It should be noticed here that there is no agreed protocol in the literature for the application of benzotriazole solutions. Dugdale and Cotton, Watkinson as well as Brostoff [9-11] reported that BTA forms a polymeric complex with copper on top of the corrosion products actin as a barrier for corrosion and that this film is very thin and chemically resistant. Recently, it was also proposed that BTA protects copper in aqueous and gaseous environments polluted with sulphur dioxide, hydrogen sulphide and salt mist [12]. Also, the chosen solvent for the preparation of BTA solution seems to be arbitrary and subject to individual practices.

### Biopatina treatment

Following the screening on the delivery systems discussed in chapter 2, two different kinds of delivery systems were first chosen for testing the application of the biological treatment: a carboxycellulose-based gel (Metylan®) and a mixture of clay products (based on Lutum®). Liquid pre-cultures of *B. bassiana* were mixed with the delivery systems adding nutrients for the fungal growth. Both systems presented the following advantages:

- Application and removal ease
- No interaction of the material with the fungus and the metal substrate
- Transparency, only for Metylan®, allowing the observation of the fungal growth.

The protocol used for biopatina treatment on “test objects” was defined in 10 steps:

1. Sterilization of artefacts and tools with 70% w/w ethanol solution
2. Preparation of a polyethylene (PE) film (Pluriball) previously punched for the packaging of artefacts. A micro-perforated PE film, for example Tredegar film, can be used as alternative
3. Application on PE film of a thin layer of the chosen delivery system by spatula
4. Application on artefacts of a thin layer of the chosen delivery system (around 5mm) by spatula and/or brush, starting from the holes and concave parts
5. Placing of artefacts on PE film and retouching of the delivery system films for a better uniformity
6. Packing of artefacts
7. Storage of artefacts in a PE box for a duration of the treatment of 2,5 weeks
8. Sampling of the delivery systems submitted to FTIR analyses
9. Cleaning under stereomicroscope with different tools and brushes using 70% w/w ethanol solution
10. Evaluation of the treatment’s performance by visual observations and FTIR analyses

After the characterization of the two delivery systems resulting in poor performance, a second optimized treatment was performed on “test objects”. The biopatina treatment application was repeated on the same objects for 4 additional weeks using the Metylan<sup>®</sup> gel and packing the objects in Tredegar<sup>®</sup> film.

Because of results obtained on “test objects” a new delivery system was used on archaeological “real objects”. Indeed, the Metylan<sup>®</sup> gel presented removal difficulties. Thus, due to the similar positive characteristic in common with Metylan<sup>®</sup> gel (i.e. transparency, neutral pH, easy application) without its removal difficulties, the GelX formulation was selected. Regarding the other parameters, the protocol remained identical in terms of nutrient concentration and active fungal culture. The “real objects” were treated for 28 days.

#### *Visual characterization*

A stereomicroscopy Olympus SZ-61 and a camera Canon 8800F were used before and after treatment and after artefacts ageing. All acquisition parameters (light, acquisition time, magnification, RVB, saturation, contrast, brightness) were set identical.

#### *Fourier Transform Infrared Spectroscopy*

Samples were analyzed taking out micro-particles (around 30  $\mu\text{m}$ ) under a stereomicroscope and positioning them onto a diamond Attenuated Total Reflectance (ATR) crystal plate. Spectra were acquired in the range using an iS5 Thermo Scientific spectrometer connected to an iD<sup>TM</sup>5 ATR accessory or a Thermo iN10MX spectrometer and recorded either in reflection (%R) or in attenuated total reflectance (ATR) mode. All the spectra were acquired in the range 4000 – 650  $\text{cm}^{-1}$ . A total of 64 scans were recorded with a resolution of 4  $\text{cm}^{-1}$  and the resulting interferogram averaged. Data collection and post-run processing were carried out using the Thermo Scientific Omnic<sup>TM</sup> software. On each sample, several measurements were carried out at different spots. The patina composition before treatment for each artefact is summarized in Table 4 (test objects) and Table 5 (real objects).

#### *Ageing procedures*

##### Accelerated ageing of “test objects”

The artificial accelerated ageing simulates an accelerated atmospheric corrosion by placing samples under controlled conditions of temperature and relative humidity cycling, as described in the International Standard ISO/FDIS 16701 [13]. The efficiency of BTA and biopatina were evaluated comparing the behaviour of treated samples to untreated reference samples. The selected ageing protocol simulated an uncontrolled indoor environment. The procedures were carried out in a climatic chamber (VC0020 by Voetsch<sup>®</sup> using Simpati4<sup>®</sup> data recording software). The “test objects” were positioned inside the chamber on an aluminium tray covered with a micro-perforated polyethylene film (Figure 17). The objects were put in a slightly leaning position using bamboo sticks in order to have a greater surface of the objects in contact with the chamber environment. The cycling conditions were fixed according with literature at 35°C and 95% RH for 12 hours and at 20°C and 50% RH for other 12 hours (Figure 18). Mild corrosion conditions were chosen by alternated wet and dry cycles. A total of 30 cycles were achieved.

##### Natural ageing of “real objects”

After treatment, “real objects” remained in the conservation-restoration laboratory of the Laténium museum in a semi air-conditioned room (uncontrolled, only ventilation). Natural storage ageing was preferred in this case in order to preserve such delicate artefacts from extreme ageing conditions. A visual control of the objects and a photographic documentation allowed to evaluate the behavior of the

treated objects. The relative humidity varied between 30% and 60% and was continuously recorded during the storage period by the dataloggers Testo 174H® (data collected every hour). Data of the ageing period are reported on Figure 19.



Figure 17. Climatic chamber used for the ageing procedures on LAT samples showing the aluminium trail covered with a micro-perforated plastic film

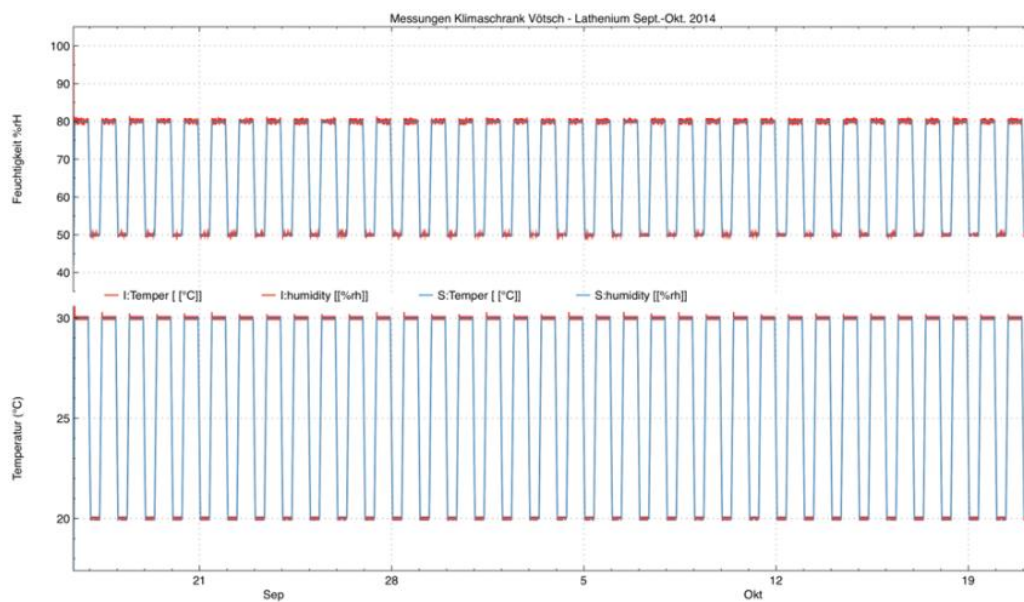


Figure 18. Data recorded during the one month cycle of ageing showing the regularity of the artificial climate generated inside the chamber: The upper chart represents the relative humidity, the lower chart the temperature

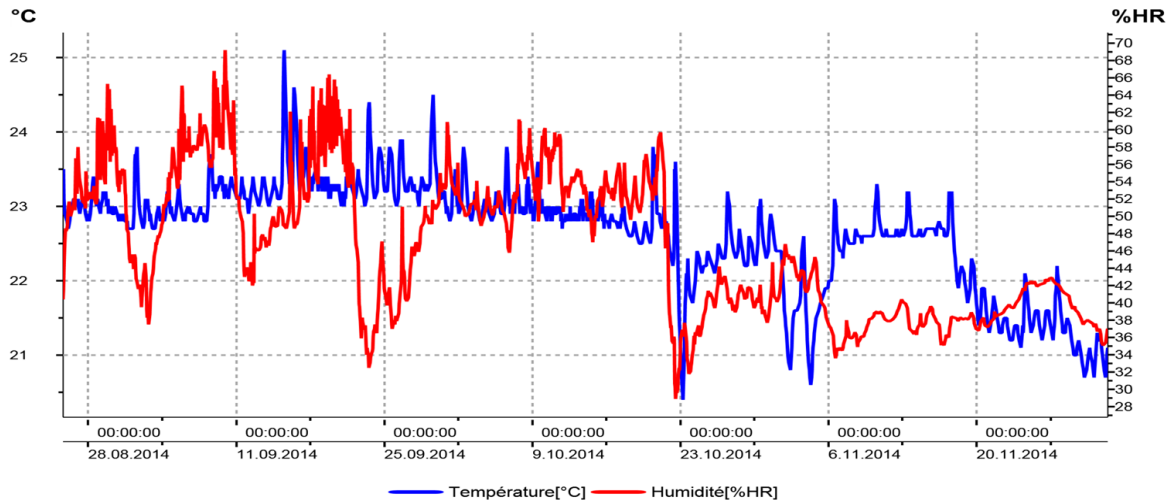


Figure 19. Climate during July and November 2014 in the laboratory of Laténium Museum, Hauterive

## Results

### *Test objects*

After BTA treatment a slight colour change and darkening of the patina were observed on the objects. In particular, some residues of BTA were visible as a thin white layer on the incised decorations or holes on objects (Figure 20 and Figure 21)

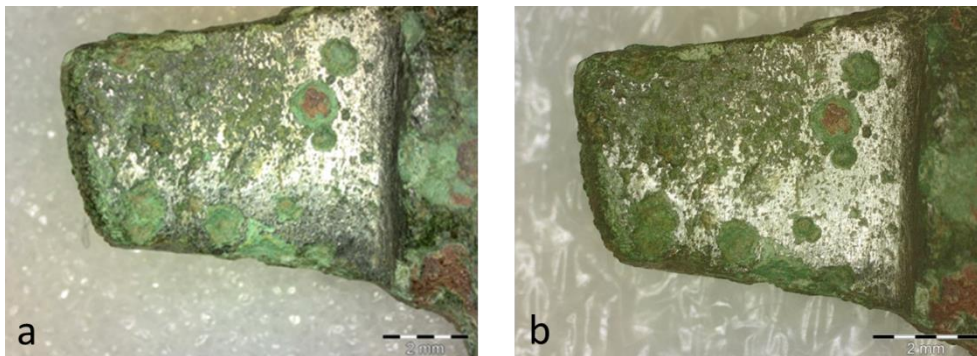


Figure 20. Fibula A-10 before (a) and after (b) BTA treatment

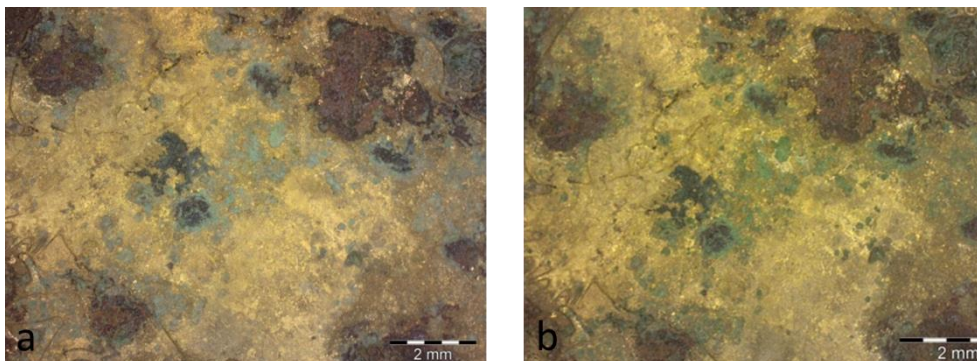


Figure 21. Coin A-3 before (a) and after (b) BTA treatment

FTIR analysis showed a low presence of benzotriazole on objects surface (characteristic peaks at  $\sim 2954$ ,  $2921$ ,  $2849$ ,  $1630$ ,  $1270$ ,  $1212$ ,  $1146$   $\text{cm}^{-1}$ ). Spectra also showed (Figure 22) the presence of malachite (characteristic peaks at  $\sim 1505$ ,  $1385$ ,  $1098$ ,  $1045$ ,  $872$ ,  $816$ ,  $750$   $\text{cm}^{-1}$ ) and, on sample Lat-A10-02, copper chlorides. A summary of the products detected on BTA treated samples is presented in Table 6.

SAMPLE	FTIR RESULTS
Lat-AGEN15-01	Malachite and benzotriazole
Lat-AGEN15-02	Malachite and benzotriazole
Lat-A10-02	Malachite and copper chlorides
Lat-A10-03	Malachite
Lat-A3-01	Malachite and benzotriazole
Lat-A3-02	Benzotriazole

Table 6. Summary of products detected with FTIR analysis on samples surface treated with benzotriazole

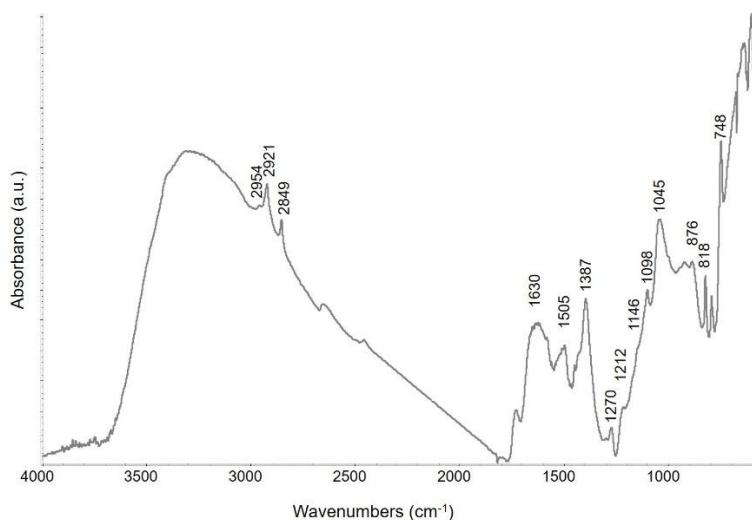


Figure 22. ATR-FTIR spectra showing the presence of malachite and benzotriazole on Lat-Agen15-02

After biopatina treatment no degradation or colour changes occurred on the surface of the objects and details were well preserved (Figure 23, 24 and 25). Moreover, the protocol using Metylan® gel appeared to be more efficient forming a higher amount of copper oxalates even if just a partial formation of this latter was observed (data not shown). Indeed, copper oxalates were not evenly distributed on the objects surface. This could be due to the medium itself, whose density could had inhibited the fungal growth, or to a low initial fungal concentration.



Figure 23. Axe blade F-23 before intervention (a), during mechanical cleaning (b), during biological treatment using a clay mixture (c), after 2,5 weeks of treatment with white spots confirm the fungal growth (d) and after treatment removal (e)

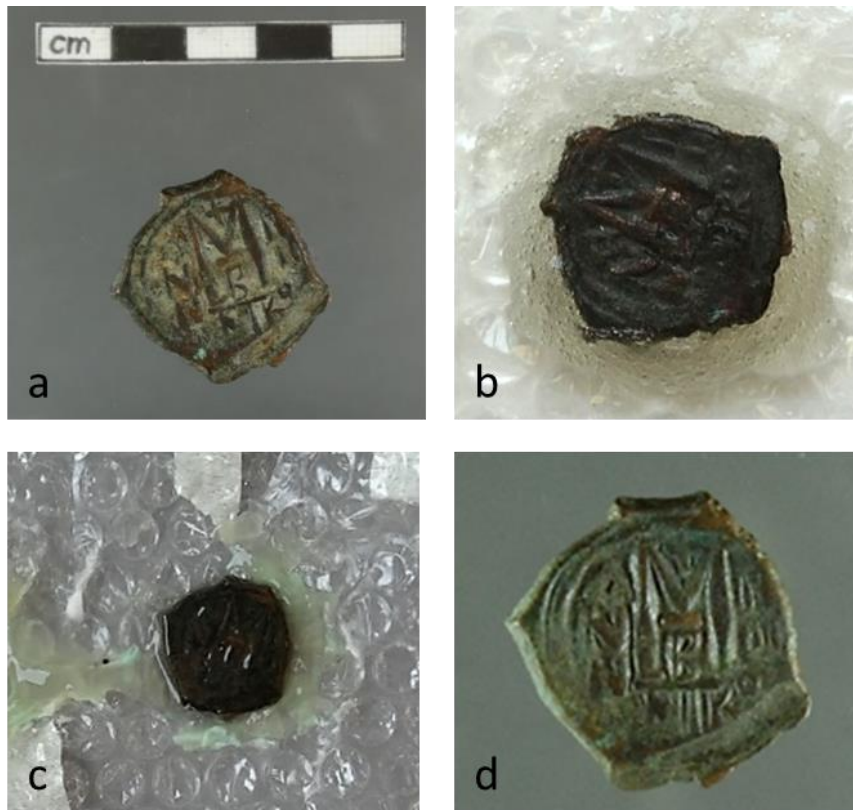


Figure 24. Coin A-5 before treatment (a), during biological treatment using Metylan® (b), after 2,5-weeks treatment with light green parts confirming the formation of copper oxalates (c) and after treatment removal (d)

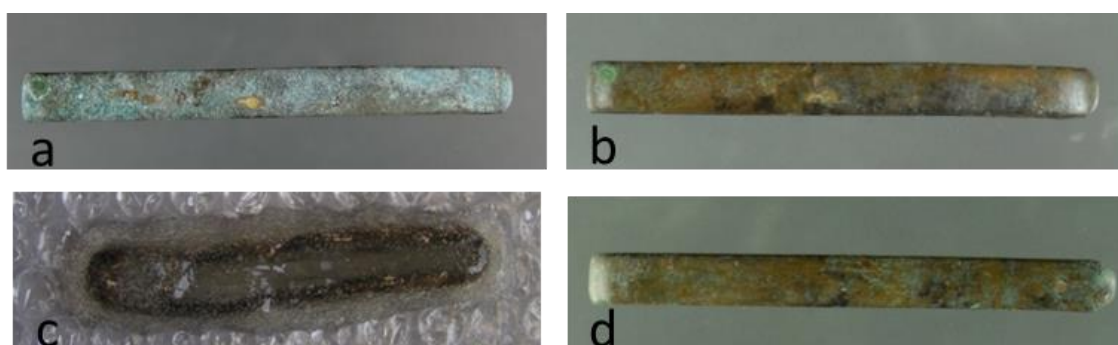


Figure 25. Belt strap A-11 before treatment (a), after mechanical cleaning with scalpel (b), c) during biological treatment using Metylan® and after treatment removal (d)

The characteristics of the two delivery systems were also evaluated. Both Metylan® and the clay mixture resulted easy to apply. However, their high density may had inhibited the fungal growth. Furthermore, the transparency of the medium was an issue for the visual control of the fungal growth and the examination of the artefact during treatment. The clay mixture is thus not optimal for these purposes. Another important characteristic of a suitable delivery system is its adherence to the treated surface and its removal ease. Regarding the surface adherence, the clay mixture presented good properties while Metylan® resulted in poor adherence, which could pose potential problem for the treatment of large dimension objects. Moreover, both delivery systems presented some difficulties during their removal. Indeed, the clay mixture is partially abrasive and, if not properly handled, could damage the treated surface. The Metylan® gel partially stuck to the surface in thin layers that were difficult to recognize and remove.

Further observation about the used protocol regarded the polyethylene film. Other films as Tredegar® were tested in the following experiments, because of a higher degree of transparency, minor thickness and breathable component.

In order to obtain a homogeneous layer of copper oxalates on the “test objects”, a second optimized treatment was thus performed. The treatment application was repeated for 4 additional weeks using the Metylan® gel and packing the objects in Tredegar® film.

The Tredegar® film allowed a visual control of the fungal growth and of the objects during treatment thanks to its transparency (Figure 26). After treatment, it was visually noted that a thin whitish layer was formed on one of the treated objects. The colour of the original patina seems also slightly modified: the black-brownish areas turned light brown, dark red areas appeared bright red and light green areas became more brownish (Figure 27).

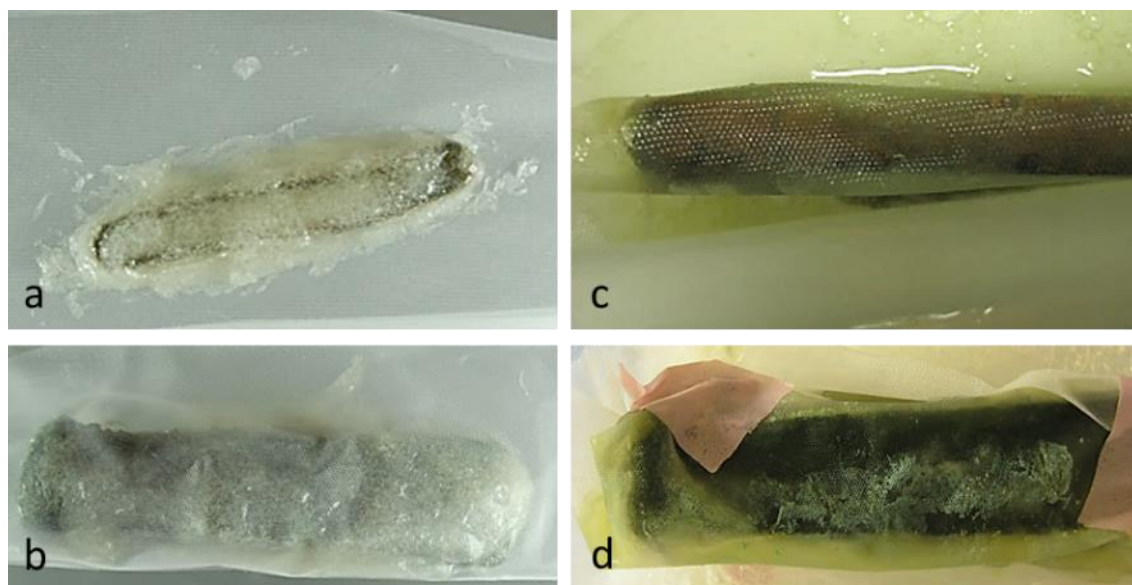


Figure 26. LAT samples treated with biopatina: A-11 (a) and F-23 (b) samples during application of Metylan® gel and packaging with Tredegar® film; A-11 (c) and F-23(d) samples after 28 days of treatment

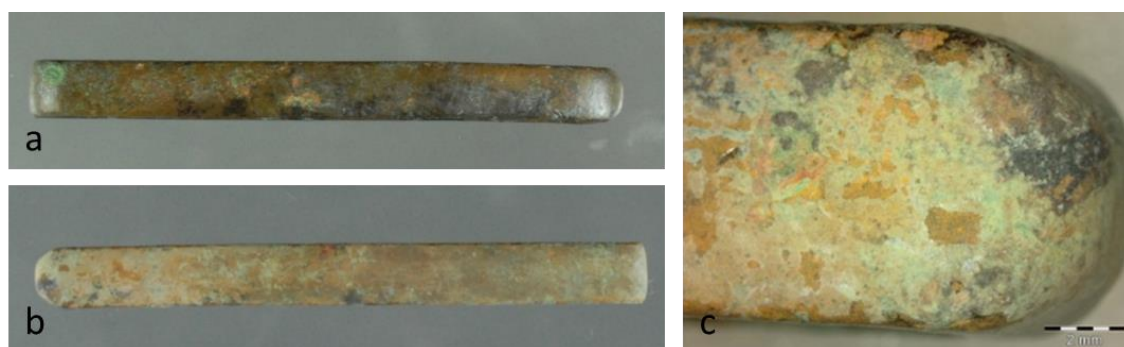


Figure 27. Sample A-11 after mechanical cleaning (a), after 28 days of biological treatment (b) with detail of the surface with a thin white layer indicating the presence of copper oxalates (c)

However, FTIR analyses after treatment demonstrated that copper oxalates were formed uniformly on all objects surfaces (Figure 28). Nevertheless, residues of methyl cellulose (Metylan®) and sugar (fungal nutrient) were observed in almost all samples (Figure 28b), suggesting that post-treatment cleaning by immersion baths and brushing was not sufficient. Therefore, cleaning was repeated by mechanical means: a soft brush first and then a scalpel. The scalpel was manipulated gently as loss of matter can occur. In order to avoid time-consuming post-treatment cleaning, another delivery system was tested for the application on “real objects”.

Before and after accelerated ageing visual observations were carried out (Table 7) on characteristic areas showing copper chlorides efflorescence (craters, pustules, blisters, etc.) as detected by FTIR analyses. Only few visible changes on objects treated with benzotriazole or with biopatina were visible after treatment, meaning that active corrosion was stabilized at the same order of magnitude by both treatments (Figures 29, 30 and 31). However, on untreated objects new efflorescence were noticed, with the exception of the object A-12. This sample may have possibly undergone previous conservation-restoration intervention and application of an anti-corrosion treatment (as organic substances were identified by FTIR analyses).

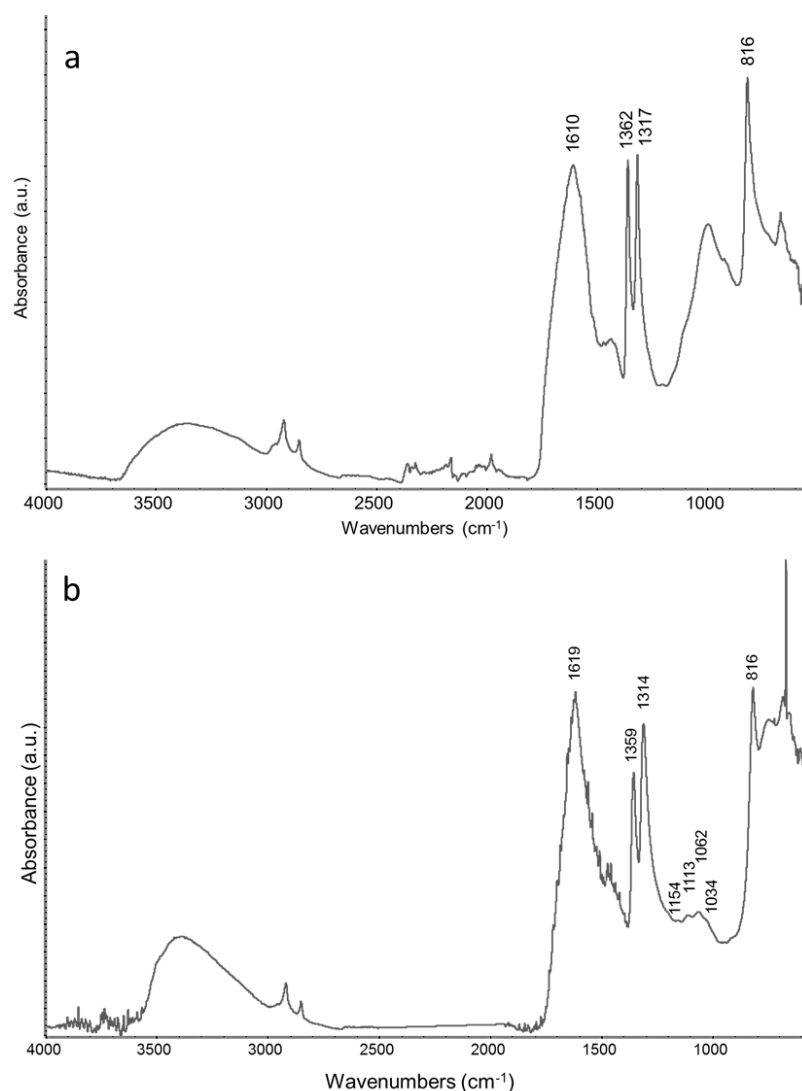


Figure 28. ATR-FTIR spectra showing the presence of copper oxalate (characteristic peaks at  $\sim 1615$ ,  $1360$ ,  $1315$  and  $1815$   $\text{cm}^{-1}$ ) on A5 (a) and on A11 (b) samples with residues of Metylan® (peaks at  $1154$ ,  $1113$ ,  $1062$  and  $1034$   $\text{cm}^{-1}$ )

Sample	Treatment	Areas observed	Corrosion reactivation after ageing
A-2	untreated	5	Yes
A-6	untreated	6	Yes
A-12	untreated	3	No
A-3	BTA	4	No, barely observable
A-10	BTA	5	No, barely observable
F-Agen-15	BTA	4	No, barely observable
A-5	Biopatina	5	No, barely observable
A-11	Biopatina	10	No, barely observable
F-23	Biopatina	5	No, barely observable
CH-518	Biopatina	2	No, barely observable
CH-947	Biopatina	2	No, barely observable

Table 7. Summary of visual observations done after ageing on test objects regarding the corrosion reactivation

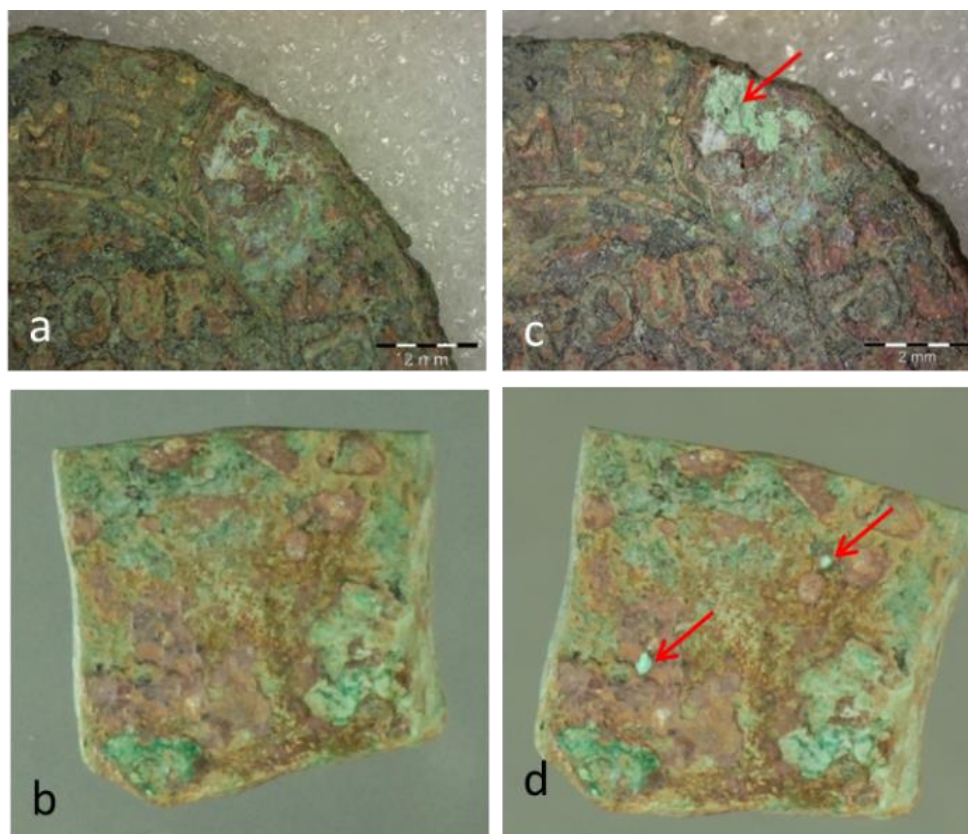


Figure 29. Untreated objects A2 and A6 before ageing (a-b) and after ageing (c-d) respectively. New efflorescences indicated by red arrows

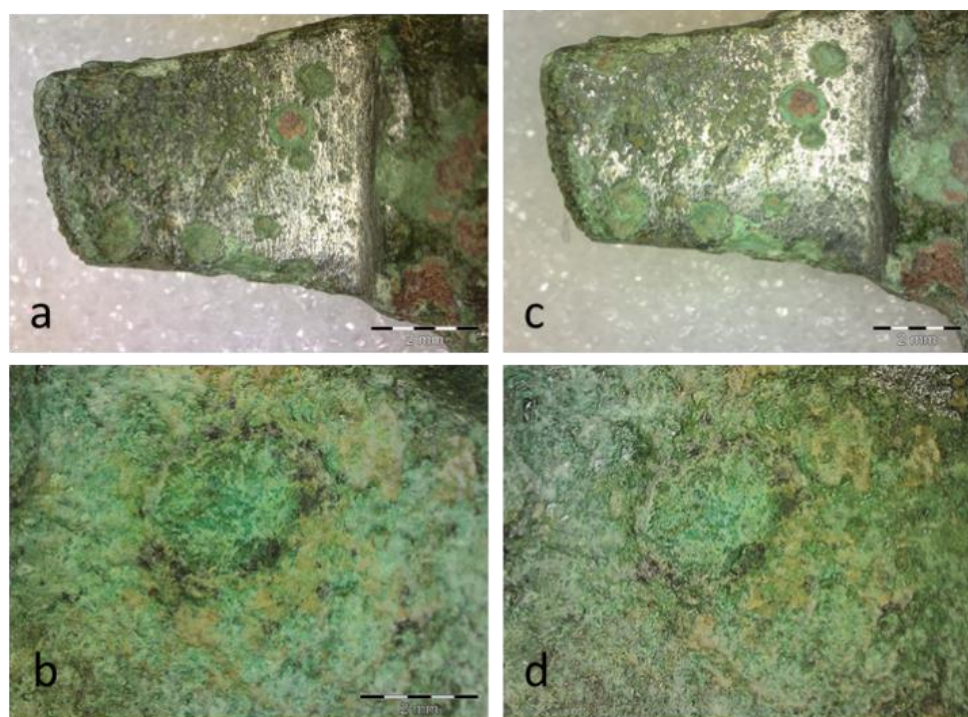


Figure 30. BTA-treated objects A10 and F-Agen-15 before ageing (a-b) and after ageing (c-d) respectively. No significant visual changes



Figure 31. Biopatina-treated objects F23 and A5 before ageing (a-b) and after ageing (c-d) respectively. No significant visual changes

#### *Real objects*

The additional delivery system used for biopatina and applied on the “real objects” remained adherent and produced a thin layer of copper oxalates on the overall treated surfaces (Figure 32). Moreover, it was easy to apply and remove, leaving no residues on the surface (Figure 33) demonstrating that this delivery system is the best option among the tested ones.

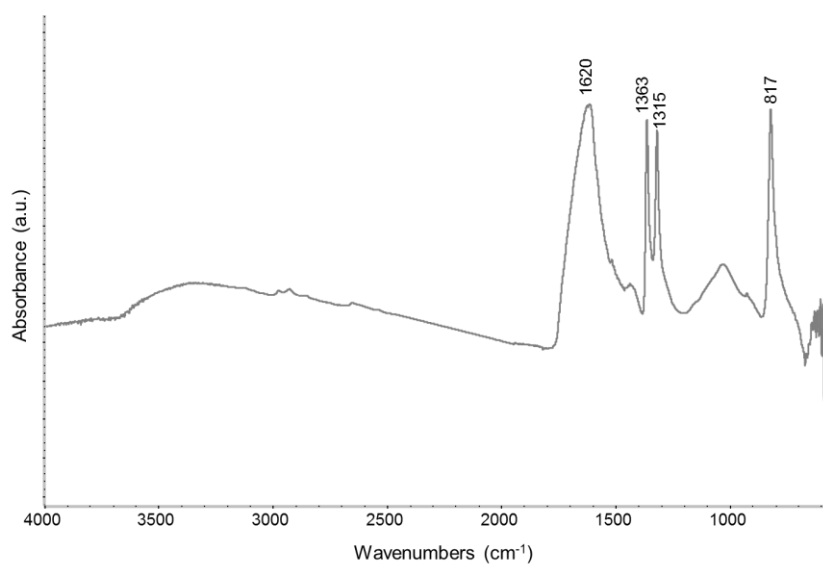


Figure 32. ATR-FTIR spectra showing the presence of copper oxalate (characteristic peaks at ~1615, 1360, 1315 and 1815  $\text{cm}^{-1}$ ) on Bracelet sample



Figure 33. Biopatina treated real object Eg-530 before treatment (a), during biopatina treatment (b-c), after treatment (d) and after natural ageing (e)

As well as for the “test objects”, visual observations were performed before and after natural indoor ageing (four months) on characteristic areas showing copper chlorides efflorescences. In this case, the objects did not present new corrosion processes, even the untreated ones (Figure 34 and Figure 35). This behaviour is probably due to the soft corrosion conditions of the museum environment that requires a longer period of time to trigger corrosion mechanisms. However, these objects will be monitored over a longer period of time since they are stored at Laténium facilities. This will allow a further comparison among BTA and biopatina inhibition effect.

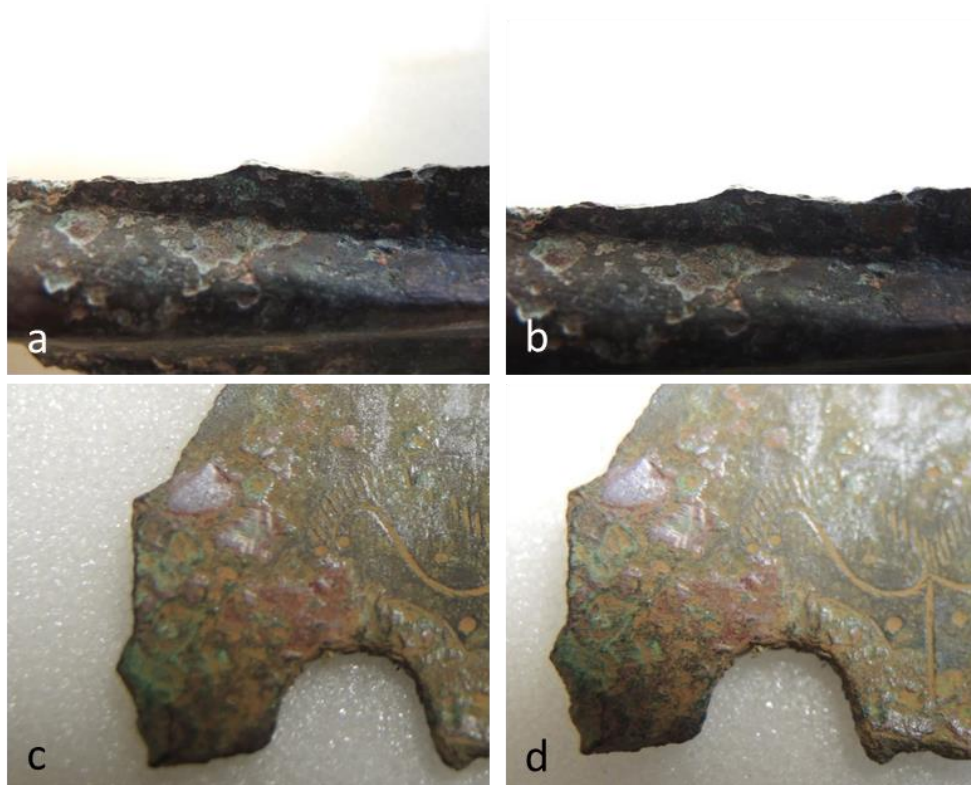


Figure 34. Untreated real object (spearhead) unnumbered before (a) and after (b) indoor storage; BTA treated real object CH-287 before (c) and after (d) indoor storage

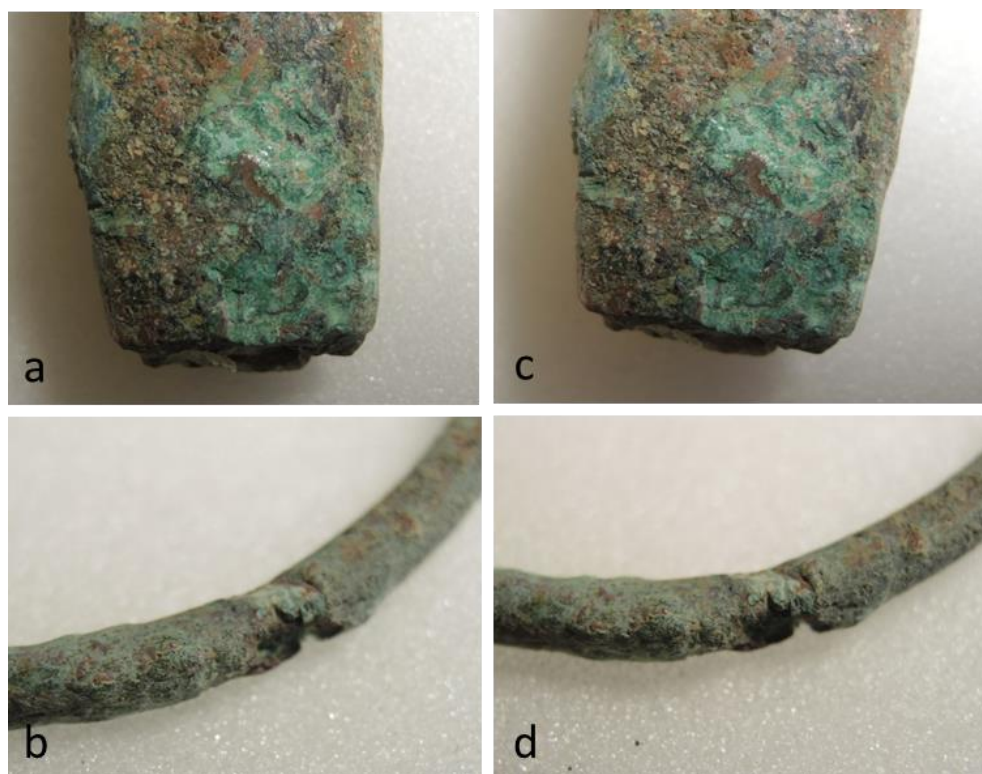


Figure 35. Biopatina treated real objects Eg-530 (a) and Bracelet (b) unnumbered before and after (c-d) indoor storage respectively

## Conclusions

In this study a first comparison between BTA and biopatina treatments for the stabilization of active corrosion on archaeological objects was made. Moreover, three different delivery systems for the biological treatment were tested. The clay mixture resulted in poor performance in terms of copper oxalates production and removal ease. Furthermore, it presented the disadvantage of being a non-transparent material. Metylan® gel appeared to be more efficient in terms of copper oxalates production but resulted difficult to remove, leaving residues on the surface. Then, GelX was tested as delivery system. It presented a high degree of transparency that, in combination with the use of Tredegar® film as micro-perforated PE film, allowed a visual monitoring of the fungal growth and of the objects behavior during treatment. Also, it was the most efficient delivery system for the production of copper oxalates, resulting to be the best one tested. Regarding the BTA-biopatina comparison, the accelerated ageing of “test objects” gave promising results about the inhibition effect of biopatina treatment, that seems to be as efficient as BTA. In-depth analysis on the inhibition effect of the two treatments needs to be performed in order to corroborate these results but a step forward has been done on the development of non-toxic inhibitors.

## 3.2 In-depth comparison between benzotriazole and Biopatina

### Abstract

This research aims at studying the effectiveness of an innovative biological treatment and of benzotriazole (BTA) for the protection of copper-based artefacts. Benzotriazole is commonly used in conservation-restoration practice in order to inhibit active corrosion due to the presence of copper chlorides on copper-based artefacts. Despite its extensive use as corrosion inhibitor, benzotriazole is considered a hazardous product for environment and human health. Therefore, in the last decades the interest for alternative and harmless treatments increased. For this study, artificial atacamite was produced on copper samples. Then, both treatments, biological and BTA, were applied and their properties investigated. The use of several analytical techniques such as Fourier Transform Infrared Spectroscopy, Scanning Electron Microscopy and Electrochemical Impedance Spectroscopy allowed to characterize the two treatments on surfaces and cross sections of corroded samples. Results showed that the biological treatment converted almost all the atacamite present on the samples surface and enhanced the inhibition against corrosion demonstrating better results than benzotriazole solution. Hence, the biopatina treatment could represent an effective alternative to the use of benzotriazole for the inhibition of active corrosion on copper alloys.

### Introduction

Artefacts made of copper and its alloys undergo progressive and inevitable corrosion processes. The identification of the degradation mechanisms and their corrosion products is, thus, important to select the best conservation approach to be used [14]. One of the most harmful degradation process for a copper-based artefact is the so called “bronze disease” [2]. This corrosion process is caused by the interaction between copper and chloride ions in presence of oxygen and high relative humidity producing nantokite (CuCl). The formation of nantokite in presence of air and moisture cause a cyclic corrosion process that form a green powdery patina of copper hydroxychlorides  $\text{Cu}_2(\text{OH})_3\text{Cl}$  [3, 4, 15]. This corrosion product has four polymorphic crystal forms: atacamite, paratacamite, clinoatacamite and botallackite. Even if generally stable, in some cases  $\text{Cu}_2(\text{OH})_3\text{Cl}$  can release  $\text{Cl}^-$  and bring to further corrosion of the artefact. This cyclic reaction is the main cause of stress cracking and eventually of the complete loss of shape. In heritage conservation, the use of corrosion inhibitors to decrease the corrosion rate of metal relics is a common practice. The most used inhibitor for copper-based objects is benzotriazole (BTA). The study of BTA inhibition mechanism, described for the first time in 1963, and its application in conservation vault a vast scientific literature even if with conflicting evidence and opinions [16-23]. Nonetheless, BTA is considered since long time the reference corrosion inhibitor in the field of copper alloys conservation, particularly for archaeological objects. The most controversial argument about the extended use of BTA is its toxicity. As reported by Cano and Lafuente [7], some authors refer to BTA as an environmental and health hazardous product recommending to handle it with care [2] while others are inclined to describe it as slightly toxic. However, in the last decades the interest about alternative sustainable and harmless products increased. Corrosion inhibitors made of plant extracts [24-27] and of amino acids [28-32] have been studied even if no experiments on real objects have been carried out so far. The biological treatment proposed in this paper relies on metal-microbe interactions studied with the BIOPATINA project. Indeed, because of their ability to immobilize metals microorganisms can be used in order to produce stable metallic compounds [33].

The Biopatina project relies on more than 10 years of research on the optimization of a biological treatment for copper surfaces using a specific strain of the fungus *Beauveria bassiana*. In fact, some fungal strains are reported for their ability to transform metal compounds into metal oxalates [34, 35]. In the field of conservation of metal artefacts, metal oxalates and more specifically copper oxalates were already identified on outdoor exposed bronzes but not associated with the phenomenon of cyclic corrosion [36].

Instead, compact patinas of an attractive green color are created on the bronze surface. Moreover, with a high degree of insolubility and chemical stability even in acidic atmosphere, copper oxalates provide the surface with good protection [37]. On this basis, a novel microbiological strategy for the conservation-restoration of copper-based artefacts was developed [38-43]. In this paper, this alternative biological treatment is compared to benzotriazole in terms of conversion and corrosion stabilization of an artificial atacamite patina. Both biological and BTA treatments were fully characterized on surfaces and cross sections of corroded samples. A multi-analytical approach using Fourier Transform Infrared Spectroscopy, Scanning Electron Microscopy and Electrochemical Impedance Spectroscopy was adopted.

## Materials and methods

### *Copper samples and artificial patina preparation*

Nine copper samples (2.5 x 2.5 cm) were cut from a naturally aged copper roof from Neuchatel, Switzerland. All copper samples exhibited a typical urban natural patina mainly composed of brochantite, a copper hydrosulphate. The samples surface was washed in ultrasound bath with acetone and then dried under pressurized air. In order to reproduce an artificial patina of copper chlorides a solution of 20g  $\text{Cu}(\text{NO}_3)_2 \cdot 3\text{H}_2\text{O}$  (Fluka Germany, purum p.a.) and 20g NaCl (Panreac Spain, PA-ACS-ISO) in 100 mL deionized water was prepared. The samples were wetted with the solution and left air dry on a soft cloth. The procedure was repeated twice a day over five consecutive days and finally all samples were rinsed with deionised water [44-46]. Fourier-Transform Infrared Spectroscopy was used to characterize the newly formed artificial patina that resulted to be mainly composed of atacamite.

### *Treatments*

The biological treatment (biopatina) is based on a culture of *Beauveria bassiana* mixed with a gelling agent and nutrients. The samples were covered with the gel during 14 days. After treatment the gel was removed and samples were rinsed with deionized water first and then with ethanol to remove any eventually remained fungi. The samples were dried under pressurized air.

A 3% w/V solution of benzotriazole in ethanol (95% w/w solution in deionized water) was prepared. Two different application protocols were employed. For the first application protocol (BTA1) the corroded samples were fully immersed and left in the solution for 24 hours according with protocols commonly employed by conservator-restorers on archaeological objects. The second application protocol (BTA2) involved a longer treatment duration. The corroded samples were fully immersed and left in the solution for 14 days in order to have the same time durations of the biological treatment and allowing a better comparison of the results. At the end of both treatments samples were rinsed with ethanol and dried under pressurized air.

Finally, a group of samples was left untreated as reference for comparison purposes.

All treatments were performed in triplicates. Before and after treatment all samples were documented with a scanner HP1110 using a resolution of 600 dpi and setting the white balance with a white paper (Figure 36).

### *Resin embedding and preparation of cross section*

One sample for each treatment (Biopatina, BTA1 and BTA2) and one untreated sample were cold embedded in resin using the EpoFix Kit (Struers). Samples were dry polished using successive silicon carbide abrasive papers with 250, 500 and 1000 grit and Micro-Mesh abrasive cloths 1800, 2400, 3200, 3600, 4000, 6000, 8000 and 12000 grade.

*Optical Microscopy*

Cross sections were characterized with a Polyvar MET optic microscope by Reichert Jung. Data collection was carried out using AxioVision LE software.


















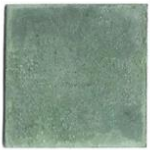
Samples		Triplicates		
		1	2	3
<b>Biopatina</b> (14 days)	Before Treatment			
	After Treatment			
<b>BTA 1</b> (24 hours)	Before treatment			
	After Treatment			
<b>BTA 2</b> (14 days)	Before treatment			
	After Treatment			

Figure 36. Samples appearance before and after treatment

*Fourier Transform Infrared Spectroscopy (FTIR)*

FTIR on the surface of the samples was performed without any sample preparation using an iS5 Thermo Scientific spectrometer with a diamond Attenuated Total Reflectance (ATR) crystal plate (iD5™ ATR accessory). All spectra were acquired in the range 4000–550  $\text{cm}^{-1}$ , at a spectral resolution of 4  $\text{cm}^{-1}$ . A total of 32 scans were recorded and the resulting interferograms averaged. Data collection and post-run processing were carried out using Omnic™ software. The FTIR mapping on samples sections was performed using a Thermo Scientific Nicolet iN10 MX FTIR microscope in ATR mode. All spectra were acquired in the range 4000–675  $\text{cm}^{-1}$ , at a spectral resolution of 4  $\text{cm}^{-1}$  and a step size of 20 x 20 mm. A total of 16 scans per point were recorded and the resulting interferograms averaged. Data collection was carried out using Omnic Picta™ software while post running processing was carried out using Omnic Atlas™ software.

### *Scanning Electron Microscopy (SEM)*

Secondary electron images were acquired using a Philips ESEM XL30 FEG scanning electron microscope with a working distance of 10mm and an acceleration voltage of 20kV.

### *Electrochemical impedance spectroscopy (EIS)*

EIS measurements were performed with a specially designed contact probe (ST15), with a nominal area of 1.77 cm<sup>2</sup>, to possibly compare measurements on artworks [47]. Spectra with 10 points per decade were acquired in potentiostatic mode with 10mV AC signal level at open circuit potential, in the frequency range 100 KHz - 10 mHz, using a Gamry REF600, with Framework/EIS300 V5.3 software©2007, Gamry Instruments, Inc. A commercial cleaning-cloth soaked with a mineral water (electrical conductivity 320µS/cm, pH=7.9) for 120 minutes is fixed to the contact cell, and the system obtained is then leant on the surface to be measured. The EIS spectra acquisition started after approximately 30 minutes to allow the stabilization of the open circuit potential. In order to properly normalise for the measurement area, the wet footprint of the EIS contact probe was recorded with a VEHO VMS-004 usb Microscope by MicroCapture software with a graph paper as background. At least two measurements for each group of samples were acquired in order to evaluate treatment reproducibility and homogeneity within the samples.

## **Results and discussion**

At a first visual observation, the aesthetical appearance of the samples changed during BTA treatment resulting in surface darkening (Figure 36). This effect is already known [6] and it has to be considered when the use of benzotriazole solutions is envisaged. The biological treatment also changed the appearance of the surface even though in a minor extent.

In order to ascertain the formation of copper oxalates and Cu-BTA complexes all samples surfaces were characterized after treatment through FTIR analyses. As showed in Figure 37, characteristic vibrational bands corresponding to copper oxalates at 1641, 1362, 1319 and 816 cm<sup>-1</sup> were recorded (Figure 2b). Peaks at 3445, 3336, 985, 948, 915, 894 and 847 cm<sup>-1</sup> corresponding to atacamite were also present. Nevertheless, these peaks presented an absorbance intensity lower than before treatment indicating a lower abundance of atacamite on the surface of treated samples. On the contrary, the intensity of copper oxalates peaks is much higher indicating a relative larger amount respect to atacamite in surface. Regarding BTA, both 24 hours and 14 days applications formed Cu-BTA complexes with characteristic peaks at 1494, 1445, 1395, 1298, 1274, 793 and 746 cm<sup>-1</sup> for BTA1 (24 hours) and at 1493, 1445, 1395, 1297, 1274, 790 and 746 cm<sup>-1</sup> for BTA2 (14 days) [11]. The difference among the two BTA applications concerned the intensity of the original patina FTIR peaks. Indeed, it seems that even if an application of 24 hours guaranteed the formation of Cu-BTA complexes, the BTA longer application of 14 days resulted in an increased intensity of Cu-BTA complexes FTIR peaks respect to those of the original patina. This result could be due to a higher degree of reaction of the benzotriazole solution with the original patina because of the longer immersion that brought to the formation of a higher amount of Cu-BTA complexes.

SEM surfaces observation confirmed the presence of copper oxalates on the biopatina-treated samples, showing the typical rosette-like habit of copper oxalates crystals (Figure 38).

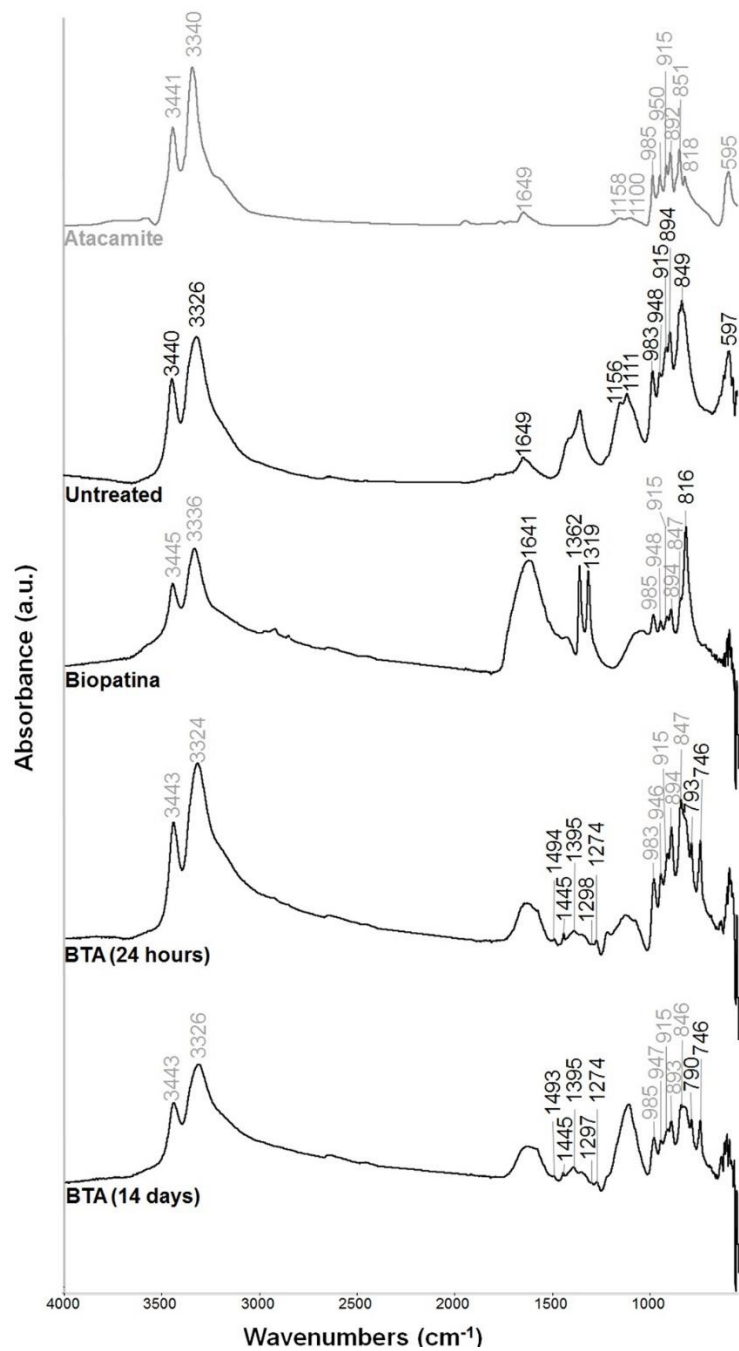


Figure 37. ATR-FTIR spectra showing from top to bottom an atacamite standard reference (grey) and its characteristics wavenumbers, the untreated sample characteristic peaks corresponding to atacamite wavenumbers, and treated samples (Biopatina, BTA1 (24hours) and BTA2 (14 days)) with the respective wavenumbers of copper oxalates and Cu-BTA complexes indicated in black. The wavenumbers corresponding to atacamite are indicated in grey in all spectra

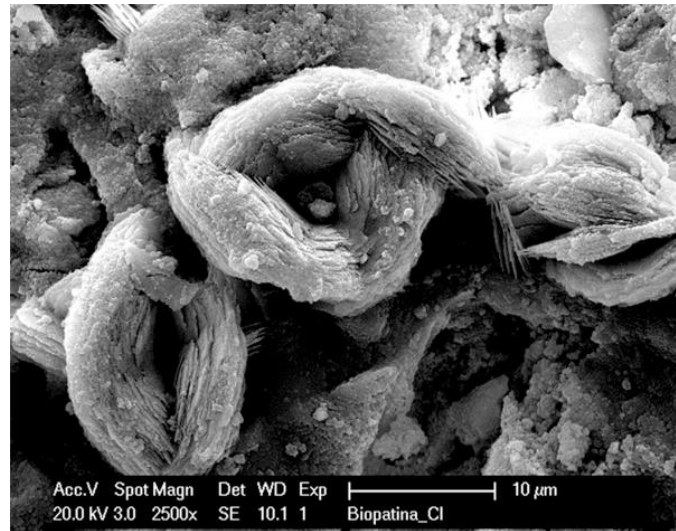


Figure 38. Secondary electrons micrograph of biopatina-treated sample showing typical habits of copper oxalates crystals

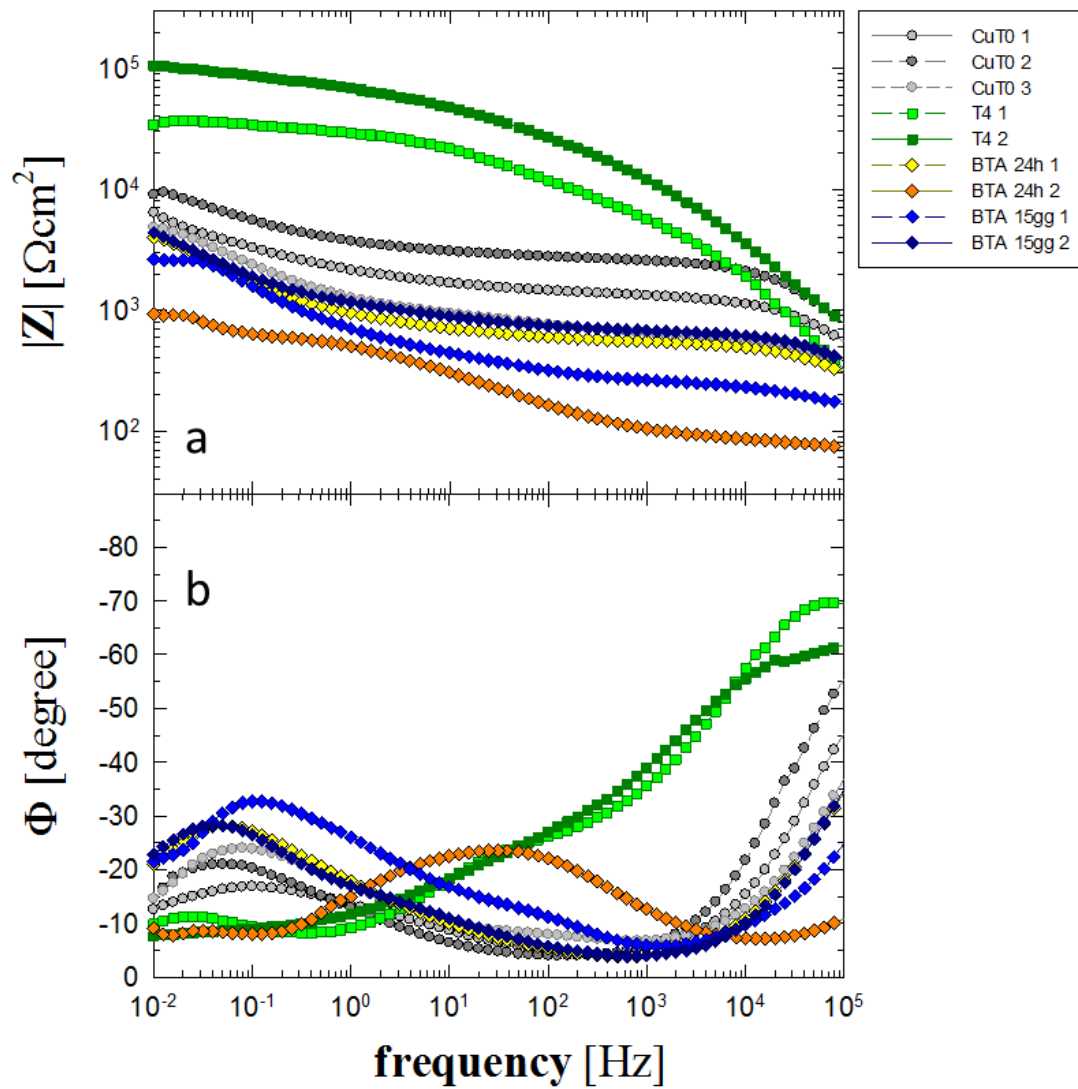


Figure 39. EIS Bode plots: impedance  $|Z|$  modulus (a) and phase plots (b) for untreated (grey dots, T0), biopatinated (green squares, T4) and BTA (yellow (24h, BTA1) and blue (14days, BTA2) diamonds) treated samples

The treatments protectiveness was evaluated through electrochemical impedance spectroscopy (EIS). The biopatina treatment increased the patina protectiveness, as indicated from the  $|Z|$  modulus limit values (Figure 39a and Table 8). In fact, they were one order of magnitude higher than untreated and BTA-treated samples. On the contrary, BTA treatment, either after an application of 24-hours or 14-days, had the  $|Z|$  modulus limit values in the same order of magnitude of the untreated samples, indicating almost no effectiveness against corrosion on atacamite-rich samples. Nevertheless, with protocol BTA2 (14 days) a better repeatability than protocol BTA1 (24h) was obtained as showed in the phase plot (Figure 39). Indeed, the phase plots recorded on two BTA1 samples differed one from each other, indicating that the formation of Cu-BTA complexes probably varied from a sample to another “and thus a poor reproducibility of the treatment.

Sample	$ Z $ K $\Omega$
Control 1	1.84
Control 2	2.45
Control 3	1.35
Biopatina1	9.91
Biopatina2	24.60
BTA1_1	1.15
BTA1_2	0.25
BTA2_1	0.59
BTA2_2	1.19

Table 8. Impedance  $|Z|$  modulus limit values  $|Z|$  for all measured samples

In order to evaluate the diffusion of the treatment within the corrosion layers and the degree of transformation of the corrosion products, optical microscopy and FTIR mapping were performed on cross sections of samples allowing the localisation of treatments. The untreated sample presented all over its surface a homogeneous green layer of atacamite (thickness range between 22 - 65  $\mu\text{m}$ ). Atacamite was the only compound detected (Figure 40). It is worth saying that the FTIR microscope has a signal cut-off at 675  $\text{cm}^{-1}$  thus copper oxides that have vibrational bands under this limit, cannot be detected. Hence, their presence can not be excluded in the underneath red-coloured layer. On biopatina-treated samples the conversion of the atacamite layer into copper oxalates was observed (Figure 41). Indeed, a continuous and intense layer of copper oxalates (thickness range between 22-50  $\mu\text{m}$ ) was identified as main compound of the sample green patina layer. Nevertheless, a low amount of atacamite in the inner part of this layer was detected, even if its presence was uneven and with low intensity (thickness range among 0-22  $\mu\text{m}$ ). Regarding the treatment with BTA, the amount and homogeneity of Cu-BTA complexes formed on the corroded surface seemed to depend on the treatment duration. In fact, a duration of 24 hours was insufficient to allow the formation of a homogeneous layer of Cu-BTA complexes (Figure 42a-c-e). Indeed, only few areas of the corrosion layers showed the presence of Cu-BTA complexes (thickness range between 0-24  $\mu\text{m}$ ) and the main component remained atacamite (thickness range between 27-50  $\mu\text{m}$ ) confirming EIS results about the lack of reproducibility of this

treatment. However, even a longer treatment duration did not guarantee the complete reaction of the atacamite with BTA. Indeed, a continuous layer of atacamite (thickness range between 24-32  $\mu\text{m}$ ) was still detected after 14-days treatment with BTA (Figure 42 b-d-f). The Cu-BTA complexes layer was, in this case, more homogeneous (thickness range among 0-32  $\mu\text{m}$ ) even though with low intensity, probably because of the simultaneous presence of atacamite in the same areas.

As general observation, it seemed that in the biopatina treatment the conversion of the atacamite present into copper oxalates started from the surface layers towards the inner core of the corrosion layers. This is probably due to the gel medium that gradually released the oxalic acid produced by the fungus allowing a progressive and homogeneous diffusion and reaction with copper ions. On the contrary, for BTA treatment, the solution diffused along the pores of the atacamite patina in the entire corrosion layer reacting simultaneously in different areas at different depth. Also, the degree of reaction seemed depended from the immersion time (24h versus 14 days).

A second observation regarded the patina thickness. The patina resulted to be thicker on untreated than on treated samples, regardless the used product. On one hand, the biopatina treatment decreased the patina thickness from a maximum of 15 micrometres. On the other hand, the BTA treatment also decreased the patina thickness, according with the treatment duration, from 15 micrometres (24 hours, BTA1) to 33 micrometres (14 days, BTA2) removing more than half of the original patina. However, this phenomenon may also be related to the detachment of the patina during the treatment and not to its conversion. Indeed, artificially-produced patinas are usually less adherent than natural ones and, thus, a physical detachment might be occurred, in particular after 2 weeks of immersion in BTA solution. It is important to notice here that a patina loss may, in some cases, preclude the readability of archaeological artefact. Indeed, inscriptions or decorations can be preserved in the corrosion layers. Thus, a removal, even partial, of the patina should be controlled and treatments that that limit such loss of material should be preferred.

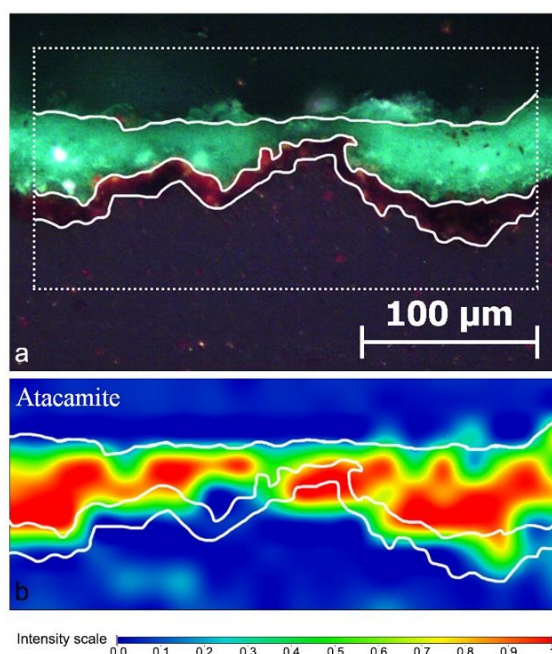


Figure 40. (a) optical micrograph of untreated sample cross section showing the area (white dotted line) where FTIR mapping was performed and (b) FTIR chemical map of the relative intensity of the entire atacamite spectrum

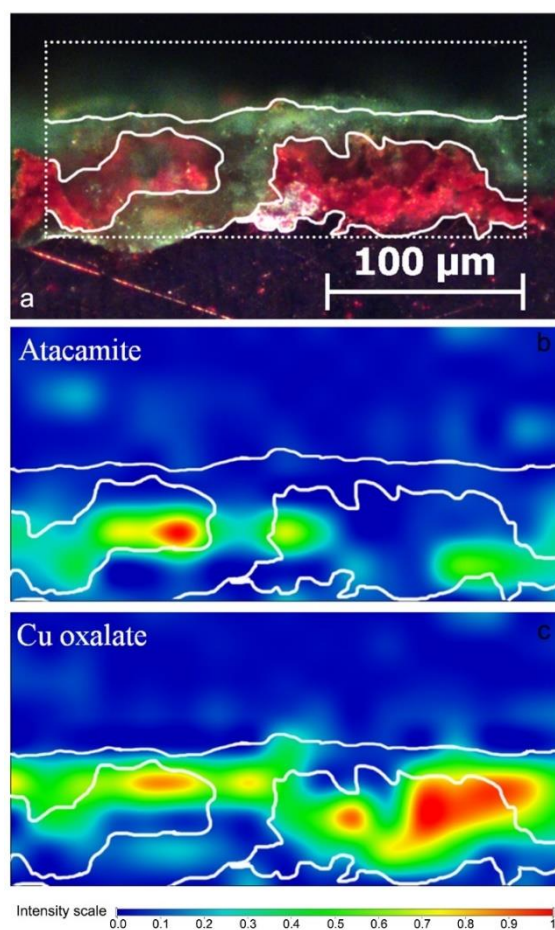


Figure 41. (a) optical micrograph of biopatinated sample cross section showing the area (white dotted line) where FTIR mapping was performed. FTIR chemical map of the relative intensity of the entire atacamite spectrum (b) and of the entire copper oxalate spectrum (c)

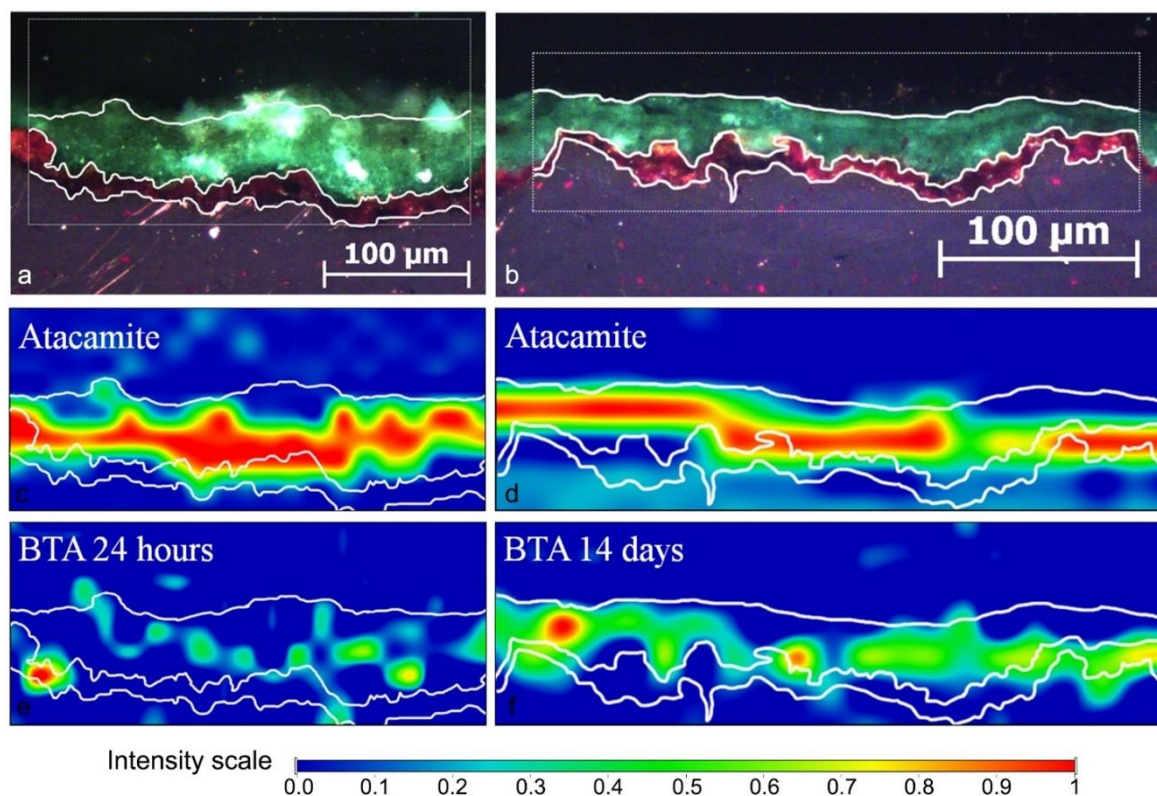


Figure 42. optical micrographs of BTA 24 hours and BTA 14 days treated samples cross section (a and b respectively) showing the area (white dotted line) where FTIR mapping was performed. FTIR chemical map of the relative intensity of the entire atacamite spectrum (c and d respectively) and of the 1397  $\text{cm}^{-1}$  characteristic peak Cu-BTA complex

## Conclusions

This paper aimed at comparing the efficiency of an innovative biological treatment and a reference corrosion inhibitor as benzotriazole in terms of conversion and corrosion stabilization of the original patina. Two BTA applications were performed: the first one (BTA1) lasted 24 hours and the second one (BTA2) lasted 14 days. The 24 hours application was insufficient to form an homogeneous layer of Cu-BTA complexes resulting in poor surface protectiveness. In order to obtain a layer of Cu-BTA complexes 14 days were needed. Nonetheless, in both cases, the efficiency in terms of corrosion inhibition was not sufficient. In fact, the protectiveness of the newly formed complexes seemed to be of the same order as the untreated samples. The biological treatment used in this study resulted to convert almost all the atacamite present into a homogeneous layer of copper oxalates. Furthermore, the presence of copper oxalates enhanced the surface inhibition against corrosion compared both with original and BTA-treated patinas. Also, the microorganism used in the biopatina treatment is reported to be non-toxic for the environment and for human health [48]. To conclude, the biopatina appears to be an efficient and safe corrosion inhibition treatment. Indeed, it could represent an effective and eco-friendly alternative to the use of benzotriazole for the inhibition of active corrosion known as bronze disease.

## References

1. Knotkova, D., et al., Indoor corrosivity in the National Museum Depository. *Strategies for Saving our Cultural Heritage*, 2007: p. 64.
2. Scott, D.A., *Copper and Bronze in Art: Corrosion, Colorants, Conservation*. 2002: Getty Publications.
3. Scott, D.A., Bronze Disease: A Review of Some Chemical Problems and the Role of Relative Humidity. *Journal of the American Institute for Conservation*, 1990. 29(2): p. 193-206.
4. Grayburn, R., et al., Tracking the progression of bronze disease—A synchrotron X-ray diffraction study of nantokite hydrolysis. *Corrosion Science*, 2015. 91: p. 220-223.
5. Argyropoulos, V., et al. A survey of the types of corrosion inhibitors and protective coatings used for the conservation of metal objects from museum collections in the Mediterranean basin. in *Strategies for Saving our Cultural Heritage. Proceedings of the International Conference on Conservation Strategies for Saving Indoor Metallic Collections 2007*. Cairo (Egypt): TEI of Athens.
6. Faltermeier, R., Colour changes induced when treating copper and copper alloy archaeological artefacts with the corrosion inhibitors benzotriazole and amino-mercapto-thiadiazole. *SSCR Journal*, 1998. 9(1): p. 5.
7. Cano, E. and D. Lafuente, Corrosion inhibitors for the preservation of metallic heritage artefacts, in *Corrosion and conservation of cultural heritage artefacts*, P. Dillmann, et al., Editors. 2013, Woodhead Publishing. p. 570-594.
8. Golfomitsou, S. and J. Merkel. Synergistic effects of corrosion inhibitors for copper and copper alloy archaeological artefacts. in *Metal 2004: proceedings of the International Conference on Metals Conservation: Canberra, Australia, 4-8 October 2004*. 2004.
9. Dugdale, I. and J. Cotton, An electrochemical investigation on the prevention of staining of copper by benzotriazole. *Corrosion science*, 1963. 3(2): p. 69-74.
10. Cotton, J.B. and I.R. Scholes, Benzotriazole and Related Compounds as Corrosion Inhibitors For Copper. *British Corrosion Journal*, 1967. 2(1): p. 1-5.
11. Brostoff, L.B., *Coating strategies for the protection of outdoor bronze art and ornamentation*. 2003, University of Amsterdam. p. 180.
12. Watkinson, D., *Preservation of Metallic Cultural Heritage*, in *Shreir's Corrosion*, J.A.R. Tony, Editor. 2010, Elsevier: Oxford. p. 3307-3340.
13. ISO, 16701: Corrosion of metals and alloys-corrosion in artificial atmosphere-accelerated corrosion test involving exposure under controlled conditions of humidity cycling and intermittent spraying of a salt solution. 2003.
14. Appelbaum, B., *Conservation treatment methodology*. 2007, Oxford: Elsevier.
15. MacLeod, I.D., Bronze Disease : An Electrochemical Explanation. *ICCM Bulletin*, 1981. 7(1): p. 16-26.
16. Hassairi, H., et al., Evaluation of the inhibitive effect of benzotriazole on archeological bronze in acidic medium. *Applied Physics A*, 2013. 113(4): p. 923-931.
17. Hassairi, H., et al., Characterization of archaeological bronze and evaluation of the benzotriazole efficiency in alkali medium. *Materials and Corrosion*, 2008. 59(1): p. 32-40.

18. Abu-Baker, A.N., et al., A comparative study of salicylaldehyde, cysteine and benzotriazole as inhibitors for the active-chloride-based corrosion of copper and bronze artifacts. *European Scientific Journal*, 2013. 9(33).
19. Mezzi, A., et al., Investigation of the benzotriazole inhibition mechanism of bronze disease. *Surface and Interface Analysis*, 2012. 44(8): p. 968-971.
20. Balbo, A., et al., Effectiveness of corrosion inhibitor films for the conservation of bronzes and gilded bronzes. *Corrosion Science*, 2012. 59: p. 204-212.
21. Faltermeier, R., Testing Corrosion Inhibitors for the Conservation of Archaeological Copper and Copper Alloys. *Journal of Conservation and Museum Studies*, 1997. 3.
22. Argyropoulos, V., et al. A survey of the types of corrosion inhibitors and protective coatings used for the conservation of metal objects from museum collections in the Mediterranean basin. in *Strategies for Saving our Cultural Heritage. Proceedings of the International Conference on Conservation Strategies for Saving Indoor Metallic Collections*, Cairo (Egypt). TEI of Athens, Athens. 2007.
23. MacLeod, I.D., Conservation of corroded copper alloys: a comparison of new and traditional methods for removing chloride ions. *Studies in Conservation*, 1987. 32(1): p. 25-40.
24. Abiola, O.K. and A. James, The effects of Aloe vera extract on corrosion and kinetics of corrosion process of zinc in HCl solution. *Corrosion Science*, 2010. 52(2): p. 661-664.
25. Banerjee, S., V. Srivastava, and M. Singh, Chemically modified natural polysaccharide as green corrosion inhibitor for mild steel in acidic medium. *Corrosion Science*, 2012. 59: p. 35-41.
26. Deng, S. and X. Li, Inhibition by Ginkgo leaves extract of the corrosion of steel in HCl and H<sub>2</sub>SO<sub>4</sub> solutions. *Corrosion Science*, 2012. 55: p. 407-415.
27. El-Haddad, M.N., Chitosan as a green inhibitor for copper corrosion in acidic medium. *International journal of biological macromolecules*, 2013. 55: p. 142-149.
28. Wang, T., J. Wang, and Y. Wu, The inhibition effect and mechanism of l-cysteine on the corrosion of bronze covered with a CuCl patina. *Corrosion Science*, 2015. 97: p. 89-99.
29. Badawy, W.A., K.M. Ismail, and A.M. Fathi, Corrosion control of Cu–Ni alloys in neutral chloride solutions by amino acids. *Electrochimica Acta*, 2006. 51(20): p. 4182-4189.
30. Ismail, K.M., Evaluation of cysteine as environmentally friendly corrosion inhibitor for copper in neutral and acidic chloride solutions. *Electrochimica Acta*, 2007. 52(28): p. 7811-7819.
31. Khaled, K., Corrosion control of copper in nitric acid solutions using some amino acids—A combined experimental and theoretical study. *Corrosion Science*, 2010. 52(10): p. 3225-3234.
32. Zhang, D.-Q., H. Wu, and L.-X. Gao, Synergistic inhibition effect of l-phenylalanine and rare earth Ce (IV) ion on the corrosion of copper in hydrochloric acid solution. *Materials Chemistry and Physics*, 2012. 133(2): p. 981-986.
33. Gadd, G.M., Metals, minerals and microbes: geomicrobiology and bioremediation. *Microbiology*, 2010. 156(3): p. 609-643.
34. Fomina, M., et al., Role of Oxalic Acid Overexcretion in Transformations of Toxic Metal Minerals by *Beauveria caledonica*. *Appl. Environ. Microbiol.*, 2005. 71(1): p. 371-381.
35. Gharieb, M.I., M.I. Ali, and A.A. El-Shoura, Transformation of Copper Oxychloride Fungicide into Copper Oxalate by Tolerant Fungi and the Effect of Nitrogen Source on Tolerance. *Biodegradation*, 2004. 15(1): p. 49.

36. Graedel, T.E., K. Nassau, and J.P. Franey, Copper Patina Formation—Copper patinas formed in the atmosphere—I. Introduction. *Corrosion Science*, 1987. 27(7): p. 639-657.
37. Marabelli, M. and R. Mazzeo, La corrosione dei bronzi esposti all'aperto: problemi di caratterizzazione. *METALLURGIA ITALIANA*, 1993. 85: p. 247-247.
38. Joseph, E., et al., Development of an analytical procedure for evaluation of the protective behaviour of innovative fungal patinas on archaeological and artistic metal artefacts. *Analytical and Bioanalytical Chemistry*, 2011. 399: p. 2899-2907.
39. Joseph, E., et al., Protection of metal artefacts with the formation of metal-oxalates complexes by *Beauveria bassiana*. *Frontiers in Microbiology*, 2012. 2.
40. Joseph, E., et al., Spectroscopic characterization of an innovative biological treatment for corroded metal artefacts. *Journal of Raman Spectroscopy*, 2012. 43(11): p. 1612-1616.
41. Joseph, E., et al. Assessment of a biological approach for the protection of copper alloys artefacts. in *Conference Proceedings of Metal*. 2013.
42. Joseph, E., et al., BIOPATINAS: Innovative biological patinas for copper-based artefacts. , in *Outdoor Metallic Sculpture from the XIXth to the Beginning of the XXth Century: Identification, Conservation, Restoration*. 2014, ICOMOS France: Paris. p. 154-162.
43. Albin, M., et al., Innovative biological approaches for metal conservation. *Materials and Corrosion*, 2016. 67(2): p. 200-206.
44. Hayez, V., et al., Micro Raman spectroscopy used for the study of corrosion products on copper alloys: study of the chemical composition of artificial patinas used for restoration purposes. *Analyst*, 2005. 130(4): p. 550-556.
45. Hayez, V., et al., Study of copper nitrate-based patinas. *Journal of Raman spectroscopy*, 2006. 37(10): p. 1211-1220.
46. Leysens, K., A. Adriaens, and C. Degryny. Electrochemical monitoring of the storage or stabilization of archaeological copper based artefacts in sodium sesquicarbonate solutions. in *ICOM-CC 14th Triennial meeting*. 2005. James & James.
47. Letardi, P., Electrochemical measurements in the conservation of metallic heritage artefacts: an overview, in *Corrosion and Conservation of Cultural Heritage Metallic Artefacts*. , P. Dillmann, et al., Editors. 2013, EFC Publications. p. 126-48.
48. Zimmermann, G., Review on safety of the entomopathogenic fungi *Beauveria bassiana* and *Beauveria brongniartii*. *Biocontrol Science and Technology*, 2007. 17(6): p. 553-596.

## Chapter 4

---

### BIOPATINA FOR OUTDOOR SCULPTURES



This chapter is based on the results of the following published articles:

M. Albini, L. Comensoli, L. Brambilla, E. Domon Beuret, W. Kooli, L. Mathys, P. Letardi, E. Joseph. BIOPATINAS: Innovative biological approaches for metal conservation. *Materials and Corrosion*, 2016, **67**(2), 200-206. doi:10.1002/maco.201408168.

E. Joseph, P. Junier, M. Albini, P. Letardi, E. Domon Beuret, L. Brambilla, L. Mathys, C. Cevey, R. Bertholon. Biologically induced patina for metal built heritage. In *Conference Proceedings of Scienza e Beni Culturali, Metalli In Architettura: Conoscenza, Conservazione e Innovazione*. Bressanone, Italy, 30th June - 3rd July 2015. Edizione Arcadia Ricerche s.r.l., Marghera Venezia, 2015; ISBN 9788895409191, 273-282.

E. Joseph, M. Albini, P. Letardi, E. Domon Beuret, L. Brambilla, L. Mathys, C. Cevey, R. Bertholon, D. Job, P. Junier. BIOPATINAS: Innovative biological patinas for copper-based artefacts. In *Conference Proceedings of Outdoor Metallic Sculpture from the XIX<sup>th</sup> to the Beginning of the XX<sup>th</sup> Century: Identification, Conservation, Restoration*. Paris, France, 4<sup>th</sup>-5<sup>th</sup> December 2014. ICOMOS France, Paris, 2014; ISBN 9782905430182, 154-162.

This part of the research was implemented in collaboration with the Haute École ARC (Neuchâtel, Switzerland), the Latènum Archaeological Park and Museum (Hauterive, Switzerland) and Institute of Marin Sciences (CNR-ISMAR, Genoa, Italy).

## Summary

In this chapter, the use of biopatina treatment on outdoor copper-based sculptures is presented. The first part is dedicated to the interaction between the biological treatment and different natural patinas formed by exposure to atmospheric agents. This study simulated the effect of an application on ancient monuments. Indeed, samples covered with various copper corrosion products were treated using different protocols in order to identify a delivery system suitable for the treatment of large surfaces. Furthermore, a comparison with microcrystalline wax, a reference treatment commonly used for the protection of outdoor sculptures, was assessed. The treated surfaces were then monitored during exposure in marine and urban environments in order to evaluate the treatments long-term behaviour.

In the second part of the chapter the use of the biological treatment on artificial modern patinas is discussed. In this case, the use of biopatina treatment on modern sculptures cast and artificially patinated in foundry was simulated. Samples presenting several of common foundry patinas were treated with both biological and reference treatment. Also in this case, different delivery systems were tested. Due to the fragile and non-cohesive nature of some of these patinas, the natural ageing was performed only in an urban environment.

Both natural and artificial patinas were analysed by Fourier transform infrared spectroscopy, scanning electron microscopy, colorimetry and electrochemical impedance spectroscopy.

Finally, the biological treatment was tested on real artefacts presenting natural and artificial patinas.

## 4.1 Natural Patinas

### Abstract

Before the transfer of a novel conservation treatment into real praxis, its properties and behaviour need to be tested. The surface of outdoor copper-based monuments is mainly composed of copper corrosion products. These corrosion layers are formed through natural ageing processes by the interaction between the metal and the surrounding environment. Corrosion scientists usually divided the outdoor environment in basic types of corrosive atmospheres, depending on their composition: *urban*, characterized by pollution composed mainly of sulphur compounds such as sulphur dioxide (SO<sub>2</sub>) and nitrogen oxides (NO<sub>x</sub>); *marine* (or *coastal*), laden with fine particles of sea mist carried by the wind to settle on exposed surfaces as salt crystals, particularly containing chloride ions; *rural*, typically the mildest atmosphere because it does not involve strong chemical contaminants. In order to predict the behaviour of a conservation treatment in various situation it is important to evaluate its performance on several patinas, formed in different environments. Furthermore, monitoring the behaviour of the treated surfaces into several corrosion atmospheres can provide information about its durability. In this research, natural patinas formed in an urban-marine and in an urban environment were studied and treated with a novel biological treatment (biopatina) and with a traditional conservation-restoration treatment as reference (microcrystalline wax). Two different application protocols were tested in order to optimize the efficiency of the biological treatment. In order to evaluate the effect of the environmental conditions, two exposure sites were used for the natural ageing: the urban-marine corrosion site (C3 corrosion class) of Genoa Harbour (Italy) and the urban environment of Neuchâtel (Switzerland).

### Introduction

Over the last decades, the exploitation of microorganisms in conservation-restoration practice has risen. Taking advantage of biochemical processes that do not require the use of toxic materials, biotechnology became a significant alternative to traditional conservation-restoration methods. In fact, as the studies of Cappitelli [1], De Belie [2] and Fernandes [3] demonstrated, soil bacteria can be successfully employed for the bio-cleaning and bio-consolidation of frescoes and ornamental stones, indicating the great opportunities offered by using such alternative biotechnological treatments. There is indeed a growing interest for the development of biological technologies that are environmentally friendly (performed close to ambient temperature and pressure and at neutral pH) and that do not require the use of toxic solvents [4]. A real progress may be expected in terms of durability, effectiveness and toxicity, fulfilling the ethical principles considered when conservation-restoration interventions are undertaken [5, 6].

In the field of metal conservation some microorganisms can be exploited because of their ability to immobilize metals either by accumulation or precipitation producing stable metallic compounds [7]. Indeed, this capability is currently used for waste treatment and for bioremediation of metal-polluted soils [8].

Traditional conservation-restoration methods for metallic artefacts involve the use of corrosion inhibitors or organic protective coatings. However, organic coatings simply create a passive and temporary barrier against aggressive environments in a non-selective way, without consideration to the difference in terms of patina composition and corrosion products stability [9-11]. For example, the use of waxes presents some disadvantages such as surface darkening, frequent maintenance and incomplete reversibility [12, 13]. Moreover, corrosion inhibitors such as benzotriazole are a potential threat to human health and to the environment [14].

In this context, the project BIOPATINA developed a novel microbiological strategy for the conservation-restoration of copper-based artefacts [15-20]. The treatment uses a specific fungal strain of *Beauveria bassiana* that is capable to transform unstable copper corrosion products into copper oxalates. Indeed, the presence of copper oxalates has been already identified on outdoor bronzes and it is not associated with the phenomenon of cyclical corrosion [21]. With a high degree of insolubility and chemical stability even in acidic atmospheres (pH 3), green and compact patinas of copper oxalates are created, providing bronze surfaces with good protection [22].

During this study, different naturally aged coupons were treated and exposed in the urban-marine corrosion site of the CNR-ISMAR facilities at Genoa Harbour (Italy) as well as in the urban environment of Neuchâtel (Switzerland). This exposure, over a 12-months period, allowed the biopatina to be proof-tested under natural ageing conditions for its appearance, resistance to corrosion and cohesion to the surface. The biological treatment was compared to a microcrystalline wax as traditional reference treatment. The properties of both biological and reference treatments were fully characterized before and after ageing through Fourier transform infrared spectroscopy, scanning electron microscopy, colorimetry and electrochemical impedance spectroscopy.

## Materials and Methods

### *Samples*

Three different copper alloys were prepared (Table 9). Regarding QQ and GMN bronze samples, twelve square coupons were cut from cast ingots with the nominal composition of Cu 90%, Sn 8%, Pb 2% and Cu 90%, Sn 5%, Pb 5%, Zn 5%, respectively. Afterwards, the samples were polished using silicon carbide (SiC) metallographic grinding paper (1200 grit) in water, washed in ethanol and cold air dried. The natural patina was created by exposure on a rack in the urban-marine environment of the CNR-ISMAR SMS site in Genoa Harbour for 30 months (QQ) and 18 months (GMN). According to ISO 9223 standard, orientation and position were selected: the samples were placed facing south, exposed skyward in the position of 45 degrees from the horizontal. The patina developed was mainly composed of atacamite and paratacamite. In parallel, twenty-four copper coupons were cut from a naturally aged copper roof in Neuchatel. All copper urban natural (CUNN) coupons exhibit a typical urban natural patina mainly composed of brochantite, a copper hydroxysulfate. The samples surface was washed in ultrasound bath with acetone and then dried with pressurized air. All samples were documented under a stereomicroscope Olympus SZ-STB1 and a scanner Canon 8800F. In order to monitor the treatments behaviour during ageing, systematic acquisition parameters were defined. Samples surface was fully characterized before, after as well as during natural ageing through several analytical techniques (Fourier transform infrared spectroscopy colorimetry, electrochemical impedance spectroscopy and scanning electron microscopy).

Coupons	Acronym	Dimension (mm)	Alloy composition	Main corrosion products	Exposure site
Copper urban natural	CUNN	60x60x1	Cu	Cu sulphates	Neuchatel & Genoa
Bronze marine natural	QQ	58x58x3	Cu85/Sn8/Pb2	Cu chlorides	Genoa
Bronze marine natural	GMN	50x50x5	Cu85/Sn5/Pb5/Zn5	Cu chlorides	Genoa

Table 9. Naturally patinated copper and bronze samples

*Treatments*

For each set three groups of triplicates were defined: untreated (T0), treated with the biological treatment (T4) and treated with a microcrystalline wax as reference treatment (TR). The biological treatment was performed according to procedures developed at the University of Neuchatel using a specific strain of *Beauveria bassiana*. A solid-matrix pre-incubated with the fungus was positioned in direct contact with the samples surface for one month. Cosmolloid H80 wax (CTS Restauro, CH-6807 Tavernes, Switzerland) was applied by a conservator-restorer by brush after heating the samples surface with a hot air gun.

*Natural ageing procedures*

CUNN samples were divided in two sets of twelve samples. The first set (CUNN Ge) was exposed, along with QQ and GMN sets, in the urban-marine environment of Genoa harbour (Experimental Marine Station of CNR-ISMAR, Italy, C3 corrosion class according to ISO 9223). The second set (CUNN Ne), was exposed in the urban environment of Neuchatel (Switzerland) on the roof of the faculty of Sciences of the University of Neuchâtel. According to corrosion classification [23], this exposure site present characteristic that make it closer to a rural environment than to a polluted urban site. Orientation and position according to ISO 9223 standard were selected as previously described. The outdoor exposure started on October 1<sup>st</sup>, 2013 and ended on November 3<sup>rd</sup>, 2014 for a total of 12 months. Data were collected every 3 months storing the samples into control environment during measurements.

*Fourier Transform Infrared Spectroscopy (FTIR)*

FTIR was performed without any sample preparation using an iS5 Thermo Scientific spectrometer with a diamond Attenuated Total Reflectance (ATR) crystal plate (iD5™ ATR accessory). All spectra were acquired in the range 4000–650 cm<sup>-1</sup>, at a spectral resolution of 4 cm<sup>-1</sup>. A total of 32 scans were recorded and the resulting interferograms averaged. Data collection and post-run processing were carried out using Omnic™ software.

*Colorimetry*

A Minolta CM-508D spectrophotometer was used with the following measurement conditions: Specular Component Included (SCI), Illuminant D65 (daylight containing UV component, colour T 6504K), d/8° geometry, 10° observer, measurement area diameter 8 mm, illumination with Xe flash light source 100% UV containing all UV components or 0% UV containing no UV components, CIE Lab 1976 colour space. On each sample, three measurements were carried out at different spots and the mean value calculated. In order to describe the colour variation before and after treatment the parameter  $\Delta E^*$  (colour difference) was calculated for each treatment using the CIE1976 equation (1).

$$\Delta E^* = \sqrt{[(\Delta L^*)^2 + (\Delta a^*)^2 + (\Delta b^*)^2]}$$

Values lower than 3 are considered not perceptible to the human eye while  $\Delta E^*$  bigger than 5 are considered clearly perceptible.

*Scanning Electron Microscopy (SEM)*

Micrographs of the samples surface were acquired using Scanning Electron Microscopy (SEM) without preparation, just positioning the specimen into the microscope chamber. A Philips ESEM XL30 FEG

environmental scanning electron microscope was used. A working distance of 10mm and an acceleration voltage between 10-20kV were employed.

#### *Electrochemical impedance spectroscopy (EIS)*

EIS measurements were performed with a specially designed contact probe (ST15) with a nominal area of 1.77 cm<sup>2</sup> using a Gamry REF600, with Framework/EIS300 V5.3 software<sup>©2007</sup>, Gamry Instruments, Inc [24]. Spectra with 10 points per decade were acquired in potentiostatic mode with 10mV AC signal level at open circuit potential, in the frequency range 100 KHz - 10 mHz. A commercial cleaning cloth soaked with mineral water (electrical conductivity 320 $\mu$ S/cm, pH=7.9) for 120 minutes was fixed to the contact cell, and the system obtained was then leant on the surface to be measured. The EIS spectra acquisition started after approximately 30 min to allow the stabilization of the open circuit potential. For each treatment, two to seven spectra were measured to verify results homogeneity and repeatability. In order to calibrate the probe area, the wet footprint of the EIS contact probe was recorded with a VEHO VMS-004 usb microscope using MicroCapture software and a graph paper as background.

### **Results and discussion**

After treatment all samples were characterized in order to assess the efficiency of biological (T4) and of wax (TR) treatments. The presence of copper oxalates on the surface was ascertained through FTIR measurements which revealed copper oxalates characteristic vibrational bands at 1622 cm<sup>-1</sup> (C=O stretching) 1364 and 1321 cm<sup>-1</sup> (O-C-O bending) and 821 cm<sup>-1</sup> (O-C=O bending). However, copper oxalates were not detected on the entire samples surface and the relative height of the corresponding FTIR vibrational peaks was low compared with those of the natural patina. Regarding TR, all treated samples presented typical aliphatic chains vibrational bands of a microcrystalline wax at 2954, 2915 and 2847 cm<sup>-1</sup> (C-H stretching), 1473, 1462 and 1377 cm<sup>-1</sup> (C-H deformation), 730 and 719 cm<sup>-1</sup> (CH<sub>2</sub> rocking) (Figure 43). SEM observations, in accordance with FTIR results, showed a poor presence of copper oxalates crystals on the samples surface (Figure 44). The aesthetical changes yielded from treatments application were evaluated through colorimetric measurement. In particular, the colour distance  $\Delta E^*$  revealed a clearly perceptible colour variation for both biological and wax treatments (Table 10). However, the colour change induced by wax application tended to be higher. Indeed, the samples treated with biopatina showed colorimetric values close to the a\* and b\* values of the natural patinas (Figure 45). On the contrary, the wax treatment presented different values concerning both a\* and b\* coordinates, but in particular for L\* values. It is possible to notice that the biopatina treatment (T4) did not affect the lightness (L\*) of the patinas as much as the wax treatment (TR) did. In fact, the coupons treated with wax became darker compared with the T4 and untreated T0 samples.

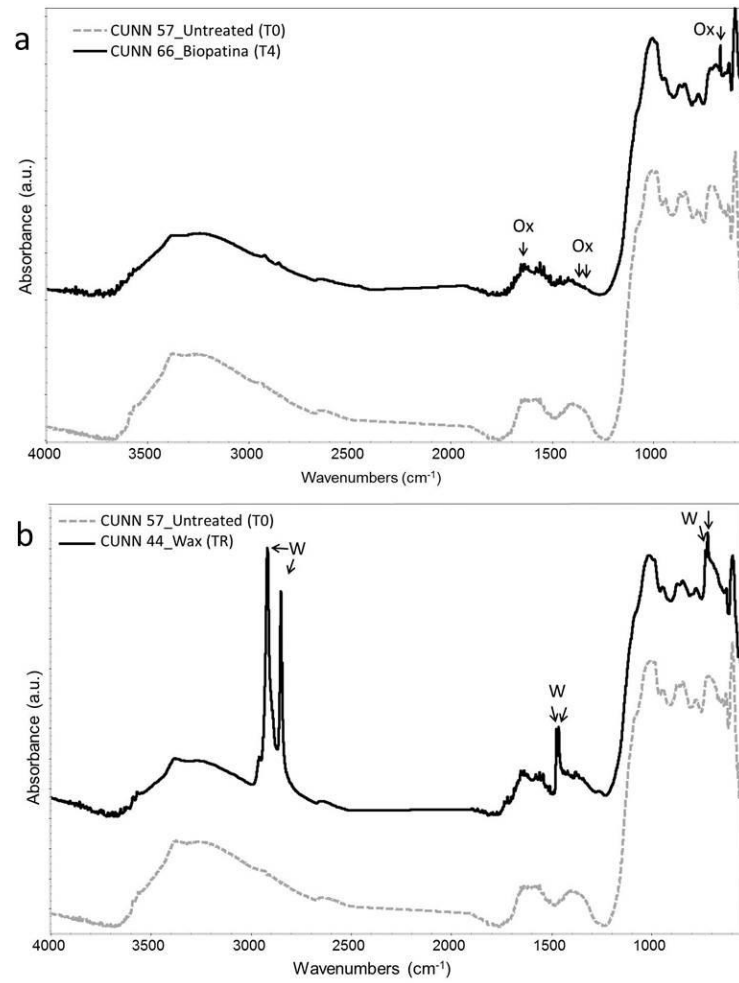


Figure 43. ATR-FTIR spectra collected on CUNN samples: untreated (grey, T0) and a) treated with biopatina (black, T4) and b) treated with wax (black, TR)

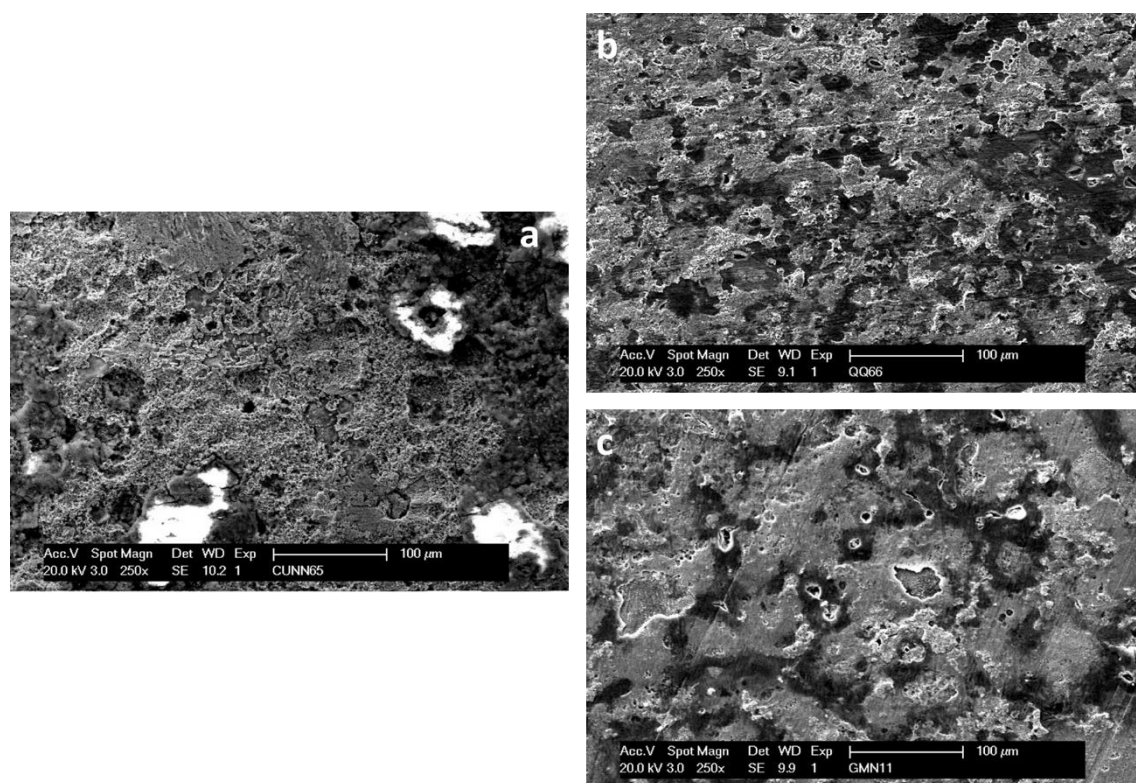


Figure 44. Secondary electrons SEM images of sample CUNN65 (a), QQ66 (b) and GMN11 (c)

Samples	Time	$\Delta E^*$		
		Untreated T0	Biopatina T4	Wax TR
CUNN Ne	0 M	$0 \pm 0$	$5 \pm 1$	$24 \pm 2$
	12 M	$1 \pm 0$	$2 \pm 1$	$23 \pm 1$
CUNN Ge	0 M	$0 \pm 0$	$6 \pm 1$	$25 \pm 1$
	12 M	$1 \pm 0$	$3 \pm 0$	$14 \pm 3$
QQ	0 M	$0 \pm 0$	$10 \pm 1$	$8 \pm 0$
	12 M	$6 \pm 1$	$4 \pm 1$	$6 \pm 1$
GMN	0 M	$0 \pm 0$	$11 \pm 2$	$8 \pm 0$
	12 M	$6 \pm 1$	$4 \pm 0$	$5 \pm 1$

Table 10. Colour difference  $\Delta E^*$  calculated before and after treatment (0 Month – 0M) and at the end of exposure (12 Months – 12M) for each set of samples. For samples coding see Table 1

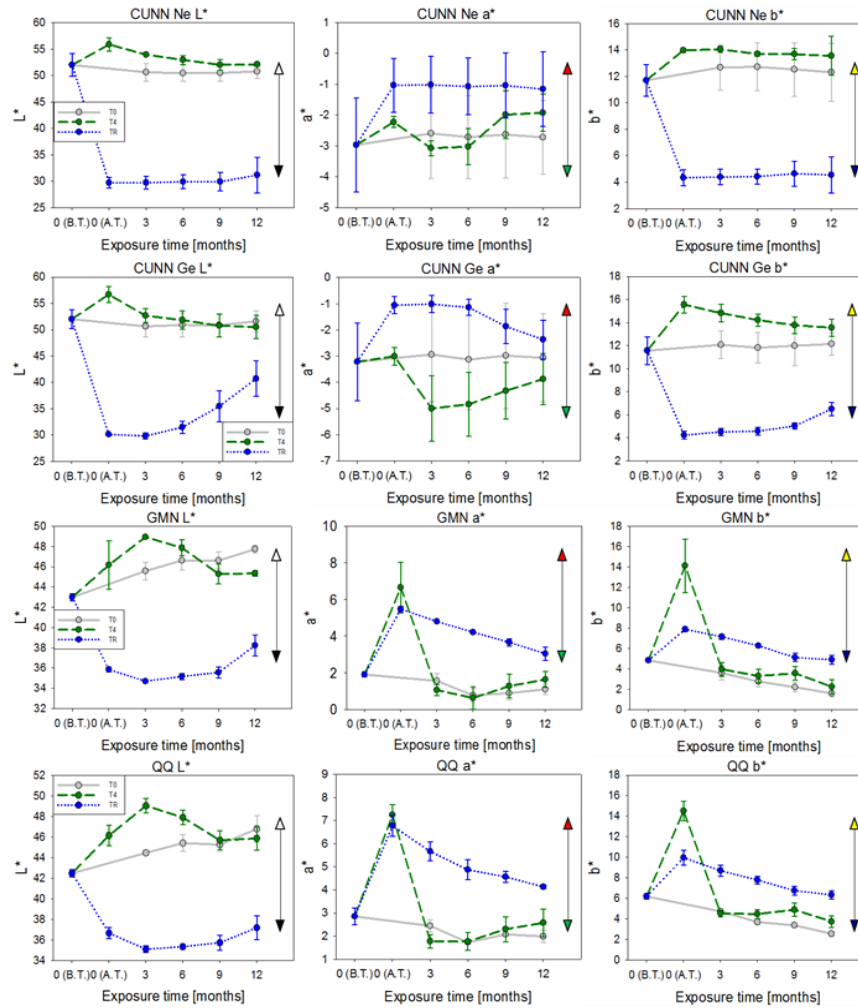


Figure 45. Evolution of the patinas colour according to the exposure time. Sets: CUNN Ge, CUNN Ne, GMN, QQ treated with wax (TR, blue), Biopatina (T4, green) and untreated (T0, grey)

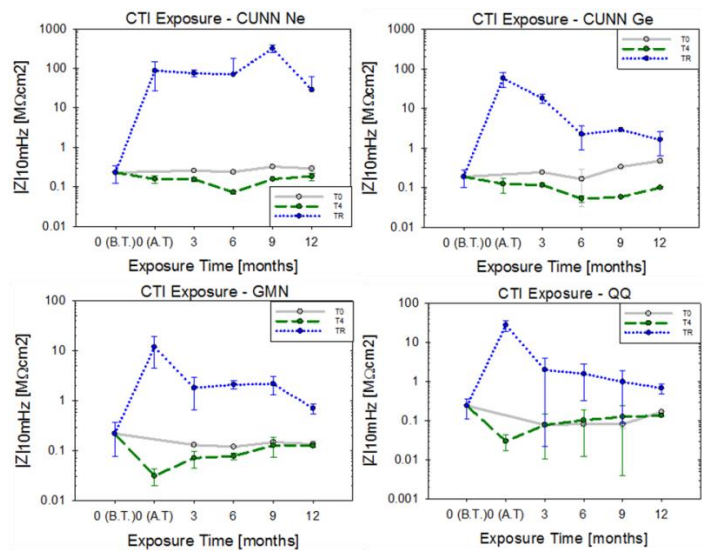


Figure 46. Impedance values showed as function of the exposure time on CUNN, GMN and QQ sets of samples treated with wax (TR, blue), Biopatina (T4, green) and untreated (T0, grey)

Finally, treatment protectiveness was estimated using Electrochemical Impedance Spectroscopy. EIS measurements allow to evaluate corrosion processes for a specific metal [25]. The lower is the measured impedance value ( $|Z|$ ) the greater a current can pass through the metal and therefore facilitates corrosion processes. That means that the value at low frequency of the impedance modulus can be used as an index of the corrosion level [24, 26]. After treatment, for T4 samples a decrease of the  $|Z|$  values was observed (Figure 46) while the TR treatment induced an increase of impedance values, as expected from a coating.

After twelve months of natural ageing, FTIR analysis did not showed the presence of copper oxalates on T4 samples surface. On the contrary, on TR samples microcrystalline wax characteristic aliphatic chain peaks were present but associated with those of copper chlorides (Figure 47). The presence of these newly formed corrosion products indicated that corrosion processes are ongoing suggesting that the wax layer is not protecting anymore the surface against environmental factors or is becoming thinner. Regarding the aesthetical aspect, the colour of the T4 samples tended to be similar to the untreated ones while TR samples showed the biggest variation also after ageing (Figure 45 and Table 10). Furthermore, samples exposed in an urban marine environment underwent a more important colour variation, especially concerning wax treatment, which seems more affected by the severe environmental conditions. Samples exposed in Neuchatel (urban environment) had less colour variation. Concerning the treatment protectiveness, EIS results show that CUNN samples exposed in Neuchatel presented a stable electrochemical behaviour during exposure. Remarkable differences between the beginning and the end of the exposure were not observed. That is probably due to the mild environmental conditions of the exposure site, in agreement with colorimetry results. An in-depth data analysis can be done for the samples exposed in the urban-marine environment of Genoa. The behaviour of biopatina treatment (T4) is quite similar to the one of natural patinas (T0) as shown in Figure 46. Indeed, T4 samples as well as T0 samples had an increase of their  $|Z|$  values while a decrease of TR protectiveness was observed within 12 months of exposure. In fact, the initial impedance modulus of wax was much higher than the biopatina one. This can be explained by the fact that wax treatment introduced extra layers that acted as a protective physical barrier against external environment. However, wax impedance value was not constant over time and decreased drastically after only 6 months of exposure in urban-marine environment underlining poor long-term protection performance. In opposition, the biological treatment does not produce a coating layer as wax but a layer of copper oxalates that is formed from the natural patina underneath. The impedance values of biopatina were stable overtime and appeared to be on the same order of magnitude of the natural patina during the whole exposure period. Also, regarding GMN and QQ samples, it is worth mentioning that the biopatina treatment seemed to slightly improve the protective ability during ageing.

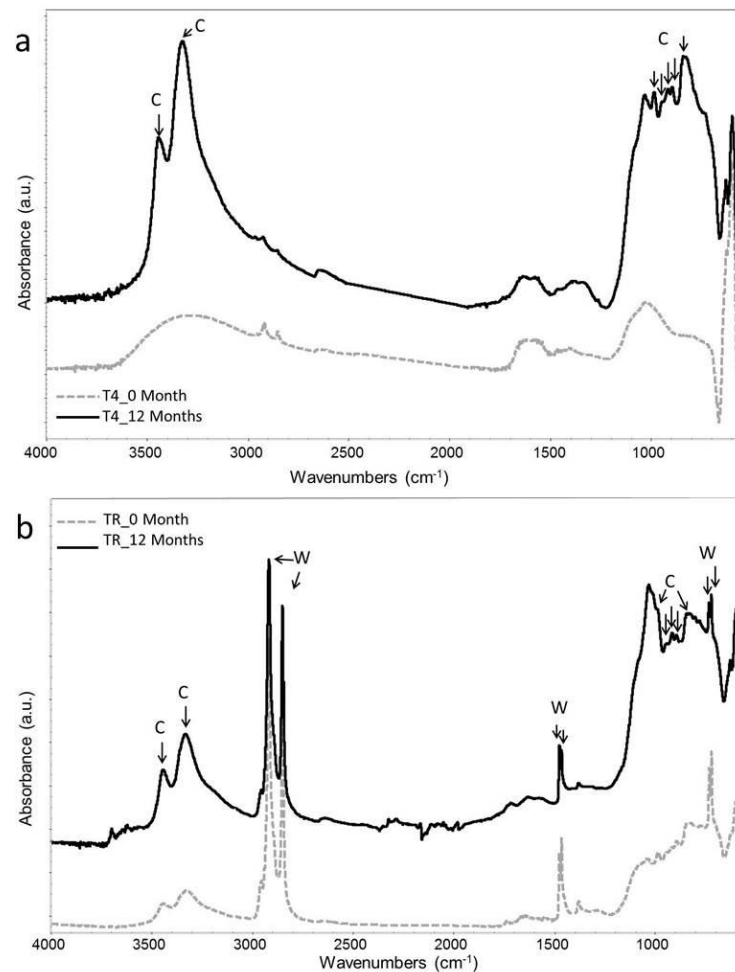


Figure 47. ATR-FTIR spectra of a) GMN11 (T4) sample and b) GMN5 (TR) sample at 0 (grey) and 12 (black) months of exposure. The spectra show the presence of copper chloride (C) and wax (W) on the sample surface

## Conclusions

The solid matrix-based application protocol of biopatina treatment resulted in the formation of an uneven copper oxalates layer. The non-homogeneous nature of this layer resulted in poor performance of the treatment that did not resist weathering. Nevertheless, the aesthetical appearance of the artefacts seems to be similar to a natural patina after treatment and during exposure. Regarding wax treatment, it drastically failed in the protection of naturally patinated copper based coupons already after 6 months of exposure in severe environmental conditions. Furthermore, this treatment provided higher colour variation compared to biopatina treatment.

However, the protective behaviour of the biological treatment needs to be further investigated, looking at a different application protocol in order to increase the homogeneity and protectiveness of biopatina. Nevertheless, according to the results, a promising ecological alternative treatment for the protection of outdoor sculpture was obtained.

## Supplementary Information

Sample	Former treatment	New treatment	Main composition	patina	Alloy
CUNN45	T0	T4			
CUNN50	T0	T4	brochantite		Cu
CUNN61	T0	T0	traces of atacamite		
QQ51	T0	T4			
QQ68	T0	T4	atacamite		Cu90/Sn8/Pb2
QQ66	T4	T0	traces of brochantite		
GMN2	T0	T4			
GMN10	T0	T4	atacamite,		Cu85/Sn5/Zn5/Pb5
GMN3	T4	T0	traces of brochantite		

Table 11. Samples used for the new application of biopatina treatment indicating the former undergone treatment (T0: untreated; T4: biological treatment)

In order to optimize the biological treatment a new application protocol was used on naturally aged coupons. Samples from the previous study were used for this new application. In Table 11 the samples employed for this new application are described. Former untreated samples were selected to undergo this new biopatina application. In the case of QQ and GMN groups, the untreated samples available were only two. Therefore, in order to reach a number of three, a former biopatinated sample was used. This choice was made because of the absence of copper oxalates on the samples surface at the end of the previous exposure. Indeed, these samples were considered as untreated with a natural patina enriched in atacamite. Nevertheless, to avoid any possible interaction with the previous biological treatment, these samples were not further treated but left as new T0.

Before treatment all samples were cleaned by applying agar on their surface for 48 hours. This allowed to remove all the soluble compounds present on the samples surface (Figures 48, 49 and 50).

The new application protocol involved the use of GelX as delivery system mixed with liquid pre-cultures of *B. bassiana* and addition of nutrients for the fungal growth. This delivery system resulted to be the most efficient for the use on archaeological objects (Chapter 3) and it was decided to test it also for outdoor applications. The treatment lasted 14 days.

After surface characterization, all samples were exposed for six months in the urban-marine environment of the Experimental Marine Station of CNR-ISMAR (Genoa, Italy) as previously described. *In situ* colour measurements were made each two months. At the end of the exposure all samples were brought back in the laboratory, washed with deionized water and dried under compressed air. For samples characterization, the same analytical techniques used during the previous study were employed.





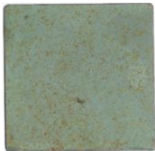



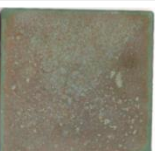

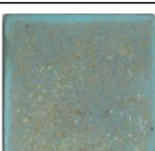
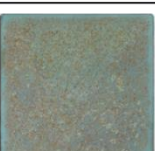
Samples		Treatment		
		CUNN 61 T0	CUNN 45 T4	CUNN 50 T4
CUNN	Before Treatment			
	After Cleaning			
	After Treatment 0M			
	After 6M ageing			

Figure 48. Visual characterization of CUNN samples before treatment, after agar cleaning, after new application of biopatina (T4) and after 6 months ageing. The untreated sample (T0) is also shown

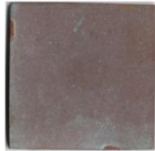
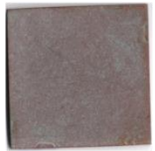


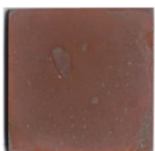

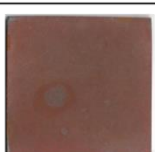

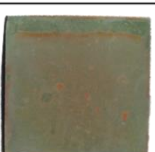
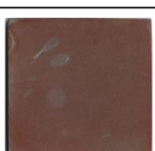
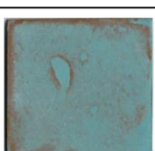
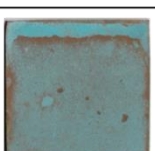
Samples		Treatment		
		QQ 66 T0	QQ51 T4	QQ68 T4
QQ	Before Treatment			
	After Cleaning			
	After Treatment 0M			
	After 6M ageing			

Figure 49. Visual characterization of QQ samples before treatment, after agar cleaning, after new application of biopatina (T4) and after 6 months ageing. The untreated sample (T0) is also shown

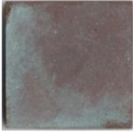
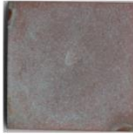

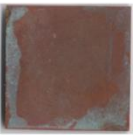
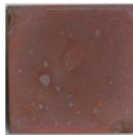
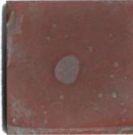
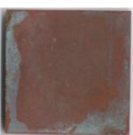

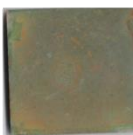
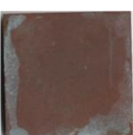

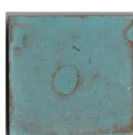
Samples		Treatment		
		GMN 3 T0	GMN 2 T4	GMN 10 T4
GMN	Before Treatment			
	After Cleaning			
	After Treatment 0M			
	After 6M ageing			

Figure 50. Visual characterization of GMN samples before treatment, after agar cleaning, after new application of biopatina (T4) and after 6 months ageing. The untreated sample (T0) is also shown

### Results and discussion

FTIR characterization showed that the agar cleaning mainly affected the atacamite patina (QQ and GMN samples), as showed in Figure 51, by the intensity decrease of its characteristic peaks at 3441, 3324, 983, 948, 913, 896, 845 and 820  $\text{cm}^{-1}$ . Indeed, the peaks at 3441, 3324 913 and 896  $\text{cm}^{-1}$  disappeared. CUNN samples did not present a modification of their chemical composition after cleaning (Figure 52). After treatment, all T4 samples exhibited a layer of copper oxalates covering the surface as showed by FTIR spectra (Figures 53, 54 and 55) and SEM images (Figure 56). Compared with the previous treatment, in this case copper oxalate characteristic peaks had a high intensity and its rosette-like crystals were clearly visible on the samples surface. The colour variation of CUNN samples after treatment indicated a slight change towards more blue colour, remaining in the same quadrant as showed in Figure 57b. In contrast, the biological treatment modified QQ and GMN samples colour to a greater extend (Figure 57c-d). Indeed, the  $\Delta E$  value for CUNN samples after treatment was 1 whereas for QQ and GMN samples was 8 (Table 12). The colour variation was, thus, strictly related to the original patina colour (reddish or greenish). In fact, it is interesting to notice that the biopatina treatment led the same colour to all samples (Figure 57a).

Impedance measurements showed a relevant effect of the agar cleaning. Indeed, all samples presented a decrease of the impedance modulus  $|Z|$  of almost one order of magnitude, indicating that soluble corrosion products actively affect the protectiveness of the patina (Figure 58 and Table 13). After the biological treatment, all samples had a decrease of  $|Z|$ , in higher extend for QQ and GMN samples. For these latter samples a change of the phase plot was observed (Figure 58b-c). This indicates a change of the corrosion behaviour due to the modification of the surface. This change did not occur on CUNN samples (Figure 58).

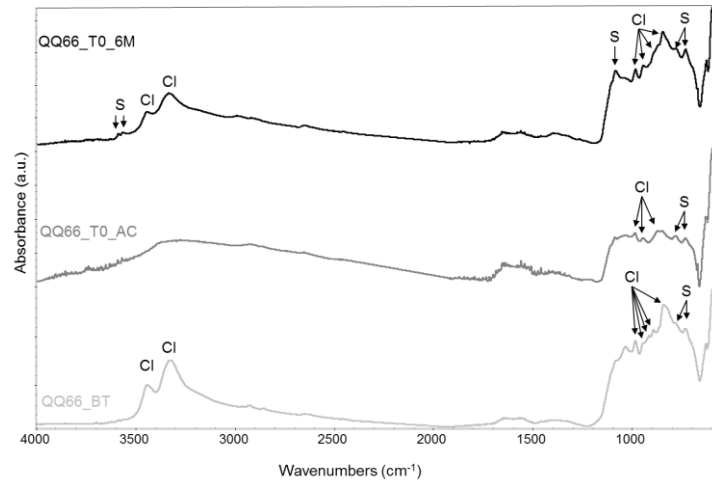


Figure 51. ATR-FTIR spectra of sample QQ66 (T0) before cleaning (BT, grey), after cleaning (AC, dark grey) and after six months of exposure (6M, black). The spectra show the presence of copper atacamite (C) and brochantite (S) on the sample surface

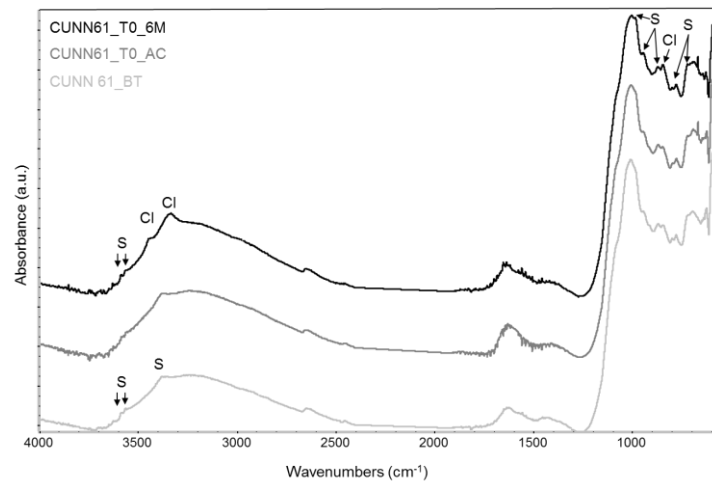


Figure 52. ATR-FTIR spectra of sample CUNN61 (T0) before cleaning (BT, grey), after cleaning (AC, dark grey) and after six months of exposure (6M, black). The spectra show the presence of copper atacamite (C) and brochantite (S) on the sample surface

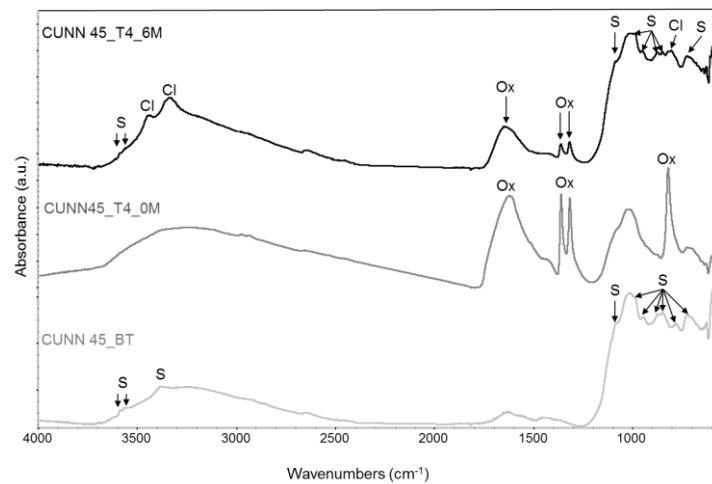


Figure 53. ATR-FTIR spectra of sample CUNN45 (T4) before cleaning (BT, grey), after biopatina treatment (0M, dark grey) and after six months of exposure (6M, black). The spectra show the presence of copper atacamite (C), brochantite (S) and copper oxalates (Ox) on sample surface

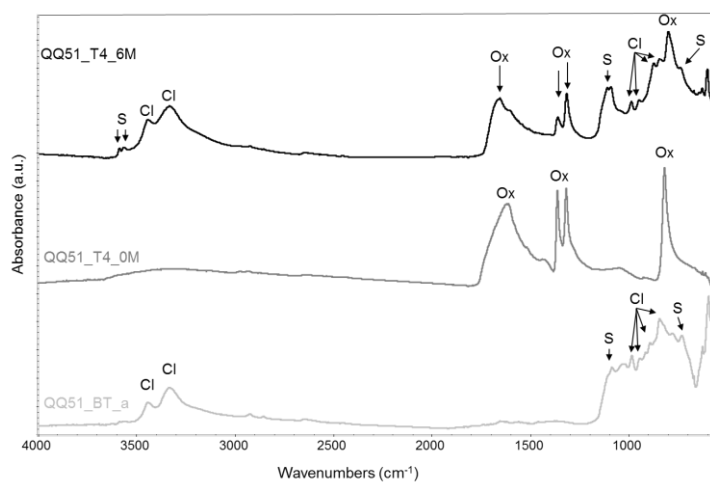


Figure 54. ATR-FTIR spectra of sample QQ51 (T4) before cleaning (BT, grey), after biopatina treatment (0M, dark grey) and after six months of exposure (6M, black). The spectra show the presence of copper atacamite (C), brochantite (S) and copper oxalates (Ox) on sample surface

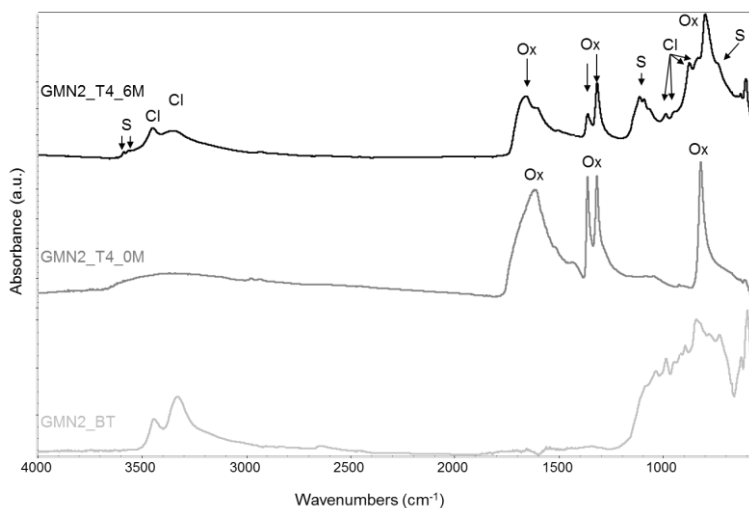


Figure 55. ATR-FTIR spectra of sample GMN2 (T4) before cleaning (BT, grey), after biopatina treatment (0M, dark grey) and after six months of exposure (6M, black). The spectra show the presence of copper atacamite (C), brochantite (S) and copper oxalates (Ox) on sample surface

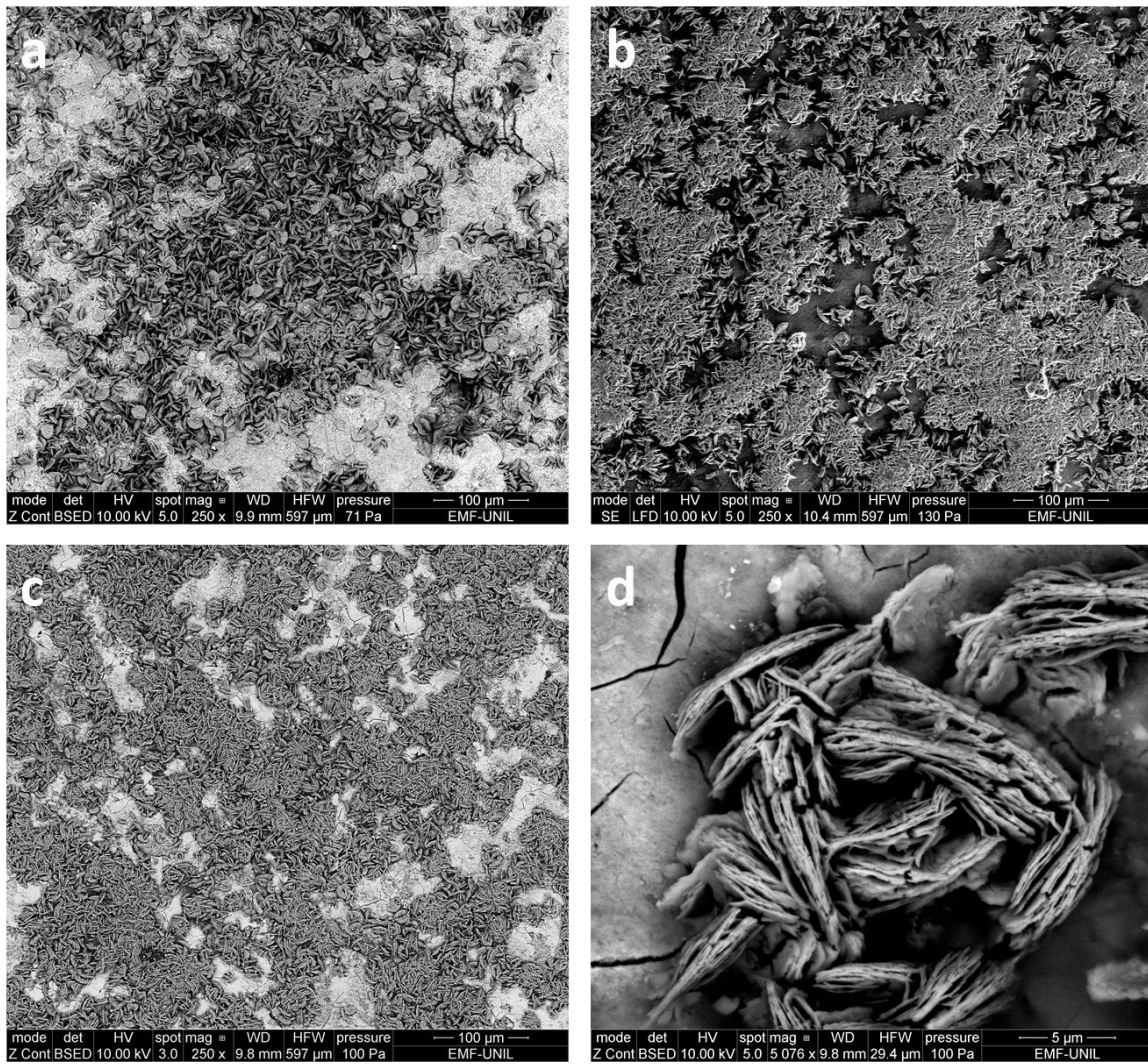


Figure 56. Secondary and backscattered electrons SEM images of rosette-like copper oxalates crystals on sample CUNN45 (a), QQ51 (b) and GMN2 (c-d)

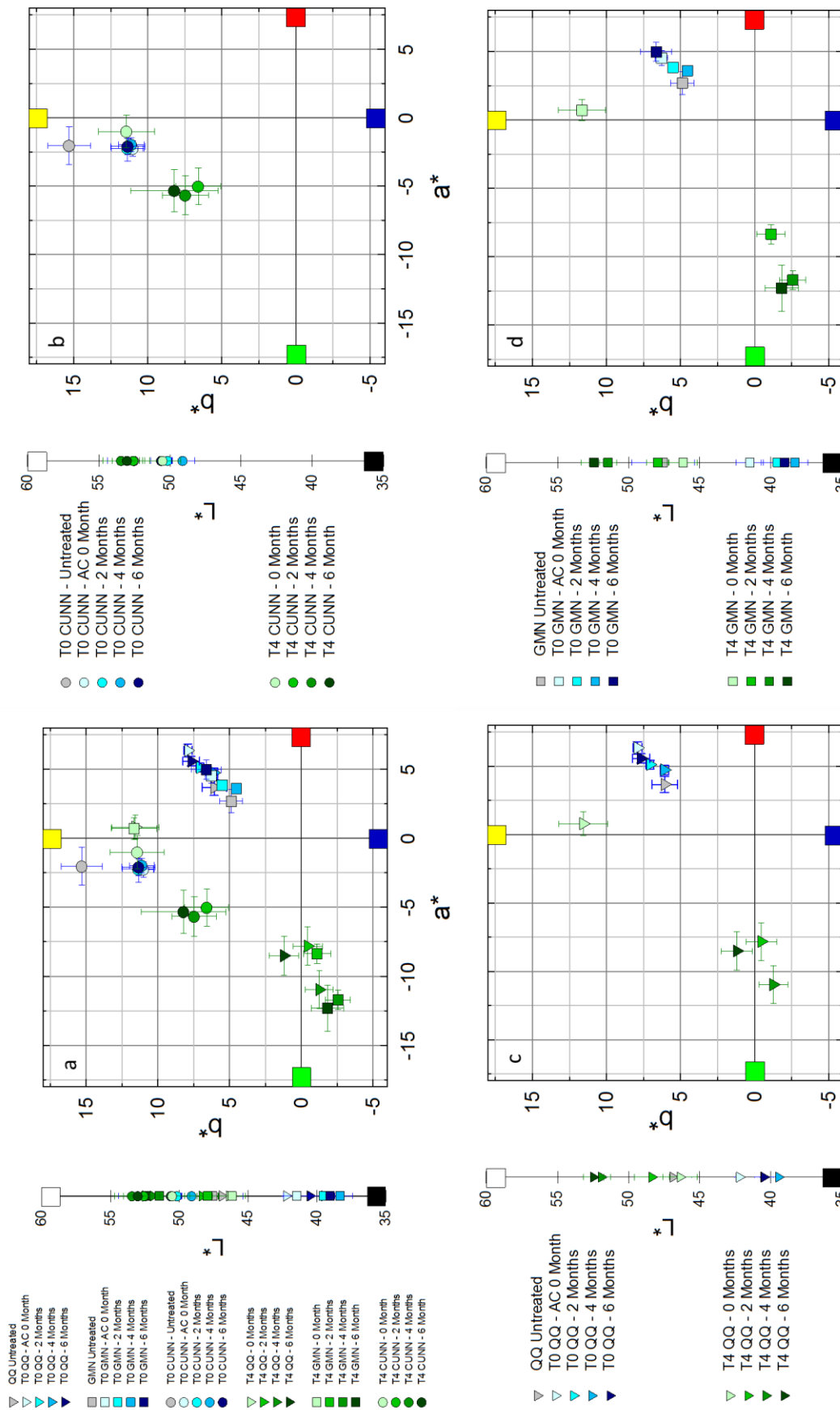


Figure 1. Colorimetry plots representing colour coordinates  $L^*$  (lightness, bright-dark)  $a^*$  (red/green opponent colours) and  $b^*$  (yellow/blue opponent colours) for all samples together (a) and CUNN (b), QQ (c) and GMN (d) samples. Measure were taken before treatment, after agar cleaning (AC), after treatment (0 Month), during exposure (2 and 4 Months) and after 6 months exposure

Exposure time	$\Delta E$					
	QQ		GMN		CUNN	
	T0	T4	T0	T4	T0	T4
Before/after cleaning	6 ± 2	6 ± 2	7 ± 4	7 ± 4	5 ± 3	5 ± 3
Before/after treatment - 0 Month	6 ± 2	8 ± 3	7 ± 4	8 ± 3	5 ± 3	1 ± 3
2 months	2 ± 1	18 ± 3	2 ± 2	16 ± 2	1 ± 2	6 ± 3
4 months	4 ± 1	22 ± 2	4 ± 2	21 ± 2	2 ± 2	6 ± 4
6 months	2 ± 1	19 ± 2	3 ± 2	22 ± 3	0 ± 2	5 ± 4

Table 12. Colour difference  $\Delta E^*$  calculated before and after cleaning, before and after treatment (0 Month) and at the end of 2, 4 and 6 months of exposure (2, 4, 6 Months) for each set of samples untreated (T0) or treated with biopatina (T4)

After six months of natural ageing the surface of the treated samples appeared highly modified (Figures 48, 49 and 50). On QQ untreated samples, FTIR analyses showed the increase of intensity of copper sulphates and copper chlorides peaks compared with the cleaned samples before exposure (Figure 51). Indeed, characteristic peaks of brochantite at 3583, 3563, 1086, 876, 781 and 733  $\text{cm}^{-1}$  and of atacamite at 3443, 3328, 983, 942, 896, 845  $\text{cm}^{-1}$  were recorded. The QQ surface composition after ageing appears to be the same as before cleaning with an increase of brochantite amount. The same results were obtained for GMN samples (data not shown). After exposure CUNN untreated samples did not show any change in the surface composition (Figure 52). On treated samples, FTIR analysis confirmed the presence of copper oxalates. Nevertheless, a remarkable increase of the corrosion products present on the surface occurred after ageing with the consequent decrease of the relative height of copper oxalates peaks (Figure 53, 54 and 55). These results indicated ongoing corrosion on samples suggesting low protectiveness against new corrosion mechanisms triggered by extreme environment.

Colorimetric measurements indicated that untreated samples did not undergo important colour variation during exposure. In fact, all  $\Delta E$  values of T0 samples (Table 12) remained lower than 3. On the contrary, a colour variation towards blue-green shades occurred for all treated samples (Figure 57). CUNN T4 samples presented the lower  $\Delta E$  value even if with a high standard deviation (Table 12). On QQ and GMN samples colour drastically changed, going in the opposite quadrant of the colorimetric plots (Figure 57 c-d) and the colour distance  $\Delta E$  resulted to be of 19 and 22 respectively. Since all the samples, treated and untreated, underwent the same exposure conditions, the colour variation must be attributed to the presence of copper oxalates on the surface. It seems that, in this specific case, the colour of copper oxalates turned into a very light green which, however, is part of the copper oxalates shades.

Regarding impedance measurement, the  $|Z|$  values of all untreated samples after six months of exposure remained similar compared with the cleaned samples before exposure (Table 13). They appear to have the same behaviour regardless the belonging group. On the contrary, all biopatina-treated samples slightly increased their  $|Z|$  values and after exposure the impedance of treated and untreated samples resulted to be of the same order of magnitude (Figure 58). Also, the phase of QQ and GMN samples modified after exposure resulting to be the same of untreated samples. These results indicate that the surface of treated and untreated samples had the same protectiveness after six months of exposure.

	$ Z  \text{ K}\Omega\text{cm}^2$					
	QQ		GMN		CUNN	
	T0	T4	T0	T4	T0	T4
Before cleaning	$0.89 \pm 0.08$		$0.77 \pm 0.36$		$1.57 \pm 0.40$	
After cleaning	$0.17 \pm 0.03$		$0.19 \pm 0.01$		$0.42 \pm 0.02$	
After treatment	$0.17 \pm 0.03$	$0.07 \pm 0.02$	$0.19 \pm 0.01$	$0.03 \pm 0.00$	$0.42 \pm 0.02$	$0.27 \pm 0.05$
6 months	$0.28 \pm 0.00$	$0.28 \pm 0.02$	$0.30 \pm 0.00$	$0.27 \pm 0.02$	$0.43 \pm 0.00$	$0.23 \pm 0.06$

Table 13. Impedance modulus  $|Z|$  measured before and after cleaning, after treatment and at the end of 6 months of exposure for each set of samples untreated (T0) or treated with biopatina (T4)

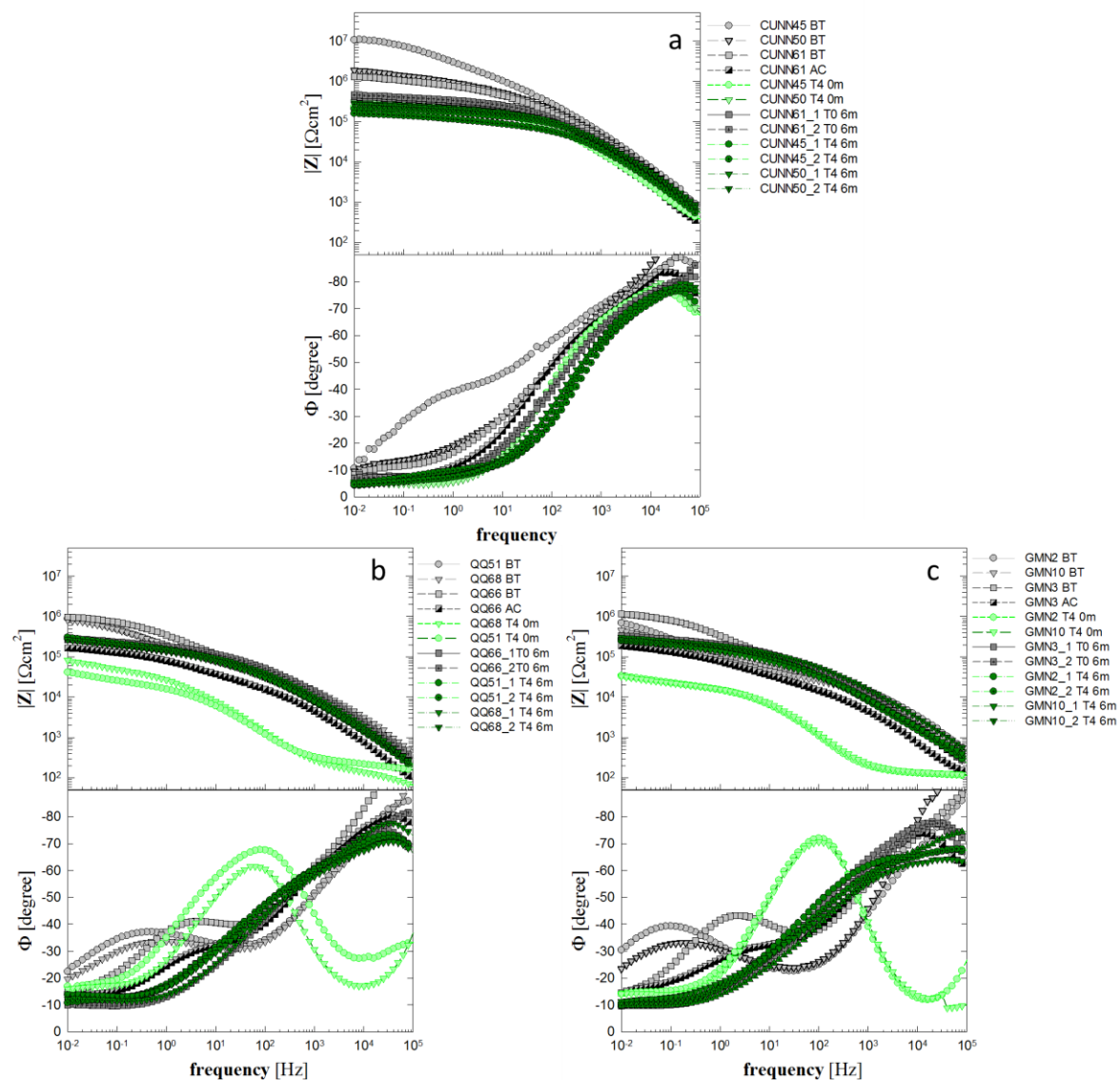


Figure 58. Bode plots (impedance modulus  $|Z|$  and phase  $\Phi$ ) of CUNN (a) QQ (b) and GMN (c) samples (2 measures for each sample). Data before treatment (BT, light grey), after agar cleaning (AC, grey/black square), after biopatina treatment (T4 0M, light green) and after 6 months exposure (6M) for the untreated (dark grey) and biopatinated (dark green) samples are shown

*Conclusions*

The new application protocol of biopatina treatment resulted in the formation of an even layer of copper oxalates. This homogeneity allowed the treatment to last during exposure in an extreme environment for six months. Nevertheless, the patina aesthetical appearance drastically changed resulting in a light green colour, in particular for red colour original patinas. For the moment, it seems that the biological treatment, did not provide a significant contribution to the protection of the treated surfaces as it did for archaeological objects. It is worth saying that due to the unstable environmental conditions and to the constant supply of moisture, pollutants and marine salts of the exposure environment, the corrosion mechanisms did not stabilise yet. Indeed, such instability is a typical behaviour in aggressive environments as Genoa. Usually a stabilization of the corrosion mechanism and thus of the patina are achieved after at least one year. Therefore, a new measurements campaign will be conducted after 12 months of exposure - in order to better compare the results with those of the previous study and to monitor the corrosion mechanisms occurred.

## 4.2 Artificial Patinas

### Abstract

In parallel to the stabilisation of natural patinas, the biological treatment was standardized for uses in contemporary art, design and architecture. Pilot tests were conducted on artificially patinated coupons reproducing foundry patinas. These coupons were treated with biopatina or Cosmolloid H80 and underwent natural ageing procedure in Neuchâtel, Switzerland. In order to improve the treatment performance the application protocol was modified according with the results obtain in the previous studies. Two delivery systems, one based on liquid fungal preculture, Japanese paper and a solid gel and another based on GelX were tested and compared on these samples. The properties of both biological and reference treatments were fully assessed before and after ageing through Fourier Transform Infrared Spectroscopy, Scanning Electron Microscopy, Colorimetry and Electrochemical Impedance Spectroscopy.

### Introduction

Metal sculptures frequently undergo patination processes in order to modify their surface appearance. Since the classical period, the manipulation of metal surfaces in order to create several colour finishes was well known, as testified by Pliny the Elder [26]. The purpose of patination usually is the embellishment of the surface but other reasons such as the emulation of antiquity, the achievement of naturalistic colours and/or the protection from environmental corrosion can bring to it. A large variety of methods to produce colours on the surface exist but the patination process involve the alteration of the metal surface by applying multiple layers of chemical solutions and, in several cases, heating. Nowadays, foundry artisans can create a great variety of colours on copper-based sculptures and contemporary artists have the possibility to use a large colour palette for their creations. Unfortunately, this kind of patinas are often powdery and unstable. Furthermore, some colours are obtained by the formation of potentially active corrosion products, such as copper chlorides. Therefore, it is important to stabilise and eventually protect artificial patinas from corrosion in order to preserve the artistic value of the artefact that is connected to the colour pallet intentionally used by the artist. In this research, five different artificial patinas applied on three different bronze alloys were characterized and treated with a novel biological treatment (biopatina) and with a traditional conservation treatment as reference (microcrystalline wax). Two different application protocols were tested in order to optimize the performance of the biological treatment. Due to the delicate and unstable nature of these patinas, the natural ageing was performed in the urban environment of Neuchâtel (Switzerland).

### Materials and Methods

#### *Samples*

Sets of 12 samples (60 x 60 x 4-5 mm) were cut from cast ingots of three bronze alloys and coated with five different artificial patinas traditionally used by the foundry Kunstgiesserei St. Gallen AG (Table 14). For the visual characterization of all samples, a scanner HP 4070 was used with a resolution of 600 dpi and the white balance set on a white paper.

Alloy	Main patina component	Acronym
Binary Bronze Cu (90%), Sn (10%)	Copper nitrate	NB
	Copper nitrate black	BNB
	Copper sulfate	SB
	Copper chloride	CB
Ternary Bronze Cu (90%), Sn (8%), Pb (2%)	Iron nitrate	IB
	Copper nitrate	NT
	Copper nitrate black	BNT
	Copper sulfate	ST
Quaternary Bronze Cu (85%), Sn (5%), Zn (5%), Pb (5%)	Copper chloride	CT
	Iron nitrate	IT
	Copper nitrate	NQ
	Copper nitrate black	BNQ
	Copper sulfate	SQ
	Copper chloride	CQ
	Iron nitrate	IQ

Table 14. Artificially patinated samples used within the project

### Treatments

For each set three groups of triplicates were defined: untreated (T0), treated with the biological treatment (T4) and treated with a microcrystalline wax as reference treatment (TR). The biological treatment was performed according to procedures developed at the University of Neuchatel using a specific strain of *Beauveria bassiana*. Two gel-based delivery systems were tested in order to compare their performance and the application ease, as summarized in Table 6. As reference treatment (TR), microcrystalline wax Cosmolloid H80 wax (CTS Restauro, CH-6807 Tavernne, Switzerland) was applied by a conservator-restorer using a brush after heating the samples surface using a hot air gun.

Method	Description	Duration	Patina nature
T4J	A liquid culture of <i>B. Bassiana</i> was dropped on samples surface. Japanese paper was laid upon coupons surface and covered with a solid gelling agent (agar) and nutrient.	4 weeks	copper nitrate, copper nitrate black and iron nitrate
T4K	A liquid culture of <i>B. Bassiana</i> was mixed with a gelling agent (GelX) and nutrient. The coupons were covered with the gel obtained.	4 weeks	copper sulfate and copper chloride

Table 15. Delivery systems and samples used for biopatina treatment

### Natural ageing procedures

All sets were exposed in the urban environment of Neuchatel (Switzerland) on the roof of the faculty of Sciences of the University of Neuchâtel. Orientation and position according to ISO 9223 standard already reported in Chapter 3.1 were selected. The outdoor exposure started in February 2014 and ended on February 2015. Data were collected at the end of the exposure time.

### Fourier Transform Infrared Spectroscopy (FTIR)

FTIR method used for this study was the same reported in Chapter 4.1.

### *Colorimetry*

The colorimetric analysis conducted for this study used the same spectrophotometer and conditions described in Chapter 4.1

### *Scanning Electron Microscopy (SEM)*

SEM analysis were performed with the same instrument and conditions reported in Chapter 4.1.

### *Electrochemical impedance spectroscopy (EIS)*

EIS measurements were performed as previously described in Chapter 4.1.

## **Results and discussion**

The first criterion to be evaluated for the two application methods compared here was the application ease. In fact, an easy-to-use delivery system is quite significant in order to transfer a laboratory protocol into real praxis in conservation-restoration. Gel method T4K presented an easier application than T4J method. This latter required the use of a solid gelling agent for fungal growth. The compact formed gel has a fragile structure that breaks easily during application and is not suitable for three-dimensional objects. On the contrary, T4K can be easily applied by hand, spatula or brush onto various surfaces and shapes.

In order to ascertain the presence of copper oxalates on the samples surface after biological treatment, FTIR measurements were performed. FTIR analysis, for both application methods, T4J and T4K, revealed the presence of intense characteristic vibrational bands of O=C-O bending at 1364 and 1321  $\text{cm}^{-1}$ , indicating the presence of copper oxalates, regardless of the patina original composition. Examples are showed in Figure 59 for copper nitrate and copper chloride patinas. Furthermore, the intensity of the peaks corresponding to the original patinas decreased concomitantly with the increasing absorbance of copper oxalates peaks. This suggested the presence of copper oxalates over the initial patina.

In accordance with FTIR results, SEM observations showed the presence of crystals aggregated as rosette-like concretions growing directly from the surface of T4J and T4K treated samples (Figure 60). These aggregates are typical of copper oxalates crystals. In order to evaluate the aesthetic effects of the two tested application methods, the colour distance  $\Delta E^*$  was calculated. Results showed that a minor colorimetric variation is obtained after T4K treatment with a maximum  $\Delta E^*$  of 6.5 (Figure 61). T4J method presented higher values dispersion that depended on the composition of treated patinas. Most of the time, the two methods presented a lower colorimetric variation compared with wax reference treatment (TR). It is also worth noticing that the final colour aspect is affected by the patina and the alloy original composition. In fact, the same method applied on different patinas resulted in different appearances. In the same way, a method applied on the same patina but with different underneath alloys led to different colour. Even considering these differences, the treatment T4K had a higher reproducibility leading to a more homogeneous colour.

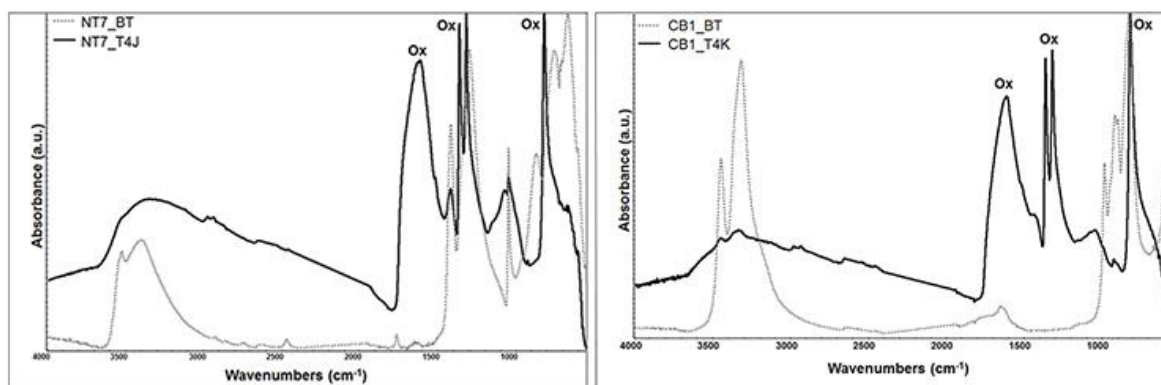


Figure 59. ATR-FTR spectra before (grey dotted line) and after (black continuous line) treatment with T4J method (left) on copper nitrate (NT) patina and T4K method (right) on copper chloride (CB) patina. Characteristic peaks of copper oxalates are indicated with the abbreviation Ox

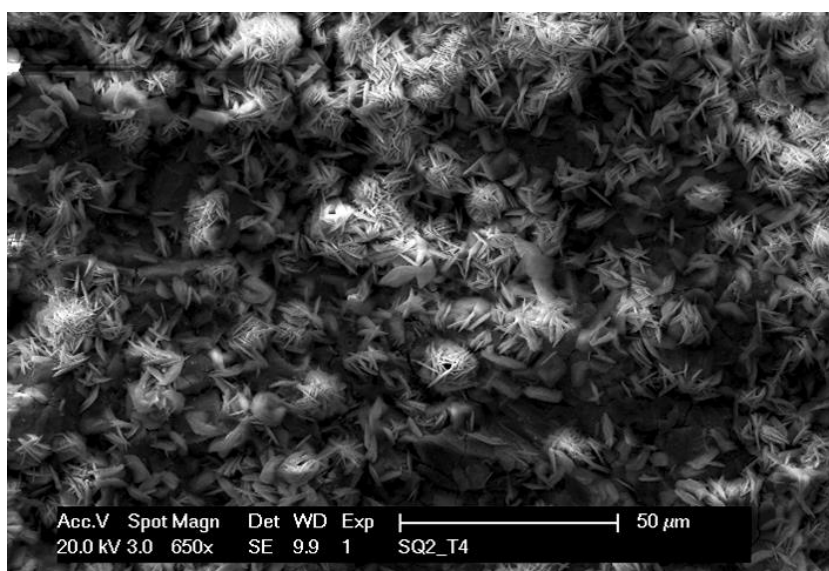


Figure 60. Secondary electrons SEM image of rosette-like copper oxalates crystals

EIS measurements showed that T4K impedance values increased, after treatment, for all the samples and  $|Z|$  values are on the same order while T4J method presented dispersed  $|Z|$  values (Figure 62). Results also showed high  $|Z|$  values on coupons treated with wax (IR), indicating an excellent protection achieved. The different impedance values between wax and biopatina are explained by the fact that the developed biological treatment does not produce an extra coating layer, as wax does, but a layer of copper oxalates that is formed from the patina underneath. This latter has a different protection mechanism from wax, making their comparison difficult. The biopatina treatment should be rather compared with conservation treatments with similar properties, such as corrosion inhibitors, e.g. benzotriazole (BTA). Experiments were performed on this comparison and results are showed in Chapter 3.

After treatment, all samples were exposed in the urban environment of Neuchâtel for 12 months. A complete characterization with the same analytical techniques employed before natural ageing was performed. In Figure 63 samples from all groups are shown before and after ageing. As a general observation, it seems that all samples underwent a colour change during ageing. Wax treated samples became darker and shinier than at the beginning of the exposure. It can be also observed, on T4 samples, a discolouration of the patina in particular for iron nitrate and copper sulphate.

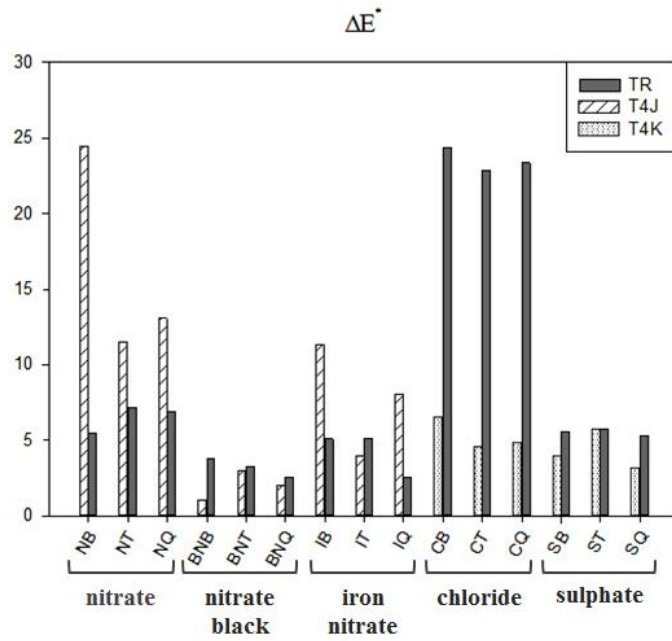


Figure 61.  $\Delta E^*$  of biological treatment applied by two different methods (T4J, T4K) compared with wax reference treatment (TR) for all the treated patinas on binary (B), tertiary (T) and quaternary (Q) bronze

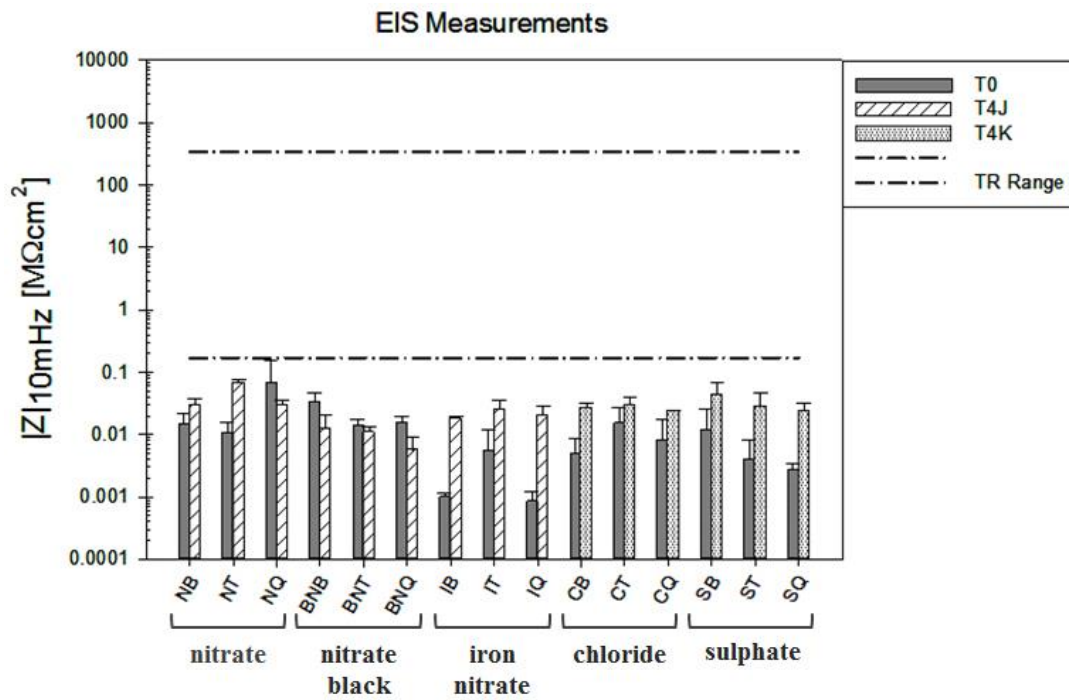


Figure 62. Comparison between impedance  $|Z|$  values of untreated samples (T0) and biological treated samples (T4J, T4K) of all the treated patinas on binary (B), tertiary (T) and quaternary (Q) bronze. The dashed lines represent the minimum and maximum  $|Z|$  values of the wax treatment (TR)



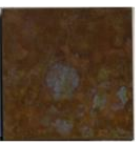
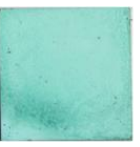

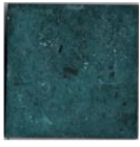






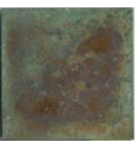
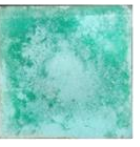









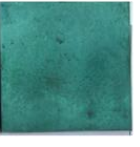




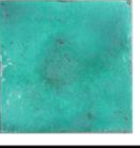

Treatment		Nitrate	Nitrate black	Iron Nitrate	Chloride	Sulfate
T0	0 Month					
	12 Months					
T4	0 Month					
	12 Months					
TR	0 Month					
	12 Months					

Figure 63. Visual characterization of the artificial patinas before exposure and after 12 months ageing. For each patina, a sample untreated (T0), treated with biopatina (T4) and microcrystalline wax (TR) is shown

Furthermore, on some samples, the trace of the impedance spectroscopy probe is visible in the central area. That could indicate an interaction between the electrolyte used on the probe and artificial patinas, which are usually more fragile than natural patinas. The electrolyte could have dissolved some products present on the artificial patina and soaked them in to the cloth used on the probe, modifying the characteristic of the contact area.

FTIR measurements showed that samples treated with Cosmoloid wax (TR) remained stable during ageing and presented typical aliphatic chain vibrational peaks, in particular at 2920 and 2851  $\text{cm}^{-1}$ . Nevertheless, the compounds of the artificial patinas were present in the spectra (Figure 64), indicating a decrease in thickness of the wax layer. Biopatinated samples (T4) showed different results depending on the artificial patina treated and on the application protocol as showed in Table 16.

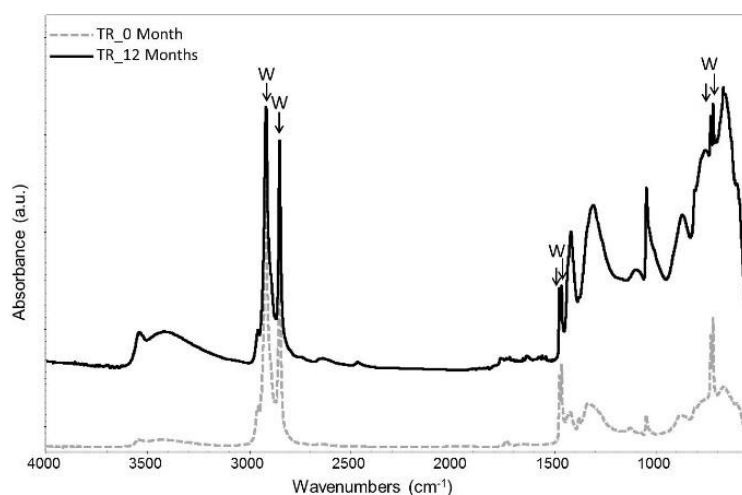


Figure 64. ATR-FTIR spectra comparison of the sample NB1 (copper nitrate original patina) treated with Cosmoloid wax H80 TR before (grey) and after 12 months of exposure (black), showing the newly increase of original patina peaks on the sample surface after ageing

Acronym	Main patina component	Alloy	Copper oxalate
NB	Copper nitrate	Binary bronze	-
NT		Ternary bronze	-
NQ		Quaternary bronze	-
BNB	Copper nitrate black	Binary bronze	-
BNT		Ternary bronze	-
BNQ		Quaternary bronze	+
IB	Iron nitrate	Binary bronze	+
IT		Ternary bronze	+
IQ		Quaternary bronze	+
CB	Copper chloride	Binary bronze	+
CT		Ternary bronze	+
CQ		Quaternary bronze	+
SB	Copper sulfate	Binary bronze	+
ST		Ternary bronze	+
SQ		Quaternary bronze	+

Table 16. Presence of copper oxalates on artificially patinated samples after 12 months of natural ageing

All samples with a copper nitrate patina did not show the presence of copper oxalates after one-year exposure regardless the alloy composition. On the black copper nitrate patina, copper oxalates were identified just on the quaternary alloy coupons, while binary and tertiary alloy samples did not show their presence. For all alloys, iron nitrate samples showed the presence of copper oxalates on their surface, even if in some cases just as traces. A unique character of this group is that most samples showed the presence of malachite on their surface, with the characteristic peaks at 1510, 1425, 1395, 1095, 1050, 880, 820 and 750  $\text{cm}^{-1}$ , changing the original patina composition after ageing (Figure 65). In fact, their surface showed a green patina that could be attributed to this newly formed compound. This compound was not identified on any other group of samples, indicating an endogenous cause.

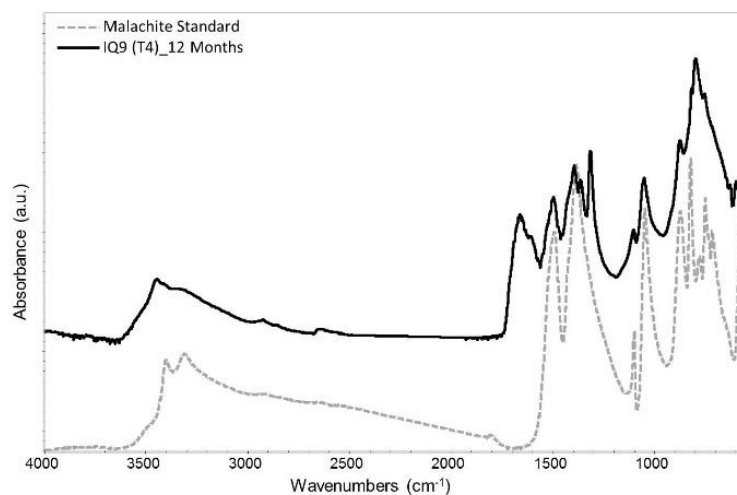


Figure 65. FTIR spectra comparison of the sample IQ9 (iron nitrate original patina) treated with biopatina after 12 months of exposure (black) and of the malachite standard (grey), revealing the presence of this latter as one of the compounds of the sample patina

Probably the recipe used by the foundry to create the artificial iron nitrate patina could explain the presence of this corrosion product after ageing. Characteristic copper oxalates vibrational bands of O-C-O bending at 1364 and 1321  $\text{cm}^{-1}$ , were also identified on all copper sulphate patinated samples, even if in most cases just as traces, as well as for copper chloride patinated samples. It appears that the T4K application protocol used on copper chloride and copper sulphate patinated samples guarantees a long-lasting adhesion of copper oxalates on artificial patinas. Furthermore, it seems that a patina composition based on copper nitrate is more difficult to treat and gives less durable results compared with the other biopatinated samples. SEM micrographs supported FTIR results. In fact, on samples with copper oxalates peaks recorded, it was possible to observe the presence of characteristic crystals with a rosette-like structure typical of copper oxalates (Figure 66a). Moreover, on wax treated samples it was possible to observe whether the coating layer was still homogeneous or if it had started to degrade (Figure 66b).

Regarding the samples aesthetical appearance after 12 months ageing, the application protocol T4J gave, in most of the cases, higher colour variation compared both to wax and untreated samples. On the contrary, application treatment T4K gave lower colour variation compared to wax and untreated samples (Figure 67).

EIS measurements showed that samples treated with Cosmoloid H80 wax (TR) had high values of  $|Z|$  indicating an excellent protection achieved by wax even after 12 months of exposure in a rural environment (Table 17).

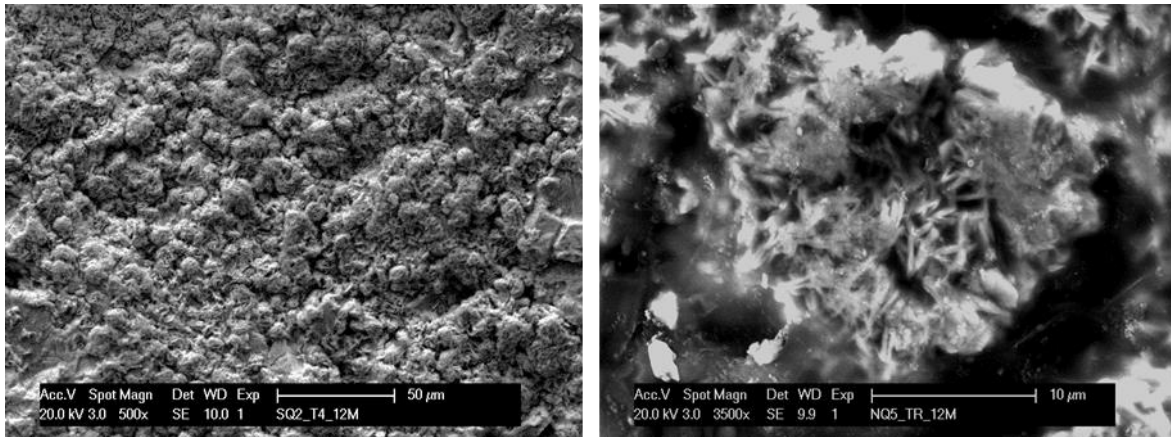


Figure 66. Secondary electron micrographs of black copper nitrate patina on quaternary bronze (BNQ, left) treated with biopatina (T4) showing copper oxalate crystals and of copper nitrate patina on quaternary bronze (NQ, right) with degraded coating layer of wax after 12 months of exposure

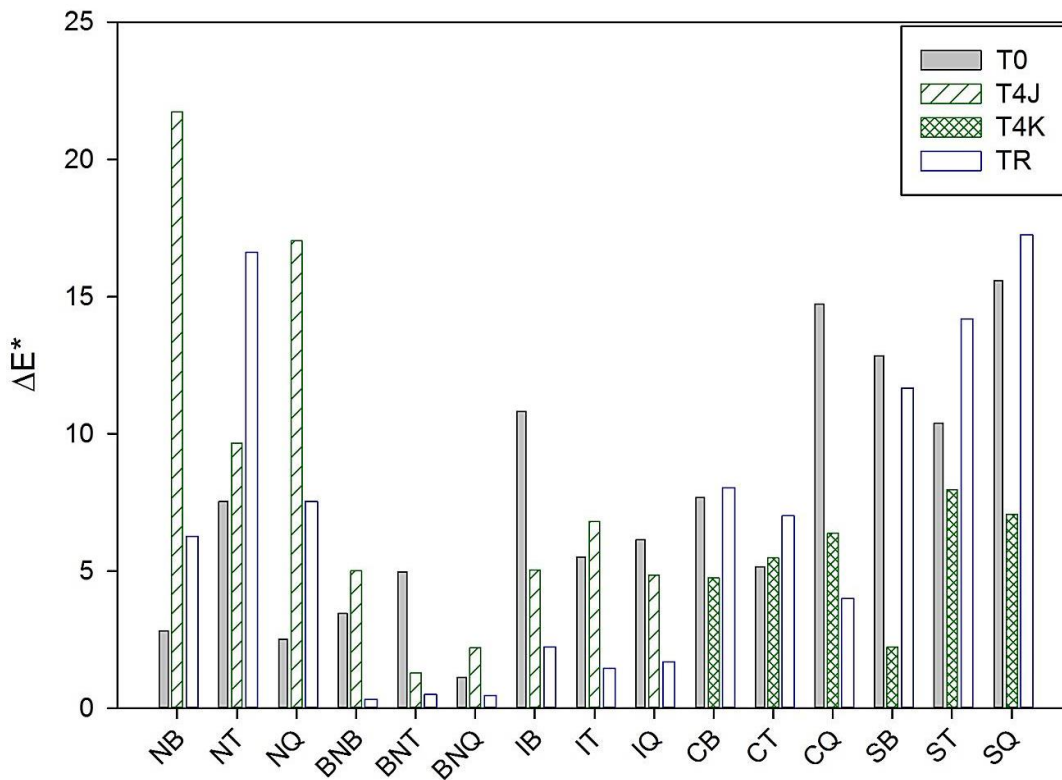


Figure 67.  $\Delta E^*$  of biological treatment applied by two different methods (T4J, T4K) compared with wax reference treatment (TR) for all treated patinas on binary (B), tertiary (T) and quaternary (Q) bronze

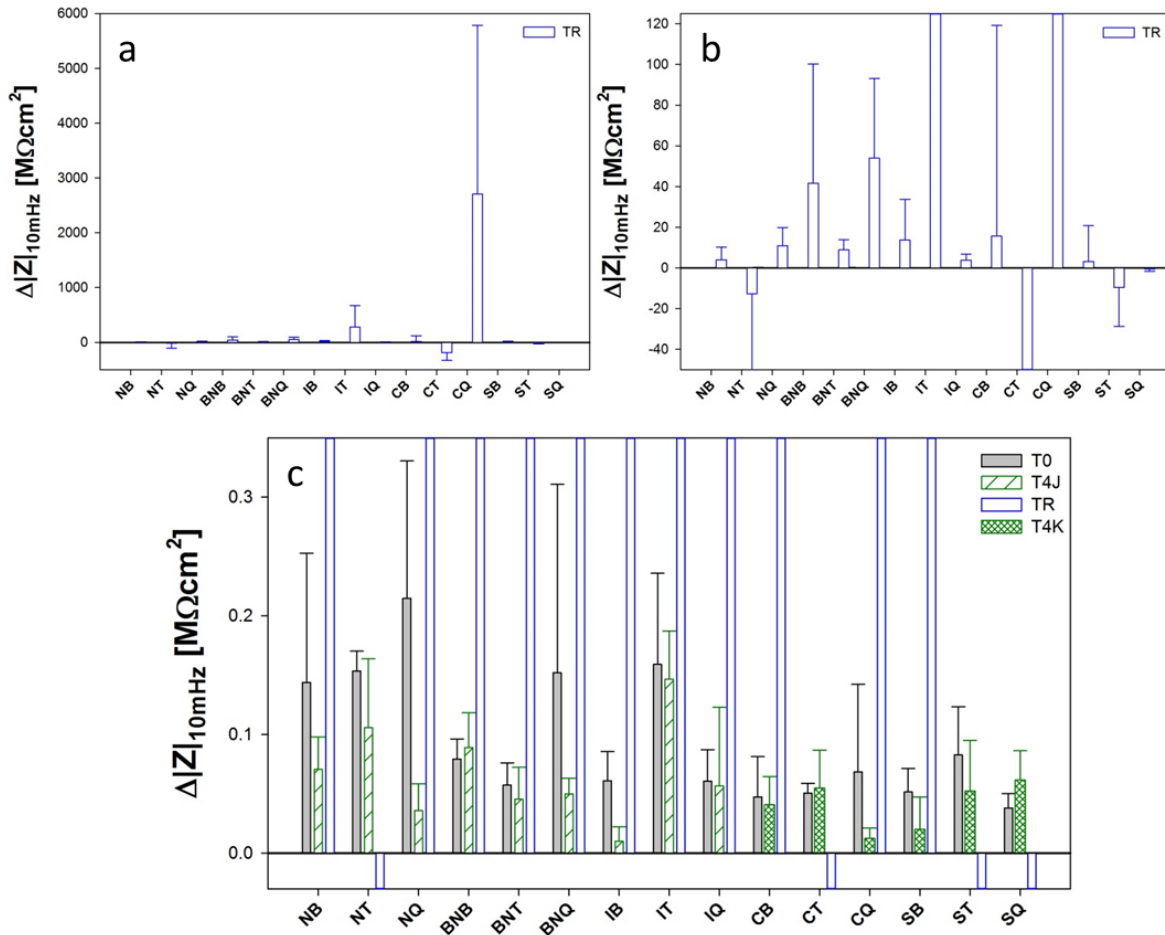


Figure 68. Variation of impedance values  $\Delta|Z|$  after 12 months of ageing obtained for the different sets of samples treated with Biopatina (T4, green), wax (TR, blue) and untreated (T0, grey). Negative values indicate a decrease of  $|Z|$  and positive values an increase of  $|Z|$  after one-year of exposure. a, b and c represent the same graph at a different scale

	T0		T4		TR	
NB	0.27	± 0.18	0.15	± 0.04	9.78	± 10.01
NT	0.28	± 0.03	0.25	± 0.10	76.19	± 32.27
NQ	0.47	± 0.33	0.09	± 0.04	26.05	± 15.27
BNB	0.18	± 0.03	0.17	± 0.05	88.26	± 98.17
BNT	0.11	± 0.04	0.09	± 0.04	23.95	± 7.68
BNQ	0.28	± 0.27	0.09	± 0.03	104.05	± 61.15
IB	0.11	± 0.04	0.04	± 0.02	24.28	± 35.363
IT	0.28	± 0.13	0.28	± 0.08	502.94	± 685.83
IQ	0.11	± 0.05	0.12	± 0.12	7.00	± 5.38
CB	0.09	± 0.06	0.10	± 0.04	80.27	± 127.80
CT	0.11	± 0.02	0.13	± 0.05	12.50	± 18.21
CQ	0.13	± 0.13	0.05	± 0.01	4826.02	± 5447.35
SB	0.11	± 0.02	0.08	± 0.03	13.92	± 22.82
ST	0.15	± 0.07	0.12	± 0.09	8.32	± 2.94
SQ	0.07	± 0.02	0.13	± 0.05	2.40	± 1.19

Table 17. Average impedance value  $|Z|$  ( $M\Omega cm^2$ ) obtained for the different sets of samples treated with biopatina (T4), wax (TR) and untreated (T0) after one-year exposure

Moreover, in 9 out of 15 cases, these wax samples drastically increased their protectiveness with the exception of NT, CT, ST and SQ groups which had a decrease of protective behaviour (Figure 68a-b). The uncommon improvement of protectiveness could be due to warm/cold temperature cycles that brought wax to melting/drying cycles causing an increase of atmospheric particulate adhesion. In fact, these cycles could have contributed to maintain a continuous and homogeneous coating layer, even if thinner, avoiding the formation of cracks and the contact of the underneath patina with environmental agents. It is worth saying that the exposure site of Neuchâtel has a low corrosivity index and that a longer time would be required for corrosion to occur. Regarding untreated and biopatina samples, all groups had an improvement of protectiveness, even if with a lower extent than wax samples (Table 17 and Figure 68c). For almost all samples (12 out of 15 sets) the  $|Z|$  values of T0 and T4 groups are comparable, indicating a similar protective behaviour after one year of exposure. Only BNB, CT, and SQ groups had higher protectiveness for biopatina-treated samples than untreated ones. This is probably due to the formation of extra corrosion layers on untreated samples at the interface between the metal and the artificial patina. These extra layers are probably formed by copper oxides that are not detectable by FTIR analyses. The formation of additional natural oxide layers could have a partial protective effect against corrosion increasing the samples  $|Z|$  values [27]. On biopatina-treated samples, the presence of copper oxalates slowed the corrosion mechanisms occurring at the metal-patina interface. It is interesting to observe that the inner nature of artificial patinas does not allow them to be electrochemically stable even after 12 months ageing.

## Conclusions

The performance the biological treatment applied on artificial foundry patinas on three different bronze alloys was here investigated. Both the application protocols tested ensured the formation of copper oxalates. However, the formation of a homogeneous layer of copper oxalates crystals, the increasing of protectiveness compared with the original patina before ageing, and a pleasant aesthetic appearance was obtained with the T4K protocol. Furthermore, it resulted to be an easy-to-use delivery system because of its gel texture, that can be easily applied by hand or using a spatula. Moreover, the comparison between biopatina and a microcrystalline wax in terms of aestheticism and colour variation resulted in favour of the biological treatment before ageing. After 12-months exposure, the T4K application method guaranteed an improved long-term adhesion of biopatina to the treated surface compared to T4J method. Furthermore, T4K method gave better results in terms of aesthetical appearance. Regarding corrosion resistance, microcrystalline wax remained stable in a mild corrosion site even if its thickness decreased. The biological treatment  $|Z|$  values remained mostly steady over time while the untreated samples showed an increase of the impedance values. This indicates a certain stability of biopatinated samples and instability of the artificial patina compounds that are still reaching a state of equilibrium with the exposure environment. Nevertheless, the protectiveness of the biological treatment could be improved in order to have, after ageing, higher protectiveness than untreated samples on artificial patinas.

Further investigations were also conducted in order to ascertain the influence of the alloy composition on the treatment behaviour and are presented in chapter 6.

## 4.3 Real Objects

### Abstract

In order to transfer the biological treatment into conservation-restoration real praxis, pilot tests were performed on real outdoor artefacts. These treatments were made in parallel with laboratory tests previously described (Chapters 3.1, 4.1 and 4.2). Indeed, each protocol used on the objects represents the one used in the laboratory at that moment.

Micro and non-destructive analyses were performed to characterise the object surface and to evaluate the efficiency of the treatment protocol.

### *Fusion sculpture*

**(Froidevaux, 1988, Neuchâtel, CH)**

In 2013 a discussion started with the City of Neuchâtel and the conservator-restorer in charge of the maintenance program for the sculptures in the public space. A real case-study was identified: the sculpture “*Fusion*” by Dominique Froidevaux (1988), located Avenue du Premier-Mars 26, 2000 Neuchâtel, Switzerland. This object is a sculpture made in three parts, of bronze and steel (Figure 69a-b). A report on the state of conservation was performed on August 2013: the presence of soluble deposits, dejections, ancient adhesives and bluish splashes at the base of the object (probably due to the garden maintenance) were observed (Figure 69c-e). Also, marks of a rotary mechanical abrasion probably due to the polishing of the object performed at the foundry were present. The sculpture presented bluish areas at the bottom and this test would permit to assess if the treatment could smooth this kind of splashing. In order to characterize the patina composition and conservation state, 4 micro-samples were taken from two areas (Figure 69-h). Those samples were analysed by FTIR spectroscopy. The surface patina appeared to be composed mainly of copper hydrosulphates (brochantite). In the blue areas at the base of the sculpture these latter are mixed with organic substances (Table 18).

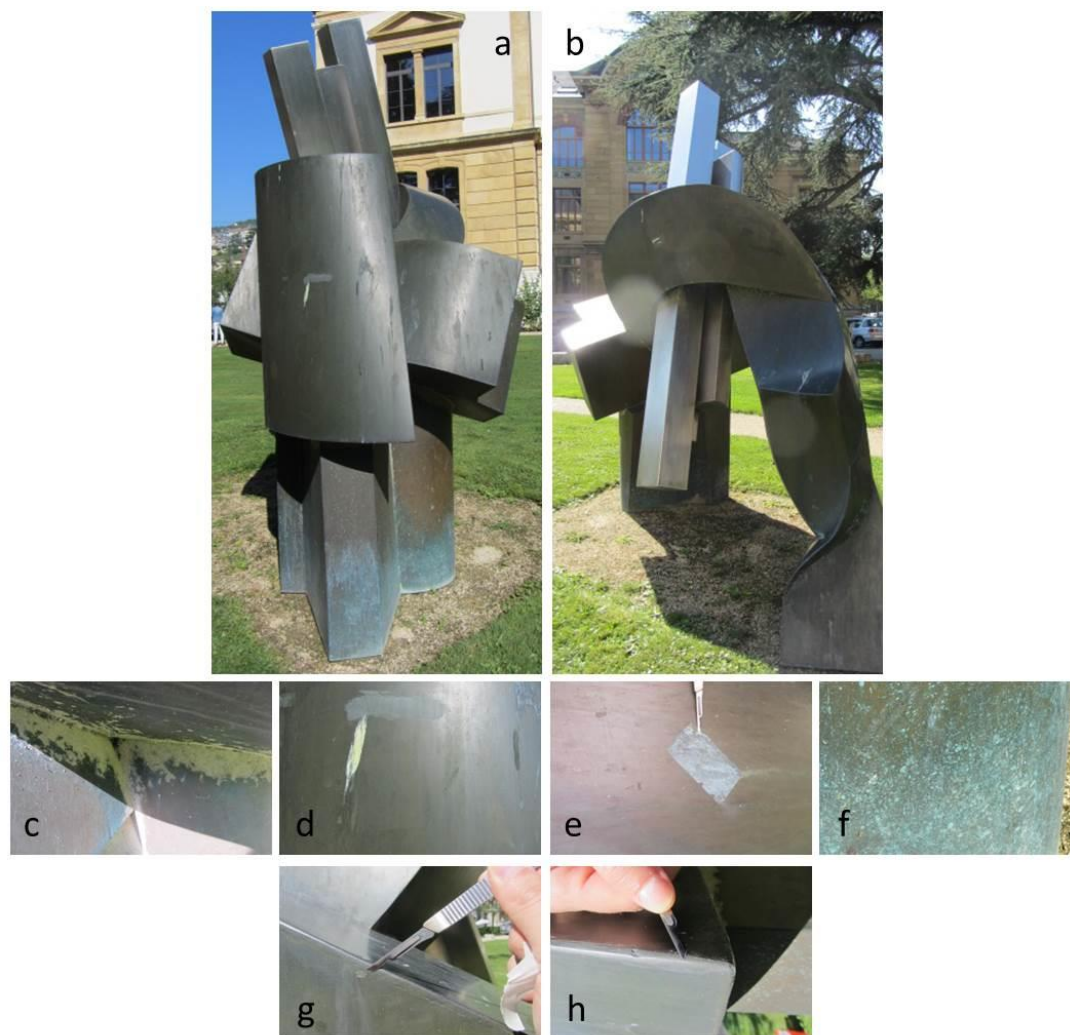


Figure 69. Fusion sculpture (Froidevaux, 1988) a-b) Before intervention. Documentation of the conservation state with c) soluble deposits, d) dejections, e) marks of ancient adhesives, f) bluish splashes and g-h) sampling points of the patina for FTIR analyses

Upper part, small area (Figure h)		Blue lower part, small area (Figure g)	
Peaks (cm <sup>-1</sup> )	Assignment	Peaks (cm <sup>-1</sup> )	Assignment
3588	brochantite	2932	organic
3561	brochantite	2851	organic
3271	brochantite	1087	brochantite
2925	organic	986	brochantite
2848	organic	944	brochantite
1087	brochantite	875	brochantite
981	brochantite	848	brochantite
944	brochantite	779	brochantite
872	brochantite	736	brochantite
848	brochantite	625	brochantite
782	brochantite		
734	brochantite		
625	brochantite		

Table 18. ATR-FTIR results on patina sample



Figure 70. Selected areas for biological treatment

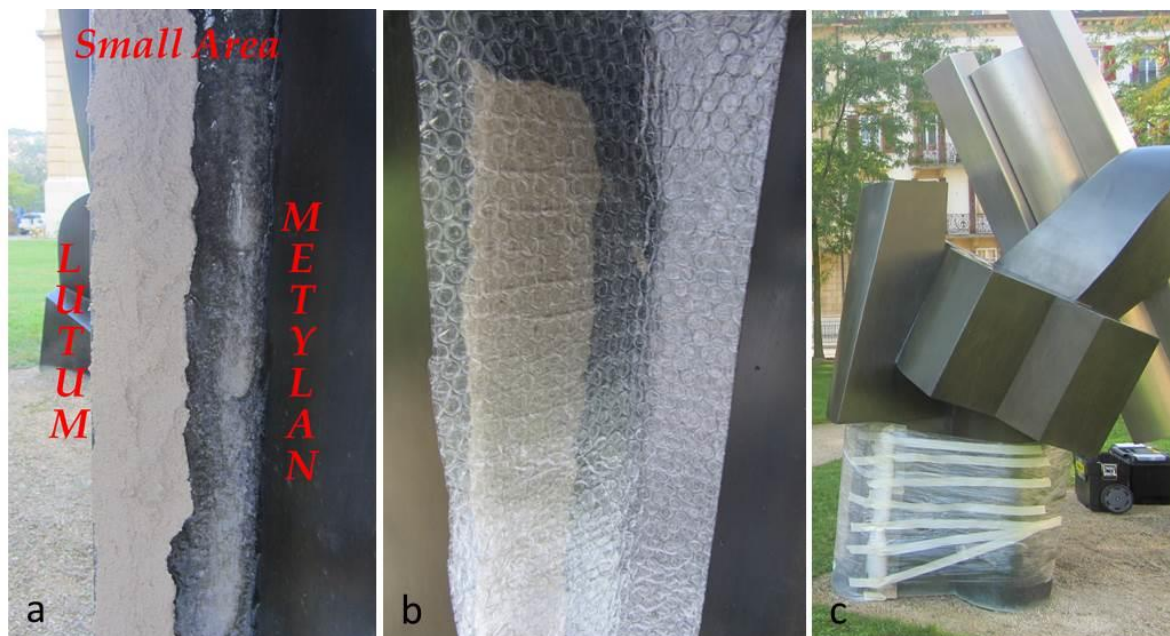


Figure 71. a) Small Area treated with a mixture of clay products (based on Lutum®) and a Metylan®-based gel; b-c) Ongoing treatment

Two test-zones of 11 x 50 cm and 80 x 20 cm respectively were identified for the application of biological treatment (Figure 70). The other bronze surfaces were treated according to the current methods used by conservator-restorers in Neuchâtel with a wax.

To perform the biological treatment, the following protocol was used:

- Characterization of the surface using non-destructive analytical techniques in order to understand the state of conservation of the artwork and the nature of the corrosion products present (FTIR)
- Cleaning of the surface of the statue in order to remove surface deposits (dust, etc.) and powdery corrosion products. Sterilization of the treated surface using 70% w/w ethanol solution in deionized water
- Application of the treatment, using procedures defined by the University of Neuchâtel. It has been decided to perform the biological treatment based on two different delivery systems in order to assess their effectiveness. The selected substrates were a mixture of clay products (based on Lutum®) and a Metylan®-based gel both mixed with *B. bassiana* precultures. The two areas identified were treated with both substrates (Figure 71a)
- Treated areas were packed with punched plastic film in order to maintain a high relative humidity and oxygen supply necessary for fungal growth (Figure 71b-c)

In order to monitor the treatment, a copper roof plate with a patina of copper hydrosulphates was treated with the same materials and exposed to similar atmospheric environment. Regular visual controls were performed on the sculpture and copper roof plate.

After 3 weeks on 17th October, Metylan®-based gel was no longer in contact with the surface due to its low density and verticality of the surface. In order to avoid an inhomogeneous treatment, this substrate was removed and analysed by FTIR spectroscopy (Table 19). The presence of copper oxalates was ascertained suggesting the effectiveness of the biological treatment.

After 5,5 weeks, on November 5<sup>th</sup>, the mixture of clay products (based on Lutum®) was removed. It is worth saying that the treatment duration was slightly extended respect to laboratory conditions due to the low outdoor temperature that inhibited fungal growth. FTIR analyses were conducted both on the copper roof plate and on removed clay-based substrate (Table 19 and Table 20). The presence of copper oxalates was not detected in the substrate but a colour variation of the treated surface was noticed, possibly due to the reaction of some compound of the delivery system with the surface.

Metylan®-based gel Large area		Clay-based gel Large area		Metylan®-based gel Small area		Clay-based gel Small area	
Peaks (cm <sup>-1</sup> )	Assignment	Peaks (cm <sup>-1</sup> )	Assignment	Peaks (cm <sup>-1</sup> )	Assignment	Peaks (cm <sup>-1</sup> )	Assignment
3354	Metylan	3343	Lutum	3351	Metylan	3370	Lutum
<b>1633</b>	<b>Cu oxalates</b>	1643	Lutum	<b>1641</b>	<b>Cu oxalates</b>	1646	Lutum
1458	Metylan	1199	Lutum	1454	Metylan	1196	Lutum
<b>1362</b>	<b>Cu oxalates</b>	1093	Lutum	<b>1377</b>	<b>Cu oxalates</b>	1087	Lutum
<b>1316</b>	<b>Cu oxalates</b>	1034	Lutum	<b>1321</b>	<b>Cu oxalates</b>	1029	Lutum
1154	Metylan	978	Lutum	1151	Metylan	984	Lutum
1111	Metylan	670	Lutum	1114	Metylan	912	Lutum
1056	Metylan			1053	Metylan	667	Lutum
948	Metylan			664	Metylan		
822	Cu oxalates						
668	Metylan						

Table 19. ATR-FTIR results on removed substrates

Copper roof plate Metylan®-based gel		Copper roof plate clay-based gel	
Peaks (cm <sup>-1</sup> )	Assignment	Peaks (cm <sup>-1</sup> )	Assignment
3588	brochantite	3588	brochantite
3564	brochantite	3564	brochantite
3383	brochantite	3381	brochantite
3277	brochantite	3271	brochantite
<b>1617</b>	<b>Cu oxalates</b>	<b>1628</b>	<b>Cu oxalates</b>
<b>1362</b>	<b>Cu oxalates</b>	1426	Lutum
<b>1318</b>	<b>Cu oxalates</b>	<b>1370</b>	<b>Cu oxalates</b>
1088	brochantite	1088	brochantite
985	brochantite	983	brochantite
948	brochantite	942	brochantite
875	brochantite	875	brochantite
<b>821</b>	<b>Cu oxalates</b>	848	brochantite
780	brochantite	778	brochantite
732	brochantite	731	brochantite
627	brochantite	631	brochantite

Table 20. ATR-FTIR results on control copper roof plate

## **Sculpture park Légende d'Automne**

**(SaraH, 2014, Lausanne, CH)**

In April 2014 a collaboration was initiated between the Laboratory of Microbiology of the University of Neuchâtel and the Association “Légende d'Automne”. The sculpture park “Légende d'Automne” is located in the heart of the Lausanne city. It is a place where touching means seeing. A set of eighteen bronze scenes to discover a story. Every scene comes with a tree trunk holding an open book; one page displays the text in braille and the other one in latin alphabet. Inspired by her own book “Légende d'Automne” Sara.H is creating this work with poetry and delicacy. The story tells why trees lose their leaves in autumn. It was the artist's wish to offer the sculpture set to the City of Lausanne and to its population. The project was entirely financed by donations from private people, companies, institutions, foundations and associations. *Légende d'Automne* was the first project to benefit from biopatina treatment at large scale and on different types of patinas. The wish of the artist was to remove all the powdery parts of the new foundry patinas from the sculptures, since they were intended to be touched. Furthermore, she wanted to contemporary create a protective layer on her artworks and tone down the foundry patina colours into more greenish, pleasant aged bronze colours. Indeed, the artist considered too shiny and vibrant the newly applied foundry patinas.

In order to characterize the artificial patinas composition, micro-samples were taken from different part of the statues, according to the colour palette employed by the foundry. FTIR results showed that the blue and green tones are characterized by the presence of copper chlorides, while the black tone is obtained with a mixture of a black pigment, probably carbon black (that cannot be identified by FTIR spectroscopy) with shellac as organic binding medium.

At the beginning of April 2014, a pilot test was performed on two sculptures (Figure 72). This pilot test had involved the artists that created the sculptures. The biopatina treatment was applied using the GelX-based delivery system tested described in chapter 4.2 on the two scenes for a 3-weeks treatment.

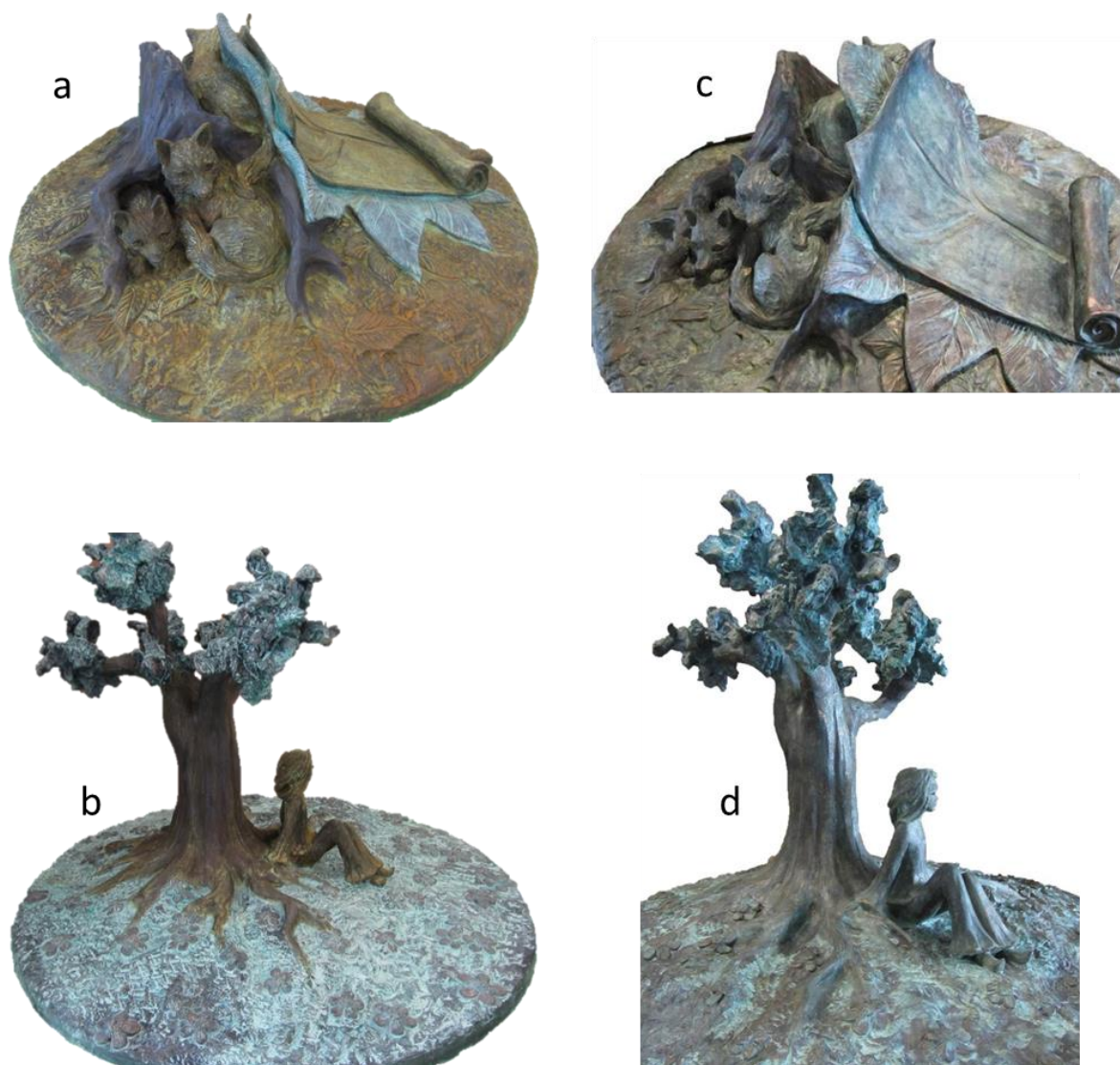


Figure 72. Pilot test: the two scenes before (a-b) and after (c-d) biological treatment

After this pilot test, the Association “Legende d’Automne” commissioned the University of Neuchâtel for an additional set of sculptures. For organisational purpose, the treatment was conducted at the premises of the University of Neuchâtel.

During 2014, 24 sculptures (11 scenes, 11 lecterns and 2 entry plates) were treated. Here below are showed some of the treated sculptures (Figure 73).



Figure 73. Scenes before (right) and after (left) 3 weeks of biological treatment

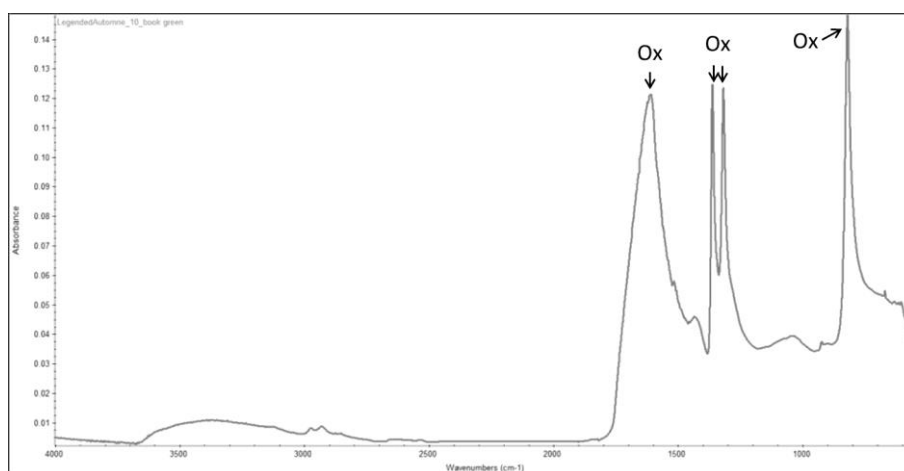


Figure 74. ATR-FTIR spectrum showing the presence of copper oxalates (Ox) on a lectern, on the front side of the book

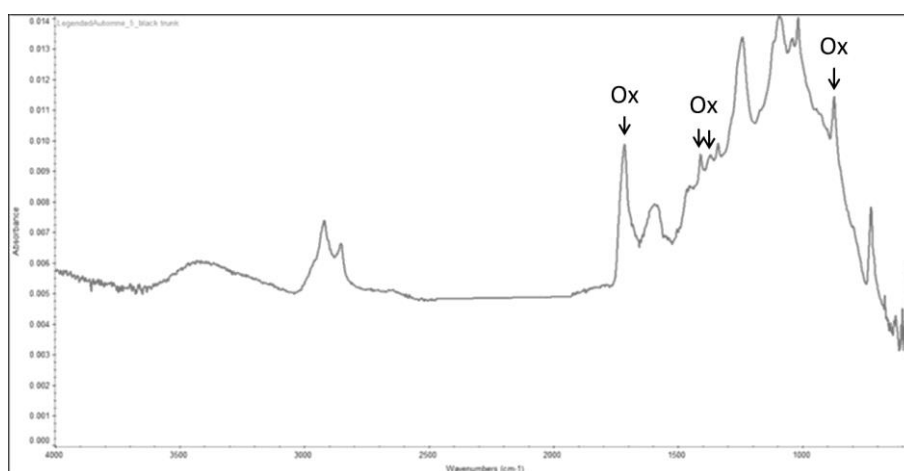


Figure 75. ATR-FTIR spectrum obtained on the black trunk of a lectern. The copper oxalates characteristic peaks (Ox) are less visible

In order to ascertain the presence of copper oxalates on the sculptures, micro-samples were taken from different part of the statues. Those samples were analysed by ATR-FTIR spectroscopy. Almost all the samples showed the presence of characteristic vibrational bands of O-C-O bending at 1364 and 1321 cm<sup>-1</sup>, attributing to copper oxalates (Figure 74). On black/brown areas, the presence of copper oxalates seemed less (Figure 75). This is probably due to the shellac applied during patination process. This compound formed a coating that acts as a barrier and did not allow the copper ions to diffuse and form a copper oxalates layer.

All treated sculptures were moved from the University of Neuchatel facilities and brought at the promenade Schnetzler in Lausanne where, in September 2014, the park was inaugurated.

## Conclusions

The use of different delivery systems on real artefacts confirmed the results obtained from laboratory tests. The Lutum® and Metylan® based delivery systems, even if suitable for the application on large outdoor objects resulted in poor efficiency in terms of copper oxalates production. Whereas, the delivery system based on GelX was efficient and easy-to-use on large surfaces. These tests on real artefacts will also allow to monitor the evolution of the treated surfaces during long-term exposure in outdoor environment since the access to the sculptures will be possible in further moments.

## References

1. Cappitelli, F., et al., Advantages of Using Microbial Technology over Traditional Chemical Technology in Removal of Black Crusts from Stone Surfaces of Historical Monuments. *Applied and Environmental Microbiology*, 2007. 73(17): p. 5671-5675.
2. De Belie, N., Microorganisms versus stony materials: a love-hate relationship. *Materials and structures*, 2010. 43(9): p. 1191-1202.
3. Fernandes, P., Applied microbiology and biotechnology in the conservation of stone cultural heritage materials. *Applied microbiology and biotechnology*, 2006. 73(2): p. 291-296.
4. Bharde, A., et al., Extracellular biosynthesis of magnetite using fungi. *Small*, 2006. 2(1): p. 135-141.
5. Appelbaum, B., *Conservation treatment methodology*. 2007, Oxford: Elsevier.
6. Brandi, C., *Teoria del restauro*. Vol. 318. 1981: Ed. di storia e letteratura.
7. Gadd, G.M., Geomycology: biogeochemical transformations of rocks, minerals, metals and radionuclides by fungi, bioweathering and bioremediation. *Mycological Research*, 2007. 111(1): p. 3-49.
8. Gadd, G.M., Metals, minerals and microbes: geomicrobiology and bioremediation. *Microbiology*, 2010. 156(3): p. 609-643.
9. Watkinson, D., Preservation of Metallic Cultural Heritage, in Shreir's Corrosion, J.A.R. Tony, Editor. 2010, Elsevier: Oxford. p. 3307-3340.
10. Dillmann, P., et al., Corrosion of metallic heritage artefacts: investigation, conservation and prediction of long term behaviour. 2007, Cambridge: Woodhead Publishing Limited.
11. Argyropoulos, V., *Metals and museums in the Mediterranean: protecting, preserving and interpreting*. 2008: Technological educational institute of Athens.
12. Johnson, R., The removal of microcrystalline wax from archaeological ironwork. *Studies in Conservation*, 1984. 29(sup1): p. 107-109.
13. Moffett, D.L., Wax coatings on ethnographic metal objects: justifications for allowing a tradition to wane. *Journal of the American Institute for Conservation*, 1996. 35(1): p. 1-7.
14. Brostoff, L.B., *Coating strategies for the protection of outdoor bronze art and ornamentation*. 2003, University of Amsterdam. p. 180.
15. Joseph, E., et al., Development of an analytical procedure for evaluation of the protective behaviour of innovative fungal patinas on archaeological and artistic metal artefacts. *Analytical and Bioanalytical Chemistry*, 2011. 399: p. 2899-2907.
16. Joseph, E., et al., Protection of metal artefacts with the formation of metal-oxalates complexes by *Beauveria bassiana*. *Frontiers in Microbiology*, 2012. 2.
17. Joseph, E., et al., Spectroscopic characterization of an innovative biological treatment for corroded metal artefacts. *Journal of Raman Spectroscopy*, 2012. 43(11): p. 1612-1616.
18. Joseph, E., et al. Assessment of a biological approach for the protection of copper alloys artefacts. in *Conference Proceedings of Metal*. 2013.

19. Joseph, E., et al., BIOPATINAS: Innovative biological patinas for copper-based artefacts. , in *Outdoor Metallic Sculpture from the XIXth to the Beginning of the XXth Century: Identification, Conservation, Restoration*. 2014, ICOMOS France: Paris. p. 154-162.
20. Albini, M., et al., Innovative biological approaches for metal conservation. *Materials and Corrosion*, 2016. 67(2): p. 200-206.
21. Nassau, K., et al., The characterization of patina components by X-ray diffraction and evolved gas analysis. *Corrosion Science*, 1987. 27(7): p. 669-684.
22. Marabelli, M. and R. Mazzeo, La corrosione dei bronzi esposti all'aperto: problemi di caratterizzazione. *METALLURGIA ITALIANA*, 1993. 85: p. 247-247.
23. ISO, 9223:2012 Corrosion of metals and alloys - Corrosivity of atmospheres - Classification, determination and estimation. 2012.
24. Letardi, P., Electrochemical measurements in the conservation of metallic heritage artefacts: an overview, in *Corrosion and Conservation of Cultural Heritage Metallic Artefacts*. , P. Dillmann, et al., Editors. 2013, EFC Publications. p. 126-48.
25. Barsoukov, E. and J.R. Macdonald, *Impedance spectroscopy: theory, experiment, and applications*. 2005: John Wiley & Sons.
26. Cano, E., D. Lafuente, and D.M. Bastidas, Use of EIS for the evaluation of the protective properties of coatings for metallic cultural heritage: a review. *Journal of Solid State Electrochemistry*, 2010. 14(3): p. 381-391.
27. Shim, J.J. and J.G. Kim, Copper corrosion in potable water distribution systems: influence of copper products on the corrosion behavior. *Materials Letters*, 2004. 58(14): p. 2002-2006.



## Chapter 5

---

### INFLUENCE OF TIN ENRICHMENT



This chapter is based on the results of the following published article:

M. Albini, C. Chiavari, E. Bernardi, C. Martini, L. Mathys, E. Joseph. Evaluation of the performances of a biological treatment on tin-enriched bronze. *Environmental Science and Pollution Research*, 2016. DOI: 10.1007/s11356-016-7361-2.

This part of the research was implemented in collaboration with the University of Bologna (Italy).

## Summary

In this chapter the influence of high amount of tin on the biopatina treatment behaviour will be investigated. Indeed, the corrosion behaviour of bronze differs from that of pure copper due to the presence of additional alloying elements. In natural environments, the selective dissolution of copper leads to a relative tin-enrichment within the corrosion layers, mostly in unsheltered areas exposed to rainwater runoff. The use of the biological treatment on outdoor exposed artefacts needs to take into account the difference in terms of patina composition. Indeed, it is important to understand the reactions occurring in these particular areas in case the biopatina treatment will be applied on the entire monument. Thus, the efficiency of the treatment, that metal oxalates are homogenously formed on the treated surface, should be ascertained whatever the patina composition underneath.

This chapter will first explore the reaction occurring applying the biological treatment on pure tin foil. Then, the issue of tin enrichment on bronze will be addressed through the artificial ageing of quaternary bronze samples by a dropping method simulating rainwater runoff conditions. These pre-aged samples will be then treated with biopatina and exposed a second time to the same ageing procedure. Finally, samples will be analysed through Fourier Transform InfraRed (FTIR) and Raman spectroscopies, Scanning Electron Microscopy coupled to Energy Dispersive Spectroscopy (SEM-EDS) and Atomic Absorption Spectrometry (AAS).

## Abstract

In the two last decades, research gave emphasis to eco-friendly and sustainable approaches for the preservation of cultural heritage that could also offer advantages in terms of compatibility, durability and safety. Hence, a biological treatment, based on a specific fungal strain of *Beauveria bassiana*, is exploited for the stabilisation of soluble and/or active copper corrosion products, converting them into copper oxalates. The chemical stability of the latter represents a real improvement for the long-term preservation of bronze, especially in case of exposure to acid rains. However, in unsheltered areas of bronze artefacts the dissolution of copper leads to a relative tin-enrichment of the patina. In order to understand the influence of tin-enriched surfaces on the formation of metal oxalates, pure tin and artificially tin-enriched bronze coupons were treated with this novel biological system and, in the case of bronze coupons, exposed to artificial ageing. Tin enrichment and accelerated ageing were performed through runoff procedures. Before and after treatment as well as after ageing, the sample surface was characterized through Fourier Transform InfraRed (FTIR) and Raman spectroscopies, Scanning Electron Microscopy coupled to Energy Dispersive Spectroscopy (SEM-EDS). Metals released in the leaching solutions were analysed through Atomic Absorption Spectrometry (AAS). The results allowed to better understand the response of unsheltered areas from outdoor bronze monuments to the biological treatment proposed.

## Introduction

Metal artefacts undergo corrosion processes since the moment of their production. Indeed, the presence of oxygen and water in the atmosphere induces oxidation processes that lead to the formation of several corrosion layers. In particular, on outdoor bronze monuments, the copper oxidation leads initially to the formation of an adherent layer of cuprite ( $\text{Cu}_2\text{O}$ ). Thereafter, depending on the environmental conditions, corrosion products such as copper chlorides (e.g. atacamite  $\text{Cu}_2\text{Cl}(\text{OH})_3$ ) and/or copper sulphates (e.g. brochantite  $\text{Cu}_4(\text{SO}_4)(\text{OH})_6$ ) are formed [1-6]. These layers are reported to partially protect the underlying metallic substrate from aggressive environmental conditions [7-9]. However, the protectiveness of these corrosion products is controversial and depends on various factors such as local pH, homogeneity, thickness, solubility and adhesion. Indeed, in the case of copper chlorides and/or copper sulphates these products are considered harmful for the artefacts. Furthermore, there is a substantial difference between sheltered and unsheltered areas of a sculpture. Hence, the geometry of the object and its exposure to acid rainwater has to be considered when proposing a conservation-restoration intervention. On sheltered areas the main conservation issue is the stagnation of a water film. This particular corrosion process is characterized by an inner layer of tin corrosion products and a second external layer mainly composed by copper corrosion products [10]. On the contrary, on unsheltered areas directly exposed to rain runoff, the main issue is the leaching action of acid rain that constantly washes out the newly formed copper corrosion products decreasing copper concentration and hence relatively increasing tin concentration on the surface [11]. The mechanism of bronze surface tin-enrichment related to the exposure conditions was previously depicted [9, 12]. In particular, the selective dissolution of copper was described. In fact, copper, zinc and partially lead species are dissolved and washed out from the surface. Furthermore, this phenomenon was related to the simultaneous formation of insoluble tin oxides, stable in aerated conditions and over a large pH range. Moreover, these unsheltered areas are typically characterised by vertical light green streaks (Figure 76) [9]. This heterogeneous surface composition requires appropriate conservation-restoration protocols that should consider the different nature and behaviour of the two corroded areas.



Figure 76. Statue “Schwinger” (Siegwart 1905) located in Lucerne before restoration intervention (2015) showing vertical light green streaks characteristic of unsheltered areas

So far, conservation-restoration treatments employed for copper-based alloys are mostly based on the application of organic protective coatings or inhibitors. These protective systems do not consider the differences in terms of patina composition and corrosion products stability. In fact, they act against aggressive environments in a non-specific way, simply creating a physical barrier (i.e. organic coatings) or forming chemical complexes (i.e. inhibitors) [13-15]. Moreover, some toxic inhibitors induce potential threats to human health and to the environment [1]. Nowadays, the exploitation of microorganisms in biotechnological applications is widespread and biological solutions start to be proposed also in cultural heritage preservation. In previous studies [16-20] a treatment based on a specific fungal strain of *Beauveria bassiana* has been designed as alternative treatment for the stabilisation of copper-based alloys artefacts. This treatment relies on the capability of copper-resistant fungi to transform soluble and/or active copper corrosion products into more stable copper oxalates. Indeed, thanks to their insolubility and stability even under acidic conditions [21] copper oxalates can provide long-term preservation to the treated objects together with a low aesthetical impact. Due to their inorganic nature, this newly formed copper oxalates are also compatible with the original patina present on the artefact, having the same physical-chemical characteristics of a natural patina. Finally, this treatment presents interesting properties for environmental and health concerns as the selected microorganism is already commonly used in organic agriculture [22]. The present work aims to evaluate the interaction between the biological treatment and bronze surfaces artificially enriched in tin, simulating the effects of the treatment on unsheltered areas of bronze outdoor monuments. To this purpose, a first experiment was conducted on pure tin coupons and the compounds formed after biological treatment were identified through Fourier Transform InfraRed (FTIR) and Raman micro-spectroscopy. Thereafter, additional coupons of bronze alloy UNS C83600 underwent tin-enrichment using the dropping method as described by Bernardi et al. in 2009 [11]. These coupons were then treated according to the same protocol as for pure tin coupons. The surface of metal coupons was characterized before and after biopatination treatment using FTIR spectroscopy and Raman micro-spectroscopy, as well as Scanning Electron Microscopy (SEM) coupled with Energy Dispersive Spectroscopy (EDS). The colour change and the aesthetical appearance of the

surface were also evaluated by colorimetric measurements. Subsequently, in order to evaluate the long-term performance of the biological treatment, untreated and biologically treated samples underwent to artificially ageing procedures using the same dropping method as mentioned above. During weathering, the amount of released metal ions was monitored by Atomic Absorption Spectroscopy (AAS) and the mass decrease was measured as well.

## Materials and methods

### *Coupons*

Three tin coupons of approximately 4 cm<sup>2</sup> were cut directly from a pure tin foil (FINOTIN 0.10mm, Original FINO GmbH, Germany). Two coupons were used for the biological treatment and one coupon was left untreated. Before treatment the surface was cleaned with ethanol and rinsed with deionized water. Bronze coupons of 2.5x1.0x0.5 cm were cut from sand cast alloy. The alloy corresponds to a quaternary bronze (UNS C83600, Cu85/Sn5/Zn5/Pb5) generally used for artistic casting. Its composition, determined by Glow Discharge Optical Emission Spectroscopy (GDOES), resulted to be 90.3 Cu, 5.7 Sn, 3.3 Pb, 0.3 Zn, 0.4 Ni (% wt). The surface was polished by abrasive papers up to 1000 grit, cleaned with acetone and rinsed with deionized water. Three bronze coupons were prepared in total: two of them (G85dx and G85sx) were used for the biological treatment and one (G85) was left untreated in order to be used as reference.

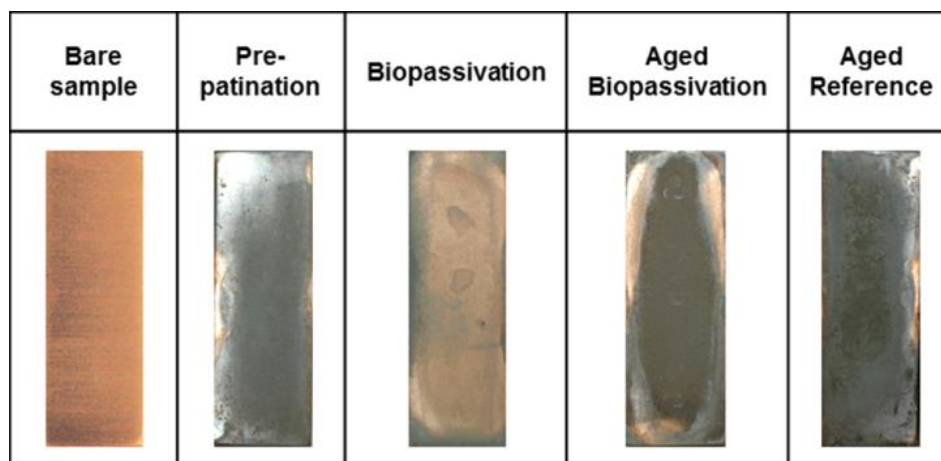


Figure 77. Surface appearance of bare, pre-patinated, treated and aged sample (G85dx) with aged reference sample (G85)

### *Pre-patination and ageing method*

All bronze samples underwent preliminary ageing procedures (pre-patination) in order to simulate the action of the rain in runoff conditions (dropping test). This procedure allowed a surface enrichment in tin on the bronze coupons (Figure 77). The coupons underwent the same weathering procedure after the biological treatment being performed (Figure 77), together with the reference coupon. Synthetic rain reproducing the mean composition of natural acid rain samples collected during the winter months in Bologna (Italy) was used. The composition was: 1.44 mg L<sup>-1</sup> CaSO<sub>4</sub>·2H<sub>2</sub>O; 1.50 mg L<sup>-1</sup> (NH<sub>4</sub>)<sub>2</sub>SO<sub>4</sub>; 1.92 mg L<sup>-1</sup> NH<sub>4</sub>Cl; 1.51 mg L<sup>-1</sup> NaNO<sub>3</sub>; 5.50 mg L<sup>-1</sup> HNO<sub>3</sub> (65 wt%); 0.32 mg L<sup>-1</sup> CH<sub>3</sub>COONa; 0.08 mg L<sup>-1</sup> HCOONa, with a measured pH of 4.3 [10, 23](Chiavari et al. 2015; Chiavari et al. 2010). The solution was periodically dropped onto 45° inclined specimens with a dropping rate of 58 ± 1 mL/h. Cycles of

2-day dropping/1-day drying and 3-day dropping/1-day drying were alternated [23]. The time of wetness (TOW) was of 30 days for pre-patination and 10 days for artificial ageing after treatment.

#### *Biological treatment*

Coupons were treated during 3 weeks with a biological treatment according to procedures developed at the Laboratory of Microbiology of the University of Neuchâtel (Switzerland), using a specific strain of *Beauveria bassiana* in a gel-based delivery system. Two tin samples and two pre-patinated bronze samples were treated with the gel directly in contact with the sample surface. Before treatment, all coupons were washed with a solution of 70% ethanol in deionized water. After treatment, all coupons were cleaned with a solution of 70% ethanol in deionized water, rinsed with deionized water and dried under pressurized air.

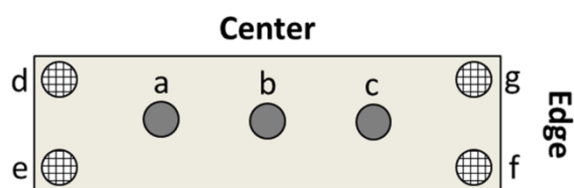


Figure 78. Mask used for Raman and FTIR measurements on bronze samples; points a, b and c (central area) and points d, e, f and g (edge area)

#### *Samples characterization*

Samples surface was characterized before and after treatment and ageing using Micro-Raman spectroscopy and Fourier transformed InfraRed spectroscopy (FTIR).

Random measurements were recorded on tin coupons while on bronze coupons Raman and FTIR measurements were performed using a mask (Figure 78). The Raman system used is a Renishaw Raman InVia Spectrometer coupled with a Leica DMLM microscope. Analysis were carried out using a Ar<sup>+</sup> laser (514.5 nm) or a diode laser (780 nm) as exciting source, the radiation power was set at 3mW for the Ar<sup>+</sup> laser and 30mW for the diode laser, the time of each scan was 10s with a total of 4 scans. FTIR measurements were carried out without preparation, just positioning the samples onto a diamond Attenuated Total Reflectance (ATR) crystal plate. ATR spectra were acquired in the range of 4000-650 cm<sup>-1</sup> on a Thermo Scientific™ Nicolet™ iS™5 FTIR Spectrometer connected to an iTR™ ATR sampling accessory. A total of 32 scans were recorded with a resolution of 4 cm<sup>-1</sup> and the resulting interferogram averaged. Data collection and post-run processing were carried out using the Thermo Scientific™ Omnic™ software. Concerning the bronze samples, their surface was characterized using several analytical techniques. Scanning Electron Microscopy (SEM) studies were performed with a Zeiss EVO 50 EP (extended pressure) system equipped with secondary and backscattered electrons detector. This system was coupled with an Oxford Instruments Energy Dispersive Spectroscopy (EDS) microprobe (software INCA 350). The EDS analyses were carried out using geological and pure metal standard compounds as reference for quantification and computed by the INCA software. Colorimetric measurements were carried out using a Datacolor CHECK II portable spectrophotometer with a D65 illuminant, a 10° observer and specular component excluded (SCE), using CIELab 1976 colour space. On each sample, before and after treatment and/or after ageing, measurements were carried out at three different points (a, b and c in Figure 78) and the mean value calculated. Colour differences were computed as equation (1):

$$\Delta E^* = \sqrt{[(\Delta L^*)^2 + (\Delta a^*)^2 + (\Delta b^*)^2]} \quad (1)$$

$\Delta E^*$  values lower than 3 are assumed as not perceivable, while values of  $\Delta E^* > 5$  are considered clearly perceivable [15, 24].

Mass measurements were carried out using a digital balance KERN AGB210\_4 with repeatability of  $\pm 0.1$  mg. The mass decrease was calculated by difference between the initial weight of the treated and reference samples and the weight of the corroded samples at different ageing times during weathering.

The concentration of alloying metals (Cu, Sn, Pb, Zn) released in the synthetic rain solution during weathering procedures was analysed by Atomic Absorption Spectroscopy (AAS) using a Perkin-Elmer AAnalyst 400 Spectrometer. After collection, the rain solutions were acidified at  $\text{pH} < 2$  with  $\text{HNO}_3$  65% suprapur and stored at  $4^\circ\text{C}$  in HDPE bottles. Cu and Zn were analysed through Flame AAS, while Sn and Pb through Graphite Furnace AAS.

## Results and discussion

### *Tin coupons*

Under visual observations, tin coupons appeared to be matt after treatment. In order to ascertain the composition of the compounds present on their surface, FTIR and Raman analysis were performed and hydrated tin oxide and tin oxalates were identified. The distribution of these compounds resulted to be heterogeneous (Figure 79). Indeed, according to the area measured, FTIR spectra showed characteristic vibrational peaks at  $1377$ ,  $1315$ ,  $1241$  and  $801\text{ cm}^{-1}$  of an hydrated tin oxide (Figure 80a) or hydrated tin oxide ( $1371$  and  $1263\text{ cm}^{-1}$ ) mixed to tin oxalates ( $1327$  and  $779\text{ cm}^{-1}$ ) (Figure 80b). Additional peaks visible at  $1070$  and  $1039\text{ cm}^{-1}$  can be assigned to some residual gel-based delivery system. Identically, Raman shifts indicated either the presence of hydrated tin oxide at  $125$  and  $580\text{ cm}^{-1}$  and/or newly formed tin oxalates at  $1465$  and  $1480\text{ cm}^{-1}$  (Figure 81). The formation of hydrated tin oxide is induced by the surface interaction with water and oxygen during the treatment. The presence of both hydrated tin oxide and tin oxalates could be due to the preferential formation of first hydrated tin oxide that then react with oxalic acid secreted by the fungus to produce tin oxalates. Thus, a treatment duration of 3 weeks seems insufficient to allow a complete conversion of hydrated tin oxide into tin oxalates and a longer time should be required to achieve a homogenous layer of tin/copper oxalates on tin-enriched surfaces. However, it is here demonstrated for the first time that the biological treatment is also efficient on tin surfaces producing tin oxalates making possible to equally apply it on sheltered and tin-enriched unsheltered areas of outdoor bronze monuments.

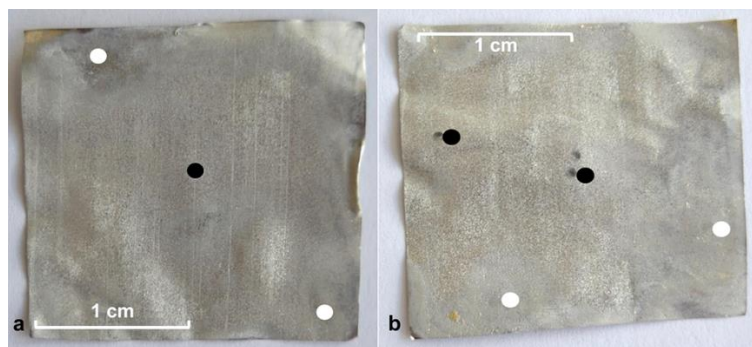


Figure 79. Tin coupons after treatment: the points indicate the position of FTIR and Raman measurements and the related composition as hydrate tin oxide (black) or mixture of tin oxalates and hydrate tin oxide (white)

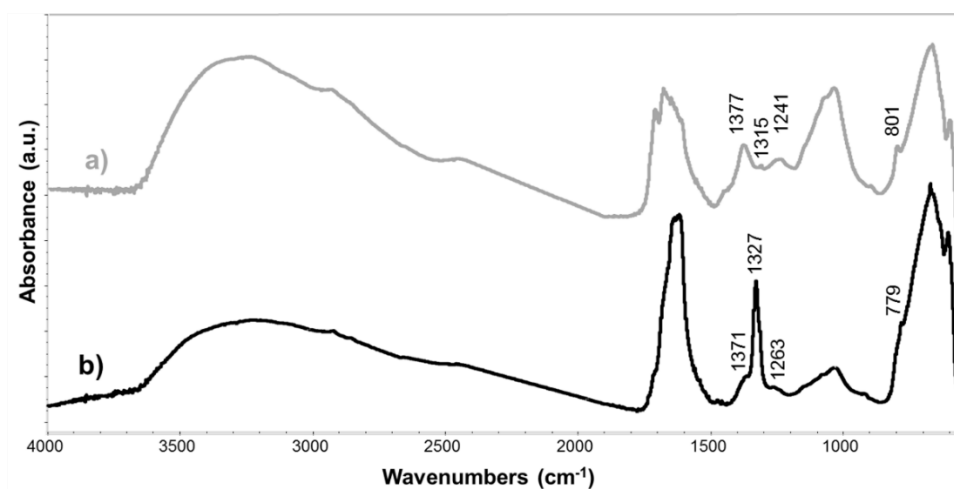


Figure 80. ATR-FTIR spectra showing characteristic vibrational bands of hydrated tin oxide (a) or the concomitant presence of tin oxalate and hydrated tin oxide (b)

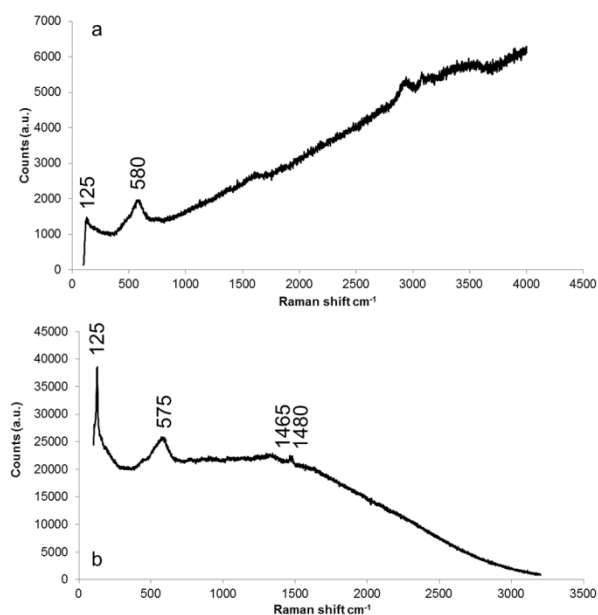


Figure 81. Raman spectra showing characteristic shifts of hydrated tin oxide (a) or the concomitant presence of tin oxalate and hydrated tin oxide (b)

### *Tin-enriched bronze coupons*

Before treatment all samples presented the same patina composition. ATR-FTIR spectra showed peaks at 2958, 2921, 2851, 1455, 1410  $\text{cm}^{-1}$  indicating the presence of an organic substance. Characteristic peaks at 1645, 1391, 1371, 1237, 830  $\text{cm}^{-1}$  can be assigned to a hydrated tin oxide. The peaks at 672, 604  $\text{cm}^{-1}$  can be assigned to tin oxide (data not shown).

After treatment/before ageing, G85dx sample presented characteristic FTIR vibrational bands of copper oxalates (at around 1650, 1364, 1321 and 824  $\text{cm}^{-1}$ ) at nearly all measured points, except two edge positions (Figure 82). On the contrary, the presence of copper oxalates on G85sx sample was only observed at the four edge positions. Characteristic peaks at 1258 and 794  $\text{cm}^{-1}$  can be assigned to tin oxalate and these were present only on the tin-enriched central zone (points a, b and c, Figure 78). As expected, the higher spatial resolution of Raman spectroscopy confirmed the presence of copper oxalates as well as some tin oxalates. Additional Raman shifts were also attributed to cuprite and hydrated tin oxide (Table 21). SEM analysis revealed that the treated surface appeared

rougher compared to the untreated one. In fact, the formation of copper oxalates seemed to follow the morphology of the dendritic structures and to visually enhance them. This can be related to pseudomorphism phenomenon where a mineral compound appears in an atypical form resulting from a substitution process and was particularly evident on G85dx sample (Figure 83) [25]. In opposition, at the edge areas where slight runoff conditions were applied and no artificial tin enrichment achieved, copper oxalates adopted their typical rosette-like habit (data not shown). Also, elemental EDS analysis indicated a lower tin/copper ratio after treatment that confirmed the effective partial conversion of the outer part of the tin-enriched corrosion layer into copper oxalates (Table 22).

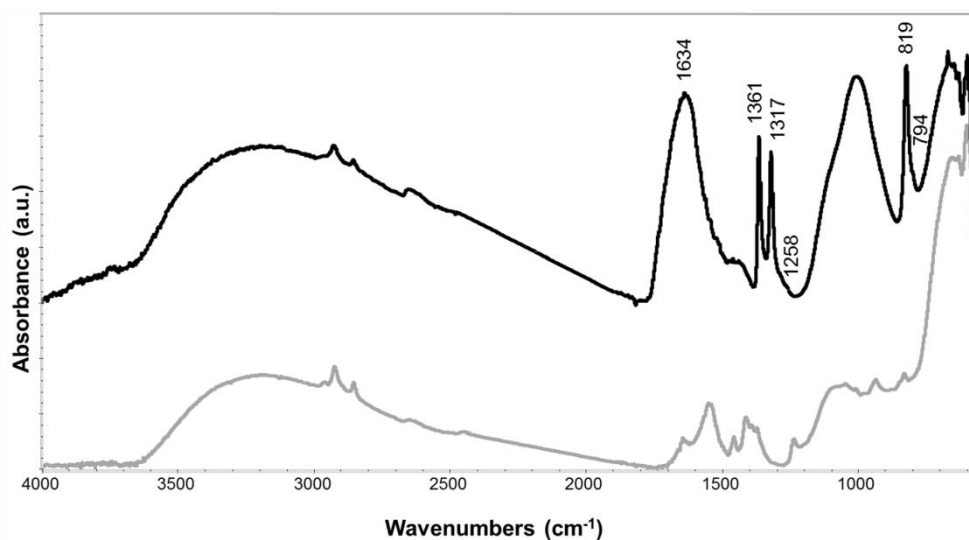


Figure 82. ATR-FTIR spectra acquired on sample G85dx before (grey) and after (black) treatment

As additional criterion, the aesthetic aspect of the treatment was considered and average colour coordinates as well as colour distances  $\Delta E^*$  were calculated (Table 23). The range of measured data, as indicated by a low standard deviation value, was less dispersed on treated samples respect to reference samples, indicating that the biological treatment provided the treated surface with a more homogenous appearance. Respect to the light green tin enriched surfaces, the partial conversion into a probable thinner tin and copper oxalates layer after treatment contributed to reveal the underneath cuprite layer as indicated by the tendency toward light orange colour of the treated surface. Such result was, however, never observed after biological treatment on natural patina and could suggest that the artificial pre-patina obtained here is less adherent to the surface and could be more easily leached out than a naturally year-aged patina. After ageing, Raman analysis showed that copper oxalates were still present on samples surface, suggesting their resistance to severe runoff conditions, even if partially washed out, and long-term stability (Table 21). However, through SEM analysis, after ageing an appearance differentiation between central areas and edge areas, not significantly affected by runoff phenomenon was observed. Especially, it was possible to observe that the central surface appearance changed and dendrite-pseudomorph oxalates are less visible (Figure 83). This could be explained by the fact that decuprification (i.e. a surface enrichment in tin) is occurring again in the weathering step, as observed in the pre-patination phase. On the contrary, at the edge areas, oxalates aggregates remained unchanged (data not shown). EDS analysis confirmed the tin enrichment of the treated surfaces after weathering, as the tin/copper ratio increased again. However, the Sn content of the treated samples is lower compared to the untreated samples (aged and not) (Table 22). Nevertheless, the increase of Sn/Cu ratio observed on the treated samples shows that tin enrichment is still occurring. Thus, at the current stage, this indicates a partial efficiency of the treatment.

	Sample	Cuprite	SnOxHy	Sn-oxalates	Cu-oxalates
Before Ageing	Reference	✓	✓	✗	✗
	Biopassivation	✓	✓	✓	✓
After Ageing	Reference	✓	✓	✗	✗
	Biopassivation	✓	✓	✗	✓

Table 21. Raman-detected compounds present on bronze coupons (treated and reference) before and after ageing procedures

Original Alloy Sn/Cu ratio 0.06	Treatment	Sn (wt%)	Cu	Sn/Cu
Before Ageing	Reference	30,9 ± 4,9	27,4 ± 6,4	<b>1,13</b>
	Biopassivation	12,4 ± 2,2	51,7 ± 4,6	<b>0,2</b>
After Ageing	Reference	34,0 ± 3,6	22,4 ± 3,2	<b>1,52</b>
	Biopassivation	24,1 ± 0,3	32,0 ± 0,1	<b>0,75</b>

Table 22. EDS averaged weight percentage of Sn and Cu and calculated Sn/Cu for the central areas of G85dx sample

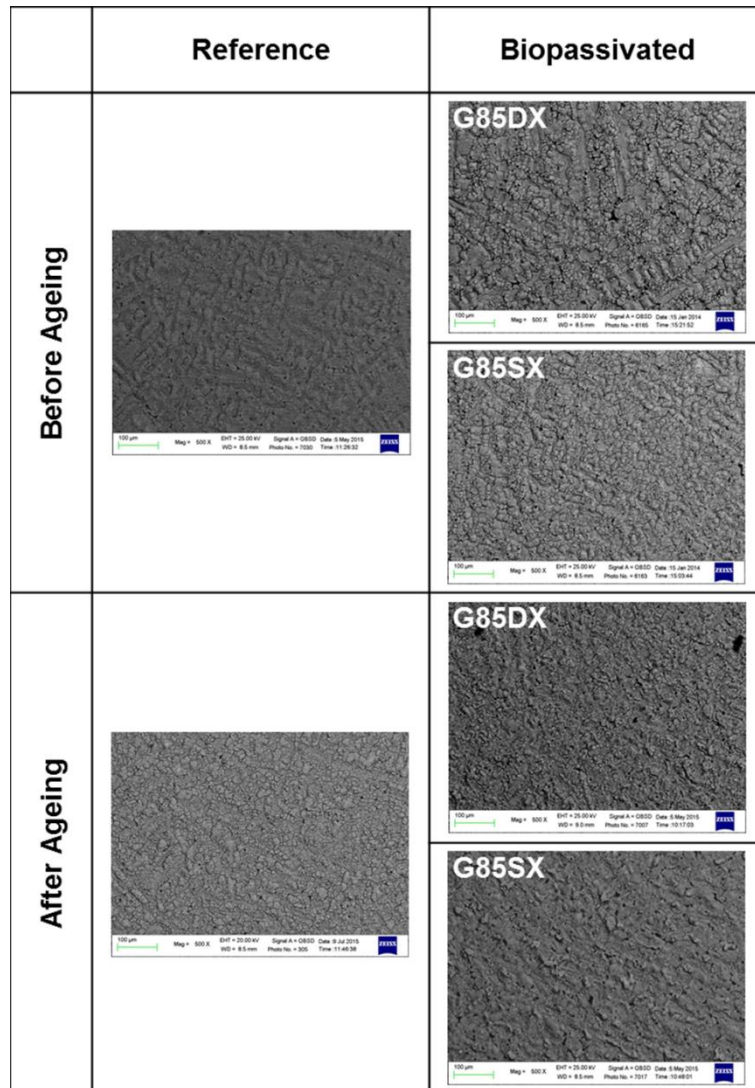


Figure 83. Backscattered electrons images of reference sample and treated G85dx and G85sx samples before and after artificial ageing (central area: points a, b and c in the mask of Figure 78)

	Reference				G85DX				G85SX			
	L*	a*	b*	$\Delta E^*$	L*	a*	b*	$\Delta E^*$	L*	a*	b*	$\Delta E^*$
<b>Pre-patination</b>	49±2	-1±2	6±1	-	62±1	-2.5±0.2	0.9±0.2	-	61±1	-4±1	1.6±0.6	-
<b>After biopatina</b>	-	-	-	-	67.3±0.3	12±1	22±1	26±2	66±2	13.8±0.2	24.2±0.5	29±2
<b>After Ageing</b>	52±1	-1±1	5±1	4±3	48±1	0.2±0.3	5.2±0.2	14.8±0.6	45±1	2.1±0.3	7.8±0.6	18± 0.4

Table 23. Colorimetric coordinates ( $L^*$ ,  $a^*$ ,  $b^*$ ) and colour variation  $\Delta E^*$  of the samples after pre-patination (tin enrichment), biopassivation and ageing.  $\Delta E^*$  are calculated with respect to pre-patination conditions. Reported values are the average of values obtained at three different points on each sample

Regarding the aesthetical aspect of the treated surface, after weathering the treated samples presented colour coordinates that tend to those of the reference sample and resulting in a grey shade, confirming that part of the oxalates outermost layer is covered by a tin enrichment (Table 23). Finally, mass decrease and metals release were measured during ageing. Treated and untreated samples followed the same trend concerning the mean mass decrease (Figure 84). Regarding metals release, copper, lead and zinc were detected in the ageing solution, while tin was always under the limit of detection ( $1.2 \mu\text{g L}^{-1}$ ). In general, metal release follow linear trends and releases from treated samples are slightly higher than from the reference one (Figure 85).

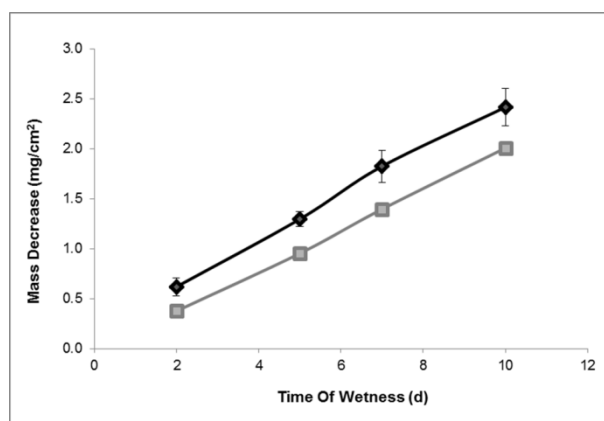


Figure 84. Mean mass decrease for treated samples (black line) and the untreated one (grey line) during ageing

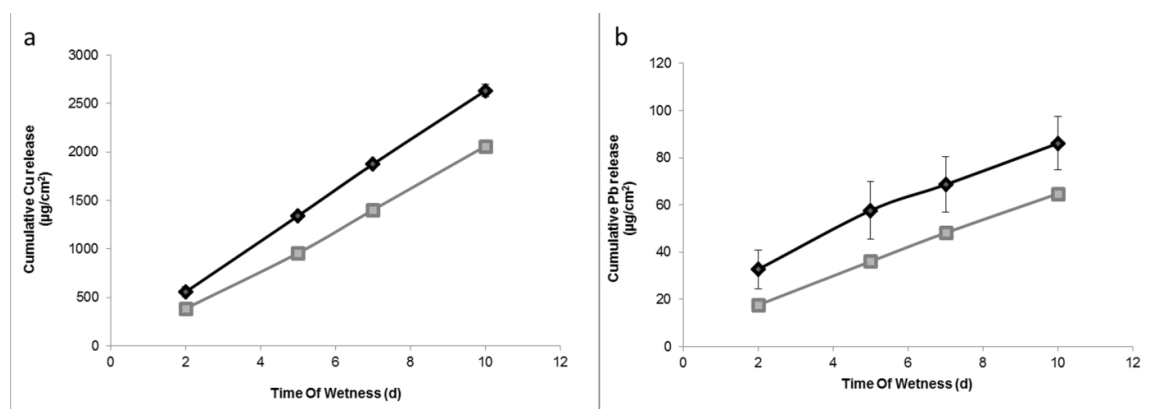


Figure 85. Release of Cu (a) and Pb (b) during ageing of treated (black line) and reference samples (grey line)

Lead release from treated and reference samples follow parallel trends (Figure 85), while copper release from treated and reference samples slightly diverged (Figure 85). Zinc concentrations always ranged between the limit of detection ( $5 \mu\text{g L}^{-1}$ ) and the limit of quantification ( $17 \mu\text{g L}^{-1}$ ), however Zn release seems to show trends analogous to those of copper (data not shown). These results could be related to the thickness of the newly formed patina. A thin patina of copper oxalates would not guarantee a complete protection to the underlying surface, confirming EDS results about surface tin-enrichment. These data could also indicate that, at this stage, the treated samples present a corrosion layer more

porous compared to the reference tin-enriched patina and probably allowed the weathering solution to soak deeper into corrosion layers, leaching metals also from the metallic substrate. However, we cannot exclude a slight simultaneous mechanical removal of the newly formed oxalates layer. A deeper understanding of the metals release should be achieved through stratigraphic analysis of the samples. Furthermore, ageing tests at longer TOW could be carried out in order to check the stability of the biopassivation at longer time. It is worth mentioning that copper oxalates are reported to be more stable than tin oxide, on the basis of their formation enthalpy ( $\text{CuC}_2\text{O}_4 \Delta fH^\circ = -751.3 \text{ kJ mol}^{-1}$ ;  $\text{SnO}_2 \Delta fH^\circ = -577.6 \text{ kJ mol}^{-1}$ ) [26, 27].

## Conclusions

The present study aimed to evaluate the feasibility of a biological treatment on unsheltered areas. In particular, interaction between tin-enriched bronze surface and the studied treatment was investigated. In this work, it has been demonstrated for the first time that this treatment is efficient on tin-enriched surfaces producing tin and copper oxalates. In particular, copper oxalates appeared to be formed preferentially even on such tin-enriched surfaces. Moreover, their presence was observed even after severe runoff condition indicating a good adhesion. Also, tin content on the treated surface remained lower compared with the one of untreated surface indicating a partial efficiency of the treatment already achieved at the current state. Besides, the biological treatment provides a homogeneous visual aspect that tends to a similar tonality than sheltered areas. However, copper release during weathering of treated samples was slightly higher compared to reference samples. Hence, the improvement of the layer porosity is required in order to enhance the treatment efficiency on these specific unsheltered areas. The process involved in the corrosion stabilization will be also deeper investigated. Fungi adopt various resistance mechanisms according to metals involved and the case of *Beauveria bassiana*, the detoxification process was only validated for copper. This mechanism could not be directly transposed to tin without adaptation. However, even if it was not evident at the beginning of the study, promising results were obtained since it was possible to produce both tin and copper oxalates on tin-enriched surfaces.

## References

- [1] L.B. Brostoff, Coating strategies for the protection of outdoor bronze art and ornamentation, 2003.
- [2] S. Cramer, S. Matthes, B. Covino, S. Bullard, G. Holcomb, Environmental factors affecting the atmospheric corrosion of copper, ASTM special technical publication, 1421 (2002) 245-264.
- [3] A. Krätschmer, I. Odnevall Wallinder, C. Leygraf, The evolution of outdoor copper patina, Corrosion Science, 44 (2002) 425-450.
- [4] F. Ospitali, C. Chiavari, C. Martini, E. Bernardi, F. Passarini, L. Robbiola, The characterization of Sn-based corrosion products in ancient bronzes: a Raman approach, Journal of Raman Spectroscopy, 43 (2012) 1596-1603.
- [5] D.A. Scott, Copper and Bronze in Art: Corrosion, Colorants, Conservation, Getty Publications, 2002.
- [6] L.S. Selwyn, N. Binnie, J. Poitras, M. Laver, D. Downham, Outdoor bronze statues: analysis of metal and surface samples, Studies in conservation, 41 (1996) 205-228.
- [7] C. Chiavari, K. Rahmouni, H. Takenouti, S. Joiret, P. Vermaut, L. Robbiola, Composition and electrochemical properties of natural patinas of outdoor bronze monuments, Electrochimica acta, 52 (2007) 7760-7769.
- [8] A. Lins, T. Power, The Corrosion of Bronze Monuments in Polluted Urban Sites: A Report on the Stability of Copper Mineral Species at Different pH Levels, in: Ancient & Historic Metals: Conservation and Scientific Research, Getty Conservation Institute, 1994, pp. 119-151.
- [9] L. Robbiola, K. Rahmouni, C. Chiavari, C. Martini, D. Prandstraller, A. Texier, H. Takenouti, P. Vermaut, New insight into the nature and properties of pale green surfaces of outdoor bronze monuments, Applied Physics A, 92 (2008) 161-169.
- [10] C. Chiavari, E. Bernardi, C. Martini, F. Passarini, F. Ospitali, L. Robbiola, The atmospheric corrosion of quaternary bronzes: The action of stagnant rain water, Corrosion Science, 52 (2010) 3002-3010.
- [11] E. Bernardi, C. Chiavari, B. Lenza, C. Martini, L. Morselli, F. Ospitali, L. Robbiola, The atmospheric corrosion of quaternary bronzes: The leaching action of acid rain, Corrosion Science, 51 (2009) 159-170.
- [12] L. Robbiola, C. Fiaud, S. Penneç, New model of outdoor bronze corrosion and its implications for conservation, in: ICOM Committee for Conservation tenth triennial meeting, 1993, pp. 796-802.
- [13] V. Argyropoulos, Metals and museums in the Mediterranean: protecting, preserving and interpreting, Technological educational institute of Athens, 2008.
- [14] P. Dillmann, G. Béranger, P. Piccardo, H. Matthiessen, Corrosion of metallic heritage artefacts: investigation, conservation and prediction of long term behaviour, Woodhead Publishing Limited, Cambridge, 2007.
- [15] S. Goidanich, L. Toniolo, S. Jafarzadeh, I.O. Wallinder, Effects of wax-based anti-graffiti on copper patina composition and dissolution during four years of outdoor urban exposure, Journal of Cultural Heritage, 11 (2010) 288-296.
- [16] E. Joseph, A. Simon, R. Mazzeo, D. Job, M. Wörle, Spectroscopic characterization of an innovative biological treatment for corroded metal artefacts, Journal of Raman Spectroscopy, 43 (2012) 1612-1616.

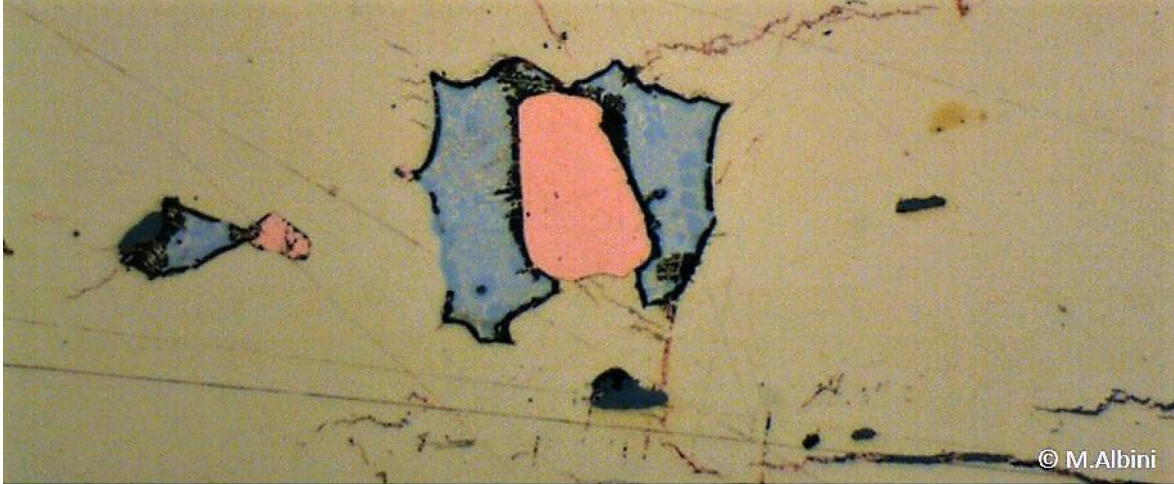
- [17] E. Joseph, S. Cario, A. Simon, M. Wörle, R. Mazzeo, P. Junier, D. Job, Protection of metal artefacts with the formation of metal-oxalates complexes by *Beauveria bassiana*, *Frontiers in Microbiology*, 2 (2012).
- [18] E. Joseph, P. Letardi, L. Comensoli, A. Simon, P. Junier, D. Job, M. Wörle, Assessment of a biological approach for the protection of copper alloys artefacts, in: *Conference Proceedings of Metal*, 2013.
- [19] E. Joseph, M. Albini, P. Letardi, E. Domon Beuret, L. Brambilla, L. Mathys, C. Cevey, R. Bertholon, D. Job, P. Junier, BIOPATINAS: Innovative biological patinas for copper-based artefacts. , in: *Outdoor Metallic Sculpture from the XIXth to the Beginning of the XXth Century: Identification, Conservation, Restoration*, ICOMOS France, Paris, 2014, pp. 154-162.
- [20] M. Albini, L. Comensoli, L. Brambilla, E. Domon Beuret, W. Kooli, L. Mathys, P. Letardi, E. Joseph, Innovative biological approaches for metal conservation, *Materials and Corrosion*, 67 (2016) 200-206.
- [21] M. Marabelli, R. Mazzeo, La corrosione dei bronzi esposti all'aperto: problemi di caratterizzazione, *METALLURGIA ITALIANA*, 85 (1993) 247-247.
- [22] G. Zimmermann, Review on safety of the entomopathogenic fungi *Beauveria bassiana* and *Beauveria brongniartii*, *Biocontrol Science and Technology*, 17 (2007) 553-596.
- [23] C. Chiavari, E. Bernardi, A. Balbo, C. Monticelli, S. Raffo, M.C. Bignozzi, C. Martini, Atmospheric corrosion of fire-gilded bronze: corrosion and corrosion protection during accelerated ageing tests, *Corrosion Science*, 100 (2015) 435-447.
- [24] G. Giuntoli, L. Rosi, M. Frediani, B. Sacchi, B. Salvadori, S. Porcinai, P. Frediani, Novel coatings from renewable resources for the protection of bronzes, *Progress in Organic Coatings*, 77 (2014) 892-903.
- [25] C.S. Hurlbut Jr, *Dana's manual of mineralogy*, John Wiley & Sons, (1971).
- [26] E. Lamprecht, G.M. Watkins, M.E. Brown, The thermal decomposition of copper (II) oxalate revisited, *Thermochimica acta*, 446 (2006) 91-100.
- [27] E.G. Lavut, B.I. Timofeyev, V.M. Yuldasheva, E.A. Lavut, G.L. Galchenko, Enthalpies of formation of tin (IV) and tin (II) oxides from combustion calorimetry, *The Journal of Chemical Thermodynamics*, 13 (1981) 635-646.



## Chapter 6

---

### INFLUENCE OF ALLOYING ELEMENTS



This chapter is based on the results of the following published article:

M. Albini, C. Chiavari, E. Bernardi, C. Martini, L. Mathys, P. Letardi, P. Junier and E. Joseph. Evaluation of the influence of alloying elements on the performances of a biological treatment. In METAL 2016, Conference Proceedings of the Interim Meeting of the ICOM-CC Metal Working Group, 26th-30th September 2016, New Delhi, India

This part of the research was implemented in collaboration with the University of Bologna (Italy).

## Summary

In this chapter, the influence of the alloying elements on the efficiency of the biological treatment studied during this PhD research project was evaluated. In the first part, a preliminary study was carried out using three alloys artificially patinated with copper sulphates. In this part, the colour change and the elemental composition before and after treatment were considered and related to the alloying elements present. In the second part of the study, an analysis of variance (ANOVA) was performed in order to provide a significant statistical model for the influence of alloying elements. In this part, the data set was broadened and the three alloys previously used were covered with five different patinas and treated either with biopatina or microcrystalline wax. The data treated here result from the assessment performed on the artificial patinas in chapter 4.2. In particular, parameters such as the colour change and the electrochemical properties of the corroded metals after treatment and after natural ageing were studied to evaluate the influence of the alloy composition.

## 6.1 Preliminary study

### Abstract

In the last decade, conservation research emphasized eco-friendly and sustainable approaches that could offer advantages in terms of durability, compatibility and safety. For example, a fungal treatment based on the use of a specific strain of *Beauveria bassiana* was proposed to convert soluble and/or active bronze corrosion products into copper oxalates. In the case of bronze exposed to acid rain, copper oxalates would improve the long-term stabilization of the corrosion patinas due to their high insolubility. The aim of this study is to proof-test a biological treatment for different bronze alloys and artificial patinas used in art and architecture. It is important to take into account that corrosion of bronze differs from that of pure copper due to the presence of additional alloying elements. In particular, in outdoor environments selective decuprification leads to a relative enrichment of tin in the corrosion layers. Understanding the influence of alloying elements on the interaction between the alloy and the protective layer is thus essential for setting up effective conservation treatments. In the present work, several pre-patinated bronze coupons were treated with the biological system and its performance was evaluated. The results of the laboratory tests will be presented on different bronze alloys: binary 90Cu/10Sn, ternary 90Cu/8Sn/2Pb, quaternary 85Cu/Sn5/Zn5/Pb5 coated with an artificial copper sulphate patina and quaternary bronze alloy (UNS C83600, 85Cu/Sn5/Zn5/Pb5) patinated with a tin enrichment obtained by artificial ageing. In particular, this study will help to better understand the response of outdoor bronze monuments in unsheltered (i.e. exposed to runoff) and sheltered areas to the biological treatment proposed, as well as to extend the application of biopatina to other metal surfaces used in contemporary art.

### Introduction

Some of the most endangered artworks are metal sculptures exposed outdoors. In order to effectively protect and inhibit the corrosion on these monuments, the conservation practice adopted should take into account the nature of the patina and its corrosion behaviour. The treatments employed so far are organic protective coatings or inhibitors. Both for coatings based on a passive barrier effect as well as for inhibitors, it has been suggested that their effectiveness against aggressive environments should depend on patina composition and on the stability of corrosion products. Furthermore, some toxic inhibitors pose potential threats to human health and to the environment [1]. The present study is part of a larger research project, the objective of which is to propose alternative biological treatments for the conservation and restoration of outdoor metal monuments. These include a ready-to-use fungal treatment as a passivating agent on copper alloys [2-4]. In order to be transferred into praxis, standardized products should be developed taking into account the following criteria:

- proof-tested for the appearance of the treated object
- resistance to corrosion and cohesion of the biopatina on to the object's surface
- proof-tested under ageing conditions through the exposure of real objects to aggressive environments (especially true for outdoor objects)
- standardized to become (and be perceived as) simple and efficient for all uses and consumers.

In previous studies, the efficiency, durability and impact of this newly developed treatment on colour was assessed. Here, to evaluate the impact of the alloying elements on the performances of the proposed biological treatment, samples of different bronze alloys were used:

- Binary (Cu: 90; Sn: 10 weight %)
- Ternary (Cu: 90; Sn: 8; Pb: 2 weight %)
- Quaternary (Cu: 85; Sn: 5; Zn: 5; Pb: 5 weight %)

These samples were coated with an artificial copper sulphate patina to simulate sheltered areas of outdoor bronze monuments. Additionally, samples of a quaternary bronze alloy (UNS C83600, Cu: 85; Sn: 5; Zn: 5, Pb: 5, weight %) patinated by artificial ageing to induce tin enrichment (as in unsheltered areas of outdoor bronze monuments) were also prepared. The different alloys-patinas systems were characterized, before and after the biological treatment, through a complement of analytical techniques. In particular, the study focused on how the fungus behaves in the presence of different alloying elements and what the consequences are in terms of aesthetic appearance and nature of chemical compounds formed. The results of this first assessment are presented here.

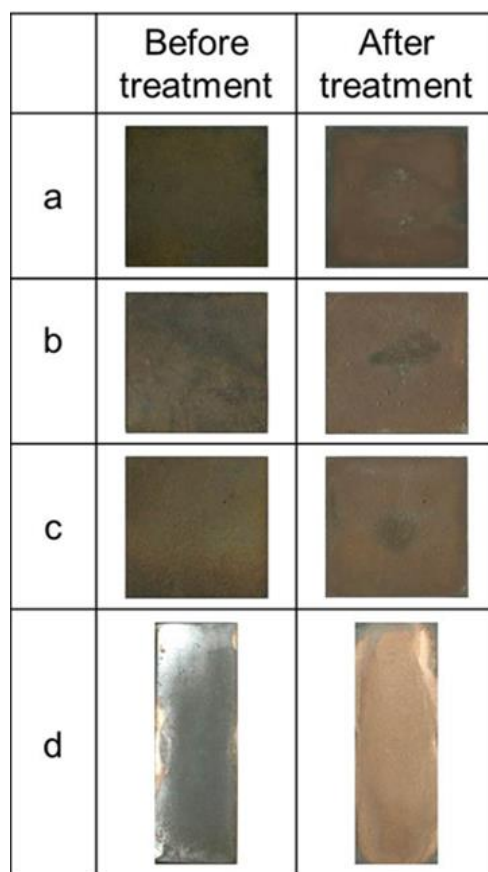


Figure 86. Macroscopic images of SB (a), ST (b), SQ (c) and TQ (d) samples before and after biological treatment

## Materials and methods

### *Coupons*

Sets of 8 samples (60 x 60 x 4-5 mm) were cut from cast ingots of binary (SB), ternary (ST) and quaternary (SQ, with Ni 1 weight %) bronze typically used in artistic foundry (Table 1). Their surface was mirror-

polished, rinsed with ethanol and air-dried before being coated with a copper sulphate artificial patina at the Kunstgiesserei St. Gallen AG (Figure 86). Another set of samples (TQ, 25 x 50 x 5 mm) was pre-patinated by artificial ageing before the biological treatment (Figure 86, Table 24). Before testing, the surface of the bronze specimens was polished with abrasive papers of decreasing granulometry (up to 1000 grit SiC), washed with deionized water and degreased with acetone. Pre-patination was carried out in conditions simulating unsheltered exposure to acid rain (dropping test). The composition of the weathering solution (artificial acid rain) used for the dropping test is reported in Table 25. It reproduced the mean composition of natural rain samples collected during the winter months in a monitoring station in Bologna (Italy) [5]. The synthetic rain was periodically dropped (58 mL h<sup>-1</sup>) onto 45°-inclined specimens. Weekly cycles were set on the basis of pluviometric data recorded in Bologna (Italy) [5]. In particular, cycles of 2-days dropping/1-day drying and 3-days dropping/1-day drying were alternated.

Alloy	Artificial Patina	Acronym	Composition
Binary Bronze	copper sulphate	SB	Cu 90% Sn 10%
Ternary Bronze	copper sulphate	ST	Cu 90% Sn 8% Pb 2%
Quaternary Bronze sheltered	copper sulphate	SQ	Cu 85% Sn 5% Zn 5% Pb 5%
Quaternary Bronze unsheltered	tin-enriched	TQ	Cu 85 % Sn 5% Zn 5% Pb 5%

Table 24. Sets of coupons prepared with artificial patinas

Chemical compounds	Concentration mg/L
CaSO <sub>4</sub> ·2H <sub>2</sub> O	1.44
(NH <sub>4</sub> ) <sub>2</sub> SO <sub>4</sub>	1.50
NH <sub>4</sub> Cl	1.91
NaNO <sub>3</sub>	1.51
CH <sub>3</sub> COONa	3.19
HCOONa	0.8
HNO <sub>3</sub> 65%	3.93

Table 25. Composition of the artificial acid rain (pH) &lt; 4.5) used for the dropping test

In total, the pre-patination procedure took 30 days of time of wetness (TOW). Artificial ageing by the dropping test, in conditions simulating the action of rainwater on unsheltered areas of outdoor bronze monuments (i.e. runoff conditions) induces Sn relative enrichment of the bronze surface, due to copper dissolution (“decuprification”). The corrosion mechanism has been discussed in detail elsewhere as well as the ability of the dropping test to simulate real patinas obtained in unsheltered areas [5-8]. Except for the TQ set (see Table 1 for sample labelling), four samples were left untreated (T0) and four samples were treated with a biological treatment (T4) applied according to procedures developed at the Laboratory of Microbiology of the University of Neuchâtel. For the TQ set, two coupons were treated with T4. All coupons were documented with Canon 8800F and HP 4070 scanners. Furthermore, a complement of analytical techniques was used to characterize the coupons before and after treatment: Fourier Transform Infrared Spectroscopy (FTIR), colorimetry and Environmental Scanning Electron Microscopy coupled with Energy Dispersive X-ray Spectroscopy (ESEM-EDS).

#### *Fourier Transform Infrared Spectroscopy*

FTIR measurements were performed directly on the coupons’ surface. An iS5 Thermo Scientific spectrometer was used. The measurements were made in attenuated total reflectance (ATR) mode using a diamond (iD5™ ATR accessory) ATR crystal. All spectra were acquired in the range 4000–650cm<sup>-1</sup>, at a spectral resolution of 4 cm<sup>-1</sup>. A total of 32 scans were recorded and the resulting interferograms averaged. Data collection and post-run processing were carried out using Omnic™ software.

#### *Colorimetry*

Colour variations were assessed by Reflectance Spectrophotometry (Datacolor CHECK II and Minolta CM-508D) with the following measurement conditions: specular component excluded (SCE), Illuminant D65 (daylight containing UV component, colour T 6504 K), d/8° geometry, 10° observer, measurement area diameter 6 (8 for Minolta) mm, UV 100% with an illumination that contains all UV components of Xe flash light source or UV 0% with an illumination that contains no UV components of Xe flash light source. Colour data were elaborated in the CIELab 1976 colour space. In this space, L\*, a\* and b\* correspond to the lightness, the red/green and the yellow/blue coordinates respectively. On each sample, three measurements were carried out in different areas and the mean value calculated. Colour distance before and after treatment was calculated according to the following formula (1):

$$\Delta E^* = \sqrt{(\Delta L^*)^2 + (\Delta a^*)^2 + (\Delta b^*)^2} \quad (1)$$

#### *Scanning Electron Microscopy - Energy-Dispersive Spectroscopy (SEM-EDS)*

A Philips ESEM XL30 FEG environmental scanning electron microscope and a Zeiss EP EVO 50 scanning electron microscope equipped with an energy-dispersive X-ray analyser were used. The metal samples were observed directly in secondary and backscattered electrons mode at an acceleration potential of 10–25 keV and a working distance of 10 mm. The samples surface was compared before and after biological treatment by recording EDS data on large areas in order to obtain representative values of the surface elemental composition.

## Results and discussion

Before treatment, SB, ST and SQ samples presented characteristic FTIR peaks at 1120, 980 (SB only), 940 (SB only) and 875  $\text{cm}^{-1}$  that can be assigned to copper sulphates (Figure 87a). TQ samples presented a layer of mixed tin oxides in surface with characteristic peaks at 1645, 1391, 1371, 1237, 830  $\text{cm}^{-1}$  that can be assigned to hydrated tin oxide and peaks at 672, 604  $\text{cm}^{-1}$  that can be assigned to tin oxide (Figure 87b).

After treatment, FTIR results showed the formation of copper oxalates on all coupons with an artificial copper sulphate patina (SB, ST and SQ), independently from the alloy composition (Figure 87c). This could be explained by the fact that copper is the major element present both in the artificial patina and in the substrate alloys. The results obtained on TQ samples allowed us to confirm a possible immobilization mechanism for tin. Indeed, the products identified on the samples' surface after treatment were copper oxalates at around 1652, 1362, 1319 and 820  $\text{cm}^{-1}$  and tin oxide (672, 604  $\text{cm}^{-1}$ ) with traces of tin oxalates at 1683, 1339, 1258, 922 and 798  $\text{cm}^{-1}$  that prevailed on the central tin-enriched area of coupons, while copper oxalates were the main product identified at the edges of the coupons (Figure 87d). The zone between 1700 and 1500  $\text{cm}^{-1}$  showed various peaks, probably from the contribution of copper and tin oxalates (Figure 87d). The tin-enrichment was not homogeneous on the coupons' surface and this explained the different products formed at the edges or in the central area of the coupons. Indeed, there is a more intensive runoff in the centre of the coupons and poorly crystallized but stable tin species (e.g.  $\text{SnOx(OH)y}$ ) are formed there together with cuprite [9].

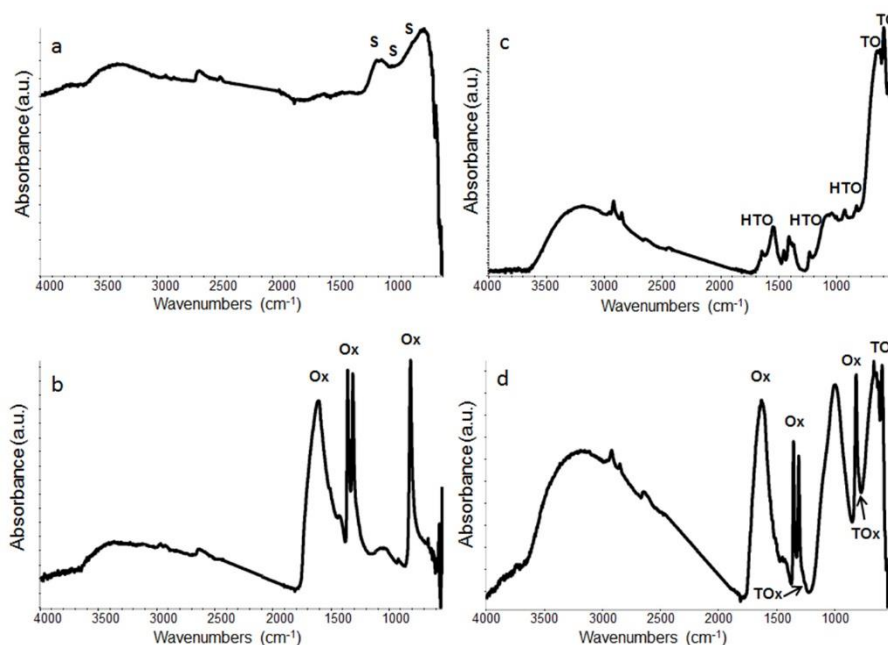


Figure 87. ATR-FTIR spectra: binary bronze with artificial copper sulphate patina before (a) and after (b) treatment, quaternary bronze with artificial tin-enriched patina before (c) and after (d) treatment. Characteristic peaks of copper oxalates (Ox) at 1662,1362,1319,820  $\text{cm}^{-1}$ , tin oxide (TO) at 672,604  $\text{cm}^{-1}$ , hydrated tin oxide (HTO) at 1645,1391,1371,1237,830  $\text{cm}^{-1}$  and tin oxalates (TOx) at 1683,1339,1258,922,798  $\text{cm}^{-1}$

		C Wt%	N	O	Al	Si	P	S	Cl	Fe	Ni	Cu	Zn	Sn	Pb
SB	T0	4.1	-	17.2	6.3	0.3	-	3.6	1.7	1.7	-	60.5	-	4.6	-
	T4	15.4	-	16.3	4.6	0.4	0.5	0.4	0.5	0.6	-	52.1	-	9.2	-
ST	T0	6.8	2.2	20.9	3.1	0.4	-	3.6	3.0	2.4	-	56.1	-	1.6	-
	T4	2.7	-	2.7	1.2	-	0.3	-	-	0.9	-	59.2	-	1.4	31.7
SQ	T0	7.4	-	-	4.7	-	-	1.4	1.9	0.8	-	75.1	-	3.1	5.6
	T4	3.0	-	3.3	1.6	-	0.3	-	-	1.2	-	77.5	-	2.7	10.4
TQ	T0	7.2	-	31.3	-	0.3	-	0.5	-	-	0.3	27.4	-	30.9	2.2
	T4	15.2	-	16.1	-	-	1.1	0.2	-	-	0.4	55.5	-	12.4	1.0

Table 26. EDS measurements of elemental composition on SB, ST, SQ and TQ samples before (T0) and after (T4) treatment expressed in weight percentage

The elemental analysis of the surface obtained by EDS measurements allows further characterization of the surface (Table 26). The SB, ST and SQ samples presented a relatively increased amount of Sn, while S concentration decreased after treatment.

The decreased concentration of S is explained by the formation of oxalates within the first micrometres of the original patina (of copper sulphate), as observed during FTIR analyses. Regarding the Sn amount, no significant change of the Cu/Sn ratio was observed for ST and SQ samples, suggesting that the presence of tin up to 5% in weight does not modify the compounds resulting from the biological treatment. In fact, only copper oxalates seemed to be formed. On the contrary, the Cu/Sn ratio was two times lower in the case of SB samples. This could suggest that copper oxalates are not the only minerals formed, but also tin oxalates. However, the latter might not be detected under the FTIR spectrometer, as the ATR method is a surface analysis with a depth penetration of 0.1-3 micrometres. In order to ascertain their presence, cross-sectioned samples could be analysed or grazing angle X-ray diffraction (XRD) measurements performed.

On TQ samples (unsheltered bronze), EDS results showed a relatively noticeable increase of the Cu/Sn ratio on the tin-enriched areas and on the edges. As mentioned, we observed here a fungal immobilization mechanism in favour of copper and probably there is copper uptake from the underlying alloy in association with assimilation of tin by *B. bassiana*, based on similar processes to those occurring in nature [10-12].

An interesting aspect was the influence of lead on the biological treatment and this was particularly visible on ternary bronze (ST samples) and to a lesser extent on sheltered quaternary bronze (SQ) samples. Indeed, the relative amount of lead considerably increased after treatment and could be explained by a selective corrosion caused by the fungal strain that aims to detoxify its environment from heavy and toxic metals (Figure 88).

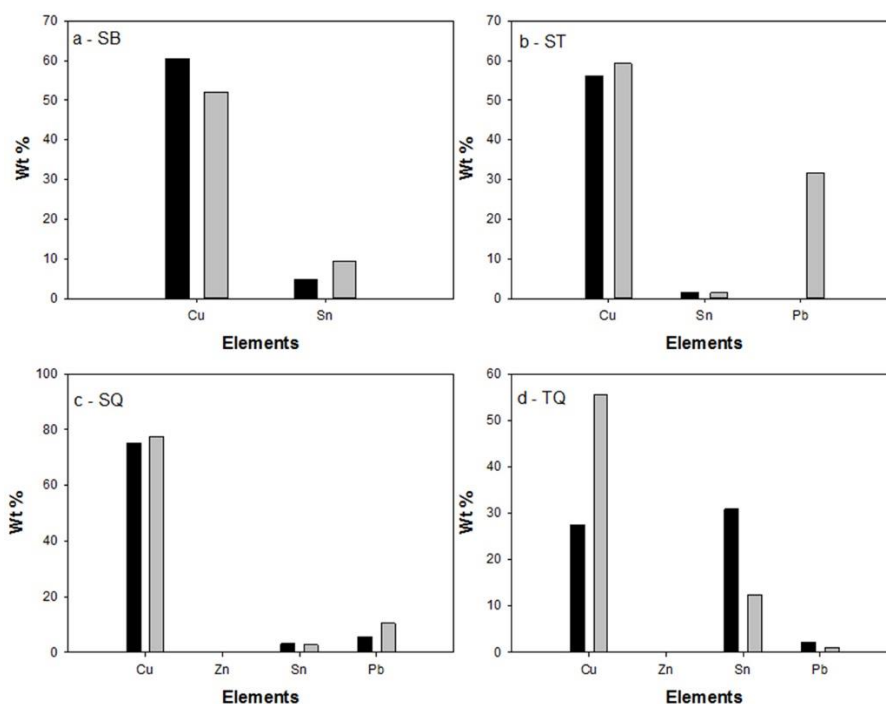


Figure 88. EDS measurements plots for the alloy elements before (T0, black) and after (T4, grey) the application of the biological treatment

Further molecular spectroscopic measurements or XRD analysis should be done in order to ascertain the presence of lead oxidized species in the patina. On the contrary, the Cu/Pb ratio remained stable after treatment of unsheltered quaternary bronze (TQ) samples. In this case, the difference between sheltered and unsheltered samples may be due to the fact that the tin-enrichment allowed a passivation of the surface that is not achieved with the artificial copper sulphates patina. Finally, the presence of zinc as an alloying element in the quaternary bronze samples (both sheltered SQ and unsheltered TQ) was not detected through the EDS measurements. Therefore, the effect of the biological treatment on this element cannot be determined here. Colorimetric results confirmed the trends highlighted with EDS analysis (Table 27).

Alloy	$\Delta E$
Binary (SB)	3.97
Ternary (ST)	5.80
Quaternary sheltered (SQ)	3.08
Quaternary unsheltered (TQ)	25.70

Table 27. Colour distance  $\Delta E$  calculated for the four alloys used in this study

Indeed, the colour distance is more important in the presence of alloying elements such as tin or lead. In particular, the higher  $\Delta E$  values were observed on ternary bronze (ST samples) that showed a high amount of lead, and on the unsheltered quaternary bronze (TQ samples) that have the highest content of tin in the patina. In addition, a colour change was observed on SB and SQ samples, although to a lesser extent, suggesting that there are thresholds in the weight percentage of the alloying elements under which colour changes are not perceivable.

## Conclusions

The current study was a first attempt to assess the influence of different alloying elements in bronze after the application of a biological treatment. In general, the biological treatment mainly induced the formation of copper oxalates, regardless of the composition of the alloy. Nevertheless, interesting results underlined the effects of alloying elements on the biological treatment and in particular on the behaviour of the fungal strain used. As showed here, it appears that *B. bassiana* might allow the immobilization of different toxic metals, such as copper, tin and lead. This was particularly evident on ternary bronze, where a drastic increase of lead concentration was observed. Furthermore, the surface colour after treatment seemed to be affected by the presence of secondary alloying elements, especially above a certain threshold. Further assessments, including the statistical analysis of the data, will be performed in order to evaluate the relevance of alloying elements influence on the biological treatment performance. To conclude, this preliminary study underlined the importance of alloy elements in the development of new conservation treatments. These elements could modify the protectiveness and aesthetic aspect of the treated artwork and the composition of the original alloy should be considered during the restoration process.

## 6.2 Statistical analysis

### Abstract

The use of statistical methods in the field of conservation science can be a valuable support in order to produce significant models useful to compare several variables and their relative importance on the mechanisms studied. Therefore, in this study, analysis of variance (ANOVA) was used to compare three different factors (*Alloy*, *Treatment* and *Patina* composition) and evaluate their relative influence on the colour of the bronze surface and protectiveness of treatment applied. The data sets included three alloys (binary, ternary and quaternary), five artificial patinas (copper black nitrate, copper chloride, iron nitrate, copper nitrate, copper sulphate), and two protective systems (biopatina and microcrystalline wax) as well as untreated samples. The data were compared using three and two-way ANOVA in order to understand the influence of each variable on the colour change and the electrochemical behaviour of the corroded bronze after treatment and after natural ageing.

### Introduction

In the previous work a possible correlation between the alloying elements and the behaviour of the biological treatment on artificial copper sulphates patina was underlined. Indeed, the biological treatment on ternary bronze seemed to immobilize lead, increasing its concentration on the surface of the alloy. Also, high concentration of lead and tin led to a higher colour variation. In this second part of the study, a statistical method was used to in-depth evaluate this correlation. In order to have a higher statistical significance, the data set was broadened. Indeed, all samples sets used in chapter 4.2 (Artificial Patinas) were analysed for a total amount of 180 samples. Also, in order to understand if the alloy composition had an influence on the efficiency of protective systems, biopatina (T4) and a wax reference treatment (TR) were selected as protective systems and included in the evaluation. Furthermore, the behaviour of untreated samples (T0) was studied. Also, the effect of alloying elements on bronze weathering behaviour was assessed. In particular, in order to assess the significance of occurring colour changes, dataset of the colour differences  $\Delta E$  among the samples before/after treatment and before/after natural ageing were included. The corrosion behaviour was considered as well, and the impedance modulus  $|Z|$  before/after treatment and before/after natural ageing was inserted in the dataset.

A three-way ANOVA analysis was selected to investigate the effect of specific factors (*Alloy* composition, *Treatment*, original *Patina* composition) and the interaction among these factors. The alloy composition (B, T, Q), the type of treatment (0, 4, R) and the original patina composition (BN, C, I, N, S) were considered. A complete sets labelling is given in Table 28. The aim of this study was to determine if the alloy composition had an influence in the colour change of the corroded surface and in the protectiveness of treatments applied as well as to observe the differences and similarities among the samples after 12 months of ageing.

### Materials and methods

#### *Coupons*

Sets of 12 samples (60 x 60 x 4-5 mm) were cut from cast ingots of three bronze alloys and coated with five different artificial patinas traditionally used by the foundry Kunstgiesserei St. Gallen AG (Table 28) as described in chapter 4.2.

*Treatments*

For each set three groups of triplicates were defined: untreated (0), treated with the biological treatment (T4) and treated with a microcrystalline wax as reference treatment (R). The biological treatment was performed according to procedures developed at the University of Neuchatel using a specific strain of *Beauveria bassiana*. As reference treatment, microcrystalline wax Cosmolloid H80 wax (CTS Restauro, CH-6807 Taverner, Switzerland) was applied by a conservator-restorer using a brush after heating the samples surface using a hot air gun.

ANOVA factors and sub-groups			
Set Acronym	<i>Patina</i>	<i>Alloy</i>	<i>Treatment</i>
BNB BNT BNQ CB CT CQ IB	Copper black nitrate (BN)	Binary Bronze (B)	Untreated (0)
IT IQ NB	Copper chloride (C)	Ternary Bronze (T)	Biopatina (4)
NT NQ SB	Iron nitrate (I)	Quaternary Bronze (Q)	Wax Reference (R)
ST SQ	Copper nitrate (N)		
	Copper sulphate (S)		

Table 28. Artificially patinated bronze samples with respective alloy composition used for this study. On each set, all treatments were applied. *Patina*, *Alloy* and *Treatment* were used as factors for the ANOVA test. The components of each factor were used as sub-groups

*Natural ageing procedures*

All sets were exposed in the urban environment of Neuchatel (Switzerland) on the roof of the faculty of Sciences of the University of Neuchâtel. Orientation and position according to ISO 9223 standard were selected: the samples were placed facing south, exposed skyward in the position of 45 degrees from the horizontal. The outdoor exposure started in February 2014 and ended on February 2015. Data were collected at the end of the exposure time.

*Colorimetry*

A Minolta CM-508D spectrophotometer was used with the following measurement conditions: Specular Component Included (SCI), Illuminant D65 (daylight containing UV component, colour T 6504K), d/8° geometry, 10° observer, measurement area diameter 8 mm, illumination with Xe flash light source 100% UV containing all UV components or 0% UV containing no UV components, CIELab 1976 colour space. On each sample, three measurements were carried out at different spots. Each measurement was

included in the data set as replicate for the same sample. The parameter  $\Delta E$  (colour difference) was calculated for each sample and replicate using the CIE1976 equation (1). The parameter  $\Delta E1$  described the colour change before/after treatment while the parameter  $\Delta E2$  described the colour change after 12 months of natural ageing.

$$\Delta E^* = \sqrt{[(\Delta L^*)^2 + (\Delta a^*)^2 + (\Delta b^*)^2]} \quad (1)$$

Values lower than 3 are considered not perceptible to the human eye while  $\Delta E$  bigger than 5 are considered clearly perceptible.

#### *Electrochemical impedance spectroscopy (EIS)*

EIS measurements were performed with a specially designed contact probe (ST15) with a nominal area of 1.77 cm<sup>2</sup> using a Gamry REF600, with Framework/EIS300 V5.3 software©2007, Gamry Instruments, Inc [13]. Spectra with 10 points per decade were acquired in potentiostatic mode with 10mV AC signal level at open circuit potential, in the frequency range 100 KHz - 10 mHz. A commercial cleaning cloth soaked with mineral water (electrical conductivity 320 $\mu$ S/cm, pH=7.9) for 120 minutes was fixed to the contact cell, and the system obtained was then leant on the surface to be measured. The EIS spectra acquisition started after approximately 30 min to allow the stabilization of the open circuit potential. For each treatment, two to seven spectra were recorded to verify results homogeneity and repeatability. In order to calibrate the probe area, the wet footprint of the EIS contact probe was recorded with a VEHO VMS-004 usb microscope using MicroCapture software and a graph paper as background. The value Z1 indicated the impedance measured after treatment while the value Z2 indicated the impedance measured after 12 months of natural ageing.

#### *ANOVA test*

The use of analysis of variance (ANOVA) provides significant statistical models useful to compare several variables and their relative importance on the studied mechanisms [14]. In particular, ANOVA test allowed us to compare the factors within the data set that may be important on the evolution of the bronze surface colour and protectiveness of treatment applied. ANOVA analysis was performed in R environment. Due to the Euclidean nature of the data, for the colour differences  $\Delta E1$  and  $\Delta E2$  a generalised lineal model (glm) was used. Among the distribution families of this model, the distribution gamma seemed to be the most appropriate to modelling the  $\Delta E1$  and  $\Delta E2$  data behaviour. The data for the treatment 0 in the matrix  $\Delta E1$  were not considered since the colour difference among the untreated samples was zero for all patinas considered (no actual treatment occurred). Regarding the impedance modulus Z1 and Z2, they presented a heavy tail distribution. Therefore, the data were transformed in to a Gaussian distribution using the R function “Gaussianize” and then analysed. The ANOVA test was made both on the entire matrix of data (three-way ANOVA) and on sub-matrixes (two-way ANOVA), fixing every time a factor sub-group and comparing the other two factors for that specific sub-group (e.g. *Treatment* and *Alloy* factors evaluated for the subgroup Patina BN).

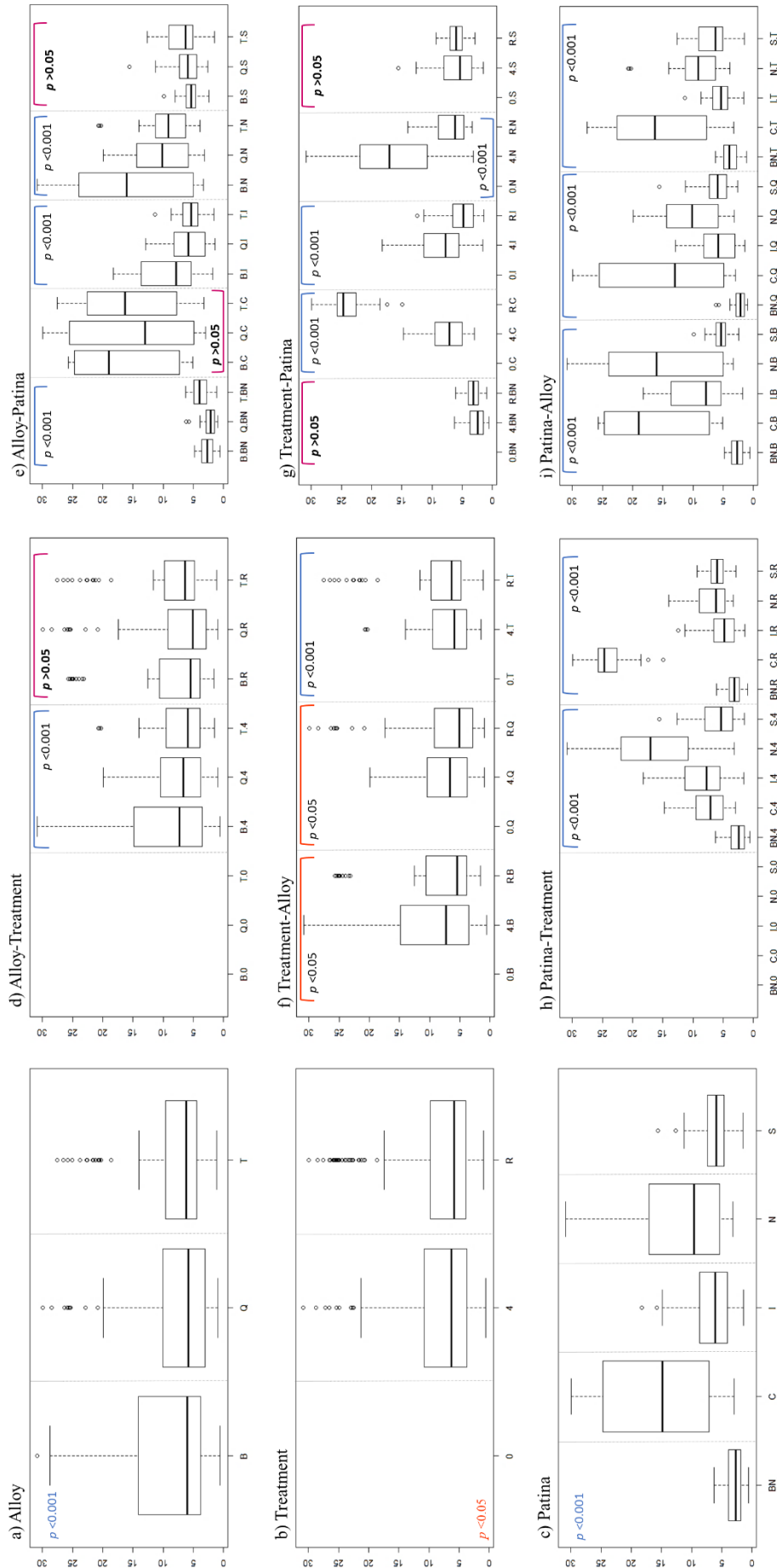


Figure 2. ANOVA boxplots with correspondent p values for  $\Delta E1$  values (colour change after treatment). Alloy (a), Treatment (b) and Patina (c) plots are referred to the entire set of data while the factor comparisons are referred to fixed subgroups (d: alloy-treatments; e: alloy-patina; f: treatment-alloy; g: treatment-patina; h: patina-treatment; i: patina-alloy). For each sub-group the correspondent p value interval is given. A colour coding further indicates the p values intervals: blue ( $p < 0.001$ ), green ( $0.001 < p < 0.01$ ), orange ( $0.01 < p < 0.05$ ) and pink ( $p > 0.05$ )



Figure 3. ANOVA boxplots with correspondent p values for  $\Delta E_2$  values (colour change after 12-months ageing). Alloy (a), Treatment (b) and Patina (c) plots are referred to the entire set of data while the factor comparisons are referred to fixed subgroups (d: alloy-treatment; e: alloy-patina; f: patina-treatment; g: treatment-alloy; h: patina-treatment; i: patina-alloy). For each sub-group the correspondent p value interval is given. A colour coding further indicates the p values intervals: blue ( $p < 0.001$ ), green ( $0.001 < p < 0.01$ ), orange ( $0.01 < p < 0.05$ ) and pink ( $p > 0.05$ )

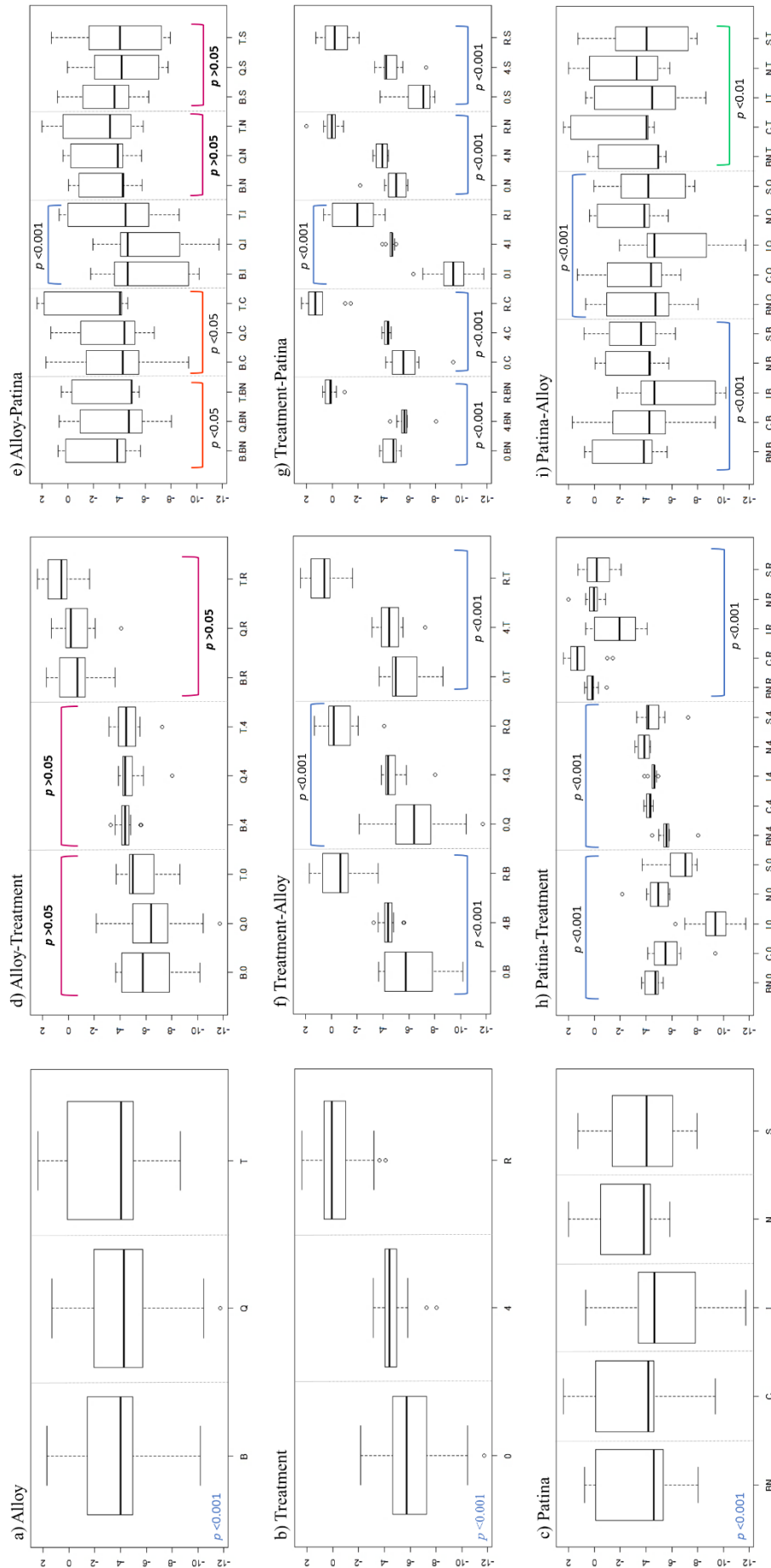


Figure 4. ANOVA boxplots with correspondent p values for Z1 values (impedance modulus after treatment). Alloy (a), Treatment (b) and Patina (c) plots are referred to the entire set of data while the factor comparisons are referred to fixed subgroups (d: alloy-treatments; e: alloy-patina; f: treatment-patina; g: treatment-patina; h: patina-treatment; i: patina-alloy). For each subgroup the correspondent p value interval is given. A colour coding further indicates the p values intervals: blue ( $p < 0.0001$ ), green ( $0.001 < p < 0.01$ ), orange ( $0.01 < p < 0.05$ ) and pink ( $p > 0.05$ )

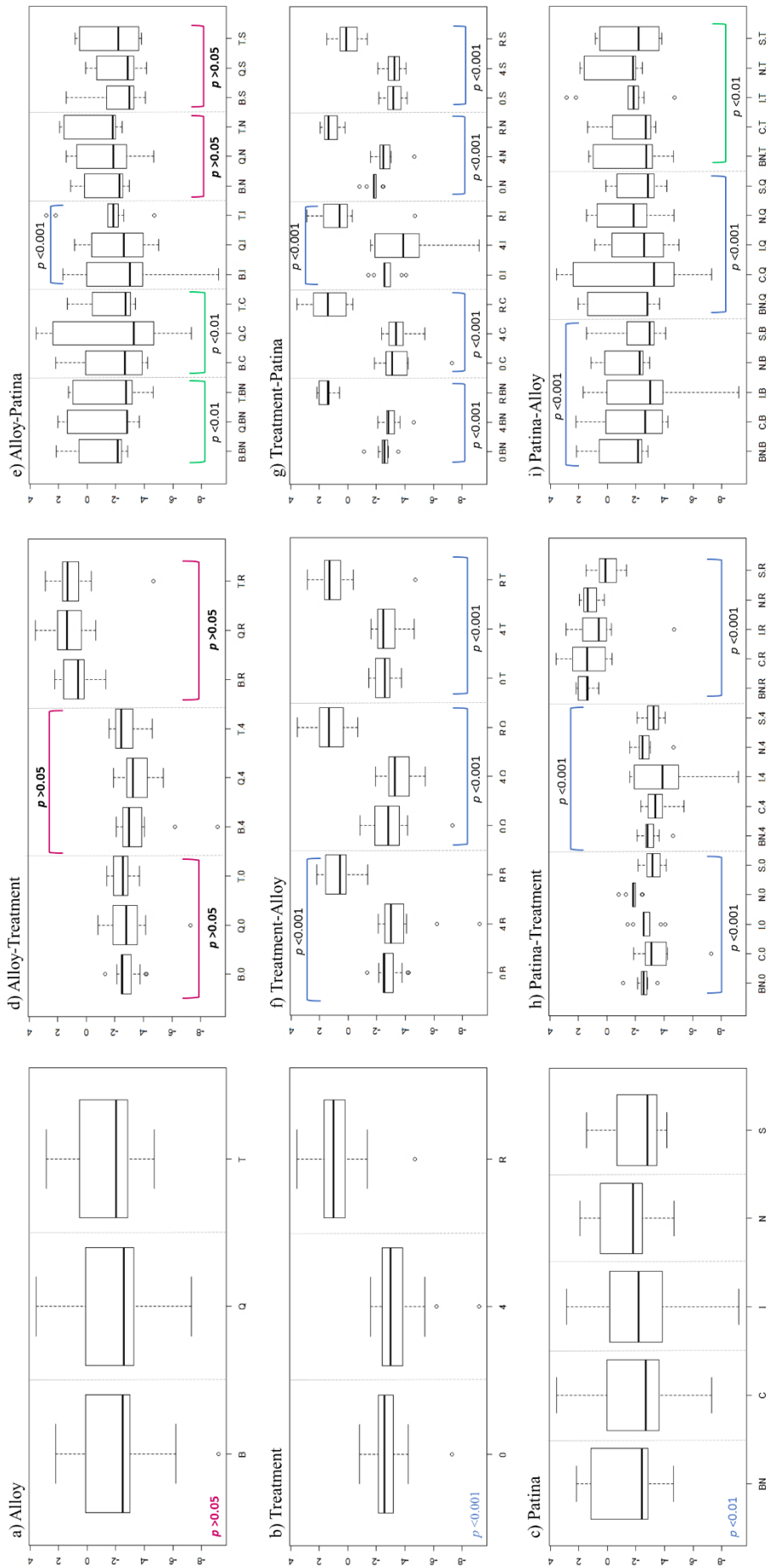


Figure 5. ANOVA boxplots with correspondent p values for Z2 values (impedance modulus after ageing Alloy (a), Treatment (b) and Patina (c) plots are referred to the entire set of data while the factor comparisons are referred to fixed subgroups (d: alloy-treatment; e: alloy-patina; f: treatment-alloy; g: treatment-patina; h: patina-treatment; i: patina-alloy). For each subgroup the correspondent p value interval is given. A colour coding further indicates the p values intervals: blue ( $p < 0.001$ ), green ( $0.001 < p < 0.01$ ), orange ( $0.01 < p < 0.05$ ) and pink ( $p > 0.05$ )

## Results and discussion

### *Alloy's influence on colour*

Each factor here considered could influence the colour of bronze surfaces. Indeed, the alloying elements could form several corrosion products that have different colour compared to copper ones. Also, the original patina colour could be an important factor influencing the treatment resulting shade after application and after ageing. In the same way, the applied treatment could modify the underneath patina, varying its colour. The ANOVA test made on the colour change after treatment ( $\Delta E1$ ) revealed that the factors mainly influencing the samples' colour variation are the *alloy* composition and the *patina* composition (p values lower than 0.001) as well as the *treatment* applied (p value between 0.05 and 0.01) but in minor extent (Figure 89a-c). It means that both biopatina and wax reference treatments contributed to the colour change but  $\Delta E1$  still strongly depends to the underneath artificial patina produced and to the bronze alloy composition. This first evaluation was done using the entire matrix of available data but a more accurate assessment was carried out considering each sub-group. Regarding the influence of the *alloy* composition on the colour change, it seemed to depend on the treatment applied. Indeed, for biopatina treatment (4) the colour change was related to the treated alloy while for wax treatment (R) the colour change depended only from the treatment itself (Figure 89d). Looking to the *Alloy-Patina* interaction, the colour change of copper chloride (C) and copper sulphate (S) patinas was not influenced by the alloy composition as it was for the other patinas (Figure 89e). The influence of *treatment* in the colour change was considered significant for all alloys, even if in major extent for the ternary alloy (Figure 89f), and for almost all patinas, except BN and S patinas (Figure 89g). Also, the influence of the *patina* composition was relevant for all the sub-groups (Figure 89h-i). From these data, it seems that the sulphate patina (S) had a different behaviour from the others and that each treatment responded differently to the alloying elements present in the bronze bulk.

The colour change occurring during ageing ( $\Delta E2$ ) seemed to be no longer dependent on the *treatment*. Indeed, the main factor influencing the colour variation was the *patina* and, in minor extent, the *alloy* (Figure 90a-c). In fact, the influence of the alloying elements decreased from  $\Delta E1$  to  $\Delta E2$ . Looking into details, the *alloy* is an influential variable only for wax treatment (Figure 90d). Also, as well as for the  $\Delta E1$  values, each patina is differently influenced by the alloy composition (Figure 90e) but no defined model could be recognised. Despite the *treatment* p-values indicated general similarities among the data, the influence of this factor was not observed for the binary and quaternary alloys (Figure 90f) and for all the patinas (Figure 90g) except copper chlorides (C). However, the *patina* remained, also during ageing, the main factor influencing the colour change for all sub-groups (Figure 90h-i).

### *Alloy influence on electrochemical behaviour*

As well as for the colour, each factor here evaluated could change the electrochemical response of the metal substrate. In fact, each alloying element have a different electrochemical behaviour that could results in a different impedance value. Also, the artificial patina composition could make the surface more or less protective against corrosion as well as the treatments do. After the ANOVA test, it seemed that the impedance modulus after treatment (Z1) was equally influenced by all factors (Figure 91a-c). Nevertheless, the *alloy* did not influence the electrochemical behaviour of any treated surface (Figure 91d). Also, the alloy composition was not an important factor for copper nitrate (N) and copper sulphate (S) patinas (Figure 91e). In this case, it appeared that the ANOVA test for the single general factors was not able to gather the subtle differences depending on each sub-group. However, the general model was confirmed for the *treatment* and the *patina* composition (Figure 91f-i). In fact, both parameters are clearly important for the electrochemical response of the samples after treatment.

After ageing, the *alloy* factor was no longer influencing the electrochemical behaviour of the samples while the *treatment* and the *patina* composition remained important factors. Indeed, the two-way ANOVA test for the sub-groups gave the same results as before ageing for almost all variable comparisons (Figure 92a-i). However, it is worth noticing here that the *alloy* influence for copper black nitrate (BN) and copper chloride (C) patinas had a relative increase (Figure 92e) while, for the general model, the *alloy* influence drastically decreased to be negligible (Figure 92a).

It seems that, in the case of electrochemical behaviour of the corroded samples, the *alloy* composition may have a role for certain patinas during treatment but generally it was not the main factor affecting the protectiveness of the applied treatments. Indeed, the *treatment* and the *patina* composition had the main influence on protection level, both after treatment and during ageing.

## Conclusions

In this study, the analysis of variance (ANOVA) was used as statistical method in order to in-depth evaluate a possible correlation between the bronze alloying elements and the behaviour of conservation treatments on artificial patinas. In particular, the colour variation and the electrochemical behaviour were analysed after treatment application and after ageing. The colour variation was mainly dependent from the colour of the original patina. The *alloy* composition had a strongest influence for the colour of the patina after treatment while during ageing its influence decreased. The same happened for the *treatments* tested here, that modified the samples colour after application but had less influence during ageing. In fact, it is known that both wax and biopatina treatment change the surface colour (towards dark, shine finishes the first and greenish shades the second). However, the colour of the original patina remains prevalent even after treatment and its interaction with the weathering environment must prevail during ageing. Nevertheless, from both  $\Delta E1$  and  $\Delta E1$  data sets, a clear model for the *alloy* influence on the colour was not identified. Regarding the electrochemical behaviour of the samples, the main influencing factors were *treatment* and *patina* both during treatment and during ageing. The alloy had an influence only on few types of patinas (BN, I, C). However, particularly in this case, the three-way ANOVA gave different responses than the two-way ANOVA. This discrepancy may be due to the data pre-treatment that could be different when the dataset is narrowed to each sub-group. In order to better understand the influence of the alloy, a further analysis of the data should be considered, using a one-way ANOVA between each sub-group of factors and considering different data pre-treatments for each sub-set. This will also allow a better understanding of the influence from each treatment on the samples behaviour. Also, interesting results could be provided by applying the same data analyses to characterize natural patinas features.

## References

1. Brostoff, L.B., Coating strategies for the protection of outdoor bronze art and ornamentation. 2003, University of Amsterdam. p. 180.
2. Joseph, E., et al., Protection of metal artefacts with the formation of metal-oxalates complexes by *Beauveria bassiana*. *Frontiers in Microbiology*, 2012. 2.
3. Joseph, E., et al., Spectroscopic characterization of an innovative biological treatment for corroded metal artefacts. *Journal of Raman Spectroscopy*, 2012. 43(11): p. 1612-1616.
4. Joseph, E., et al. Assessment of a biological approach for the protection of copper alloys artefacts. in *Conference Proceedings of Metal*. 2013.
5. Chiavari, C., et al., The atmospheric corrosion of quaternary bronzes: The action of stagnant rain water. *Corrosion Science*, 2010. 52(9): p. 3002-3010.
6. Chiavari, C., et al., Composition and electrochemical properties of natural patinas of outdoor bronze monuments. *Electrochimica acta*, 2007. 52(27): p. 7760-7769.
7. Robbiola, L., et al., New insight into the nature and properties of pale green surfaces of outdoor bronze monuments. *Applied Physics A*, 2008. 92(1): p. 161-169.
8. Bernardi, E., et al., The atmospheric corrosion of quaternary bronzes: The leaching action of acid rain. *Corrosion Science*, 2009. 51(1): p. 159-170.
9. Ospitali, F., et al., The characterization of Sn-based corrosion products in ancient bronzes: a Raman approach. *Journal of Raman Spectroscopy*, 2012. 43(11): p. 1596-1603.
10. Burford, E.P., M. Fomina, and G.M. Gadd, Fungal involvement in bioweathering and biotransformation of rocks and minerals. *Mineralogical Magazine*, 2003. 67(6): p. 1127-1155.
11. Gadd, G.M., Geomycology: biogeochemical transformations of rocks, minerals, metals and radionuclides by fungi, bioweathering and bioremediation. *Mycological Research*, 2007. 111(1): p. 3-49.
12. Gadd, G.M., Metals, minerals and microbes: geomicrobiology and bioremediation. *Microbiology*, 2010. 156(3): p. 609-643.
13. Letardi, P., Electrochemical measurements in the conservation of metallic heritage artefacts: an overview, in *Corrosion and Conservation of Cultural Heritage Metallic Artefacts.* , P. Dillmann, et al., Editors. 2013, EFC Publications. p. 126-48.
14. Faraway, J.J., *Practical regression and ANOVA using R*. 2002, University of Bath.

## Chapter 7

---

### FINAL DISCUSSION AND CONCLUSIONS



The aim of the biopatina project is to develop an alternative biological conservation treatment for copper-based artefacts using the specific strain S6 of the fungus *Beauveria bassiana*. This microorganism is able to modify existing corrosion products into copper oxalates, stable and insoluble compounds, while preserving the artefacts physical appearance. Indeed, instead of using a sacrificial layer of organic coating, this research aims at producing passivating patinas having the same composition of naturally occurring copper minerals enhancing the compatibility between applied treatment and corroded surface of artefacts. The selection of the fungal strain, its ability to produce copper oxalates and first attempts of application were developed during the projects EU-ARTECH (EU-6FP, 2005-2009) and BAHAMAS (EU-7FP-IEF, 2010-2012).

The purpose of the present work was to further investigate and optimise the use of biopatina treatment in order to bring the treatment from the laboratory tests to real praxis.

First of all, in Chapter 2, the ability of the strain S6 to produce oxalic acid was examined. In particular, it was observed that, in presence of copper oxide, the fungus over-produced oxalic acid as defensive mechanism against copper toxicity. This behaviour is of great importance for the purpose of this thesis. Indeed, since copper oxide is the first corrosion product formed on any copper-based artefacts, the high efficiency of oxalic acid production is guaranteed during the biological treatment. Therefore, the production of biogenic copper oxalates will be efficient due to the ability of oxalate ions to complex copper ions. The presence of copper ions on the surface of the treated artefact is due to the solubility of copper corrosion products, either in neutral water (e.g. copper sulphates) or in acidic pH (e.g. copper oxide). The presence of oxalic acid make the delivery system acidic, therefore all copper corrosion product will be gradually dissolved when in contact with the delivery system and the copper ions will be chelated to form copper oxalates. However, the oxidation state of copper corrosion products does not influence the formation of copper oxalates. Indeed, in aqueous solutions such as all the delivery systems used for this study, when corrosion products are dissociated copper (I) ions will spontaneously disproportionate ( $2\text{Cu}^+ \rightarrow \text{Cu}^{2+} + \text{Cu}^0$ ) [1, 2] and only Cu (II) ions will react forming copper (II) oxalate ( $\text{Cu(II)C}_2\text{O}_4$ ). During the reaction it is possible that molecular water might be incorporated into the crystalline structure of the newly formed minerals, forming an hydrated copper oxalate ( $\text{Cu(II)C}_2\text{O}_4 \cdot n(\text{H}_2\text{O})$ ). A naturally occurring hemihydrated copper oxalate was discovered in 1977 in Western Australia close to the Mooloo Downs station homestead and it has been named as Moolooite  $\text{Cu}^{2+}(\text{C}_2\text{O}_4) \cdot 0.44(\text{H}_2\text{O})$ .

A potential risk of using a strong organic acid, such as oxalic acid, to form biogenic copper oxalates, is the possibility of solubilise all the corrosion layers, leaving the bare metal exposed. This may potentially happen if the concentration of oxalic acid in contact with the surface is too high. Therefore, the duration of the treatment is crucial to allow the conversion of the active and unstable corrosion products avoiding the contact between the oxalic acid and the stable layers of the patina. Indeed, the duration of the treatment needs to be carefully evaluated for each artefact depending on the patina thickness. However, in most of the cases, stable and unstable corrosion products are simultaneously present on artefacts surface. In such cases, conservator-restorers would need to evaluate the extension of the active corrosion (spots or wide areas) and decide if localised intervention could be an alternative to the treatment of the entire object. In the event that the treatment of the whole surface is necessary, the conversion of both stable and unstable corrosion products should be envisaged and carefully considered by conservator-restorers in order to choose the best option in the interest of the degraded artefacts.

Following the study of the production of oxalic acid by the selected microorganism, the application protocol of the biological treatment was evaluated. In order to be applied on cultural heritage, conservation-restoration products need to fulfil several ethical requirements:

- no or minimal aesthetical impact
- reversibility or at least re-treatability
- long-term and predictive performance
- easy application and removal
- non-toxicity

Most of the time, conservation treatments are also required to have high performance on porous, uneven, fragile and chemically unstable patinas. Here, during the evaluation of the treatment performance all these requirements were addressed. The aesthetical impact of the treatment was evaluated throughout colorimetric measurements. The long term and predictive performance on corrosion rate was evaluated by measurement campaigns performed during natural exposure and artificial ageing. The application and removal ease were evaluated by a conservator-restorer using several delivery systems and identifying the most appropriate. The non-toxicity is an important characteristic of this treatment due to the absence of chemicals and to the harmless of the microorganism involved. Regarding the reversibility of the treatment, it was not evaluated because of the nature of the treatment. Indeed, this treatment can be easily removed by mechanical abrasion as for all naturally occurring copper patinas.

As already mentioned in chapter one, the corrosion mechanisms of copper-based objects differ depending on the exposure environment. Therefore, the biological treatment was evaluated both for archaeological and outdoor artefacts. Moreover, in order to evaluate the protectiveness of biopatina treatment, it was assimilated and compared with traditional protective treatments, currently used in conservation-restoration practice.

In the case of archaeological objects (Chapter 3), the biological treatment was compared with benzotriazole (BTA), a commonly used corrosion inhibitor. This part of the research focused its attention particularly on avoiding the corrosion instigated by copper chlorides that cause “bronze disease”. This form of corrosion is the most dangerous for copper-based artefacts and, if left untreated, it may cause the complete loss of the artefacts. In this chapter, three different delivery systems for the biological treatment were tested. The clay mixture and Metylan® gel resulted in poor performance either in the production of copper oxalates and/or in removal ease. The GelX formulation was considered the most efficient delivery system. This gel was used to compare the biological treatment with BTA in terms of conversion and corrosion stabilization of the original patina. It was demonstrated that the BTA 24-hours immersion application, commonly used by conservator-restorers, was insufficient to form a homogeneous layer of Cu-BTA complexes resulting in poor surface protectiveness. On the contrary, a consistent layer of Cu-BTA complexes was observed after 14 days of immersion. The same time required to the biological treatment to transform the copper chlorides patina into a layer of copper oxalates. Nevertheless, while the 14-days layer of Cu-BTA complexes did not change the corrosion behaviour of copper chlorides original patina, the biological treatment enhanced the surface inhibition against corrosion. Treated objects also underwent accelerating ageing showing no reactivation of cyclic corrosion processes either on BTA- or biopatina-treated objects. Based on the obtained results, it is thus possible to affirm that the biopatina treatment could be a valid and sustainable alternative to the use of BTA for the inhibition of bronze disease. Also, the replacement of BTA would avoid the potential threat to human and environment due to its toxicity. In fact, even though no in depth-studies have been conducted so far on its toxicity, BTA is currently under evaluation of the European Chemical Agency as potential endocrine disruptor substance. Also, the Globally Harmonized System of Classification and Labelling of Chemicals identify benzotriazole as: Acute Toxicity - Oral (Cat. 4), Dermal (Cat. 4), Inhalation (Cat. 4); Eye Irritation (Category 2A); Acute Aquatic Toxicity (Category 3); Chronic Aquatic

Toxicity (Category 3). Therefore, a less toxic and more efficient alternative to BTA as biopatina should be carefully evaluated. However, it would be interesting for the future to compare the biopatina treatment with other stabilisation treatments commonly used in conservation such as the immersion in sesquicarbonate solution [3, 4] or the Rosenberg method [5, 6]. For instance, the immersion of corroded copper-based artefacts in sodium sesquicarbonate ( $\text{NaHCO}_3 \cdot \text{Na}_2\text{CO}_3$ ) solution is a recognised stabilization technique, in particular for the conservation of artefacts recovered from marine environments and therefore saturated with chlorides. In fact, the hydroxyl ions of the alkaline solution react chemically with the insoluble copper chlorides to form cuprous oxide and to neutralize any hydrochloric acid formed by hydrolysis to produce soluble sodium chlorides. Due to the increase of chloride concentration in the solution over time, the bath needs to be frequently changed. At the end of the treatment, the object is rinsed in several deionized water baths until the pH is neutral. This treatment is quite slow and depending on the chloride content can take months and in some cases years [3]. Furthermore, it produces high amount of waste that needs to be neutralized before their disposal. Therefore, it would be an interesting perspective the comparison of other stabilisation methods with the biopatina treatment. In the same way, the electrochemical reduction method proposed by Rosenberg in 1917 and still used could be compared with the biopatina treatment. The Rosenberg conservation method consist in coating the object with a gel that is able to retain water, wrap the coated object with an aluminium foil and expose this system to high humidity (higher than 90%). The active chlorides present in the object would react with the aluminium foil forming localised aluminium chlorides spots on the foil reducing the copper chlorides to cuprite or tenorite. However, this method pose many problems due to the lack of control on the electrochemical processes involved and may cause more harm than benefit [7].

The use of biopatina on outdoor monuments corrosion was also assessed. In this case, the traditional protective treatment used as reference for comparison was microcrystalline wax. The use of wax on outdoor monuments presents some disadvantages such as surface darkening, frequent maintenance and incomplete reversibility. Moreover, some microorganisms are able to use wax as a carbon/energy source (i.e. hydrocarbon-degrading bacteria)[8-10], leading to the possible colonisation of the coating. The metabolites of these microorganisms, particularly organic acids, can then further corrode the artefact surface. therefore, the use of waxes should be carefully considered since their use could cause more harm than benefit with time. The use of wax could also lead to an increase of the corrosion rate in case of breakage of the coating film. Indeed, when a metal surface is exposed to differential air or oxygen concentrations differential aeration corrosion may occur. This kind of corrosion is the result of the formation of an oxygen concentration cell due to the uneven supply of air on the metal surface. The part of the metal exposed to higher oxygen concentration acts as cathode while the part exposed lower oxygen concentration acts as anodic region and undergoes corrosion [11, 12].

During the study of the biopatina treatment on outdoor artefacts, a distinction was made among natural patinas, formed during outdoor exposure to environmental agents, and artificial patinas, made for artistic purposes by foundry during the creation of the sculpture. For both natural and artificial patinas, the treatment was tested on coupons and on real objects.

As first attempt on natural patinas, a solid matrix-based application protocol was used. It resulted in the formation of an uneven copper oxalates layer affecting the performance of the treatment, which was ineffective against natural ageing. However, the aesthetical appearance of the artefacts seems to be similar to a natural patina after treatment and during exposure. Thereafter, a second application protocol based on the GelX formulation was tested. The new application resulted in the formation of an even layer of copper oxalates that lasted in an extreme environment weathering for six months. However, for the moment it seems that the biological treatment did not provide a significant contribution to the protection of the treated surfaces as it did for archaeological objects. Nevertheless, in aggressive environments such as Genoa harbour, the stabilization of the corrosion mechanisms and thus of the patinas are usually

achieved after at least one year of weathering. Therefore, a new measurements campaign will be conducted after 12 months of exposure in order to better compare the results with those of the previous study and to monitor the corrosion mechanisms occurring. Regarding wax treatment on natural patinas, it provided higher colour variation compared to biopatina. Furthermore, wax drastically failed in the protection of naturally patinated copper-based coupons already after 6 months of exposure in severe environmental conditions. As future perspective, a metallographic study on the sections of such patinas, as already done for the archaeological objects, would help to understand the evolution over time of treatment.

On artificial foundry patinas, two different application protocols were tested. One used Japanese paper and agar while the other used the GelX formulation. Both application protocols ensured the formation of copper oxalates but the best performances were obtained with the GelX-based protocol. Also in this case, the comparison between biopatina and a microcrystalline wax in terms of colour variation resulted in favour of the biological treatment. Regarding the protectiveness of the treatments, microcrystalline wax remained stable during ageing in a mild corrosion site even if its thickness decreased. The same stability was observed in the biologically treated samples while untreated samples showed an increase of the impedance values. Indeed, it seemed that the artificial patinas were still unstable and did not reach yet an equilibrium even after 12-months ageing. As for natural patinas, a metallographic study of the sections of these samples would improve the knowledge about the treatment protectiveness and performance. On real outdoor artefacts, such as the sculpture *Fusion* and the sculpture park *Légende d'Automne*, the best performing application method was the one using the GelX formulation. These tests will allow to monitor the evolution of biopatina overtime with future measurements campaigns.

During the assessment of the biopatina treatment on outdoor artefacts, many impedance measurements were carried out in order to compare the protectiveness of biopatina treatment with microcrystalline wax. The results obtained underlined some limitations of this technique for the comparison of coating systems with non-coating systems. In fact, due to the intrinsic differences of the two treatments protective mechanisms, their comparison resulted difficult. Indeed, impedance measurements indicate how prone to corrosion is the analysed object in presence of an electrolyte solution. Due to its hydrophobic properties, a coating system impedes the interaction of the object with the electrolyte solution giving, therefore, high impedance values. Hence, the use of this technique to evaluate two protective coatings provides good information for their comparison. However, the biopatina treatment does not operate as a coating, preventing the contact with the electrolyte solution. On the contrary, the biogenic copper oxalates are inorganic compounds that can be found as natural corrosion layers on copper-based artefacts. Their protectiveness is due to the stabilisation of active corrosion products and their non-solubility rather than to the physical isolation of the artefact from the environment. Therefore, the use of EIS results for the comparison of such different treatments should be reconsidered. However, for the evaluation of the electrochemical behaviour of the biopatina treatment, this technique can provide useful information. Indeed, in order to in-depth understand the protective mechanism of biopatina and the influence of ageing on its efficiency it will be interesting to further interpret the impedance spectra. In fact, it would be possible to model the protective behaviour of biopatina using its equivalent circuit that describes the measured electrochemical processes in terms of a “classical” electric circuit consisting of electrical components as resistances, capacitors, constant phase elements, and so on.

During the development of the biological treatment for outdoor exposed monuments, the issue of the corrosion due to different rainfall exposure was raised. Indeed, on unsheltered areas the content of tin in the patina is much higher than in sheltered areas. Also, this tin-enriched zones are characterized by light green vertical strikes that impair the aesthetical aspect of the artefact. At that point of the research, the interaction between the biological treatment and high concentration of tin was still unknown. Furthermore, it was not sure if this interaction might have prevented the formation of copper oxalates due to the lower availability of copper ions. Therefore, the biopatina treatment was tested on tin-enriched

specimens aged by simulated unsheltered conditions (chapter 5). It seemed that the porosity of the biological treatment on tin-enriched areas was slightly higher than on the control and an improvement of this feature would enhance the treatment efficiency on these specific zones. However, for the first time it was demonstrated that biopatina treatment is efficient on tin-enriched surfaces producing both tin and copper oxalates. However, copper oxalates appeared to be formed preferentially even on such tin-enriched surfaces with good adhesion properties even after severe runoff conditions. Furthermore, the biological treatment provided a homogeneous visual aspect that tended to a similar tonality than sheltered areas. This part of the study demonstrated that the biopatina treatment can be applied on the entire surface of outdoor monuments forming a stable layer of copper oxalates regardless of the high tin concentration of the original patina and the exposure to rainfalls.

As final part of this thesis, the influence of the alloy composition on the performance of the biological treatment was studied. As mentioned all through this thesis, the corrosion behaviour of bronze differs from the one of pure copper. Indeed, tin, lead and zinc may be present as alloying elements in bronze casting and influence bronze behaviour. Therefore, a first attempt to evaluate the influence of the alloy on biopatina treatment was assessed using three different alloys with copper sulphate artificial and tin-enriched patinas. Results showed that, both the colour and the surface composition after treatment may be influenced by the alloy composition. Thus, an in-depth evaluation of the possible correlation between alloying elements and conservation treatments applied on artificial patinas was assessed using ANOVA. In particular, the colour variation and the electrochemical behaviour were analysed after the application of treatment and after ageing procedures. It appeared that the alloy composition had a strongest influence for the corroded surface's colour after treatment while during ageing its influence decreased. However, a clear model for the alloy composition's influence on the colour was not identified. Regarding the electrochemical behaviour, the alloy composition had an influence only on few patinas and the main factors influencing it were the treatment applied and the original patina composition both after treatment and after ageing. In order to better understand the influence of the alloy composition, a data analysis using a one-way ANOVA should be evaluated. Also, the same data analysis from natural patinas may provide an interesting characterization to help in the understanding of alloying elements influence on bronze artefacts.

To conclude, this research allowed a better understanding of the protective behaviour of biopatina treatment. It positioned the biological treatment in the range of corrosion inhibitors rather than protective coatings and developed the application protocol currently used on real artefacts. Biopatina can be used to replace benzotriazole solutions as innocuous and more efficient treatment for archaeological objects. It can also be applied on outdoor objects, regardless the geometry of exposure conditions and its efficiency is not influenced by the bronze composition, however it is not comparable to a coating system. Finally, a ready-to-use kit is currently under evaluation for commercialization and available for small trials to conservators-restorers (Annex1). In Figure 93 the main findings of this thesis were added to the results of the previous "biopatina projects".

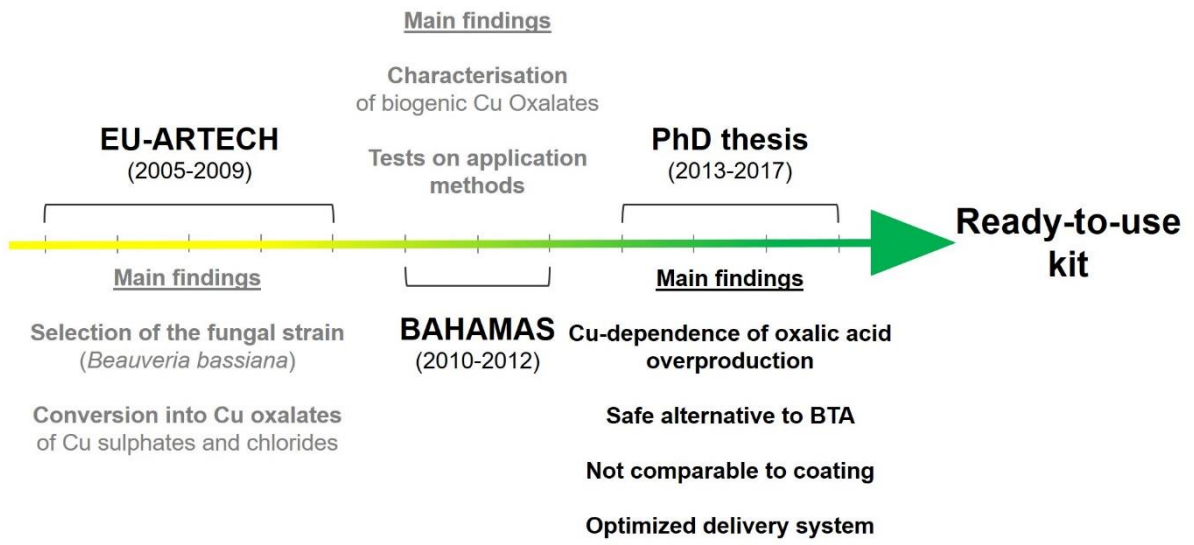


Figure 93. Main findings of this thesis with the results of the previous “biopatina projects”

## References

1. Burgot, J.L., *Ionic Equilibria in Analytical Chemistry*. 2012: Springer New York.
2. Gadd, G.M., Geomicrobiology of the built environment. *Nature Microbiology*, 2017. 2: p. 16275.
3. Adriaens, A., et al., Insights into electrolytic stabilization with weak polarization as treatment for archaeological copper objects. *Analytical and bioanalytical chemistry*, 2007. 387(3): p. 861-868.
4. Oddy, W. and M. Hughes, The stabilization of 'active' bronze and iron antiquities by the use of sodium sesquicarbonate. *Studies in conservation*, 1970. 15(3): p. 183-189.
5. Brown, B.F., *Corrosion and metal artifacts: a dialogue between conservators and archaeologists and corrosion scientists*. Vol. 479. 1977: US Department of Commerce, National Bureau of Standards.
6. Rosenberg, G.A., *Antiquites en fer et en bronze 1917*, Copenhagen.
7. Scott, D.A., *Copper and Bronze in Art: Corrosion, Colorants, Conservation*. 2002: Getty Publications.
8. Ghazali, F.M., et al., Biodegradation of hydrocarbons in soil by microbial consortium. *International Biodeterioration & Biodegradation*, 2004. 54(1): p. 61-67.
9. Hanstveit, A.O., Biodegradability of petroleum waxes and beeswax in an adapted CO<sub>2</sub> evolution test. *Chemosphere*, 1992. 25(4): p. 605-620.
10. Marino, F., *Biodegradation of paraffin wax*. 1998, McGill University, Montréal.
11. Revie, R.W., *Corrosion and corrosion control*. 2008: John Wiley & Sons.
12. Roberge, P.R., *Corrosion Engineering*. 2008: McGraw-Hill New York, NY, USA:.

# ANNEX 1 – APPLICATION PROTOCOL OF BIOPATINA

The current protocol, sent with the biopatina ready-to-use kit and available for small trials to conservators-restorers, is here reported.

## Description

BIOPATINA is a new ecological and sustainable solution for preserving copper-based artefacts using selected microorganisms. This technology is based on the natural capacity of some microorganisms to form copper oxalates on the corroded surface of copper alloys. Existing unstable and pulverulent corrosion products are converted into an insoluble and chemically stable biopatina that provides the treated surfaces with a stabilization of the corrosion process and an aesthetically attractive green colour. This treatment allows to stabilize the active corrosion induced by copper chlorides and to prevent green staining of surrounding materials (stone pedestal, wall...) due the leaching of copper sulphates.

## Properties-characteristics:

- not associated with cyclic corrosion
- stable in acidic atmosphere
- simulating naturally-aged green patina
- no glossy effects
- mineral composition as the treated surface
- smooth and adherent film (no discontinuity with the underneath corrosion patina)

## Advantages

- BIOPATINA can operate between 10 and 30°C, optimal 20°C
- No use of toxic materials or solvents - Respect of the environment

## Stability

The thickening and nutrient doses can be stored at room temperature, avoiding heat and moisture. The BIOPATINA dose should be kept at 4°C and is stable over 6 months. The mixed components are stable over 6 months if stored at 4°C avoiding external contamination.

## Procedure

The treatment is carried out in two phases. Prior to intervention, the area to be treated must be cleaned as with traditional methods. All surfaces and material used for the application must be clean with ethanol or isopropyl alcohol 70% (w/w) in deionized water and dry with clean paper.

*Phase 1- Preparation of the formulation*

Put together the tubes A and B in a container of 150-200 mL (cleaned with ethanol 70%). With tweezers (previously cleaned with ethanol 70%), get rid of the white filaments and leave the remaining solution with only whitish flakes. Add then the thickening dose C slowly under strong agitation (sieving the powder can help in this operation to avoid lumps). The gel is ready to be used. For better results, keep the gel some hours at 4°C as it will get thicker. Put the filaments taken off and paper used for cleaning in a plastic waste container and before throwing away, spray ethanol 70% on them (waste treatment to be checked according to each country regulations). The waste can also be neutralized in oven (minimum 45 min at 100°C).

*Phase 2- Application*

spray the surface with ethanol 70% (w/w in deionized water) and, if desired, dry with cold air

apply on the surface the gel with a thickness of 3-8 mm. May be applied by hand or using plastic spatula cover the treated surface with micro-perforated plastic film (and/or wet gauze to avoid extra drying of the gel) and let undisturbed for 1-2 weeks. Extra time up to 3-4 weeks might change the result on thin corrosion layers (less than 10 microns)

in case of outdoor intervention, protect the treated area from sun and rain (i.e. plastic greenhouse, closed and opaque container). Avoid drying and keep a high humidity atmosphere (90%) could be achieved also with a humidifier (shut on 1/4h off)

in case of treatment of small objects, these latter can be stored in hermetic boxes during treatment. The humidity produced will be enough to avoid desiccation

check after 72h that small white spots appeared on the surface of the formulation indicating the treatment works fine. After one week, the whole treated surface should be covered with white snow clusters. The formulation will gradually become green and should be kept wet

in case white spots are not visible after maximum 72h (this has been observed with objects highly contaminated with copper chlorides), repeat the application with fresh formulation till the apparition of the white spots.

*Phase 3- Stop of the treatment*

take off as much as possible of the gel by hand in a plastic waste container and before throwing away, spray ethanol 70% all over (waste treatment to be checked according to each country regulations). The formulation can also be neutralized in oven (minimum 45 min at 100°C)

wash the treated surface with water or alternatively (when water should be avoided) dry under cold air. Small residues of formulation can be eliminated by brushing with ethanol 70%. - clean the surface with spraying of ethanol 70%.

**Risks and toxicity**

The kit does not contain toxic nor pathogenic agents (class 2-microorganisms with weak risk). Inhalation of powder or spores can cause allergic reactions in sensitized persons. In case of contact with skin, it can cause irritation. The use of gloves and masks is recommended.

## **Packaging**

100 mL kit is enough to cover surface of 10 x 10 cm<sup>2</sup>.

KIT for 100 mL of formulation COMPOSED OF:

1 BIOPATINA dose (tube A)

1 nutrient dose (tube B)

1 thickening dose (tube C)



## ANNEX 2 – CV and PUBLICATIONS

### Personal Information

---

First name/Surname Monica Albini  
 Telephone +41 79 655 26 79  
 E-mail monica.albini@gmail.com  
 Nationality Italian  
 Date of Birth 23 / 12 /1984

### Research Experience

---

- May 2013 - Present **Scientific Collaborator – University of Neuchatel**  
 Development of a novel microbiological treatment for the conservation of copper-based alloys.  
 Neuchatel, Switzerland  
 Supervisors: Prof. Edith Joseph and Prof. Pilar Junier
- May 2013 - present **Short-term scientific stays – Institute of Marine Sciences – CNR**  
 Study of corrosion behaviour by Electrochemical Impedance Spectroscopy (EIS) measurements of copper-based and iron-based artefacts during natural ageing and conservation treatments development  
 Genoa, Italy  
 Supervisor: Dr. Paola Letardi
- May 2015 **Short-term scientific stay - Diamond Light Source Synchrotron facilities**  
 X-ray Absorption Spectroscopy (XAS) and X-Ray Fluorescence (XRF) mapping for the assessment of novel biological conservation treatment for archaeological wood  
 Didcot, United Kingdom  
 Supervisor: Dr. Konstantin Ignatyev
- april – December 2011 **Internship – Vatican Museums**  
 Study of the conservation state of artworks exhibited in museum collections, evaluation of the efficiency of conservation methods, development of conservation materials  
 Rome, Italy  
 Supervisor: Dr. Fabio Morresi and Prof. Ulderico Santamaria
- March - December 2010 **Internships – Institute of Nanostructured Materials – CNR**  
 and Use of analytical techniques (optical and metallographic microscopy, SEM-EDS, X-ray diffractometry) for the study of archaeological bronzes.  
 November 2006 - October 2007  
 Rome, Italy  
 Supervisor: Prof. Gabriel Maria Ingo

## Other professional activities

---

- May 2013 - Present **Teaching assistant**
- Laboratory and practical course in Microbiology, B.Sc. in Biology
  - Problem-based learning course in Microbiology, M.Sc in Biology and in Biogeosciences
- University of Neuchatel, Neuchatel, Switzerland
- December 2015 **FTIR in-situ analysis** of mural paintings of the Saint-Maire castle  
Lausanne, Switzerland
- January - December 2009 **Students' tutor**  
Faculty of Science, "Sapienza" University of Rome, Italy

## Education

---

- May 2013 - Present **Ph.D. in Science**  
**Conservation science / Microbiology**  
Biotechnology applied to the conservation of Cultural Heritage metal artefacts  
Faculty of Science, University of Neuchatel, Switzerland
- December 2010 **Master of Science Degree**  
**Science applied to Cultural Heritage**  
Faculty of Science, "Sapienza" University of Rome, Italy
- Grade in national classification **110/110 summa cum laude**
- October 2007 **Bachelor of Science Degree**  
**Science applied to diagnostic and conservation of Cultural Heritage**  
Faculty of Science, "Sapienza" University of Rome, Italy
- Grade in national classification **106/110**

## Further Education

---

- April 2017 Course **Obtain post-doctoral fellowships**, Neuchatel, Switzerland
- March 2017 Course **Create a project budget**, Neuchatel, Switzerland
- December 2016 Course **Time Management**, Lausanne, Switzerland
- November 2016 Course **Planning a career strategy - Part 1**, Neuchatel, Switzerland
- October 2016 Course **Negotiation skills**, Lausanne, Switzerland
- June 2016 Workshop **Patent and licence in science**, Murten, Switzerland
- September 2015 Course **Planning a career strategy - Part 2**, Neuchatel, Switzerland
- November 2014 Course **Write a review**, Neuchatel, Switzerland
- October 2014 Course **Effective public speaking**, Neuchatel, Switzerland
- July 2014 Field course **Environmental Microbiology**, Lake Cadagno, Switzerland
- May 2014 Course **Scanning Electron Microscopy**, Neuchatel, Switzerland
- January 2014 School of **Chemometrics**, Genoa, Italy
- September 2004 – July 2007 Practical course **Restoration of ancient materials**, Rome, Italy

## Grants and Awards

---

- September 2016 **Conference travel award** for attendance at Metal 2016 conference, New Delhi, India
- September 2014 **Grant “Egalite des Chances”** for Short term scientific stays at ISMAR – CNR, Genoa, Italy (total amount 2’630 CHF)
- September 2013 **Grant “Egalite des Chances”** for Short term scientific stays at ISMAR – CNR, Genoa, Italy (total amount 3’390 CHF)

## Technical skills

---

- Optical microscopy (O.M.)
- Scanning Electron Microscopy (SEM)
- Energy Dispersive Spectroscopy (EDS)
- Infrared spectroscopy (FTIR)
- Electrochemical Impedance Spectroscopy (EIS)
- Colorimetry
- Ion Chromatography (IC)

## Language skills

---

CFRL level

**Italian:** Native speaker

**English:** C2

**French:** B2

## Publications

---

L. Comensoli, J. Maillard, M. Albin, F. Sandoz, P. Junier and E. Joseph. Use of bacteria to stabilize archaeological iron. *Applied and Environmental Microbiology*. 2017. In press.

M. Albin, C. Chiavari, E. Bernardi, C. Martini, L. Mathys, P. Letardi, P. Junier and E. Joseph. Evaluation of the influence of alloying elements on the performances of a biological treatment. In *METAL 2016 Interim Meeting of the ICOM-CC Metal Working Group Conference Proceedings. New Delhi, India, 26<sup>th</sup>-30<sup>th</sup> September 2016*.

P. Letardi, B. Ramirez-Barat, M. Albin, P. Traverso, E. Cano and E. Joseph. Copper alloys and weathering steel used in outdoor monuments: Weathering in an urban-marine environment. In *METAL 2016 Interim Meeting of the ICOM-CC Metal Working Group Conference Proceedings. New Delhi, India, 26<sup>th</sup>-30<sup>th</sup> September 2016*.

M. Albin, C. Chiavari, E. Bernardi, C. Martini, L. Mathys, E. Joseph. Evaluation of the performances of a biological treatment on tin-enriched bronze. *Environmental Science and Pollution Research*, 2016. DOI: 10.1007/s11356-016-7361-2.

E. Joseph, S. Bindschedler, M. Albin, L. Comensoli, W. Kooli, L. Mathys. Microorganisms for safeguarding built heritage. *The Fungal Community: Its Organization and Role in the Ecosystem*, Eds. J. Dighton, J. White, P. Oudemans CRC press Taylor and Francis group, 2016. In press.

M. Albin, L. Comensoli, L. Brambilla, E. Domon Beuret, W. Kooli, L. Mathys, P. Letardi, E. Joseph. BIOPATINAS: Innovative biological approaches for metal conservation. *Materials and Corrosion*, 2015. doi:10.1002/maco.201408168.

E. Joseph, P. Junier, M. Albin, P. Letardi, E. Domon Beuret, L. Brambilla, L. Mathys, C. Cevey, R. Bertholon. Biologically induced patina for metal built heritage. In *Conference Proceedings of Scienza e Beni Culturali, Metalli In Architettura: Conoscenza, Conservazione e Innovazione*. Bressanone, Italy, 30<sup>th</sup> June - 3<sup>rd</sup> July 2015. Edizione Arcadia Ricerche s.r.l., Marghera Venezia, 2015; ISBN 9788895409191, 273-282.

E. Joseph, M. Albini, P. Letardi, E. Domon Beuret, L. Brambilla, L. Mathys, C. Cevey, R. Bertholon, D. Job, P. Junier. BIOPATINAS: Innovative biological patinas for copper-based artefacts. In *Conference Proceedings of Outdoor Metallic Sculpture from the XIXth to the Beginning of the XXth Century: Identification, Conservation, Restoration*. Paris, France. 4th-5th December 2014. ICOMOS France, Paris, 2014; ISBN 9782905430182, 154-162.

E. Domon Beuret, L. Mathys, L. Comensoli, L. Brambilla, M. Albini, C. Cevey, R. Bertholon, P. Junier, E. Joseph. Biopatines: des champignons au service des alliages cuivreux. In *Conference Proceedings of JOURNEES DES RESTAURATEURS EN ARCHEOLOGIE 2014 « restaurer l'ordinaire, exposer l'extraordinaire : du site au musée » Arles, France. 16th-17th October 2014*. Atelier de Conservation-Restauration du Musée Départemental Arles Antique (MDAA) et A-CORROS, Arles, 2014; *Cahier technique de l'ARAAFU* 2015, 22, 45-48.

E. Joseph, P. Letardi, M. Albini, L. Comensoli, W. Kooli, L. Mathys, E. Domon Beuret, L. Brambilla, C. Cevey, R. Bertholon, D. Job, P. Junier. Innovative biological approaches for metal conservation. In *Conference Proceedings of EUROCORR 2014, European Corrosion Congress*. Pisa, Italy. 8th-12th September 2014. DECHEMA e.V., Frankfurt and AIM – Associazione Italiana di Metallurgia, Milano, 2014; ISBN 9783897461598, 1-10.

M.P. Casaletto, G.M. Ingo, M. Albini, A. Lapenna, I. Pierigè, C. Riccucci, F. Faraldi An integrated analytical characterization of corrosion products on ornamental objects from the necropolis of Colle Badetta-Tortoreto (Teramo, Italy). *Applied Physics A: Materials Science & Processing*, 2010, Vol. 100, pp. 801-808

## Conference Communications

---

M. Albini, C. Chiavari, E. Bernardi, C. Martini, L. Mathys, P. Letardi, P. Junier and E. Joseph. *Evaluation of the influence of alloying elements on the performances of a biological treatment*. METAL 2016 Interim Meeting of the ICOM-CC Metal Working Group. New Delhi, India, Previewed from 26th to 30th September 2016. (Oral presentation)

M. Albini, L. Mathys-Paganuzzi, J. Schröter, P. Junier and E. Joseph. *Biological treatment for the conservation of copper-based alloys*. New strategies for the conservation of metallic cultural heritage. Paris, France, 11th – 12th April 2016. (Oral presentation)

M. Albini, P. Letardi, L. Mathys, P. Junier, E. Joseph. *Biopatina treatment for the stabilization of contemporary bronze artworks*. Green Conservation of Cultural Heritage. Rome, Italy, 27th-28th October 2015. (Oral presentation)

M. Albini, C. Chiavari, E. Bernardi, C. Martini, L. Mathys, E. Joseph. *Evaluation of the performances of a biological treatment on tin-enriched bronze*. EUROANALYSIS 2015, 18th European Conference on Analytical Chemistry, Bordeaux, France, 6th-10th September 2015. (Oral presentation)

M. Albini, P. Letardi, L. Mathys, P. Junier, E. Joseph. *Biopatina treatment for the stabilization of contemporary bronze artworks*. 73rd Annual Assembly of the Swiss Society for Microbiology (SSM), 2015, Lugano, Switzerland. (Poster)

M. Albini, L. Comensoli, W. Kooli, L. Mathys, P. Junier, E. Joseph. *Biotechnology and metal protection*. 15th International Symposium on Microbial Ecology (ISME), 2014, Seoul, South-Corea. (Poster)

M. Albini, P. Letardi, L. Mathys, P. Junier, E. Joseph. *Biopatinas: Microbiological Treatment for Conservation of Copper-Based Alloys*. 72nd Annual Assembly of the Swiss Society for Microbiology (SSM), 2014, Fribourg, Switzerland. (Poster)

## ACKNOWLEDGEMENTS

This doctoral research was financially supported by the Commission for Technology and Innovation CTI (grant agreement n° 14573.2 PFLS-LS, 2013-2014), the Gebert Rűf Stiftung (grant agreement n° GRS 054/12, 2013-2016), and the Stiftung zur Fűrderung der Denkmalpflege (New ecological and sustainable solution for protecting architectural metals using an ecologically friendly biological treatment, 2015-2018). The Haute Ecole ARC Conservation-restauration of Neuchatel (Switzerland), the Institute of Marine Sciences (CNR-ISMAR, Italy) and the University of Bologna (Italy), are also gratefully acknowledged for the research support and fruitful collaboration.

I also would like to thank all people that guided, supported and helped me during these four years. I also realised that most of those people are women in science that successfully harmonize work and private life. You all are a great example for me and I hope to find a perfect balance as you did.

First of all, I want to thank Edith Joseph. Four years ago you choose me to be part of your team and I will always be grateful for it. I am also really thankful for your unconditional support. You taught me how to be a better scientist and your example inspired me to always look for new achievements.

A huge thank you goes to Pilar Junier, the most encouraging and optimistic co-supervisor that I could ever had. Thank you very much for welcome me in your lab, I have been very happy here and I discovered the beauty of microbiology thanks to you.

Lidia, cette thèse n'aurait jamais été possible sans toi. En effet, ils devraient donner un doctorat aussi à toi! Merci pour tout le support, les sourires et la bonne humeur que tu m'as transmis dans ces ans.

Paola Letardi, you are an amazing researcher, an amazing woman and an amazing friend. You showed me how to face any unexpected problem with grace, humourism and a smile on the face. Thank you for welcome me in your lab and in your house, making me feel part of a family. I also would like to thank all the other researchers from the CNR-ISMAR of Genoa, Pierluigi Traverso, Roberto Stifanese, Milena Toselli as well as Lucrezia and Pino that made me feel always like home.

Thanks to Cristina Chiavari, who showed me that be an excellent researcher in Italy is still possible.

## ACKNOWLEDGEMENTS

I am also particularly grateful to Laura Brambilla and Julie Schröter, for their help and support throughout this four years.

This PhD would not have been the same without my friend and colleague Lucrezia Comensoli. Abbiamo iniziato questa esperienza insieme e avere un'amica su cui poter sempre contare e con cui condividere i momenti belli e meno belli è stata una grandissima fortuna. Grazie per tutte le risate, i consigli, i thè e le caramelle rilassanti!

Thanks to all the LAMUN and LATHEMA friends and colleagues, in particular Sevi, Tina, Wafa, Andrea, Nicole, Andrej, Saskia, Isha, Magda and Mathilde.

I want to sincerely thank my adoptive Greek/Balkan family here in Neuchatel: Sevi, Amalia, Nathalie, Elena, Tony and Dimitri. Having you in my life made it better. Thanks for all the funny, amazing and happy moments we spent together.

Thank to my long-standing friends, gli amici di una vita: Mabel, Michele, Diego, Giovanna e Irene. È bello sapere che anche se lontani, possiamo ritrovarci come se il tempo non fosse mai passato.

Un grazie speciale va a i miei genitori, per avermi dato solide basi per partire avendo la sicurezza di poter tornare e essere sempre amata. Grazie anche al mio “fratellino”, che mi mostra ogni giorno come si diventa adulti con leggerezza e a cui voglio tanto bene, anche se non te lo dico mai.

Finally, a special thank goes to Giulio, per l'amore, l'incoraggiamento e la pazienza nella distanza.

## FIGURES INDEX

Figure 1. Potential – pH diagram of Cu in aqueous medium ( $10^{-6}$ mol·dm <sup>-3</sup> ) .....	19
Figure 2. Pourbaix diagram for the system Cu – SO <sub>4</sub> – H <sub>2</sub> O at 20°C with 46 ppm of SO <sub>4</sub> .....	24
Figure 3. Pourbaix diagram for the system Cu – Cl – H <sub>2</sub> O at 20°C at chlorine concentration of 35 ppm (a), 350 ppm (b), 3550 ppm and 35500 ppm (d) .....	25
Figure 4. Roman coin affected by bronze disease.....	26
Figure 5. Pourbaix diagram for the system Cu – CO <sub>2</sub> – H <sub>2</sub> O at 20°C at carbon dioxide concentrations of 44 ppm (a), 440 ppm (b), 4400 ppm and 44000 ppm (d).....	31
Figure 6. Main copper and tin minerals found on corroded bronze artefacts.....	32
Figure 7. Chronological timeline of biopatina projects and main outcomes of previous studies .....	38
Figure 8. Summary of the main focuses of this PhD project.....	39
Figure 9. Front and reverse of <i>Beauveria bassiana</i> colony in Malt Agar .....	49
Figure 10. Microscopic aspect of <i>B.bassiana</i> conidia.....	50
Figure 11. Secondary electron micrographs of <i>B. bassiana</i> hyphae and biosynthesised crystals of copper oxalates. On the top images some copper oxalates crystals are indicated by circles .....	52
Figure 12. Plots of the oxalic acid concentration in control (black), copper oxide (red) and copper sulphate (blue) amended culture media during the first seven (a), thirty-one (b) and hundred-seventy (c) days. The asterisks indicate the sets where one outlier was excluded from the calculation of the mean. ....	55
Figure 13. HPLC chromatograms of control, copper sulphate and copper oxide amended culture media after 3 days of incubation.....	56
Figure 14. HPLC chromatograms of control, copper sulphate and copper oxide amended culture media after 5 days of incubation.....	57
Figure 15. HPLC chromatograms of control, copper sulphate and copper oxide amended culture media after 10 days of incubation.....	57
Figure 16. HPLC chromatograms of control, copper sulphate and copper oxide amended culture media after 31 days of incubation.....	58
Figure 17. Climatic chamber used for the ageing procedures on LAT samples showing the aluminium trail covered with a micro-perforated plastic film.....	70
Figure 18. Data recorded during the one month cycle of ageing showing the regularity of the artificial climate generated inside the chamber: The upper chart represents the relative humidity, the lower chart the temperature.....	70
Figure 19. Climate during July and November 2014 in the laboratory of Laténium Museum, Hauterive .....	71
Figure 20. Fibula A-10 before (a) and after (b) BTA treatment.....	71
Figure 21. Coin A-3 before (a) and after (b) BTA treatment .....	71
Figure 22. ATR-FTIR spectra showing the presence of malachite and benzotriazole on Lat-Agen15-02 .....	72

Figure 23. Axe blade F-23 before intervention (a), during mechanical cleaning (b), during biological treatment using a clay mixture (c), after 2,5 weeks of treatment with white spots confirm the fungal growth (d) and after treatment removal (e).....	73
Figure 24. Coin A-5 before treatment (a), during biological treatment using Metylan® (b), after 2,5-weeks treatment with light green parts confirming the formation of copper oxalates (c) and after treatment removal (d) .....	73
Figure 25. Belt strap A-11 before treatment (a), after mechanical cleaning with scalpel (b), c) during biological treatment using Metylan® and after treatment removal (d).....	74
Figure 26. LAT samples treated with biopatina: A-11 (a) and F-23 (b) samples during application of Metylan® gel and packaging with Tredegar® film; A-11 (c) and F-23(d) samples after 28 days of treatment .....	75
Figure 27. Sample A-11 after mechanical cleaning (a), after 28 days of biological treatment (b) with detail of the surface with a thin white layer indicating the presence of copper oxalates (c).....	75
Figure 28. ATR-FTIR spectra showing the presence of copper oxalate (characteristic peaks at ~1615, 1360, 1315 and 1815 cm <sup>-1</sup> ) on A5 (a) and on A11 (b) samples with residues of Metylan® ( peaks at 1154, 1113, 1062 and 1034 cm <sup>-1</sup> ) .....	76
Figure 29. Untreated objects A2 and A6 before ageing (a-b) and after ageing (c-d) respectively. New efflorescences indicated by red arrows .....	77
Figure 30. BTA-treated objects A10 and F-Agen-15 before ageing (a-b) and after ageing (c-d) respectively. No significant visual changes.....	77
Figure 31. Biopatina-treated objects F23 and A5 before ageing (a-b) and after ageing (c-d) respectively. No significant visual changes .....	78
Figure 32. ATR-FTIR spectra showing the presence of copper oxalate (characteristic peaks at ~1615, 1360, 1315 and 1815 cm <sup>-1</sup> ) on Bracelet sample .....	78
Figure 33. Biopatina treated real object Eg-530 before treatment (a), during biopatina treatment (b-c), after treatment (d) and after natural ageing (e) .....	79
Figure 34. Untreated real object (spearhead) unnumbered before (a) and after (b) indoor storage; BTA treated real object CH-287 before (c) and after (d) indoor storage.....	80
Figure 35. Biopatina treated real objects Eg-530 (a) and Bracelet (b) unnumbered before and after (c-d) indoor storage respectively .....	80
Figure 36. Samples appearance before and after treatment.....	84
Figure 37. ATR-FTIR spectra showing from top to bottom an atacamite standard reference (grey) and its characteristics wavenumbers, the untreated sample characteristic peaks corresponding to atacamite wavenumbers, and treated samples (Biopatina, BTA1 (24hours) and BTA2 (14 days)) with the respective wavenumbers of copper oxalates and Cu-BTA complexes indicated in black. The wavenumbers corresponding to atacamite are indicated in grey in all spectra.....	86
Figure 38. Secondary electrons micrograph of biopatina-treated sample showing typical habit of copper oxalates crystals.....	87
Figure 39. EIS Bode plots: impedance  Z  modulus (a) and phase plots (b) for untreated (grey dots, T0), biopatinated (green squares, T4) and BTA (yellow (24h, BTA1) and blue (14days, BTA2) diamonds) treated samples.....	87
Figure 40. (a) optical micrograph of untreated sample cross section showing the area (white dotted line) where FTIR mapping was performed and (b) FTIR chemical map of the relative intensity of the entire atacamite spectrum.....	89

Figure 41. (a) optical micrograph of biopatinated sample cross section showing the area (white dotted line) where FTIR mapping was performed. FTIR chemical map of the relative intensity of the entire atacamite spectrum (b) and of the entire copper oxalate spectrum (c).....	90
Figure 42. optical micrographs of BTA 24 hours and BTA 14 days treated samples cross section (a and b respectively) showing the area (white dotted line) where FTIR mapping was performed. FTIR chemical map of the relative intensity of the entire atacamite spectrum (c and d respectively) and of the 1397 cm <sup>-1</sup> characteristic peak Cu-BTA complex .....	91
Figure 43. ATR-FTIR spectra collected on CUNN samples: untreated (grey, T0) and a) treated with biopatina (black, T4) and b) treated with wax (black, TR).....	101
Figure 44. Secondary electrons SEM images of sample CUNN65 (a), QQ66 (b) and GMN11 (c).....	102
Figure 45. Evolution of the patinas colour according to the exposure time. Sets: CUNN Ge, CUNN Ne, GMN, QQ treated with wax (TR, blue), Biopatina (T4, green) and untreated (T0, grey).....	103
Figure 46. Impedance values showed as function of the exposure time on CUNN, GMN and QQ sets of samples treated with wax (TR, blue), Biopatina (T4, green) and untreated (T0, grey).....	103
Figure 47. ATR-FTIR spectra of a) GMN11 (T4) sample and b) GMN5 (TR) sample at 0 (grey) and 12 (black) months of exposure. The spectra show the presence of copper chloride (C) and wax (W) on the sample surface.....	105
Figure 48. Visual characterization of CUNN samples before treatment, after agar cleaning, after new application of biopatina (T4) and after 6 months ageing. The untreated sample (T0) is also shown...	107
Figure 49. Visual characterization of QQ samples before treatment, after agar cleaning, after new application of biopatina (T4) and after 6 months ageing. The untreated sample (T0) is also shown...	107
Figure 50. Visual characterization of GMN samples before treatment, after agar cleaning, after new application of biopatina (T4) and after 6 months ageing. The untreated sample (T0) is also shown...	108
Figure 51. ATR-FTIR spectra of sample QQ66 (T0) before cleaning (BT, grey), after cleaning (AC, dark grey) and after six months of exposure (6M, black). The spectra show the presence of copper atacamite (C) and brochantite (S) on the sample surface.....	109
Figure 52. ATR-FTIR spectra of sample CUNN61 (T0) before cleaning (BT, grey), after cleaning (AC, dark grey) and after six months of exposure (6M, black). The spectra show the presence of copper atacamite (C) and brochantite (S) on the sample surface.....	109
Figure 53. ATR-FTIR spectra of sample CUNN45 (T4) before cleaning (BT, grey), after biopatina treatment (0M, dark grey) and after six months of exposure (6M, black). The spectra show the presence of copper atacamite (C), brochantite (S) and copper oxalates (Ox) on sample surface.....	110
Figure 54. ATR-FTIR spectra of sample QQ51 (T4) before cleaning (BT, grey), after biopatina treatment (0M, dark grey) and after six months of exposure (6M, black). The spectra show the presence of copper atacamite (C), brochantite (S) and copper oxalates (Ox) on sample surface .....	110
Figure 55. ATR-FTIR spectra of sample GMN2 (T4) before cleaning (BT, grey), after biopatina treatment (0M, dark grey) and after six months of exposure (6M, black). The spectra show the presence of copper atacamite (C), brochantite (S) and copper oxalates (Ox) on sample surface.....	111
Figure 56. Secondary and backscattered electrons SEM images of rosette-like copper oxalates crystals on sample CUNN45 (a), QQ51 (b) and GMN2 (c-d) .....	111
Figure 15. Colorimetry plots representing colour coordinates L* (lightness, bright-dark) a* (red/green opponent colours) and b* (yellow/blue opponent colours) for all samples together (a) and CUNN (b), QQ (c) and GMN (d) samples. Measure were taken before treatment, after agar cleaning (AC), after treatment (0 Month), during exposure (2 and 4 Months) and after 6 months exposure.....	112

Figure 58. Bode plots (impedance modulus  $|Z|$  and phase  $\Phi$ ) of CUNN (a) QQ (b) and GMN (c) samples (2 measures for each sample). Data before treatment (BT, light grey), after agar cleaning (AC, grey/black square), after biopatina treatment (T4 0M, light green) and after 6 months exposure (6M) for the untreated (dark grey) and biopatinated (dark green) samples are shown ..... 114

Figure 59. ATR-FTIR spectra before (grey dotted line) and after (black continuous line) treatment with T4J method (left) on copper nitrate (NT) patina and T4K method (right) on copper chloride (CB) patina. Characteristic peaks of copper oxalates are indicated with the abbreviation Ox..... 119

Figure 60. Secondary electrons SEM image of rosette-like copper oxalates crystals ..... 119

Figure 61.  $\Delta E^*$  of biological treatment applied by two different methods (T4J, T4K) compared with wax reference treatment (TR) for all the treated patinas on binary (B), tertiary (T) and quaternary (Q) bronze ..... 120

Figure 62. Comparison between impedance  $|Z|$  values of untreated samples (T0) and biological treated samples (T4J, T4K) of all the treated patinas on binary (B), tertiary (T) and quaternary (Q) bronze. The dashed lines represent the minimum and maximum  $|Z|$  values of the wax treatment (TR)..... 120

Figure 63. Visual characterization of the artificial patinas before exposure and after 12 months ageing. For each patina, a sample untreated (T0), treated with biopatina (T4) and microcrystalline wax (TR) is shown ..... 121

Figure 64. ATR-FTIR spectra comparison of the sample NB1 (copper nitrate original patina) treated with Cosmoloid wax H80 TR before (grey) and after 12 months of exposure (black), showing the newly increase of original patina peaks on the sample surface after ageing..... 122

Figure 65. FTIR spectra comparison of the sample IQ9 (iron nitrate original patina) treated with biopatina after 12 months of exposure (black) and of the malachite standard (grey), revealing the presence of this latter as one of the compounds of the sample patina ..... 123

Figure 66. Secondary electron micrographs of black copper nitrate patina on quaternary bronze (BNQ, left) treated with biopatina (T4) showing copper oxalate crystals and of copper nitrate patina on quaternary bronze (NQ, right) with degraded coating layer of wax after 12 months of exposure..... 124

Figure 67.  $\Delta E^*$  of biological treatment applied by two different methods (T4J, T4K) compared with wax reference treatment (TR) for all treated patinas on binary (B), tertiary (T) and quaternary (Q) bronze ..... 124

Figure 68. Variation of impedance values  $\Delta|Z|$  after 12 months of ageing obtained for the different sets of samples treated with Biopatina (T4, green), wax (TR, blue) and untreated (T0, grey). Negative values indicate a decrease of  $|Z|$  and positive values an increase of  $|Z|$  after one-year of exposure. a, b and c represent the same graph at a different scale ..... 125

Figure 69. Fusion sculpture (Froidevaux, 1988) a-b) Before intervention. Documentation of the conservation state with c) soluble deposits, d) dejections, e) marks of ancient adhesives, f) bluish splashes and g-h) sampling points of the patina for FTIR analyses ..... 128

Figure 70. Selected areas for biological treatment..... 129

Figure 71. a) Small area treated with a mixture of clay products (based on Lutum®) and a Metylan®-based gel; b- c) Ongoing treatment ..... 129

Figure 72. Pilot test: the two scenes before (a-b) and after (c-d) biological treatment ..... 133

Figure 73. Scenes before (right) and after (left) 3 weeks of biological treatment ..... 134

Figure 74. ATR-FTIR spectrum showing the presence of copper oxalates (Ox) on a lectern, on the front side of the book..... 135

Figure 75. ATR-FTIR spectrum obtained on the black trunk of a lectern. The copper oxalates characteristic peaks (Ox) are less visible.....	135
Figure 76. Statue “Schwinger” (Siegwart 1905) located in Lucerne before restoration intervention (2015) showing vertical light green streaks characteristic of unsheltered areas.....	142
Figure 77. Surface appearance of bare, pre-patinated, treated and aged sample (G85dx) with aged reference sample (G85).....	143
Figure 78. Mask used for Raman and FTIR measurements on bronze samples; points a, b and c (central area) and points d, e, f and g (edge area).....	144
Figure 79. Tin coupons after treatment: the points indicate the position of FTIR and Raman measurements and the related composition as hydrate tin oxide (black) or mixture of tin oxalates and hydrate tin oxide (white).....	145
Figure 80. ATR-FTIR spectra showing characteristic vibrational bands of hydrated tin oxide (a) or the concomitant presence of tin oxalate and hydrated tin oxide (b).....	146
Figure 81. Raman spectra showing characteristic shifts of hydrated tin oxide (a) or the concomitant presence of tin oxalate and hydrated tin oxide (b).....	146
Figure 82. ATR-FTIR spectra acquired on sample G85dx before (grey) and after (black) treatment .	147
Figure 83. Backscattered electrons images of reference sample and treated G85dx and G85sx samples before and after artificial ageing (central area: points a, b and c in the mask of Figure 78).....	149
Figure 84. Mean mass decrease for treated samples (black line) and the untreated one (grey line) during ageing.....	150
Figure 85. Release of Cu (a) and Pb (b) during ageing of treated (black line) and reference samples (grey line).....	150
Figure 86. Macroscopic images of SB (a), ST (b), SQ (c) and TQ (d) samples before and after biological treatment.....	158
Figure 87. ATR-FTIR spectra: binary bronze with artificial copper sulphate patina before (a) and after (b) treatment, quaternary bronze with artificial tin-enriched patina before (c) and after (d) treatment. Characteristic peaks of copper oxalates (Ox) at 1662,1362,1319,820 $\text{cm}^{-1}$ , tin oxide (TO) at 672,604 $\text{cm}^{-1}$ , hydrated tin oxide (HTO) at 1645,1391,1371,1237,830 $\text{cm}^{-1}$ and tin oxalates (TOx) at 1683,1339,1258,922,798 $\text{cm}^{-1}$ .....	161
Figure 88. EDS measurements plots for the alloy elements before (T0, black) and after (T4, grey) the application of the biological treatment.....	163
Figure 89. ANOVA boxplots with correspondent p values for $\Delta E1$ values (colour change after treatment). Alloy (a), Treatment (b) and Patina (c) plots are referred to the entire set of data while the factor comparisons are referred to fixed subgroups (d: alloy-treatments; e: alloy-patina; f: treatment-alloy; g: treatment-patina; h: patina-treatment; i: patina-alloy). For each sub-group the correspondent p value interval is given. A colour coding further indicates the p values intervals: blue ( $p < 0.001$ ), green ( $0.001 < p < 0.01$ ), orange ( $0.01 < p < 0.05$ ) and pink ( $p > 0.05$ ).....	168
Figure 90. ANOVA boxplots with correspondent p values for $\Delta E2$ values (colour change after 12-months ageing). Alloy (a), Treatment (b) and Patina (c) plots are referred to the entire set of data while the factor comparisons are referred to fixed subgroups (d: alloy-treatments; e: alloy-patina; f: treatment-alloy; g: treatment-patina; h: patina-treatment; i: patina-alloy). For each sub-group the correspondent p value interval is given. A colour coding further indicates the p values intervals: blue ( $p < 0.001$ ), green ( $0.001 < p < 0.01$ ), orange ( $0.01 < p < 0.05$ ) and pink ( $p > 0.05$ ).....	169
Figure 91. ANOVA boxplots with correspondent p values for Z1 values (impedance modulus after treatment). Alloy (a), Treatment (b) and Patina (c) plots are referred to the entire set of data while the	

factor comparisons are referred to fixed subgroups (d: alloy-treatments; e: alloy-patina; f: treatment-alloy; g: treatment-patina; h: patina-treatment; i: patina-alloy). For each sub-group the correspondent p value interval is given. A colour coding further indicates the p values intervals: blue ( $p < 0.001$ ), green ( $0.001 < p < 0.01$ ), orange ( $0.01 < p < 0.05$ ) and pink ( $p > 0.05$ ) ..... 170

Figure 92. ANOVA boxplots with correspondent p values for Z2 values (impedance modulus after ageing Alloy (a), Treatment (b) and Patina (c) plots are referred to the entire set of data while the factor comparisons are referred to fixed subgroups (d: alloy-treatments; e: alloy-patina; f: treatment-alloy; g: treatment-patina; h: patina-treatment; i: patina-alloy). For each sub-group the correspondent p value interval is given. A colour coding further indicates the p values intervals: blue ( $p < 0.001$ ), green ( $0.001 < p < 0.01$ ), orange ( $0.01 < p < 0.05$ ) and pink ( $p > 0.05$ ) ..... 171

Figure 93. Main findings of this thesis with the results of the previous “biopatina projects” ..... 181

# TABLES INDEX

Table 1. Standard reduction potentials ( $E_0^{\text{red}}$ ) by decreasing order.....	18
Table 2. Mean and standard deviation of the oxalic acid concentration measured in control, copper oxide and copper sulphate amended culture media. The asterisks indicate the sets where one outlier was excluded from the calculation of the mean. ....	55
Table 3. Main characteristics of the different substrates tested (x: yes; -: no; $\pm$ : partially).....	60
Table 4. Test objects: patina composition determined by FTIR analysis and respective treatment assignment.....	67
Table 5. Real objects: patina composition determined by FTIR analysis and respective treatment assignment.....	67
Table 6. Summary of products detected with FTIR analysis on samples surface treated with benzotriazole.....	72
Table 7. Summary of visual observations done after ageing on test objects regarding the corrosion reactivation.....	76
Table 8. Impedance $ Z $ modulus limit values $ Z $ for all measured samples.....	88
Table 9. Naturally patinated copper and bronze samples.....	98
Table 10. Colour difference $\Delta E^*$ calculated before and after treatment (0 Month – 0M) and at the end of exposure (12 Months – 12M) for each set of samples. For samples coding see Table 1.....	102
Table 11. Samples used for the new application of biopatina treatment indicating the former undergone treatment (T0: untreated; T4: biological treatment).....	106
Table 12. Colour difference $\Delta E^*$ calculated before and after cleaning, before and after treatment (0 Month) and at the end of 2, 4 and 6 months of exposure (2, 4, 6 Months) for each set of samples untreated (T0) or treated with biopatina (T4).....	113
Table 13. Impedance modulus $ Z $ measured before and after cleaning, after treatment and at the end of 6 months of exposure for each set of samples untreated (T0) or treated with biopatina (T4).....	114
Table 14. Artificially patinated samples used within the project.....	117
Table 15. Delivery systems and samples used for biopatina treatment.....	117
Table 16. Presence of copper oxalates on artificially patinated samples after 12 months of natural ageing.....	122
Table 17. Average impedance value $ Z $ ( $M\Omega\text{cm}^2$ ) obtained for the different sets of samples treated with biopatina (T4), wax (TR) and untreated (T0) after one-year exposure.....	125
Table 18. ATR-FTIR results on patina sample.....	128
Table 19. ATR-FTIR results on removed substrates.....	131
Table 20. ATR-FTIR results on control copper roof plate.....	131
Table 21. Raman-detected compounds present on bronze coupons (treated and reference) before and after ageing procedures.....	148
Table 22. EDS averaged weight percentage of Sn and Cu and calculated Sn/Cu for the central areas of G85dx sample.....	148

Table 23. Colorimetric coordinates ( $L^*$ , $a^*$ , $b^*$ ) and colour variation $\Delta E^*$ of the samples after pre-patination (tin enrichment), biopassivation and ageing. $\Delta E^*$ are calculated with respect to pre-patination conditions. Reported values are the average of values obtained at three different points on each sample .....	149
Table 24. Sets of coupons prepared with artificial patinas .....	159
Table 25. Composition of the artificial acid rain (pH) < 4.5) used for the dropping test.....	160
Table 26. EDS measurements of elemental composition on SB, ST, SQ and TQ samples before (T0) and after (T4) treatment expressed in weight percentage.....	162
Table 27. Colour distance $\Delta E$ calculated for the four alloys used in this study.....	163
Table 28. Artificially patinated bronze samples with respective alloy composition used for this study. On each set, all treatments were applied. Patina, Alloy and Treatment were used as factors for the ANOVA test. The components of each factor were used as sub-groups .....	166





